Optimizing the Costs of Solid Sorbent-Based CO_2 Capture Process Through Heat Integration

Final Technical Report

DOE Award DE-FE0012914

Project Period Start Date: October 1, 2013

Reporting Period End Date: December 31, 2015

ADA-ES, Inc.

9135 South Ridgeline Boulevard, Suite 200

Highlands Ranch, CO 80129

ADA-ES Document No. RP-15-0137 R0

ADA-ES Project No. 1017-13

Principal Investigator: Sharon Sjostrom

Report Co-Authors: Jayson Denney, William Morris

Report Date: March 18, 2016

Revised June 2, 2016

Disclaimer

Acknowledgements

This report is based upon work supported by the U.S. Department of Energy, National Energy Technology Laboratory. Award DE-FE0012914, with cost share from ADA-ES, Inc.. The authors gratefully acknowledge the support of our NETL Project Manager, Bruce Lani. Key subcontractors included Dr. Edward K. Levy and Joshua Charles from The Energy Research Center at Lehigh University, Caroline Richard, Robert McGillivary, and Ashley Bbyman from Solex Thermal Science, David Adam and Roy Silverman from Technip Stone and Webster, and Mike Richard and Bhurisa Thitakamol from Stantec.

Abstract

This report is the Final Technical Report for DOE Award DE-FE0012914 for the project period October of 2013 through December of 2015. The primary objective of this program was to advance the development post-combustion CO_2 capture technologies that utilize solid sorbents by reducing the energy penalty and/or overall levelized cost of electricity through heat integration or other process optimization.

The focus of this project was the ADAsorb™ CO_2 Capture Process, a temperature-swing adsorption process that incorporates a three-stage fluidized bed as the adsorber and a single-stage fluidized bed as the regenerator. ADAsorb™ system was designed, fabricated, and tested under DOE award DE-FE0004343. Two amine-based sorbents were evaluated in conjunction with the ADAsorb™ process: "BN", an ion-exchange resin; and "OJ", a metal organic framework (MOF) sorbent. Two cross heat exchanger designs were evaluated for use between the adsorber and regenerator: moving bed and fluidized bed. The fluidized bed approach was rejected fairly early in the project because the additional electrical load to power blowers or fans to overcome the pressure drop required for fluidization was estimated to be nominally three times the electrical power that could be generated from the steam saved through the use of the cross heat exchanger.

The Energy Research Center at Lehigh University built and utilized a process model of the ADAsorb™ capture process and integrated this model into an existing model of a supercritical PC power plant. The Lehigh models verified that, for the ADAsorb™ system, the largest contributor to parasitic power was lost electrical generation, which was primarily electric power which the host plant could not generate due to the extraction of low pressure (LP) steam for sorbent heating, followed by power for the CO_2 compressor and the blower or fan power required to fluidize the adsorber and regenerator.

Sorbent characteristics such as the impacts of moisture uptake, optimized adsorption and regeneration temperature, and sensitivity to changes in pressure were also included in the modeling study. Results indicate that sorbents which adsorb more than 1-2% moisture by weight are unlikely to be cost competitive unless they have an extremely high CO_2 working capacity that well exceeds 15% by weight. Modeling also revealed that reductions in adsorber pressure drop could negatively affect the CO_2 adsorption characteristics for sorbents with certain isobar adsorption characteristics like sorbent BN. Thus, reductions in pressure drop do not provide the efficiency benefits expected.

A techno-economic assessment conducted during the project revealed that without heat integration, the a metal organic framework (MOF) sorbent used in conjunction with the ADAsorb™ process provided the opportunity for improved performance over the benchmark MEA process. While the addition of a cross heat exchanger and heat integration was found to significantly improve net unit heat rate, the additional equipment costs required to realize these improvements almost always outweighed the improvement in performance. The exception to this was for a supported amine sorbent and the addition of a moving bed cross heat exchanger alone or in conjunction with waste heat from the compressor used for supplemental regenerator heating.

Perhaps one of the most important points to be drawn from the work conducted during this project is the significant influence of sorbent characteristics alone on the projected COE and LCOE associated with the ADAsorb™ process, and the implications associated with future improvements to solid sorbent CO_2 capture. The results from this project suggest that solid sorbent CO_2 capture will continue to see performance gains and lower system costs as further sorbent improvements are realized.

Table of Contents

Table of Figures

Table of Tables

Executive Summary

This report is the Final Technical Report for DOE Award DE-FE0012914. The primary objective of this program was to advance the development post combustion CO_2 capture technologies that utilize solid sorbents by reducing the energy penalty and/or overall levelized cost of electricity through heat integration or other process optimization. The focus of this project was the ADAsorb^{TM} CO_2 Capture Process, a temperature-swing adsorption process that incorporates a three-stage fluidized bed as the adsorber and a single-stage fluidized bed as the regenerator. ADAsorb™ system was designed, fabricated, and tested under DOE award DE-FE0004343.

This heat integration and optimization project began in October of 2013 and continued through December of 2015. The original end date of the project was extended from December 2014 to 2015 to incorporate results from extended testing of the ADAsorb^{TM} CO_2 Capture Process Pilot under the separate DOE project.

Two sorbents were evaluated during this project: “BN”, an ion-exchange resin that incorporates covalently-bonded amines; and “OJ”, a metal organic framework (MOF) sorbent that incorporates amines. BN was also included in ADAsorb^{TM} pilot testing, which provided additional insights to this heat integration project.

Two fundamental design approaches, moving-beds and fluidized beds, were assessed for their applicability incorporated into the ADAsorb™ process as cross heat exchangers between the adsorber and the regenerator. Solex Thermal Science provided the moving bed design, testing, and modeling support. Technip Stone and Webster provided support for the fluidized bed design. The fluidized bed approach was rejected fairly early in the project because the additional electrical load to power blowers or fans to overcome the pressure drop required for fluidization was estimated to be nominally three times the electrical power that could be generated from the steam saved through the use of the heat exchanger. The moving bed was tested independently by Solex and also incorporated into a cold-flow model of the ADAsorb™ process while using sorbent BN to better assess the impact to operations resulting from reactions with CO_2.

The Energy Research Center at Lehigh University independently built a process model of the ADAsorb^{TM} capture process and integrated this model into an existing model of a supercritical PC power plant that they developed on a separate DOE project. The Lehigh models allowed process modifications to be evaluated independently and in combination with one another. The primary combined process model was built using Aspen Plus software with individual components of the process built within Excel for verification of results. Analysis and modeling of the ADAsorb^{TM} CO_2 Capture System has resulted in not only a better understanding of how the system operated, but also has resulted in recommended changes in design and process conditions, which have the potential to significantly improve the performance of a coal-fired plant equipped with an ADAsorb™ system.

The Lehigh models verified that, for the ADAsorb™ system, the largest contributor to parasitic power is lost electrical generation, which is primarily electric power which the host plant cannot generate due to

the extraction of low pressure (LP) steam for sorbent heating, followed by power for the CO_2 compressor and the blower or fan power required to fluidize the adsorber and regenerator. Pump and refrigeration power only account for a small percentage of the total parasitic power.

Lehigh modeled an "ideal" cross heat exchanger to determine the extent that parasitic load could be minimized. As the exchanger efficiency approached 100%, the modeled net unit heat rate for a power plant with an ADAsorb™ CO_2 capture system could be decreased by up to 14.4% for sorbent BN compared to a power plant with an ADAsorb™ CO_2 capture system and no heat integration. The addition of a cross heat exchanger primarily decreased the overall parasitic power through decreasing the lost electrical generation. The reason for this is that the cross heat exchanger adds heat to the rich sorbent stream that otherwise would come from the LP steam. Blower power is slightly reduced by the use of a cross heat exchanger as fewer cooling water tubes are required in the top adsorber bed, resulting in a shallower bed and lower bed pressure drop. As system parasitic power is reduced, overall unit efficiency increases, decreasing the coal flow rate, which results in a lower CO_2 flow rate for a $550MW_{net}$ plant. A lower CO_2 flow rate further reduces the capture demand on the ADAsorb™ CO_2 capture system, resulting in lower parasitic power for each component of the capture and compression system.

In addition to evaluating cross heat exchanger efficiencies ranging from 0 to 100%, Lehigh also included an evaluation of heat recovered from the compressors used to heat sorbent entering the regenerator and heat steam cycle feedwater, and heat recovered from the flue gas cooler used to heat boiler combustion air and to heat steam cycle feedwater.

Every heat integration option considered in Lehigh's modeling exercise resulted in a reduction in net unit heat rate for a power plant with an installed ADAsorb™ system relative to implementing the ADAsorb™ CO_2 capture system without heat integration. The best-performing case at a representative cross heat exchanger of 75% efficiency included all other heat recovery options evaluated. This configuration resulted in a 13.0% reduction and 3.4% reduction in net unit heat rate for the power plant from the ADAsorb™ case without heat integration for sorbents BN and OJ, respectively. Using heat from the compression system contributes most significantly to this improvement, as there is a greater quantity of high-temperature heat available from this source than from the flue gas cooling system. Conversely, the case with the smallest heat rate improvement is the case without a cross heat exchanger, where heat from the flue gas cooler is used to heat steam cycle feedwater, which only reduces net unit heat rate by 0.46% and 0.36% for sorbents BN and OJ, respectively. The reason for the small performance improvement for these cases is the low quantity of low quality heat, which is available from the flue gas cooler for feedwater heating. Cases utilizing compressor heat for regenerator and/or feedwater heating perform better, with heat rate reductions between 3.3% and 6.7% for the BN sorbent and 1% and 1.5% for the OJ sorbent.

Although the OJ sorbent is still under development, assumptions were made regarding performance characteristics for this material produced at scale. The OJ sorbent is projected to have more optimal characteristics than BN in the ADAsorb™ process. If the OJ sorbent is used instead of the BN sorbent, for the case with no heat integration, the net unit heat rate at a power plant with an ADAsorb™ system

installed is reduced by between 10% and 17% , or an increase in net power plant unit efficiency from 25.6% to 30.9% when compared to the BN sorbent. This reduction is partially due to a reduction in the sorbent flow rate due to higher CO_2 loading capacity of the OJ sorbent. Specifically, the OJ sorbent has the potential to provide three times the CO_2 loading of the BN sorbent. A lower sorbent flow rate reduces the energy needed to heat and cool the sorbent in the regenerator and adsorber.

Another factor promoting the enhanced thermodynamic performance of the OJ sorbent is the optimal operating temperatures of the adsorber and regenerator. For the BN sorbent, optimal adsorber and regenerator temperatures of 40°C (104°F) and 120°C (248°F) respectively were found. However, for the OJ sorbent, optimal adsorber and regenerator temperatures were found to be 38°C (100°F) and 59°C (140°F) respectively. If the lower adsorber operating temperatures can be realized, the increased capacity and lower temperature can potentially cut the sorbent flow rate for OJ compared to BN by around 66%. With a lower temperature difference between the adsorber and regenerator, heating and cooling demands by the sorbent in the adsorber and regenerator are further reduced.

As a cross heat exchanger and heat integration are added to the ADAsorb^{TM} CO_2 capture system, the heat rate benefit through use of the OJ sorbent compared to the BN sorbent diminishes. However, for the modeled case with a cross heat exchanger (effectiveness of 75%) and all four heat integration options being utilized, the use of the OJ sorbent still lowers net unit heat rate by a significant 8.0% over the BN case.

The CO_2 compressor is the second highest parasitic load resulting from an ADAsorb™ system installed at a power plant. The CO_2 compression system modeled by Lehigh consisted of a seven-stage compression system with an output of 2,215 psia. This discharge pressure is a typical pressure discussed in literature. If the captured CO_2 were to be sequestered, there may be different wellhead pressure requirements. Model results indicate that a 1,000 psia reduction in the CO_2 discharge pressure results in a predicted 2% decrease in net unit heat rate corresponding to a 12.5% decrease in compression power.

Other options evaluated to improve the overall efficiency of the integrated process included optimizing the moisture level and reducing pressure drop in the adsorber and regenerator to reduce the electrical demand resulting from the fan power requirements.

The solid sorbent utilized in the ADAsorb^{TM} pilot, sorbent BN, is known to adsorb moisture as well as CO_2. Investigation of the sorption of moisture by to the CO_2 sorbent within the ADAsorb^{TM} process is of interest as varying the moisture uptake has an effect on the system efficiency. The impacts of flue gas moisture uptake on the sorbent turned out to be significant for sorbent BN. Sorbent BN's design working capacity, the delta loading between adsorption and regeneration, was measured to be 7% by weight for CO_2 and 0.9% by weight for H_2O. If the sorbent could be made to not adsorb water, the net plant heat rate for Illinois #6 coal would be reduced by 5.7%. These reductions are largely due to increased CO_2 sorption, decreased regenerator heat requirements, and decreased mass flow into the CO_2 compression system. This indicates that moisture adsorbed by the sorbent should be minimized to increase the net power plant efficiency. It also indicates that, based on the size of the possible reductions, this should clearly be a development priority and that sorbents which adsorb more than 1-

2% moisture by weight are unlikely to be cost competitive unless they have an extremely high CO_2 working capacity that well exceeds 15% by weight.

Another option to reduce the moisture uptake on the sorbent is to decrease the moisture in the flue gas at the inlet to the ADAsorb™ system. The concentration of the water vapor will be at the saturation point entering the adsorber, since it has to be cooled below the saturation point of an upstream wet flue gas desulfurization unit. The impact of moisture will be a function of either sorbent moisture uptake or flue gas cooling. Using the process model and fundamental heat and mass transfer analyses, simulations were performed for a 550 MW_{net} coal fired power plant to estimate heat exchanger surface areas, power needs for refrigeration systems, and water capture energy costs for different flue gas moisture levels entering the CO_2 adsorber. Not surprisingly, this investigation led to the conclusion that the temperature and pressure of the gas entering the adsorber dominate the energetic and fiscal costs associated with moisture removal and flue gas cooling. Reducing flue gas moisture and temperature through the combined use of a spray cooler and refrigeration cycle has little effect on capital costs while the power usage increases by two or three times. Development focus on sorbents with lower moisture uptake will have a much larger impact on the efficiency of the overall system than the addition of flue gas cooling.

The third largest parasitic load from an installed ADAsorb™ system is from the booster fan required to maintain fluidization in the adsorber. Results from Lehigh's modeling suggest that nominally a third of the heat rate impact of the ADAsorb^{TM} CO_2 capture system is due to this added fan power. Lehigh modeled the heat rate impact of reduced pressure drop in the adsorber. For a 1 and 2 psia reduction in adsorber pressure drop, unit heat rate dropped by 0.5% and 1.1% respectively as a result of a reduction in booster fan power from 51 MW to 44 MW and 37 MW respectively. Upon first review, the expectation was that such a significant reduction in fan power should result in a much larger reduction in net unit heat rate. However, the reduction in adsorber pressure drop negatively affects the CO_2 adsorption characteristics as the partial pressure of CO_2 is reduced in the adsorber. This lowers the equilibrium loading potential of the sorbent and effectively reduces its working capacity necessitating a higher sorbent recirculation rate. For each 1 psia reduction in adsorber pressure drop, the sorbent flow rate corresponding to 90% CO_2 capture increases by approximately 1,000,000 lb/hr. This results in a larger regenerator duty, extraction steam flow, increasing the turbine cycle heat rate. Thus, reductions in pressure drop do not provide the efficiency benefits for a sorbent with isobar adsorption characteristics like sorbent BN.

The Solex heat exchanger test results and Lehigh modeling efforts were incorporated into a techno-economic assessment to determine both the projected costs of the base ADAsorb™ system in conjunction with sorbents BN and OJ, and the potential benefits of other heat integration approaches. Without heat integration, the OJ sorbent used in conjunction with the ADAsorb™ process provides the opportunity for improved performance over the benchmark MEA process. Many of these are summarized in Table ES-1. For reference, the cost of electricity (COE) is the annual cost per kWh (expressed in base-year dollars) of electricity produced. The levelized cost of electricity (LCOE) involves the addition of a levelization factor to the COE. The LCOE is expressed in operational year (first year of operation) dollars, which means that any LCOE costs expressed in base-year dollars (throughout

construction period) must be scaled to operational year dollars using an inflation rate. The assumptions used in the cost assessment are critical to the cost projections. These assumptions and related calculations are provided in more detail in the report and associated reference documents.

Table ES-1 Results of Techno Economic Analysis

Case	Sorbent BN		Sorbent OJ	
	COE	**LCOE**	**COE**	**LCOE**
ADAsorb™ without heat integration	$154.4/MWh	$194.8/MWh	$126.2/MWh	$159.2/MWh
Cost increase from no CO_2 capture	66%		36%	
Comparison to 90% CO_2 capture with MEA	15% higher		6% lower	
ADAsorb™ with 75% cross heat exchanger	$148.4/MWh		$125.9/MWh	
ADAsorb™ with 75% cross heat exchanger with regenerator heat	$147.4/MWh			

While the addition of a cross heat exchanger and heat integration was found to significantly improve net unit heat rate, the additional equipment costs required to realize these improvements almost always outweighed the improvement in performance. The exception to this was for sorbent BN and the addition of a moving bed cross heat exchanger alone or in conjunction with a regenerator heater for supplemental heating of the regenerator with waste heat. For sorbent OJ, the addition of cross heat exchanger with an effectiveness of 75% only lowered the COE by $0.3/MWh, or by 0.2%. Given this very small difference in COE between the OJ case with and without a cross heat exchanger, it is suggested that it would be best not to include a cross heat exchanger for this sorbent. The additional complexity of adding such a system will most likely outweigh the minimal improvement in COE. For each of the other heat integration opportunities modeled, which include the addition of waste heat to provide supplemental feedwater heating or supplemental combustion air heating for the BN case, or supplemental heating to the regenerator for the OJ sorbent case, COE and LCOE increased.

Perhaps one of the most important points to be drawn from the work conducted during this project is the significant influence of sorbent characteristics alone on the projected COE and LCOE associated with the ADAsorb™ process, and the implications associated with future improvements to solid sorbent CO_2 capture. ADA has supported steady progress in developing and testing new sorbents. For instance, the

BN sorbent represents a sorbent tested prior to the initiation of this project, while sorbent OJ was characterized in the year leading up to publication of this report. Improvements to the OJ sorbent are in progress under a separately funded project. We believe that solid sorbent CO_2 capture will continue to see performance gains and lower system costs as further sorbent development is conducted.

1 Introduction

1.1 Overview of Project

According to the International Energy Agency (IEA), post-combustion carbon dioxide (CO_2) capture (PCCC) and storage will be an important component of reducing worldwide CO_2 emissions from stationary point sources, such as coal-fired power plants.[1] An existing 550 MW_{net} coal-fired power plant can produce over 4 million tons of CO_2 per year. Aqueous amine processes, which are the most developed for removing CO_2 from process gases, are projected to significantly increase the cost of electricity. Amine processes also pose environmental impacts such as increased water usage and increased emissions of hazardous chemicals into the air or wastewater resulting from volatile components in the solvents or chemicals added to the process. ADA-ES, Inc. (ADA), through a separate DOE contract, DE-FE0004343, has been developing a sorbent-based process, termed ADAsorb™, which addresses many of these negative environmental challenges.

There are several options for optimization that could significantly reduce the costs associated with PCCC, and while such options have largely been explored for aqueous amine capture systems, a similar development effort for sorbent-based processes has yet to be completed. For example, heat integration could significantly improve the economics of solid-based capture processes. The options for heat integration that were evaluated under this program include using heat from CO_2 compressors and flue gas coolers, integrating the capture process with the power plant, and designing and implementing a cross heat exchanger (HXTX) to recover sensible heat from the sorbent leaving the regenerator and add it to the sorbent entering the regenerator.

In addition to heat integration, there are other considerations that could also reduce the overall energy penalty and the related costs, such as optimizing the moisture content in the flue gas, reducing pressure drop through the system, optimizing CO_2 discharge pressure, and optimizing adsorption and desorption vessel temperatures. This program examined optimization of these parameters for sorbent-based CO_2 capture processes. Key components of the effort included addressing the technology gap of a cross heat exchanger for solids through bench-scale testing of select concepts, computational modeling, and a techno-economic assessment. While this effort was based on a specific CO_2 capture process, the optimization study includes a trend analysis across a range of sorbent properties so that the general conclusions will be applicable to most sorbent-based CO_2 capture processes.

1.1.1 Project Description

This project was divided into four tasks with several subtasks. The tasks, described in the sections below, include:

Task 1. Project Management;

Task 2. Bench-Scale Testing and Technical Analysis of Heat Exchanger Designs

Bench-scale testing of a heat exchanger concept with a single sorbent was conducted to collect the data required for scale-up modeling with subsequent computational modeling;

Task 3) Heat Integration and Optimization, where modeling using ASPEN Plus and custom tools were used to

a) Determine the optimal operating conditions for a heat exchanger in moving-bed and fluidized bed arrangements that was integrated into the overall CO_2 capture process to minimize capital and operating cost;
b) Assess the viability of heat integration options with the power plant and the CO_2 compressors;
c) Optimize the flue gas moisture level;
d) Assess adsorber and regenerator designs to reduce pressure drop; and

Task 4) Incorporate Process Optimization into ADAsorb^{TM} CO_2 Capture Process Techno-Economic Assessment, where a techno-economic assessment of the optimized equipment and operating conditions were incorporated into a 550 MW_{net} supercritical plant using ADA's existing techno-economic model developed under DE-FE0004343. The techno-economic assessment also included identification of sorbent properties to meet the DOE's CO_2 capture cost goals.

1.1.2 Project Schedule

The project began in October of 2013 and continued through December of 2015. The original end date of the project was extended from December 2014 to 2015 due to extended testing at the ADAsorb^{TM} Pilot under DOE award DE-FE0004343. The project timeline is presented in Figure 1.

1.1.3 Project Team

In this program, ADA was the prime contractor and managed all project efforts. The project team consisted of ADA, Solex Thermal Science (Solex), Technip Stone and Webster (Technip), and the Energy Research Center at Lehigh University (Lehigh). Solex and Technip were chosen because of their expertise in moving and fluidized beds, respectively. Lehigh provided an objective assessment of the technology options and conducted optimization studies.

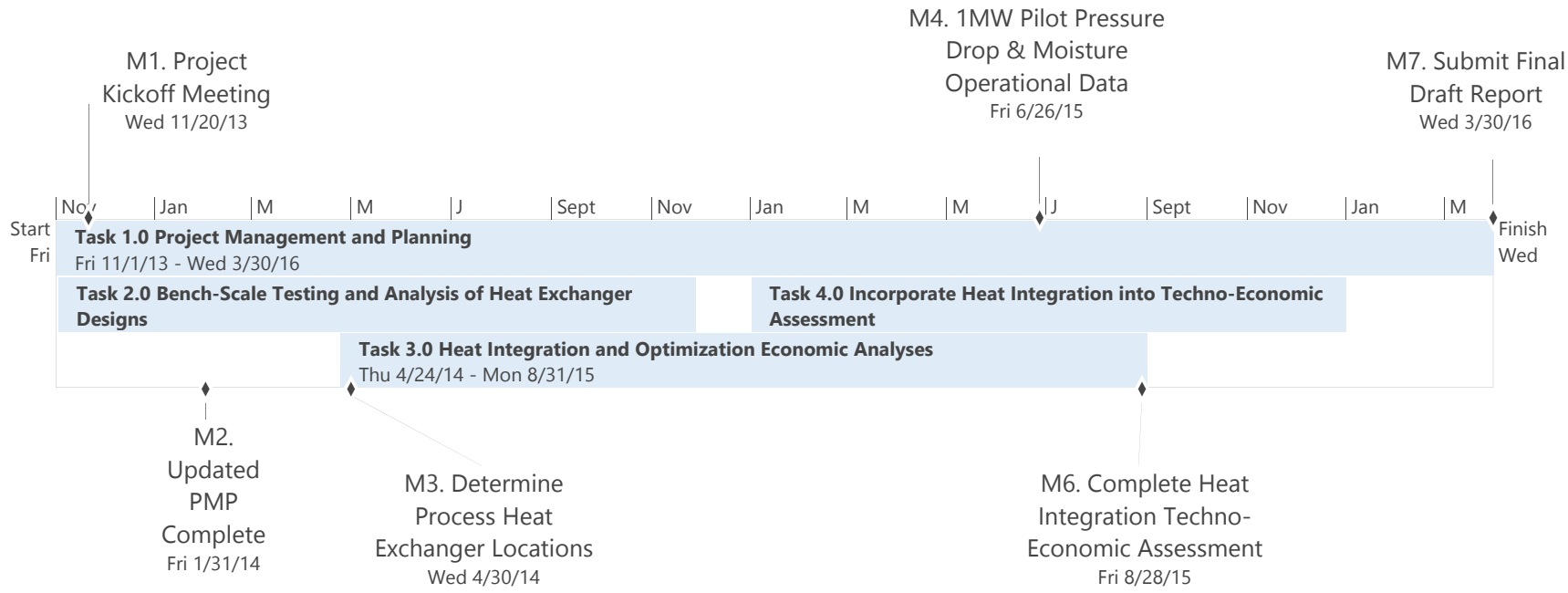

Figure 1. Project Timeline

1.2 Objectives of the Project

The primary objective of this program was to advance the development PCCC technologies that utilize solid sorbents by reducing the energy penalty and/or overall levelized cost of electricity. This objective facilitated progress towards meeting the overall DOE Carbon Capture Program performance goals of 90% CO_2 capture rate with 95% CO_2 purity at a cost of approximately $40/tonne of CO_2 captured by 2025 and a cost of less than $40/tonne of CO_2 captured by 2035.

Specific focus areas for this project included:

- Bench-scale testing to collect the empirical data necessary to evaluate moving bed heat exchangers for use as a cross heat exchanger. Data for fluidized beds was collected under DE-FE0004343;
- Using computational modeling to evaluate multiple configurations of cross heat exchangers and identify the most cost-effective option.
- Optimizing the approach temperature and cross heat exchanger designs to minimize overall CO_2 capture costs while taking into account both capital and operating costs.
- Completing a sensitivity analysis of the technical capabilities, projected capital costs, and operating costs for incorporating the following into the sorbent-based CO_2 capture process:
    - Heat Integration;
        - Integrating the process with the CO_2 compression system and the power plant.
        - Heat recovery using the optimal cross heat exchanger.
    - Flue gas drying;
    - Optimized design to reduce pressure drop;
- Completing a techno-economic analysis that:
    - Identified costs and expected energy requirements for an optimized ADAsorb™ process;
    - Provided a pathway for heat recovery research and development to accelerate the development of sorbent-based CO_2 capture through development of general energy and cost trends for a range of key sorbent properties;
    - Identified sorbent characteristics necessary to achieve the target technical performance of 90% CO_2 capture while reducing levelized costs by reducing parasitic plant load (i.e., steam and auxiliary power) and capital costs associated with capture and compression.

ADA has developed and refined a techno-economic assessment of its ADAsorb™ post-combustion capture process without advanced heat integration through DOE contract DE-FE0004343. Significant additional cost reductions for the ADAsorb™ process were expected to be achievable based on process and sorbent improvements. The sorbent ADA is using for a 1 MWe ADAsorb™ process validation study (DE-FE0004343) has been identified for bench-scale evaluations and as the basis of the computational models described in this proposal. Process modeling and techno-economic evaluations were conducted across a range of representative sorbent properties to assure broad applicability of the concepts evaluated under the project and to identify optimal sorbent characteristics for future development.

1.3 Significance of the Project

This project is significant in that it focuses on the potential for process optimization rather than sorbent development and screening. While sorbent properties are critically important for PCCC applications, considerably less effort has been expended analyzing how a practical solid sorbent based system could be integrated into the power plant in the most efficient way possible. The impact on the absolute efficiency optimization of the plant and process, and the impact to levelized cost of electricity (LCOE) were compared. A key component of the project included addressing the technology gap of a cross heat exchanger for solids through bench-scale testing of select concepts, computational modeling, and a techno-economic assessment. Two types of cross heat exchangers were evaluated for this unique application.

2 Technology Description

2.1 Description of the Technology

In 2011 a team led by ADA developed a conceptual design for a PCCC process, ADAsorb™, to treat flue gas from a 550 MW_{net} coal-fired power plant. The ADAsorb™ process was designed to maximize heat and mass transfer during the uptake and release of CO_2. While the optimization study to be completed in this effort will have applicability to different sorbent-based CO_2 capture processes, the ADAsorb^{TM} CO_2 capture process was used as a basis to complete a detailed techno-economic analysis.

Figure 2 is a simplified sketch of the ADAsorb™ process integrated into an existing coal-fired power plant. Similar to the aqueous amine process, the sorbent-based CO_2 capture process is implemented immediately upstream of the stack.

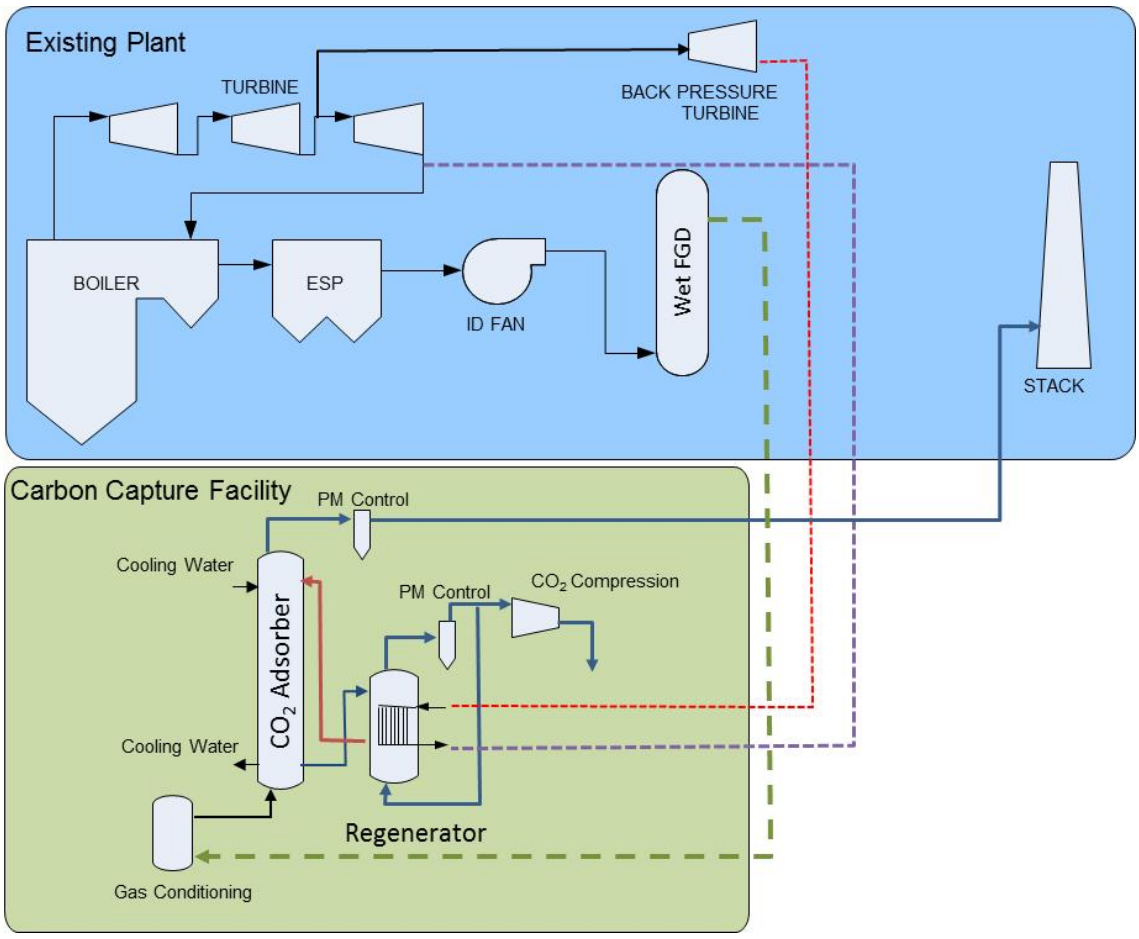

Figure 2. Process Flow Diagram of a Sub-Critical PC Power Plant Retrofitted with a Solid-Based CO_2 Capture Process

The ADAsorb™ process is sorbent agnostic, meaning that the process can be designed to provide process conditions to minimize CO_2 capture costs by tailoring the process conditions for a given sorbent.

The ADAsorb™ process is shown in Figure 3 with additional detail. Flue gas enters the bottom of the adsorber vessel after passing through a SO_2 scrubber. The gas progressively flows upwards through a series of staged fluidized beds. The gas velocity is controlled to maintain each of the beds in a bubbling regime to optimize mass and heat transfer. While the gas is flowing upwards, the sorbent, which is introduced at the top of the adsorber vessel, progressively flows downward through each of the fluidized beds. Heat is generated as the sorbent reacts exothermically with CO_2. Because the CO_2 loading is negatively impacted by increased temperature, isothermal conditions are maintained within the adsorber vessel by the use of cooling water inside tubes. CO_2 lean gas exits the top of the adsorber vessel through particulate control devices to capture entrained sorbent. CO_2 rich sorbent is pneumatically conveyed from the fluidized bed at the base of the adsorber to the top of the regenerator. Figures 2 and 3 represent the system without any heat recovery, thus the sorbent entering the regenerator at the adsorption temperature and thus must be heated up in the regenerator. Similarly, the top bed of the adsorber is responsible for removing sensible heat (because the sorbent is

still hot from the regenerator) and latent heat (from the reactions with CO_2 and H_2O). The size of the adsorber and regenerator are based upon the amount of heat transfer surface area necessary to maintain isothermal operation as well as the kinetics of the adsorption and desorption processes. Therefore, if heat recovery is added to the process the top bed of the adsorber and the regenerator could potentially be smaller and the corresponding pressure drop through the beds will be smaller.

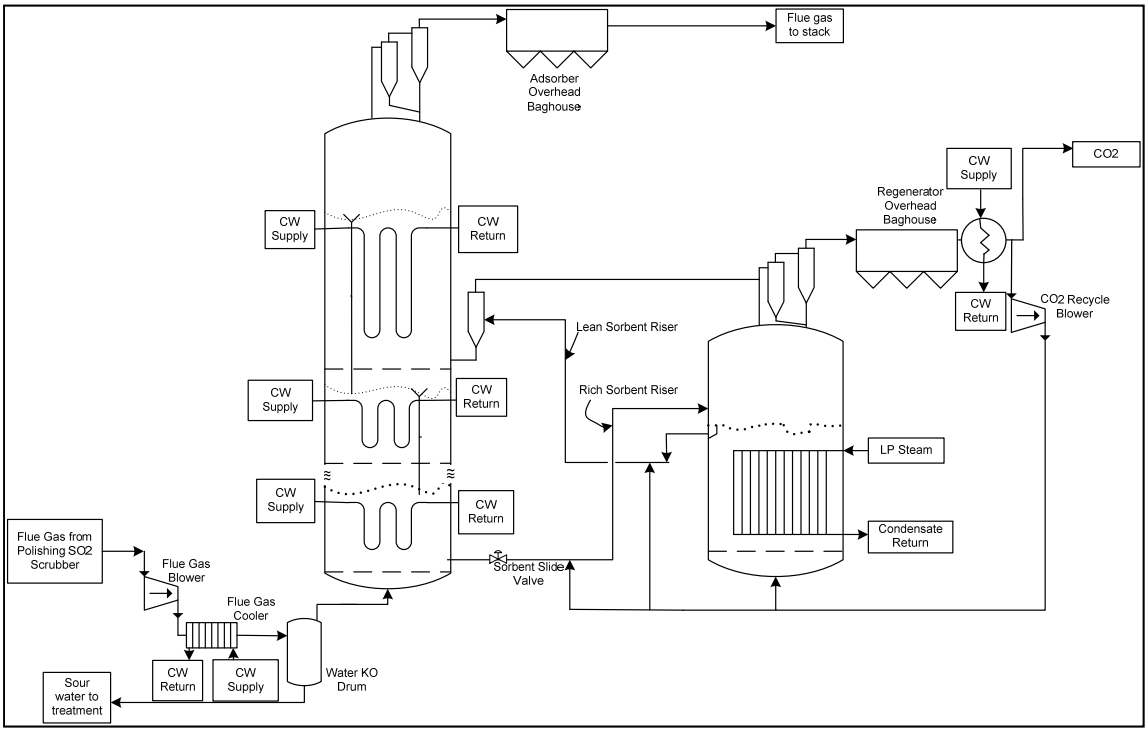

Figure 3. Sketch of the ADAsorb™ CO_2 Capture Temperature Swing Adsorption System

The regeneration process is operated isothermally via the use of indirect steam. The sorbent in the regenerator is fluidized using recycled CO_2. As the sorbent particles reach the regeneration temperature, the equilibrium loading of CO_2 decreases and CO_2 is released. The evolved CO_2 exits the regenerator through a particulate collection system.

ADA conducted an ADAsorb™ process validation test during 2014 and 2015 under DOE contract DE-FE0004343 using a 1 MWe pilot-scale version of the process shown in Figure 3 and an amine-functionalized sorbent. This pilot did not include any heat integration features and, other than initial development of the concepts presented in this report, heat integration was not included in the scope of that DOE project.

The main purpose of the this project was to determine how much energy can be saved through heat integration (i.e., integrating the CO_2 capture process with CO_2 compression and the power plant and recovering heat using a cross heat exchanger), flue gas drying, and design optimization to reduce pressure drop and improve the overall cost for CO_2 capture.

A key component of the effort was the development and analysis of a cross heat exchanger for heat recovery. The sensible heat duty component of the energy penalty for aqueous MEA CO_2 capture processes have been dramatically reduced by the addition and optimization of cross heat exchangers. Similarly, investigating the amount of energy that could be saved and the overall cost implications of including heat integration, especially a cross heat exchanger, for solid-based CO_2 capture processes was necessary. Two configurations of a cross heat exchanger for solids, fluidized beds and moving beds, were chosen for development. Because a solids/solids heat exchanger is not feasible, it was envisioned that a heat transfer fluid would be circulated between two or more exchangers, effectively heating the CO_2-laden sorbent and cooling the CO_2 lean sorbent. A process sketch of the proposed configuration is shown in Figure 4.

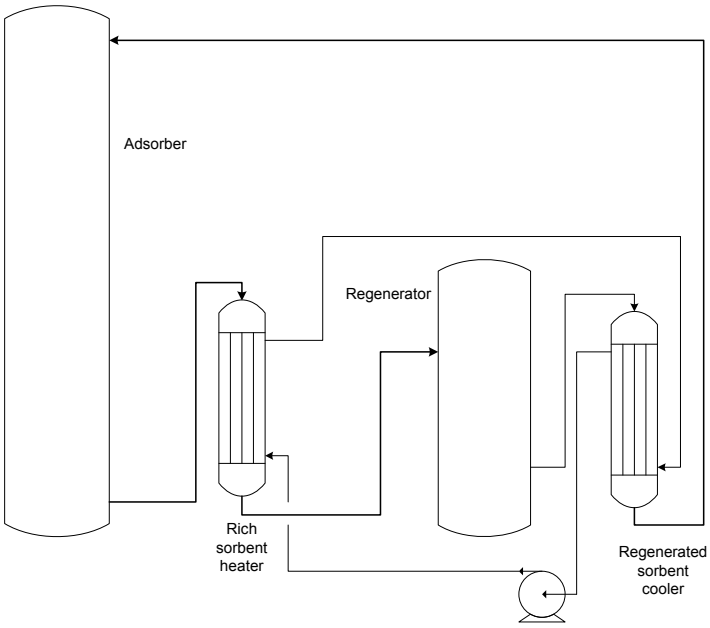

Figure 4. Heat Exchanger Concept

Additionally, optimization of the moisture content in the flue gas, which affects the energy penalty resulting from the latent heat of vaporization of water, was considered for sorbents that adsorb various amounts of water. System improvements that reduce the heat transfer surface area required, such as recovering sensible heat and reducing the heat of vaporization, were also included in this evaluation. Such system improvements can result in smaller fluidized beds in the ADAsorb™ process with a corresponding lower system pressure drop, and reduced flue gas blower loads which allow for the use of smaller flue gas blowers.

2.2 Solid Sorbent Technology

While most solid sorbents offer the benefit of a lower specific heat compared to aqueous solutions, the mechanism in which such materials remove CO_2 from flue gas can vary significantly. Sorbents can be

classified into two general families: those that chemically react with the CO_2, called supported reactants, and those that adsorb or use their molecular structure or Van der Waals forces to screen CO_2 from other gases, called non-reacting adsorbents. Chemically reacting sorbents usually include an inert, high surface area support, with an immobilized amine or other reactant on the surface. The surface area provides numerous sites for the desired reaction to occur. Many different types of solid materials for CO_2 capture have been or are currently being investigated including: supported amines[2-8], carbon-based sorbents[9-12], supported carbonates[13,14], zeolites[15], metal organic frameworks (MOFs)[16-20], etc. These materials are being developed and tested at universities, government laboratories, and private institutions worldwide.

Extensive sorbent screening programs were previously completed by ADA under cooperative agreements DE-NT0005649 and DE-FE0004343 as well as several other funding mechanisms including ADA internal research. In 2011, based on testing over 250 solid sorbent variations, ADA made the determination that for the ADAsorb™ Pilot Program, a supported amine sorbent presented the best potential to significantly reduce the energy penalty associated with post-combustion CO_2 capture. The sorbent utilized for that program, identified as sorbent BN, is also utilized for this program and is the basis for the baseline Techno-Economic Analysis (TEA). Properties of an additional available sorbent, sorbent OJ, were selected in 2015 as the basis for a comparison sorbent to be examined within the TEA of this project. Sorbent OJ is a metal organic framework (MOF) sorbent. The inclusion of the two sorbents within this program's analysis allows for heat integration benefits to be compared against sorbent characteristics improvements.

Data available from the extensive laboratory characterization of the two sorbents was used within the process modeling of this project. The key sorbent characteristics identified for process design consideration are listed below:

- CO_2 working capacity;
- Cyclic stability;
- Reaction kinetics;
- Effect of flue gas constituents including SO_2 and moisture;
- Heat of reaction;
- Resistance to attrition
- Physical characteristics: particle size distribution and density;
- Sorbent cost;
- Sorbent fluidization and handling properties;
- Heat transfer coefficient.

A summary of properties needed for the modeling effort within this program can be seen in Table 1.

Table 1. Summary of Sorbent Properties

	Unit	BN	OJ
Equilibrium CO_2 Working Capacity	lb CO_2/100 lb Sorbent	7	12
Heat of Reaction	kJ/mol	77	58
Attrition	lb Sorbent/hour	Negligible	Assumed Same
Sorbent Cost	$USD	5.62	Assumed Same
Moisture Uptake	lb H_2O/100 lb Sorbent	0.9	Negligible

2.2.1 Sorbent BN

Sorbent BN has been extensively characterized under the ADAsorb™ Pilot Program. This sorbent is a commercially available supported amine. CO_2 loading and moisture loading isotherms are presented in Figure 5 and Figure 6, respectively.

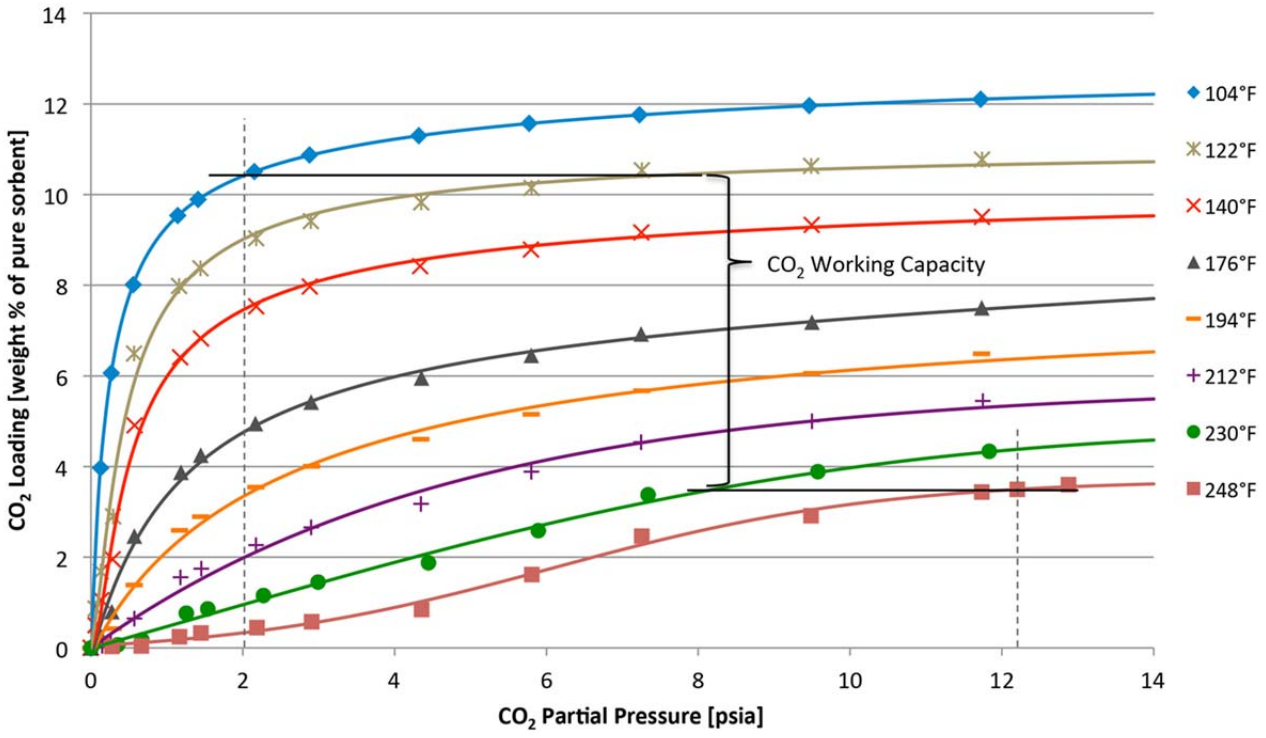

Figure 5. CO_2 Loading Isotherm Data and Curve Fits for Sorbent BN [26]

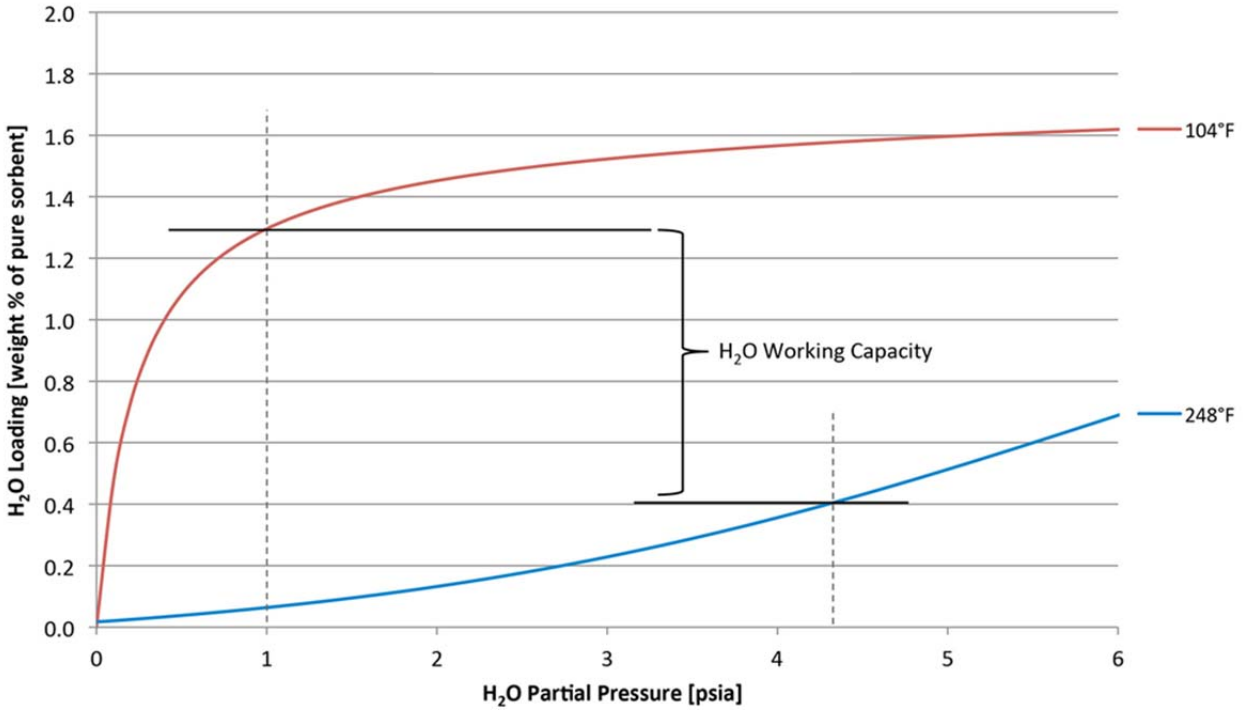

Figure 6. H_2O Loading Isotherms [26]

2.2.2 Sorbent OJ

Sorbent OJ is an experimental metal organic framework (MOF) sorbent that incorporates amines. This sorbent is in the development stage and has not been fully characterized for process use. Some assumptions, as presented in Table 1, were made to facilitate process evaluations conducted during this project. Measured CO_2 loading isotherms for sorbent OJ are presented in Figure 7. These measured data show a spike in adsorption at very low CO_2 partial pressure. Because the ADAsorb™ system does not operate within this range of partial pressure and due to the complexity in modeling the observed adsorption spike, the isotherm curves seen in Figure 8 were used for the modeling efforts conducted during this project.

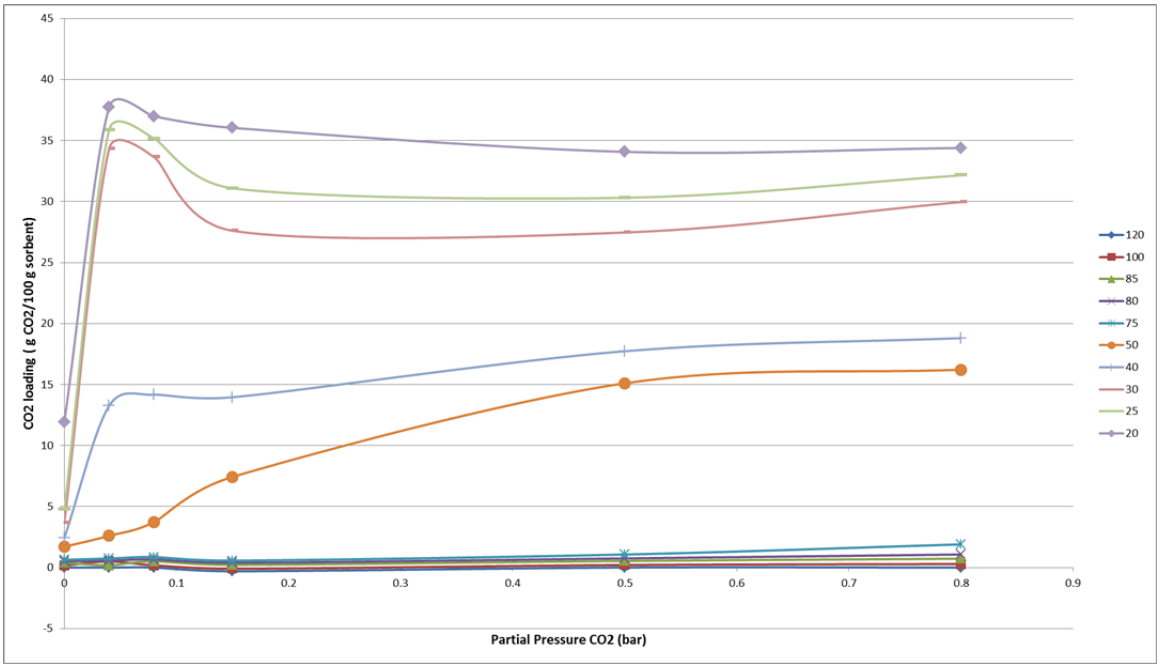

Figure 7. Measured CO_2 Loading Isotherm Data Sorbent OJ

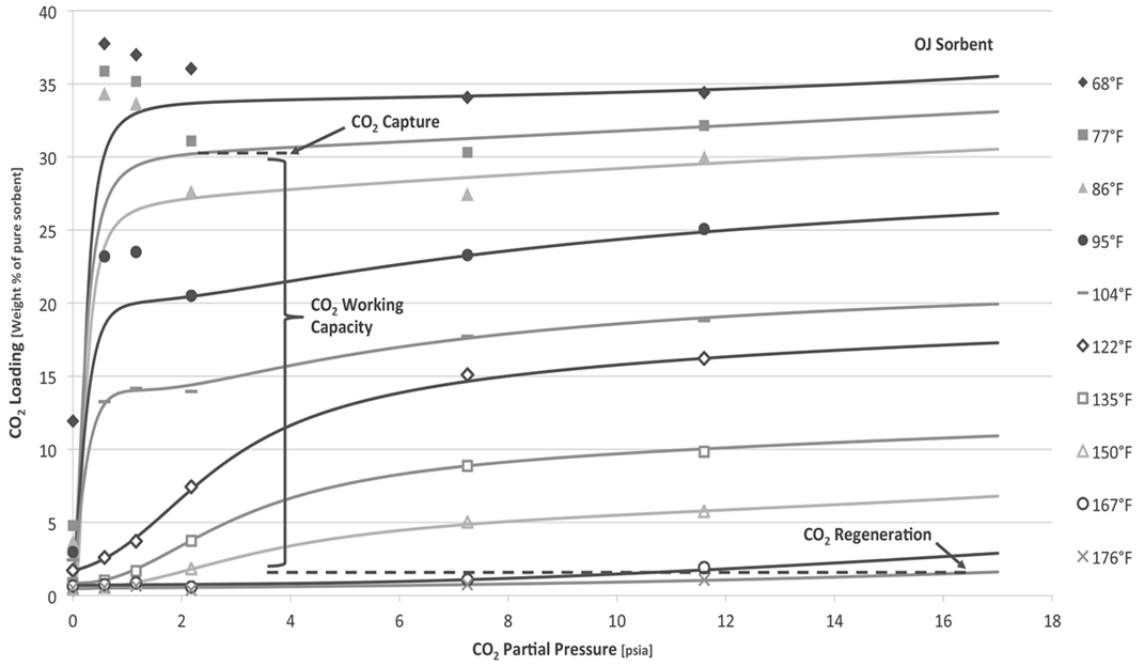

Figure 8. CO_2 Loading Isotherm Data and Curve Fits for Sorbent OJ used for modeling[29]

2.3 Options for Heat Transfer with Solids

In the ADA system, represented in Figure 3, the cold, rich sorbent stream is conveyed by recirculated CO_2 to the top of the regenerator. The sorbent is heated in the top of the regenerator bed from 104°F to 248°F. Following regeneration, the hot, lean sorbent is conveyed to the top of the adsorber where it is cooled from 248°F to 104°F. Conceptually, heating of the rich sorbent requires steam to be extracted from the power plant's steam cycle, and cooling of the lean sorbent requires cooling of the adsorber through a refrigeration system or cooling water. A heat exchanger which exchanges heat between these two streams, also known as a cross heat exchanger, would help to reduce these heating and cooling loads, potentially reducing the parasitic power losses to the power plant that are associated with operating the CO_2 capture system.

2.3.1 Fluidized Beds

Fluidized beds were one configuration option for the cross heat exchanger that was investigated under this project. One of the most important characteristics of fluidized beds is that the heat transfer coefficient can be maximized compared to moving beds. This means that for the same amount of heat transferred less surface area is necessary, which could lead to lower capital costs for the vessel. Behavior of the heat transfer coefficient at different conditions is illustrated in Figure 9. Figure 9 was collected by Xavier et al.[21,22] to measure the effect of pressure on heat transfer between a flat surface and glass spheres in an N_2 atmosphere.

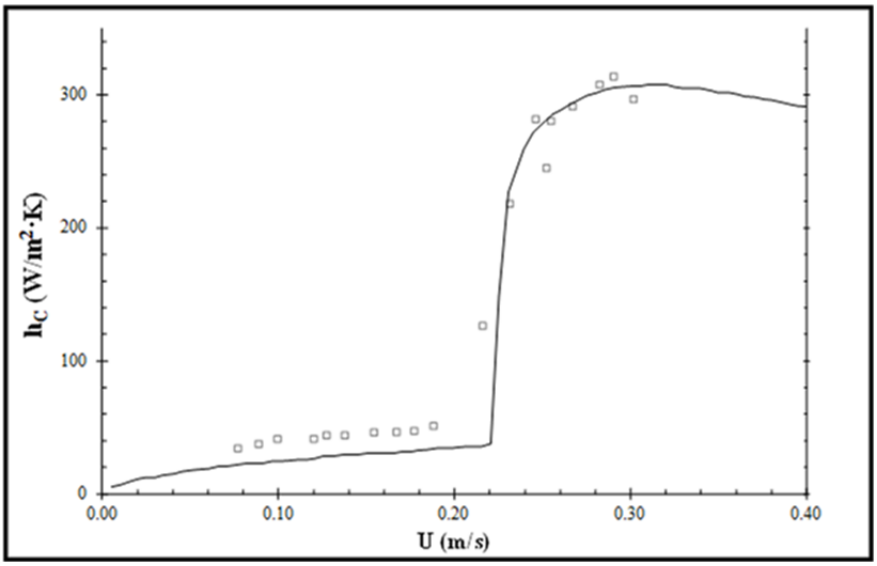

Figure 9. Experimentally measured overall heat transfer coefficient. (Specifically the purpose of this figure is to illustrate the step change in the overall heat transfer coefficient when a material is fluidized.[21,22])

As is shown in Figure 9, the gas velocity has a relatively small effect on the heat transfer coefficient within the fixed or moving bed regime. However, as the bed achieves the minimum fluidization velocity (in the lowest pressure drop case this occurs at about 0.23 m/s), the overall heat transfer coefficient

increases as a step change from approximately 30 to 270 $W/m^2 \cdot K$. It should be noted that the maximum heat transfer coefficient is observed in the bubbling fluidized bed regime.

Bench-scale fluidized bed testing of one CO_2 sorbent, identified in this report as BN, was completed under a separate DOE contract (DE-FE0004343) to support development of the ADAsorb™ process. The following parameters were measured using an 11.5-inch diameter column over a range of superficial gas velocities for each of several particle size distributions:

- Bed density;
- Quality of fluidization - determined both visually, and by means of high frequency ΔP bed fluctuation measurements;
- Entrainment rate;
- Dip-leg density (combined first and second stage);
- Heat transfer coefficient;
- Bubble volume fraction.

An example of how fluidized beds could be used for heat recovery is shown in Figure 10. In this diagram the vessels labeled “heater” and “cooler” are both fluidized beds and operate isothermally. Heat transfer fluid is moved between the two beds and, thus, heat is transferred from the hot sorbent leaving the regenerator to the cool sorbent entering the regenerator. Note that because the capacity of the sorbent for CO_2 is highly temperature dependent, and reactions with CO_2 affect the energy balance, integrated modeling was required to determine the optimal CO_2 partial pressure of the fluidizing gas to manage the CO_2 both on the sorbent and in the conveying gas at the exit of the heat exchangers.

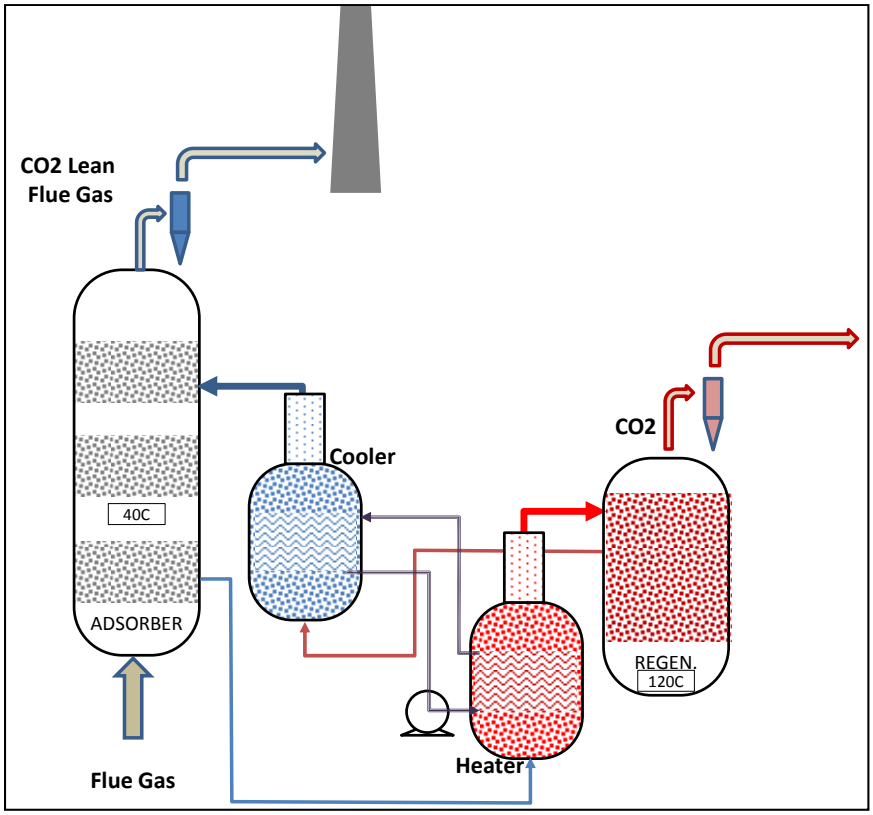

Figure 10. Schematic of Fluidized Bed used for Heat Recovery

2.3.2 Moving Beds

Although it was shown that the heat transfer coefficient of a sorbent in a moving bed will be lower than that of the same sorbent in a fluidized bed, there are also significant advantages for using moving beds for heat integration. For example, in a moving bed the sorbent moves down through the bed based on gravity, so little or no fluidizing gas is necessary. In addition, a clear benefit of moving bed systems is that, unlike fluidized beds, indirect heating and cooling can be readily employed, allowing the solids and heat transfer media to move in opposite directions. This means that aggressive approach temperature and high heat recovery using only two moving beds per CO_2 capture train, one moving bed for heating and one for cooling, is possible. The optimal approach temperature must be determined based on the overall costs for CO_2 capture.

With a moving bed and indirect cooling technology, a heat transfer fluid is pumped through a vertical bank of hollow plates while the bulk solid passes between the plates at a rate sufficient to achieve the required cooling. A sketch of the process is shown in Figure 11. In this case the moving bed is being used to cool a solid with water as the heat transfer medium. The water circulates counter-current to the solid flow. Solex conducted an assessment of applying their exchanger design to recover some of the sensible heat from a post-combustion solid sorbent application. The design concept is quite similar to large oilseed dryers. A photo of a full-scale oilseed dryer is shown in Figure 12.

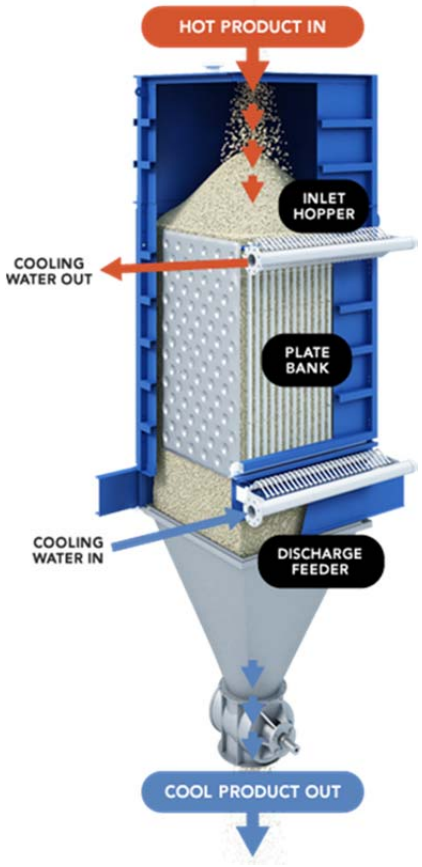

Figure 11. Solex Plate and Frame Heat Exchanger Diagram [23]

Figure 12. Solex Oil Seed Dryer

An example of how moving beds might be used for heat recovery is shown in Figure 13. In this example a heat transfer fluid is circulated between a separate moving-bed rich-sorbent heater and a moving-bed sorbent cooler. The heat exchanger surface area required is very dependent on the approach temperature, the temperature difference between the sorbent and heat transfer fluid, becoming larger as the approach temperature narrows. An option is to incorporate a separate heater and cooler in the heat exchanger fluid circuit. This may reduce the heat transfer surface area required and, thus, impact the overall costs.

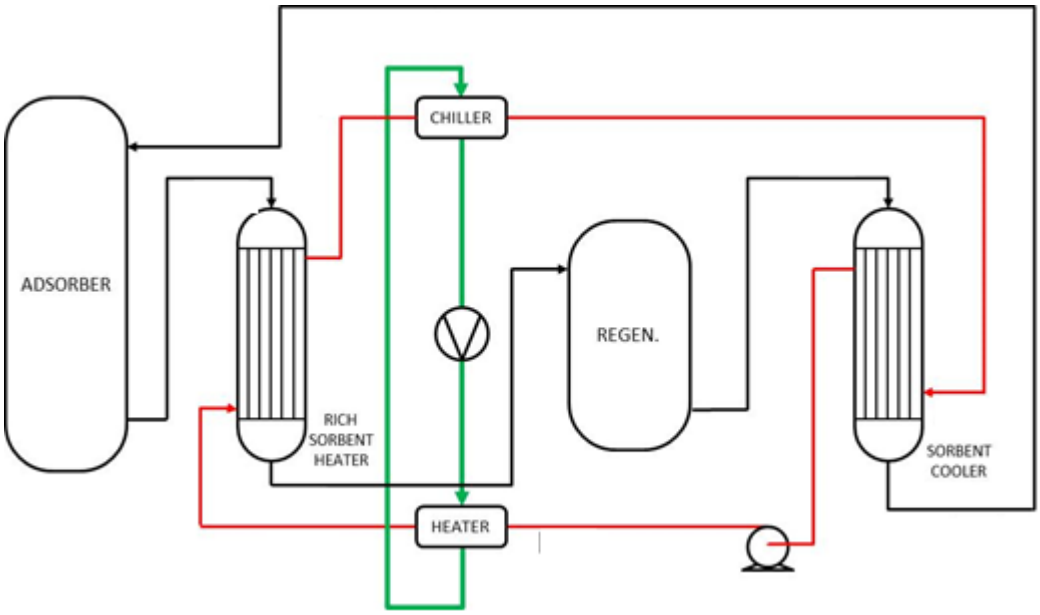

Figure 13. Sketch of Moving Beds used for Heat Recovery

2.4 Modeling

A team at the Energy Research Center at Lehigh University was contracted to independently build a process model of the ADAsorb™ capture process and integrate this model into an existing model of a supercritical PC power plant. The Lehigh model allowed process modifications to be evaluated independently and in combination with one another. Multiple models were built using different software. The primary combined process model was built using Aspen Plus software with individual components of the process built within Excel software for results verification.

Aspen Plus is the market-leading chemical process optimization software used by the bulk, fine, specialty, and biochemical industries, as well as the polymers industry for the design, operation, and optimization of safe, profitable manufacturing facilities. [24]

2.4.1 Steam Cycle

The supercritical steam cycle represented in Figure 14 was modified in Aspen Plus in such a way that the steam flow rate could be varied in order to meet a desired net electric power output. As the steam flow rate was varied, the heat duty on the boiler changed accordingly. Coal flow rate was then adjusted to

meet the condition where flue gas exits the economizer at 600°F. The air feed to the boiler was also adjusted to result in an O_2 mole-fraction of 3.5 vol% at the economizer exit. Air was assumed to leak into the boiler at a rate of 8 vol% of the flue gas flow rate, the air preheater seals are assumed to leak at a rate equal to 6 vol% of the flue gas mass flow rate, and the ductwork downstream of the air preheater is assumed to leak air into the duct at a rate equal to 5 vol% of the flue gas mass flow rate.

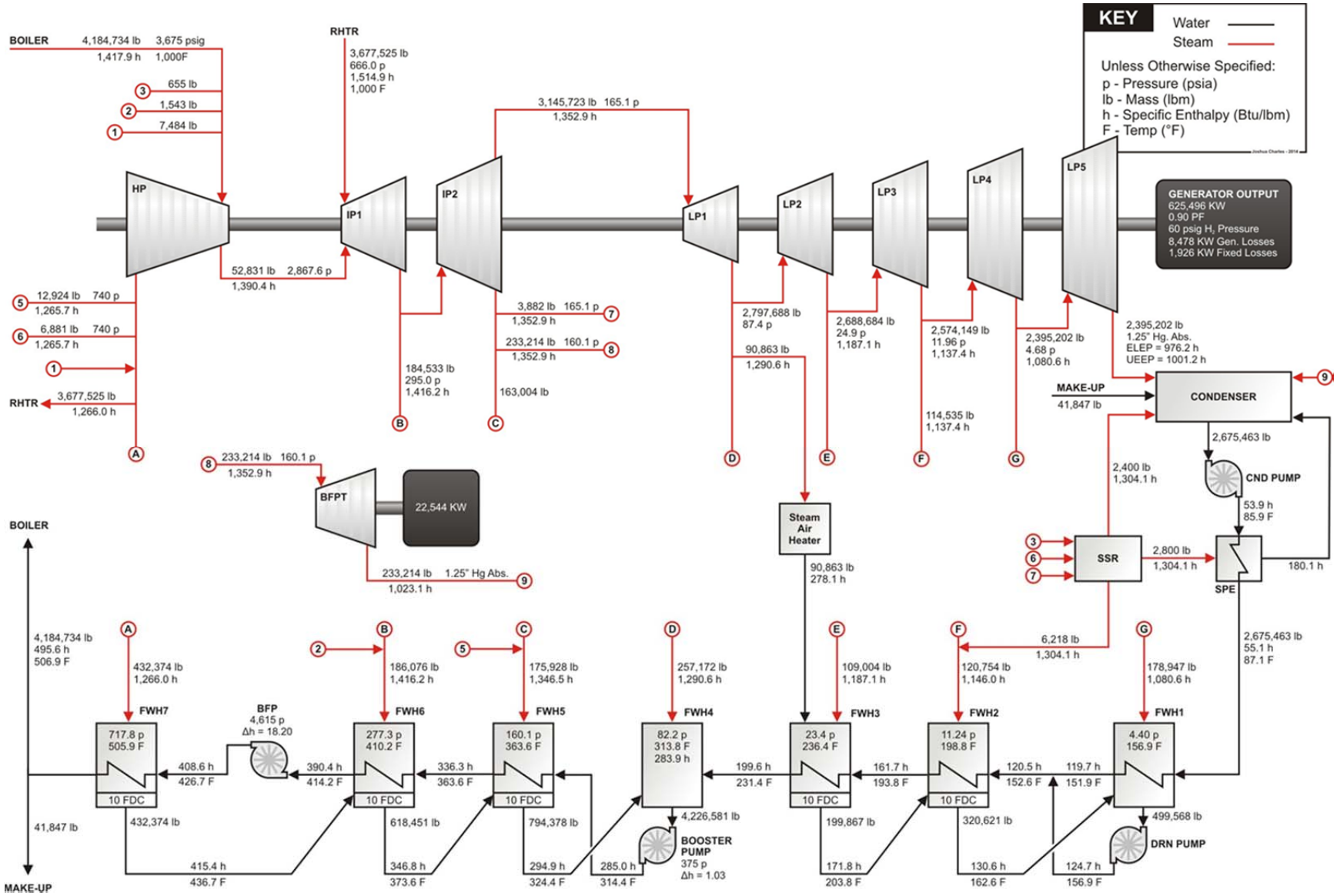

Figure 14. Supercritical Steam Cycle Used for Model Analyses [26]

2.4.2 Coal

The model was run using the three coals presented in Table 2. For each of the coals, net plant electric output was specified at 550 MW_{net}, while the steam and coal flow rates were allowed to vary accordingly.

Table 2. Coal Compositions used for Process Modeling [26]

Coal	Illinois #6	Powder River Basin	North Dakota Lignite
	AR Proximate Analysis (weight %)		
Fixed Carbon	44.19	32.98	21.87
Volatile Matter	34.99	32.17	27.33
Ash	9.70	6.31	12.30
HHV (Btu/lb)	11,666	8,426	6,406
	AR Ultimate Analysis (weight %)		
Moisture	11.12	28.09	38.50
Carbon	63.75	49.21	34.03
Hydrogen	4.50	3.51	2.97
Nitrogen	1.25	0.73	0.72
Chlorine	0.29	0.02	0.00
Sulfur	2.51	0.45	0.51
Ash	9.70	6.31	12.30
Oxygen	6.88	11.67	10.97

3 Design Program, Testing and Analysis

3.1 Task 1: Project Management and Planning

This task included the necessary activities to ensure coordination and planning of the project with DOE/NETL and other project participants. These activities include, but are not limited to, monitoring and controlling of the project scope, cost, schedule, and risk, and the submission and approval of required National Environmental Policy Act (NEPA) documentation, and preparation of all reports including quarterly technical reports and a comprehensive final report.

This task also included all work elements required to maintain and revise the Project Management Plan, and to manage and report on activities in accordance with the plan.

3.1.1 Project Organization, Structure, and Stakeholders

ADA developed an organizational structure to facilitate the performance of the tasks described in the Statement of Project Objectives. ADA managed all project efforts and oversaw all aspects of the project.

All other team members were subcontractors under the project. Two subcontractors, Solex Thermal Science (Solex) and Technip Stone and Webster (Technip), were chosen because of their expertise in moving and fluidized beds, respectively. Technip also led the detailed engineering efforts for the ADAsorb™ process development under DE-FE0004343. The Energy Research Center at Lehigh University provided an objective assessment of the technology options, developed a process model based on an ASPEN Plus model developed under DOE-FE0002146, and conducted optimization studies. The ADA Principal Investigator worked closely with the Project Managers and Technology Managers to assure that the Project Management Plan was executed on schedule and within budget. ADA has an active team of intellectual property experts who managed intellectual property developed during the project according to DOE regulations that apply to small businesses.

3.1.2 Briefings and Technical Presentations

ADA prepared detailed briefings for presentation to the Project Officer including:

- Project kick-off meeting.
- Update briefing to explain the plans, progress, and results of the technical effort.
- At least one briefing was given at a national conference each year.
- A final briefing will be given at DOE offices.

3.1.3 Risk Management

Risk management was planned and documented formally through a Risk Management Plan. The project manager obtained input from team members as well as stakeholders relative to the risks associated with the project. A risk register was used to record identified risks, their severity, and the actions steps to be taken. The process allowed quick identification of risks and their relative severity to the project. Resources were identified and assigned to mitigate risks. The register associated with the project can be found in the Appendix.

3.2 Task 2. Bench-Scale Testing and Technical Analysis of Heat Exchanger Designs

During this task, a cross heat exchanger operating in both a moving-bed regime and a fluidized bed regime were evaluated as potential options for reducing the overall energy penalty of a CO_2 capture process associated with sensible heating and cooling of the sorbent. Bench-scale results from fluidized bed testing are available through a separate DOE contract, DE-FE0004343. Bench-scale testing of a moving bed was conducted using Solex's bench scale testing apparatus. Analysis of both designs was conducted to determine the optimal amount of heat recovery and relative equipment size and costs. The sorbent used by ADA during 1 MWe pilot testing, sorbent BN, under DE-FE0004343 was used during bench-scale testing for consistency.

3.2.1 Subtask 2.1: Bench-Scale Testing of Moving Bed Heat Exchangers

Collecting experimental data at the bench-scale was the first step to analyzing performance of a moving bed heat exchanger in a PCCC application. The data collected focused on what must be known to complete the subsequent computational modeling efforts and techno-economic analysis. In order to accomplish this task, Solex's existing bench-scale moving bed test unit, shown in Figure 15, was operated in different configurations to collect key operating data for the sorbent being used in ADA's 1 MWe pilot, under DE-FE0004343. This sorbent, BN, was chosen for the experiments because it had been used for bench-scale fluidized bed experiments.

Figure 15. Solex Bench-Scale Heat Exchanger

The bench-scale moving bed related experiments were conducted in concert with various tools developed by Solex. Specific tests are described subsequently.

3.2.1.1 <u>Thermal Property Analysis</u>

Determining the thermal characteristics of a bulk solid material is critical for heat exchanger design. The two key variables that must be known to assess the behavior of a material in a moving bed for heat transfer are the thermal conductivity and the specific heat capacity. The thermal conductivity of a bulk solid is dependent on base material composition, size distribution and temperature. Since the thermal conductivity is sensitive to many variables, Solex measured this in its lab using an advanced hot wire

method. The specific heat capacity of the sorbent under investigation has already been measured under a separate DOE program, but was confirmed by Solex during bench-scale testing.

3.2.1.2 Flowability

Flowability testing determines the optimum heat exchanger plate spacing to ensure that the material will flow without bridging or blocking. This test work was carried out in a transparent test chamber fitted with heat exchanger plates, seen in Figure 16. The material flow pattern was observed at various plate spaces to determine the critical clear space required between the plates.

Flowability testing was conducted under cold flow conditions to determine if the material would bridge in tight plate spacing. Initial testing results were very promising and displayed excellent handling characteristics that facilitated tight plate spacing to maximize heat transfer surface area for a given heat exchanger structure size.

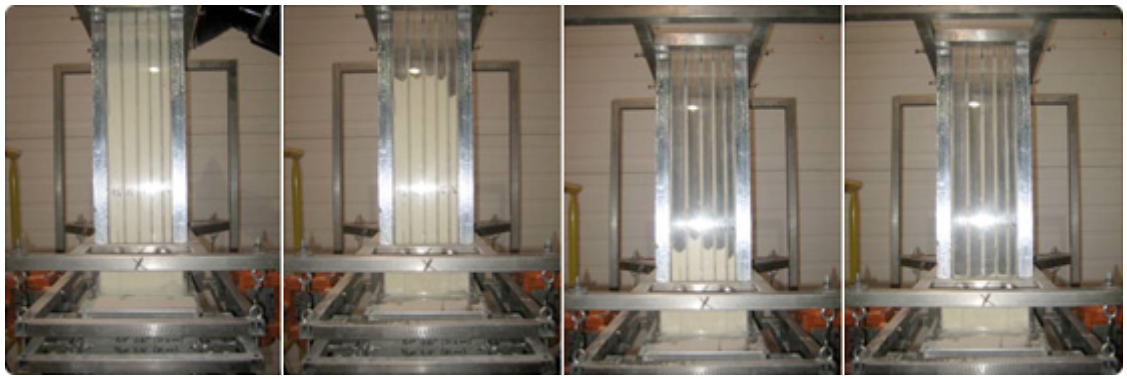

Figure 16. Solex Bench-Scale Moving Test Bed setup to Measure Flowability

3.2.1.3 Mass Flow Testing

Mass flow testing was carried out to observe material flow characteristics and ensure that uniform velocity of the sorbent could be obtained in the moving bed, particularly in a mass flow discharge hopper, if it were used to make up the cross heat exchanger. Again, initial tests suggested excellent handling characteristics, indicating that a moving bed heat exchanger could be a viable option for this particular sorbent based on material handling.

3.2.1.4 Performance at Simulated Process Conditions

Due to the success of the initial testing, which used a dry sorbent at room temperature that was not representative of actual process conditions, further testing was warranted. In order to examine process conditions and loaded sorbent, the bench scale heat exchanger was shipped to ADA's facilities in Highlands Ranch, CO for testing at simulated process conditions.

At ADA's facilities, Solex's bench scale heat exchanger was connected to ADA's cold flow model of the top two stages of the ADAsorb™ adsorber. This model features a scale representation of the top bed of the three adsorber beds in the ADAsorb™ process where hot sorbent from the regenerator is cooled

from 248^{o} F to 104^{o} F. It also features a second bed that is a scale model of the identical bottom two beds of the ADAsorb™ facility. The cold flow model also contains cooling coils, installed so that it may be modified as a reacting flow model. This setup allowed the model to function as an adsorber so that sorbent laden with CO_2 and H_2O could be introduced to the Solex heat exchanger for simulated process conditions testing.

The experimental setup was plumbed together, as seen in Figure 17, so that sorbent could be pneumatically conveyed from the adsorption beds into the Solex plate and frame heat exchanger. CO_2 and moisture were introduced to the fluidizing gas for the adsorption beds to provide similar gas conditions to pilot and commercial applications. A concern existed that the sorbent that had adsorbed CO_2 and moisture may exhibit different handling characteristics than sorbent which had only been exposed to an ambient environment.

In addition, the Solex heat exchanger was equipped with an oil heater that could circulate hot oil as a working fluid through the plates in the heat exchanger. This allowed the heat exchanger to test the sorbent for flowability across all ranges of projected operation temperatures and gather useful information for Solex's design purposes.

After the experimental setup was completed, a series of bench-scale tests were conducted to determine the potential performance of the heat exchanger at conditions simulating expected process conditions at full-scale. Testing included examination of critical process data that Solex deemed necessary to engineer a solution for the cross heat exchanger scaled to a 550 MW_{net} application. After testing, Solex interpreted the data and initiated their modeling efforts.

Figure 17. Moving Bed Heat Exchanger Connected to the ADA Cold Flow Model, Modified to Simulate Process Conditions.

3.2.2 Subtask 2.2: Computational Modeling and Design Integration of Moving-Bed Heat Exchangers

Solex developed their initial heat exchanger design over 20 years ago and has developed ThermaPro, a proprietary Solex Thermal Modeling Software Program, to characterize performance of their designs. Indirect heat transfer in bulk solids follows a conduction model that is defined by a Fourier series. This conduction model, in a modified form to take into account variations in fluid-side temperatures, is engineered into ThermaPro. ThermaPro enables Solex to provide its customers with guaranteed thermal performance and accurate predictions of product temperatures. The software performs detailed thermal calculations based on inputs of key process and material parameters, including:

- Product flow rate;
- Product temperature;
- Heat transfer media temperature;
- Material bulk density;
- Material specific heat;

- Thermal conductivity;
- Heat exchanger plate spacing.

ThermaPro enables accurate modeling of the following:

- Steam systems;
- Multiple heat exchanger banks;
- Co-current and counter-current flow of heat transfer media;
- Heating and cooling loads.

Preliminary modeling was carried out to establish basic viability of the cross heat exchanger concept. Figure 18 shows an example of the solids and heat exchanger fluid temperature for the cooler with a 20°C (68°F) approach temperature between the solid stream and the fluid stream. For this example, there were four banks of heat exchanger plates stacked vertically. It was observed that the sorbent could be cooled from 120°C (248°F) to 40°C (104°C) using moving beds as cross heat exchangers.

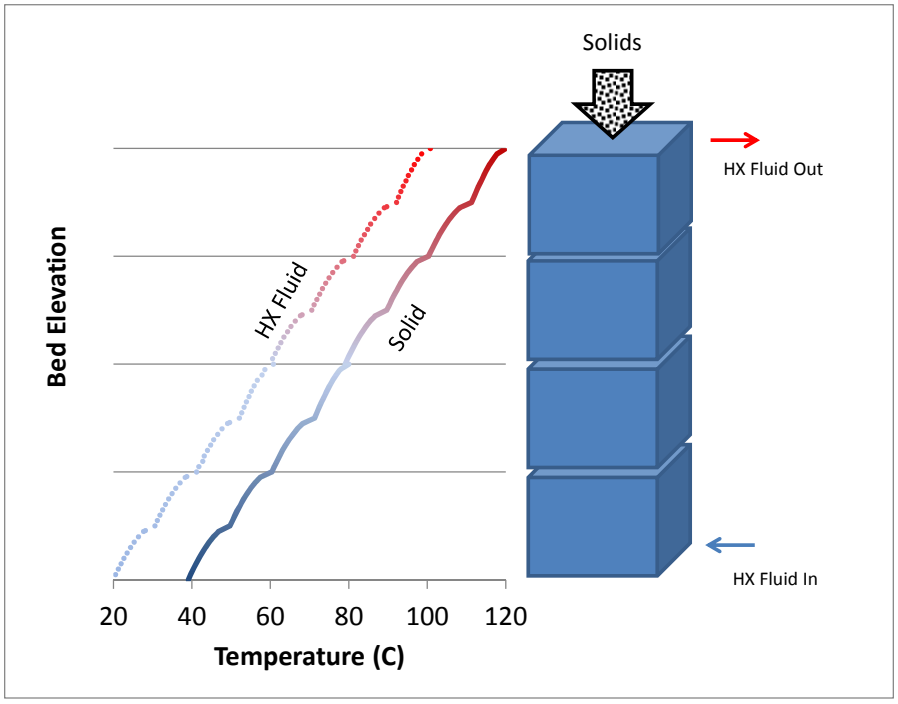

Figure 18. Initial ThermaPro Model of Solex Heat Exchanger and ADAsorb™

Data from the bench scale testing was analyzed by Solex once the simulated process condition testing was completed. These data provided the necessary inputs for the ThermaPro modeling effort. Results of the modeling allowed Solex to determine equipment size and configuration for the full scale 550 MW_{net} application. ADA, Solex, and Lehigh then collaborated on integrating the finalized design into the Lehigh process model.

3.2.3 Subtask 2.3: Design Integration of Fluidized Bed Heat Exchangers

The data collected during previous bench-scale testing under a separate project, DE-FE0004343, were used to evaluate how fluidized beds could be employed to accomplish heat transfer between hot and cool sorbent.

One of the most challenging aspects of integrating fluidized bed heat exchangers into the ADAsorb™ process included evaluating the appropriate CO_2 partial pressure of the fluidization gas to minimize any negative impacts on the working capacity of the sorbent. For example, in the ADAsorb™ process, CO_2 product is used to fluidize the sorbent in the regenerator. If high partial pressure CO_2 was utilized in the sorbent cooler, as the sorbent cooled it would begin to adsorb the CO_2, which is undesirable as the effective CO_2 working capacity would be decreased. If CO_2 lean gas were used for fluidization some of the CO_2 still adsorbed after regeneration could be released based on the equilibrium loading at the lower CO_2 partial pressure causing captured CO_2 to be released into the flue gas.

Therefore, detailed analysis was required to determine the process gas that should be used for fluidization in the heat recovery heat exchangers. In addition, the optimal CO_2 partial pressure for fluidizing the sorbent in the heat exchangers is also related to the operating temperature, which must be optimized based on overall economics. ADA and Technip collaborated on this difficult design problem.

Ultimately, a system with multiple fluidization gas streams was examined and modeled to determine the impact on process performance. The heat exchanger reduced 372 MMBtu/hr of sensible heat duty in the regenerator for an additional net 28,000 hp of electrical load requirements for fluidizing gas blowers and additional water circulation. There was some reduction in horsepower requirements for the adsorber blower, but it was more than offset by new requirements.

It was then necessary to determine whether the sensible heat saving outweighed the additional electrical load requirements. In order to do that, a simple modeling exercise was conducted. It is assumed that the steam entering the regenerator must be approximately 154°C (310°F) to maintain a regenerator temperature of 140°C (248 °F). Furthermore, at 154°C, a temperature change of +/- 5.5°C does not really impact the specific enthalpy of the steam very much so even if the temperature fluctuates, this remains a reasonable assumption.

In the ADAsorb™ regenerator design, the latent heat of the steam is the primary energy used to drive the thermal load for heating and regenerating the sorbent. At 154°C, the change in enthalpy from saturated steam to water is 903 Btu/lb of steam. As a result, an additional ~412,000 lb/hr of steam at 154°C would be saved if a cross heat exchanger were incorporated that recovered 372 MMBtu/hr sensible heat duty.

The reduced steam load was converted to equivalent electrical energy to compare with the additional fan power required to fluidize the bed that resulted in the steam load savings. The enthalpy of the steam at 154°C and 77 psia is about 1183 Btu/lb and the enthalpy of steam at 2 psia at the outlet of a steam turbine at 52°C (126°F) is about 1116 Btu/lb, so the difference is only 67 Btu/lb. Assuming that

the steam withdrawn at 154°C were allowed to continue to pass through the turbine at 85% efficiency, that steam would produce 9,200 hp worth of electrical energy.

The fluidized bed heat exchanger design requires an additional 28,000 hp of electrical load to provide power to the blowers. Thus, the additional electrical load required to overcome the additional pressure drop required for fluidization in this heat exchanger deign is three times the amount of sensible heat duty saved in the regenerator. Although this analysis is not strictly accurate as the steam for the regenerator is not likely to be withdrawn from a turbine at a saturated condition, it is sufficient to determine a first approximation of in the additional electrical energy consumed to operate the blowers is three times the thermal energy saved. This first-order estimate resulted in a decision to cease any ongoing efforts to integrate a fluidized bed heat exchanger into the process.

3.3 Task 3: Heat Integration and Optimization

During this task, Lehigh's process model of a supercritical PC power plant was used to compute baselines for the three coals described in Table 2. The results for these three coals without CO_2 capture can be seen in Table 3.

A process model of the ADAsorb™ CO_2 capture process was then developed and integrated into the PC plant model. The model was subsequently systematically modified to evaluate the effects on the integrated capture process energy requirements. Initial equipment costs were calculated for the necessary equipment to implement the modeled modifications. Several potential process modifications were evaluated and optimized, including:

- Heat integration;
    - Cross heat exchanger for heat recovery applied:
        - Between the CO_2 capture process and the power plant;
        - Between the CO_2 compression system and the CO_2 capture process;
        - Between the CO_2 compression system and the power plant;
- Moisture of incoming flue gas;
    - The energy penalty and economics of reducing the incoming flue gas moisture content was evaluated;
- Adsorber design;
    - The design was evaluated to determine if the pressure drop could be reduced;
    - The vessel temperature was optimized for varying coals;
- Regenerator vessel temperature was optimized for varying coals;
- CO_2 compression system discharge pressure.

Table 3. BASE PC Plant Aspen Model Results without CO_2 Capture[26]

		Illinois #6	PRB	ND Lignite
Generator Power	MW	581	578	580
TC Net Power	MW	574	571	573
Net Power$_e$	MW	550	550	550
Cond. Pump Power	kW	263	262	263
Drain Pump Power	kW	62	62	62
Boost Pump Power	kW	1,264	1,258	1,262
Cond. Circ. Pump Power	kW	5,078	5,056	5,073
TC Pump Pow.	kW	6,667	6,637	6,659
Main Steam Flow	lb/hr	3,882,313	3,865,288	3,878,071
Main Steam Q	Btu/hr	3.574E+09	3.559E+09	3.570E+09
Reheat Steam Q	Btu/hr	8.608E+08	8.570E+08	8.599E+08
TC Q	Btu/hr	4.435E+09	4.416E+09	4.430E+09
TCHR	Btu/kWh	7,728	7,728	7,728
FD Fan Power	kW	1,784	1,895	1,841
PA Fan Power	kW	2,724	2,893	2,811
ID Fan Power	kW	7,338	7,315	7,566
Total Fan Power	kW	11,846	12,103	12,218
Mill Power	kW	2,200	3,145	4,289
ESP Power	kW	663	734	752
FGD Power	kW	6,225	2,426	3,056
Other Aux Power	kW	3,007	2,994	3,004
Total SS Power	kW	30,607	28,040	29,979
Coal Flow	lb/hr	415,651	594,347	810,377
Coal HHV	Btu/lb	11,666	8,426	6,406
Coal Q (Combustion)	Btu/hr	4,849,147,920	5,007,790,350	5,191,144,760
Boiler Efficiency	%	91.5	88.2	85.3
Unit Heatrate	Btu/kWh	8,817	9,105	9,439
Unit Efficiency	%	38.7	37.5	36.2

3.3.1 Subtask 3.3.1: Assess Costs of Heat Integration

During the cross heat exchanger design process, the best locations for the components of a fixed bed cross heat exchanger, the required sizes, and the necessary heat transfer surface area for different approach temperatures were verified independently. The next step was to investigate if the use of the

cross heat exchanger could lead to a reduction in the energy penalty. The heat exchanger design concept assumed a heat transfer medium will be circulated between two or more heat exchangers to transfer heat from the hot sorbent stream leaving the stripper to the cold sorbent stream leaving the adsorber.

Heat exchanger effectiveness was used to express the performance of the cross heat exchanger system. At a cross heat exchanger effectiveness of 1, the sorbent stream returning to the adsorber is cooled to the adsorber operating temperature, while the sorbent going to the regenerator is heated accordingly with no system losses. Figure 19 and Table 4 present the results of the modeled cross heat exchanger over a range of heat exchanger effectiveness levels from zero (no exchange) to 1 (no losses).

The results from modeling indicate that addition of a cross heat exchanger would improve the heat rate of a power plant that incorporated the ADAsorb™ CO_2 capture system. It is also clear that the actual operating effectiveness of any proposed cross heat exchanger design is crucial with regard to its positive impact on the plant. As the effectiveness approaches 1, net unit heat rate is suggested to decrease by 12.0% to 14.4% depending on the coal.

To express the ADAsorb™ CO_2 capture system parasitic power load one must consider the electric power which it utilizes in combination with the electric power which the host plant cannot generate due to the extraction of low pressure steam for sorbent heating. Figure 19 and Table 4 also illustrate the parasitic power load of the ADAsorb™ CO_2 capture system utilizing a cross heat exchanger of different effectiveness levels.

Table 4. Effect of a Cross Heat Exchanger on Net Unit Heat Rate and Parasitic Power[26]

	Illinois #6		PRB		ND Lignite	
XHTX Effectiveness	Net Unit HR [Btu/kWh]					
0	13,356	ΔHR	14,854	ΔHR	15,232	ΔHR
0.25	12,958	-3.0%	14,307	-3.7%	14,687	-3.6%
0.5	12,551	-6.0%	13,768	-7.3%	14,149	-7.1%
0.75	12,151	-9.0%	13,232	-10.9%	13,617	-10.6%
1	11,749	-12.0%	12,709	-14.4%	13,096	-14.0%
XHTX Effectiveness	Parasitic Power [MW]					
0	290	ΔPP	355	ΔPP	345	ΔPP
0.25	264	-8.9%	321	-9.6%	312	-9.5%
0.5	238	-17.9%	287	-19.1%	280	-18.8%
0.75	212	-26.8%	254	-28.4%	248	-28.1%
1	186	-35.7%	222	-37.6%	217	-37.2%

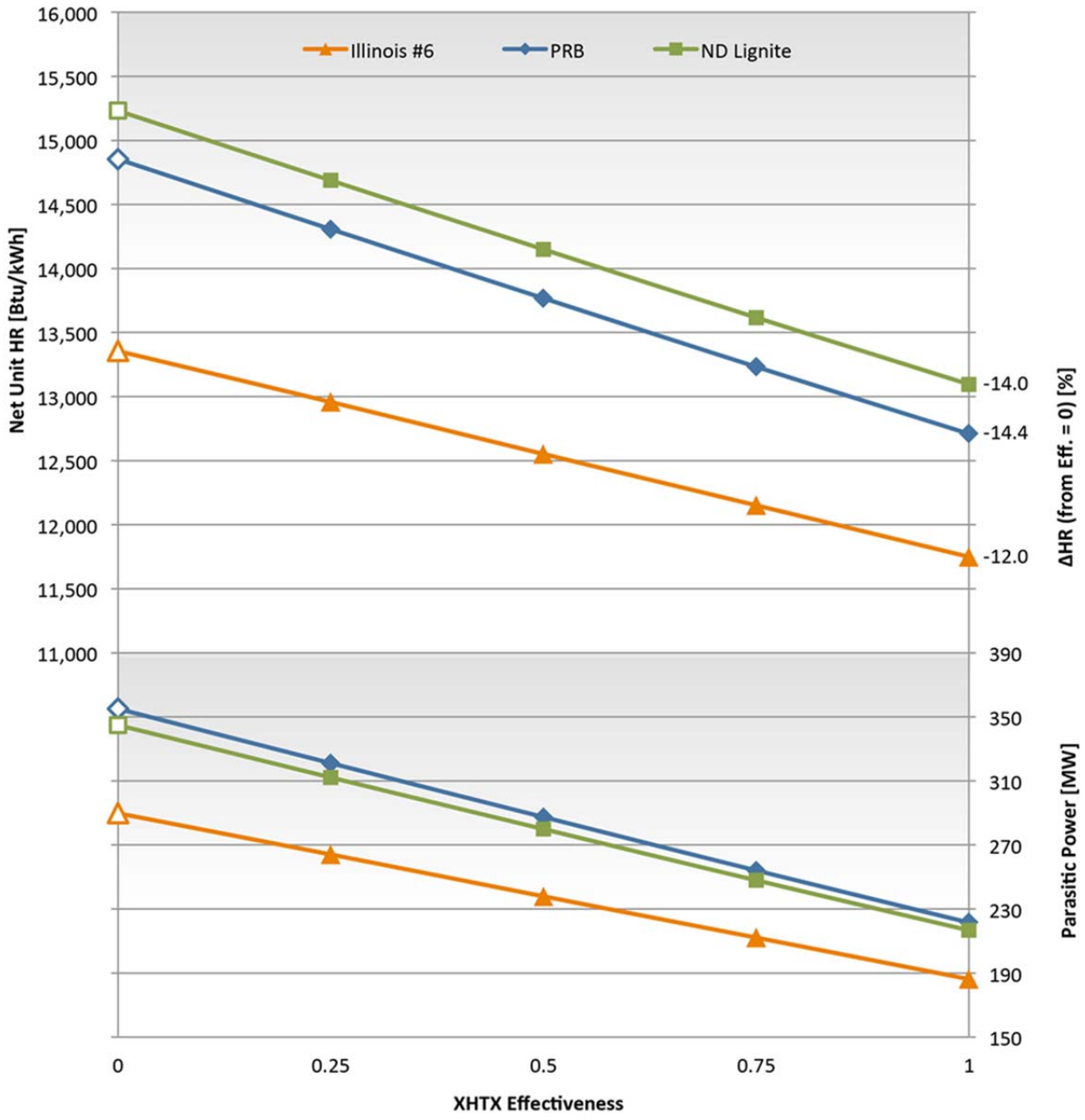

Figure 19. Effect of a Cross Heat Exchanger on Net Unit Heat Rate and Parasitic Power[26]

A breakdown of the parasitic power of the CO_2 capture system for cross heat exchanger (XHTX) effectiveness values between 0 and 1 for the case of the Illinois #6 bituminous coal is presented in Figure 20. As shown, the largest contributor to parasitic power is lost electrical generation, followed by compression power and the blower or fan power. Pump and refrigeration power only account for a small percentage of the total parasitic power. Figure 20 also shows that the addition of a cross heat exchanger primarily decreases the overall parasitic power through decreasing the lost electrical generation. The reason for this is that the cross heat exchanger adds heat to the rich sorbent stream

that otherwise would come from the low pressure (LP) steam. Blower power is slightly reduced by the use of a cross heat exchanger as fewer cooling water tubes are required in the top adsorber bed, resulting in a shallower bed and lower bed pressure drop. As system parasitic power is reduced, overall unit efficiency increases, decreasing the coal flow rate, which results in a lower CO_2 flow rate for a $550MW_{net}$ plant. A lower CO_2 flow rate further reduces the capture demand on the ADAsorb^{TM} CO_2 capture system, resulting in lower parasitic power for each component of the capture and compression system.

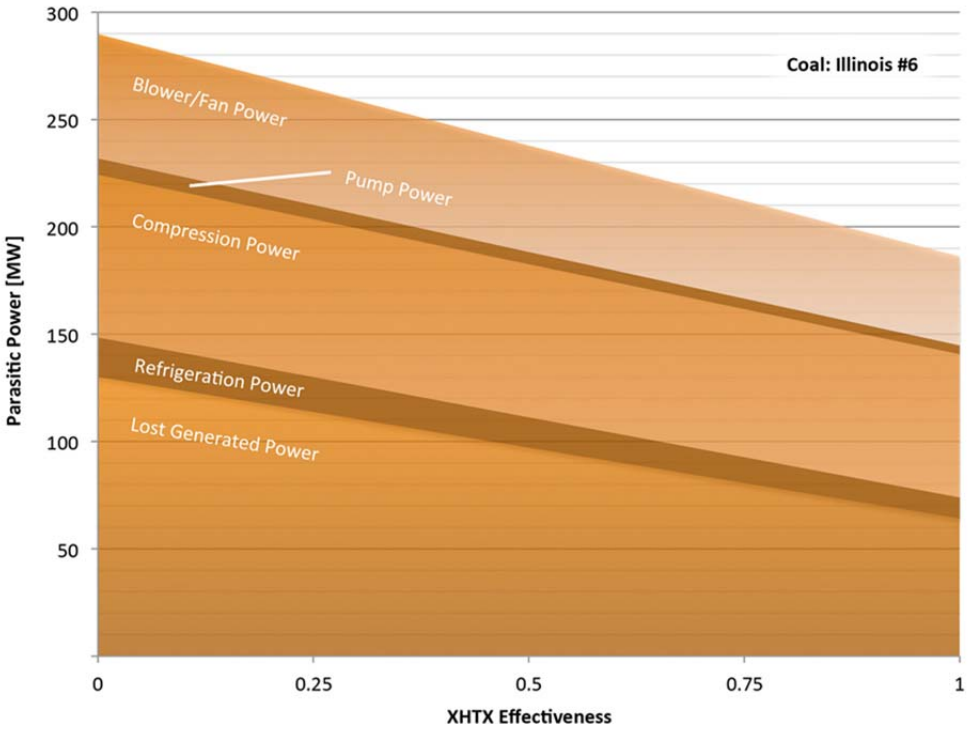

Figure 20. Parasitic Power Breakdown vs. Cross Heat Exchanger Effectiveness [26]

The capital cost of the heat exchangers varies depending on the amount of heat recovered and the approach temperature. Of course, for heat integration to be employed, the cost reduction from the decrease in energy penalty must be larger than the additional equipment costs. During this subtask, 3.3.1, an equipment cost analysis for a full-scale system as a function of heat recovery was developed for a moving bed system for several different potential approach temperatures for each design. As explained in Section 3.2.3, the fluidized bed heat exchanger concept was determined not to be an effective solution, so it was not modeled.

Following the technical assessment, a sensitivity analysis of the estimated additional equipment capital cost associated with heat recovery was incorporated into the techno-economic assessment to determine the break-even increase in capital costs compared to the reduction in operating costs associated with heat recovery.

A significant quantity of heat is rejected from both the flue gas cooler upstream of the adsorber and the CO_2 compressors. It was determined that the quality of this heat was sufficient to accomplish heating of boiler combustion air, steam cycle feedwater, and the cold CO_2 rich sorbent entering the regenerator. The examined sources and sinks of heat outside of a cross heat exchanger are illustrated in Figure 21. The capital costs related to providing this heat to the CO_2 capture process as well as areas of the power plant and the energy penalty savings were quantified.

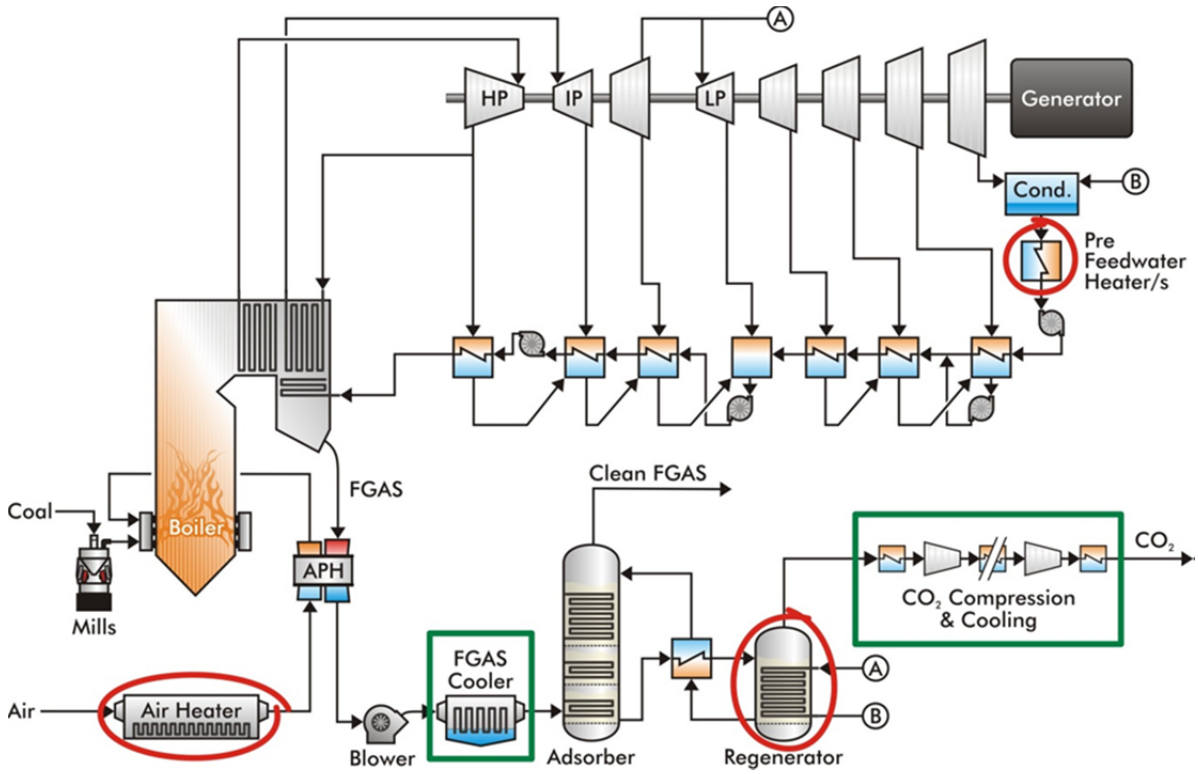

Figure 21. Sources and Possible Destinations for Capture Waste Heat. (Thermal Sources in Green Rectangles and Sinks in Red Ellipses) [26]

The following five heat integration cases were examined in depth for two different sorbents, sorbent BN and sorbent OJ, using the developed model:

- HI REG – Heat from the compressors used to heat sorbent entering the regenerator
- HI FWH – Heat from the compressors used to heat steam cycle feedwater
- HI FG AIR – Heat from the flue gas cooler used to heat boiler combustion air
- HI FG FWH – Heat from the flue gas cooler used to heat steam cycle feedwater
- XHTX 0.75 eff – Cross heat exchanger with a 75% effectiveness
- OPTI – Case without a cross heat exchanger or heat integration at optimal adsorber and regenerator operating temperatures

Combinations of these four cases were also analyzed. For instance, HI ALL is a case where all four heat integration cases are examined simultaneously.

**Figure 22 clearly shows that every cross heat exchanger and/or heat integration option considered resulted in a reduction in net unit heat rate relative to the CO_2 capture process omitting potential temperature improvements (OPTI) case. The best-performing case is the cross heat exchanger of 75% efficiency combined with all other modifications (XHTX 0.75 eff. & HI ALL) configuration, which results in a 13.01% reduction in net unit heat rate for the BN sorbent and a 3.39% reduction in net unit heat rate (HR), from the OPTI case, for the OJ sorbent. The case with the smallest heat rate improvement is the case in which heat from the flue gas cooler is used to heat steam cycle feedwater (HI FG FWR), which only reduces net unit heat rate by 0.46% for the BN sorbent and 0.36% for the OJ sorbent. The reason for the small performance improvement for this case is the low quantity of low quality heat, which is available from the flue gas cooler for feedwater heating. Cases utilizing compressor heat for regenerator and/or feedwater heating perform better, with heat rate reductions between 3.3% and 6.7% for the BN sorbent and 1% and 1.5% for the OJ sorbent.

If the OJ sorbent is used instead of the BN sorbent, net unit heat rate is reduced by between 10% and 17%. This reduction is partially due to a reduction in the sorbent flow rate due to higher CO_2 loading capacity of the OJ sorbent. A lower sorbent flow rate reduces the energy needed to heat and cool the sorbent in the regenerator and adsorber. Another factor promoting the enhanced thermodynamic performance of the OJ sorbent is the optimal operating temperatures of the adsorber and regenerator. For the BN sorbent, optimal adsorber and regenerator temperatures of 40°C (104°F) and 120°C (248°F) respectively were found. However, for the OJ sorbent, optimal adsorber and regenerator temperatures were found to be 38°C (100°F) and 59°C (140°F) respectively. With a lower temperature difference between the adsorber and regenerator, heating and cooling demands by the sorbent in the adsorber and regenerator are further reduced.

A more comprehensive discussion of all heat exchange cost options as well as all plant costs and contributions to LCOE are included in "*Thermo-Economic Analysis of ADA Solid Sorbent CO_2 Capture System: Effects of Sorbent Properties and Waste Heat*" in the Appendix.

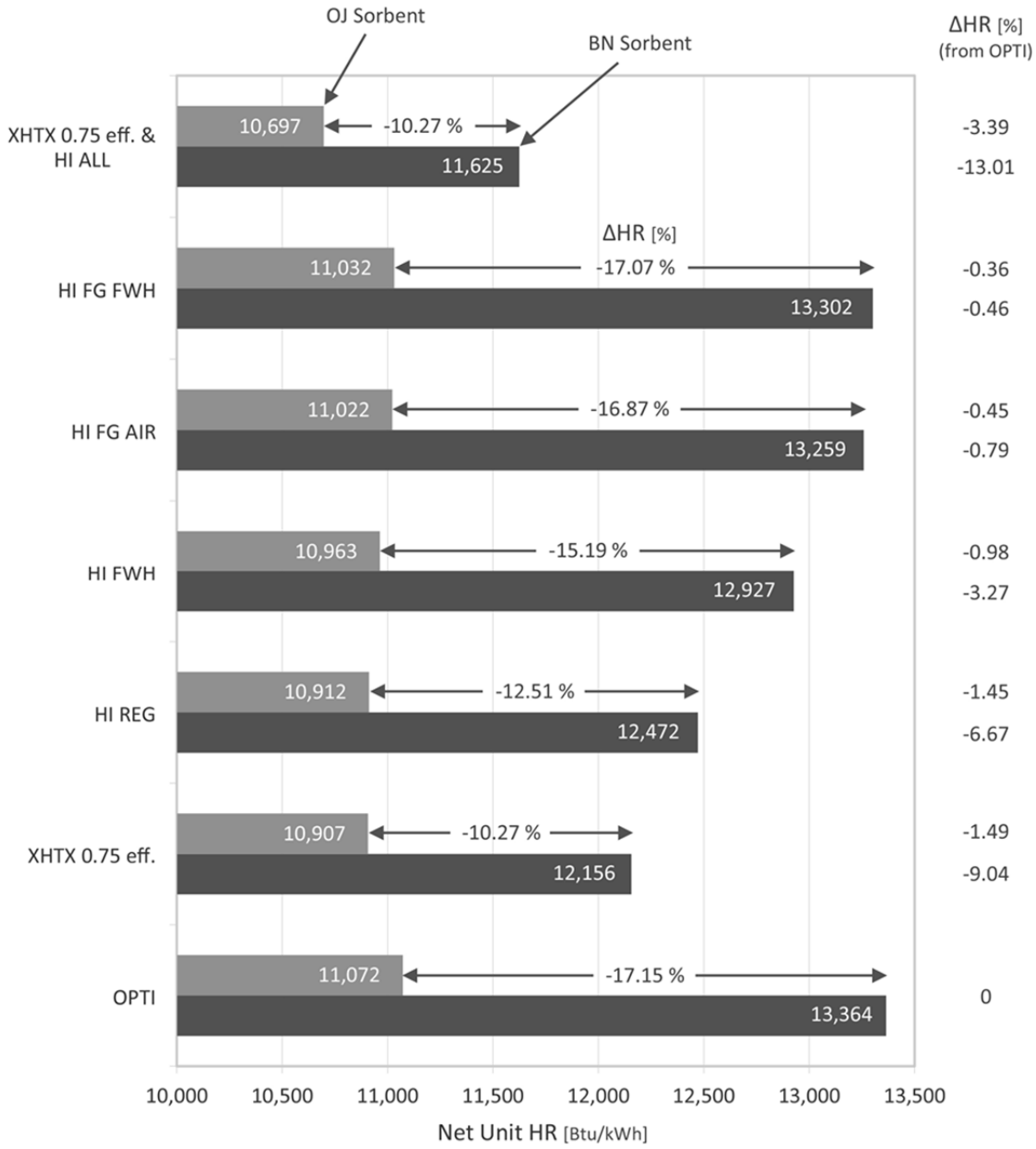

Figure 22. Net Unit Heat Rate for Both Sorbents & for Cross Heat Exchanger & Heat Integration Cases using an Illinois #6 coal[28]

3.3.2 Subtask 3.3.2: Assess Impacts of Flue Gas Moisture

The solid sorbent utilized in the ADAsorb™ pilot, sorbent BN, is known to adsorb moisture as well as CO_2. Investigation of the sorption of moisture by to the CO_2 sorbent within the ADAsorb™ process is of interest as varying the moisture uptake has an effect on the system efficiency.

The impacts of flue gas moisture uptake on the sorbent turned out to be significant for sorbent BN. Sorbent BN's design working capacity, the delta loading between adsorption and regeneration, was measured to be 7% by weight for CO_2 and 0.9% by weight for H_2O. If the sorbent could be made to not adsorb water, the net plant heat rate for Illinois #6 coal would be reduced by 5.7%, for PRB coal the reduction is 6.9%, and for North Dakota Lignite, the reduction is 6.6%. A summary of these results can be seen in Table 5. These reductions are largely due to increased CO_2 sorption, decreased regenerator heat requirements, and decreased mass flow into the CO_2 compression system. This indicates that moisture adsorbed by the sorbent should be minimized to increase the net power plant efficiency. It also indicates that based on the size of the possible reductions, that this should clearly be a development priority and that sorbents which adsorb more than 1-2% moisture by weight are unlikely to be cost competitive unless they have an extremely high CO_2 working capacity that well exceeds 15% by weight. Additional information and detail of this sensitivity analysis and impact of sorbent moisture can be found in Lehigh's appended report "*Aspen Plus Modeling of ADA Solid Sorbent* CO_2 *Capture System*".

Table 5. Impact of Water Adsorption Multiplier on Net Unit Heat Rate and Sorbent Flow Rate for Sorbent BN[26]

	Illinois #6		PRB		ND Lignite	
Water Multiplier	Net Unit HR [Btu/kWh]					
0	12,595	-5.7%	13,836	-6.9%	14,223	-6.6%
0.25	12,792	-4.2%	14,098	-5.1%	14,481	-4.9%
0.5	12,978	-2.8%	14,348	-3.4%	14,728	-3.3%
0.75	13,165	-1.4%	14,602	-1.7%	14,978	-1.7%
1	13,358	-	14,855	-	15,233	-
1.25	13,477	0.9%	14,997	1.0%	15,382	1.0%
1.5	13,521	1.2%	15,051	1.3%	15,438	1.3%
Water Multiplier	Sorbent Flow Rate [Mlb/hr]					
0	16.7	-22.6%	19.4	-23.0%	18.3	-23.1%
0.25	17.8	-17.5%	20.8	-17.7%	19.6	-17.8%
0.5	19.0	-11.9%	22.2	-12.0%	20.9	-12.1%
0.75	20.3	-5.9%	23.8	-5.8%	22.4	-5.9%
1	21.5	-	25.3	-	23.8	-
1.25	22.2	3.2%	26.0	3.0%	24.6	3.1%
1.5	22.5	4.6%	26.4	4.4%	24.9	4.6%

Using the process model and fundamental heat and mass transfer analyses, simulations were performed for a 550 MW_{net} coal fired power plant to estimate heat exchanger surface areas, and power needs for refrigeration systems and water capture energy costs for different flue gas moisture levels entering the CO_2 adsorber. Not surprisingly, this investigation led to the conclusion that the temperature and pressure of the gas entering the adsorber dominate the energetic and fiscal costs associated with moisture removal and flue gas cooling. The concentration of the water vapor will be at the saturation point entering the adsorber since it has to be cooled below the saturation point of an upstream wet flue gas desulfurization unit, the impact of moisture will be a function of either sorbent moisture uptake or flue gas cooling.

For flue gas cooling, an example case looking at PRB coal determined the power requirement of the cooling system as a function of flue gas outlet temperature, which is directly correlated to moisture content, at various flue gas flow rates is shown in Table 6. The capital costs for the same conditions are shown in Table 7. In both cases, the increase in flue gas flow rate has a dramatic increase in both energy cost and capital cost requirements. This highlights the need to have an efficient plant with a high heat rate to minimize flue gas production per unit electrical output.

Interestingly, with a fixed cooling system outlet temperature when the mass flow rate of flue gas is varied from 7,343,850 to 10,634586 lb/hr a two- to three-fold increase is noted for power requirements while, the capital cost is relatively insensitive to the choice in flow rate.

Table 6. Total Power Needed of Flue Gas Cooling System with Refrigeration System[27]

Mass Flow of Flue Gas (lbs/hr)	Outlet Temperture (°F)				
	100	104	110	120	130
	Total Power Requirement (MW)				
10,634,586	31.41	28.16	32.16	17.91	12.04
9,561,430	23.53	21.42	19.29	12.82	895
8,452,640	16.32	16.47	13.54	9.58	7.07
7,343,850	11.02	10.14	8.44	6.38	7.56
Note: inlet temperature and pressure; 219°F, 21.7psia					

Table 7. Installed Capital Costs of Flue Gas Cooling System with Refrigeration System[27]

Mass Flow of Flue Gas (lbs/hr)	Outlet Temperture (°F)				
	100	104	110	120	130
	Cost (Million $)				
10,634,586	16.68	14.82	12.98	9.27	7.42
9,561,430	14.82	12.98	11.12	9.27	7.42
8,452,640	14.82	12.98	11.12	9.27	7.43
7,343,850	14.82	12.99	11.12	9.29	5.56
Note: inlet temperature and pressure; 219°F, 21.7psia					

Extensive discussion of the design requirements, power requirements, and cost justification can be found in the appended report, *"Investigation on Flue Gas & Condensing Heat Exchanger (CHX) Cooling Water Cooling Processes and CHX Design*" by Lehigh University. Additional discussion of the cost benefits of this system and all other power plant systems are also discussed in section 3.3.4.

3.3.3 Subtask 3.3.3: Assess Impacts to System Pressure Drop

The flue gas booster fan upstream of the adsorber contributes to a large portion of the heat rate penalty to the plant due to the PCCC system. Results from Lehigh's modeling presented in Table 8 suggest that around a third of the heat rate impact of the ADAsorb^{TM} CO_2 capture system is due to this added fan power. The purpose of this fan is to overcome the pressure drop through the system of which the main contributor is the pressure drop within the fluidized beds in the adsorber. Reducing the pressure drop through the adsorber beds, most likely due to a reduction in bed depth, should result in a reduction in fan power. Two models were completed with the overall pressure drop being manually reduced by 1 psia and then by 2 psia.

Because the top bed of the adsorber is the deepest, the modeled pressure drop is more than twice as large as that of either of the lower beds. Therefore, for the 1 psia reduction in pressure drop model, the

pressure drop across this top bed section was simply reduced by 1 psia, which resulted in a 1 psia reduction in fan discharge pressure. For the case with a 2 psia reduction in pressure drop, each of the beds was given equal pressure drop reductions. Table 8 presents the plant results for these models.

It is interesting that for the 1 and 2 psia reduction in adsorber pressure drop, unit heat rate drops by 0.5% and 1.1% respectively. The reason for this is that booster fan power is reduced from 51 MW to 44 MW and 37 MW respectively. Such a significant reduction in fan power should result in a larger reduction in net unit heat rate, but it appears that a reduction in adsorber pressure drop negatively affects the CO_2 adsorption characteristics as the partial pressure of CO_2 is reduced in the adsorber. This lowers the equilibrium loading potential of the sorbent and effectively reduces its working capacity necessitating a higher sorbent recirculation rate. For each 1 psia reduction in adsorber pressure drop, the sorbent flow rate corresponding to 90% CO_2 capture increases by approximately 1,000,000 lb/hr. This results in a larger regenerator duty, extraction steam flow, increasing the turbine cycle heat rate. It is understood that as the fluidizing gas pressure is reduced, the partial pressure of the CO_2 is proportionally reduced. By looking at the 40°C (104°F) CO_2 loading curve in Figure 5, it can be easily deduced that a lower partial pressure of CO_2 will result in a lower loading of CO_2 on the sorbent, thus the requirement for a larger sorbent flow rate. As more sorbent is circulated through the system, the sensible heat loads associated with the heating and cooling of the sorbent will increase.

Table 8. Plant Model with ADA Capture – Pressure Drop Results (Illinois #6 – NETL / IG-1 Compressor)

Case		BASE (no Cap.)	ADA w/Wat Cap	ADA w/Wat Cap (-1 psia across ADS)	ADA w/Wat Cap (-2 psia across ADS)
#		1	2	6	7
Coal Flow	[lb/hr]	414,724	612,965	609,675	606,401
HHV	[Btu/hr]	8,426	8,426	8,426	8,426
Q_{coal}	[Btu/hr]	3,494,467,171	5,164,844,640	5,137,120,059	5,109,535,391
TC Gen. Power	[MW]	578	717	710	703
TC Net Power	[MW]	577	715	708	701
TC Pump Power	[kW]	1,584	2,316	2,303	2,290
FD Fan Power	[kW]	1,195	1,765	1,755	1,746
ID Fan Power	[kW]	8,412	12,387	12,320	12,253
Boost Fan Power	[kW]	0	51,081	44,258	37,272
Recirc. Fan Power	[kW]	0	3,578	3,595	3,615
Total Fan Power	[kW]	9,608	68,810	61,928	54,886
Pulv. Power	[kW]	2,196	3,244	3,226	3,209
Aux. Power	[kW]	15,000	15,000	15,000	15,000
CO_2 Cap.	[%]	0	90	90	90
Comp. Power	[kW]	0	77,973	77,764	77,577
SS Power	[kW]	28,387	167,342	160,221	152,962
Net Power	[kW]	550	550	550	550
Sorbent Flow	[lb/hr]	0	24,487,781	25,325,044	26,208,635
CO2 Cap. Ads.	[lb/hr]	0	1,328,955	1,322,420	1,315,822
H2O Cap. Ads.	[lb/hr]	0	216,477	223,930	232,013
CO2 In	[lb/hr]	967,132	1,429,533	1,421,848	1,414,218
CO2 Emissions	[lb/hr]	967,132	142,946	142,178	141,414
Cap. HT Duty	[Btu/hr]	0	1,973,689,620	2,009,912,250	2,048,661,270
TCHR	[Btu/kWh]	7,659	9,049	9,089	9,131
Unit HR	[Btu/kWh]	8,796	13,002	12,932	12,863
Unit Efficiency	[%]	38.8	26.2	26.4	26.5
ΔUnit HR (From 1)	[%]	0.0	47.8	47.0	46.2
ΔUnit HR (From 2)	[%]	-32.3	0.0	-0.5	-1.1

The CO_2 compressor represented an additional focal area for reducing system pressure. The CO_2 compression system modeled consisted of a seven-stage compression system with an output of 2,215 psia. This discharge pressure is a typical pressure discussed in literature. If the captured CO_2 were to be sequestered, there very well may be different wellhead pressure requirements. In order to determine the effect of CO_2 discharge pressure on net unit heat rate, the discharge pressure was decreased by 200 psia increments to 1,215 psia. Table 9 and show the reductions in net unit HR and compression power for this range of CO_2 pressures. These results show that a 1,000 psia reduction in the CO_2 discharge

pressure results in a predicted 2% decrease in net unit heat rate corresponding to a 12.5% decrease in compression power.

Table 9. Effect of CO_2 Pressure on Net Unit Heat Rate and Compression Power[26]

	Illinois #6		PRB		ND Lignite	
CO_2 Pressure [psia]	Net Unit HR [Btu/kWh]					
2215	13,358	-	14,855	-	15,233	-
2015	13,321	-0.3%	14,802	-0.4%	15,182	-0.3%
1815	13,282	-0.6%	14,747	-0.7%	15,129	-0.7%
1615	13,240	-0.9%	14,689	-1.1%	15,072	-1.1%
1415	13,195	-1.2%	14,625	-1.5%	15,010	-1.5%
1215	13,146	-1.6%	14,557	-2.0%	14,943	-1.9%
CO_2 Pressure [psia]	CO_2 Compression Power [MW]					
2215	75.8	-	90.0	-	84.1	-
2015	74.2	-2.1%	88.0	-2.2%	82.2	-2.2%
1815	72.4	-4.4%	85.8	-4.6%	80.3	-4.5%
1615	70.6	-6.9%	83.6	-7.1%	78.2	-7.0%
1415	68.6	-9.5%	81.1	-9.8%	75.9	-9.7%
1215	66.4	-12.4%	78.5	-12.8%	73.4	-12.7%

3.3.4 Subtask 3.3.4: Evaluate Process Improvements from Operations

Development of cross heat exchanger designs for use in the ADAsorb™ process has led to analysis to quantify the tradeoffs between the capital and operating costs of a cross heat exchanger. The impacts on net unit heat rate and on the cost of carbon capture were determined. The optimal configuration, approach temperature, and number of heat exchangers were determined. A further refinement of the optimization included an evaluation of additional energy recovery through the use of a heat pump to supplement outside heat exchanger fluid heating and cooling requirements to achieve more aggressive approach temperatures and reduce capital costs associated with heat transfer surface area.

Analyses have also been performed to quantify the heat rate benefits which would result from using heat generated by the CO_2 compression process and flue gas cooler to provide heat for the feedwater heaters in the steam cycle, to provide heat for boiler combustion air, and/or to provide heat for the CO_2 capture systems sorbent regenerator. The impacts on net unit heat rate and on the cost of carbon capture were determined.

Additional analyses were performed to quantify the tradeoffs between the capital and energy costs required to reduce flue gas moisture levels and the energy costs required to evaporate higher levels of adsorbed moisture in the regenerator in cases where the flue gas moisture level to the adsorber had not been reduced. The analyses were performed for the H_2O working capacity for sorbent BN. Removal of the moisture through flue gas condensing and cooling also allowed the effect of lowering flue gas temperatures to be examined. The impacts on net unit heat rate and on the cost of carbon capture were determined.

The optimal adsorber and regenerator vessel temperatures were also modeled to reduce the net unit heat rate and overall cost of carbon capture. Varying the vessel temperatures has a direct impact on the sorbent flow rate, adsorber cooling requirements, and on the regenerator heating requirements. To find the optimal operating temperatures, modeling was completed based on both measured and extrapolated isotherms for CO_2 loading on sorbent BN. The adsorber temperature was varied within the model between 37.8°C (100°F) and 47.8°C (118°F) while the regenerator was varied between 106.7°C (225°F) and 123.9°C (255°F) for cases using all three coals. The analysis of both vessels resulted in tends showing a range of operation where the net unit heat rate varied very little while the sorbent flow rate varied. The optimal temperatures were selected from the minimal heat rate range which had the lowest sorbent flow rate to minimize any costs associated with increasing sorbent flow rate. Figure 23 and Figure 24 display the results of this modeling.

The optimal operating temperatures for the adsorber and regenerator for an ADAsorb^{TM} CO_2 capture system operating on sorbent BN at a supercritical PC power plant burning an Illinois #6 coal were found to be the same as the base case temperatures, 40°C (104°F) and 120°C (248°F) respectively. However, for the OJ sorbent, optimal adsorber and regenerator temperatures were found to be 38°C (100°F) and 59°C (140°F) respectively.

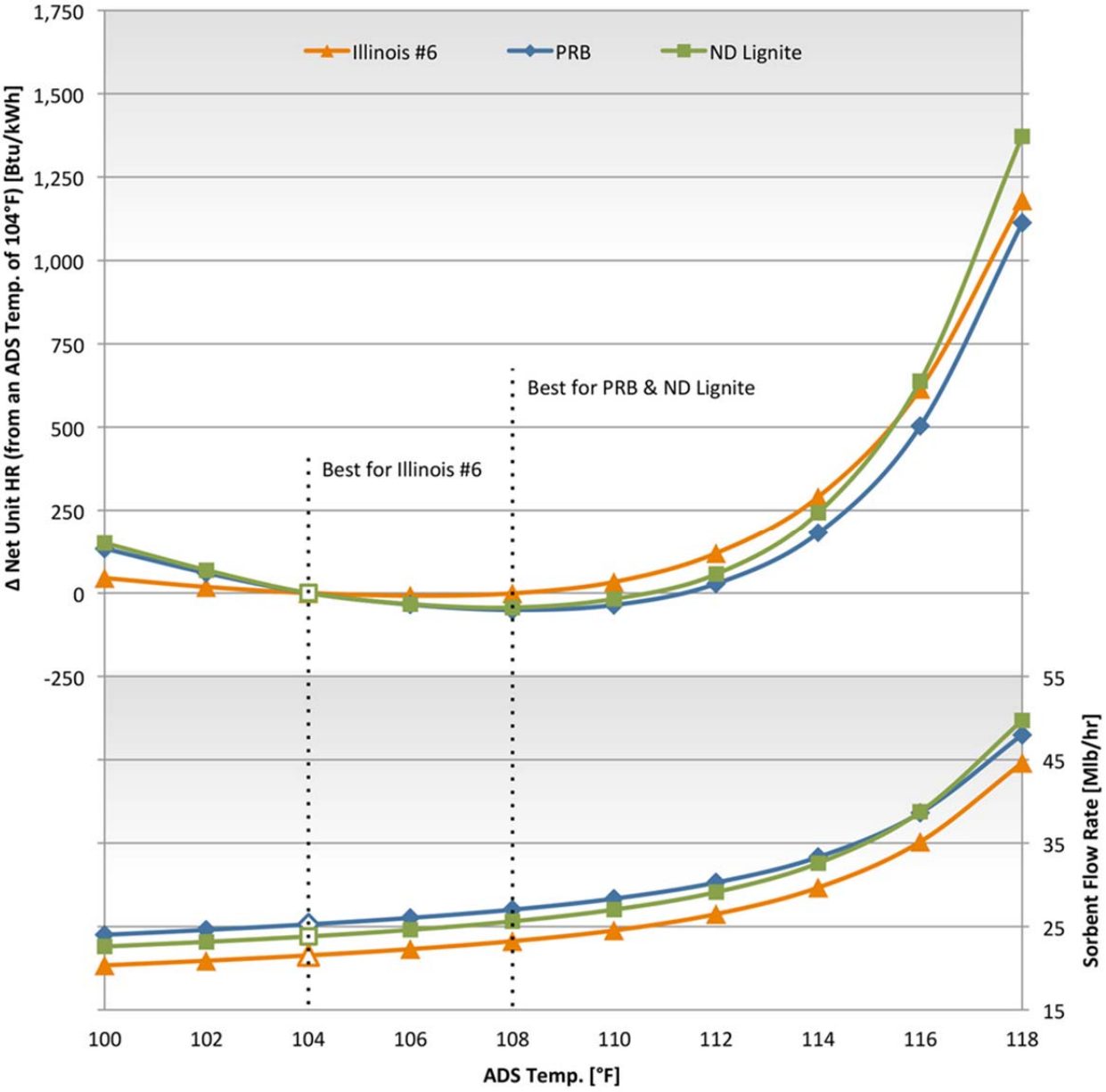

Figure 23. : Impact of Adsorber Temperature on Net Unit Heat Rate and Sorbent Flow Rate[26]

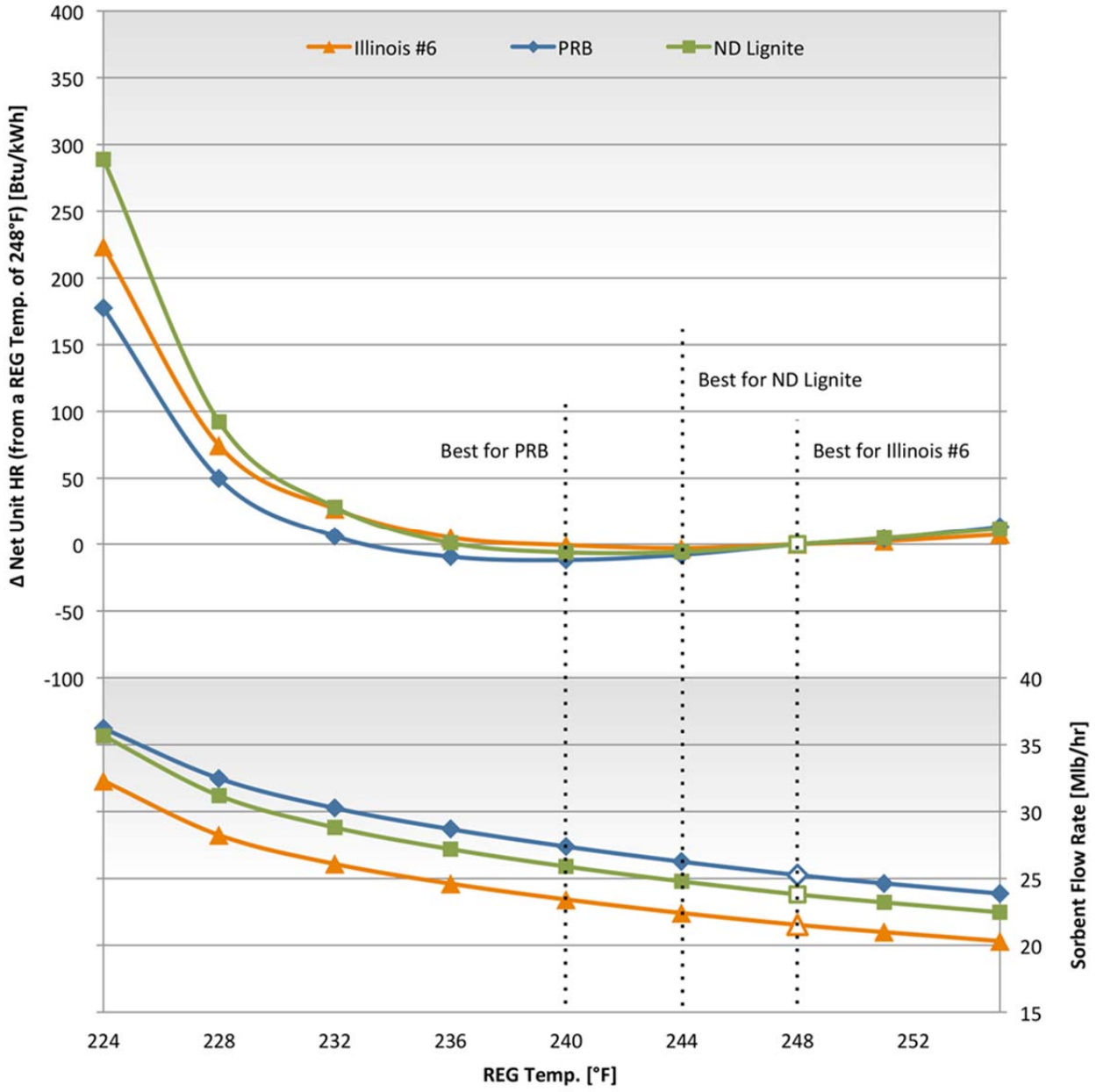

Figure 24. Impact of Regenerator Temperature on Net Unit Heat Rate and Sorbent Flow Rate[26]

A summary of the net heat rate savings for each of the investigated process modifications are shown in Figure 25. This summary is based on using sorbent BN within the ADAsorb™ system combined with a supercritical steam cycle utilizing an Illinois #6 coal.

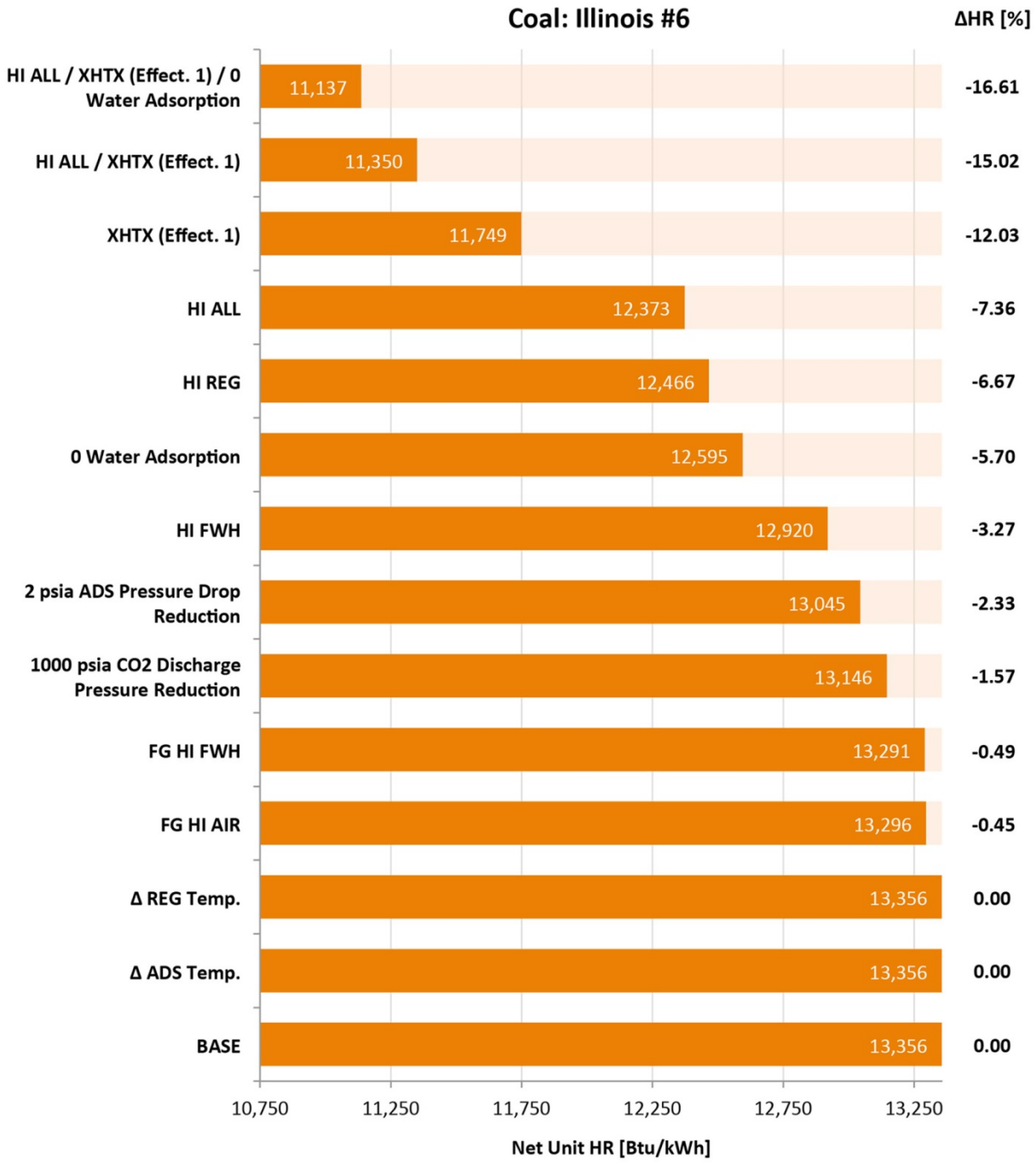

Figure 25. Summary of Heat Rate Findings for Illinois #6 and Sorbent BN[26]

It was found that changes in the operating conditions of the ADA CO_2 capture system, the addition of a cross heat exchanger, and heat integration can all have a major positive impact on net unit heat rate, especially when the various changes are combined. Detailed approaches and analysis can be found in the appended reports "*Aspen Plus Modeling of ADA Solid Sorbent CO_2 Capture System*".

The collected heat rate change data was utilized to assess the costs of each of the process modifications and a detailed analysis and optimization was conducted to compile and incorporate into a Techno-Economic Analysis found in section 3.4 of this report.

3.4 Task 4: Incorporate Process Optimization into ADAsorb™ process Techno-Economic Assessment

A schematic of the ADAsorb™ CO_2 capture process is provided in Figure 26. The ADAsorb™ process was the basis of the techno-economic analysis, although it should be noted that many of the components of the techno-economic analysis could be extrapolated to any sorbent-based CO_2 capture process based on temperature swing adsorption.

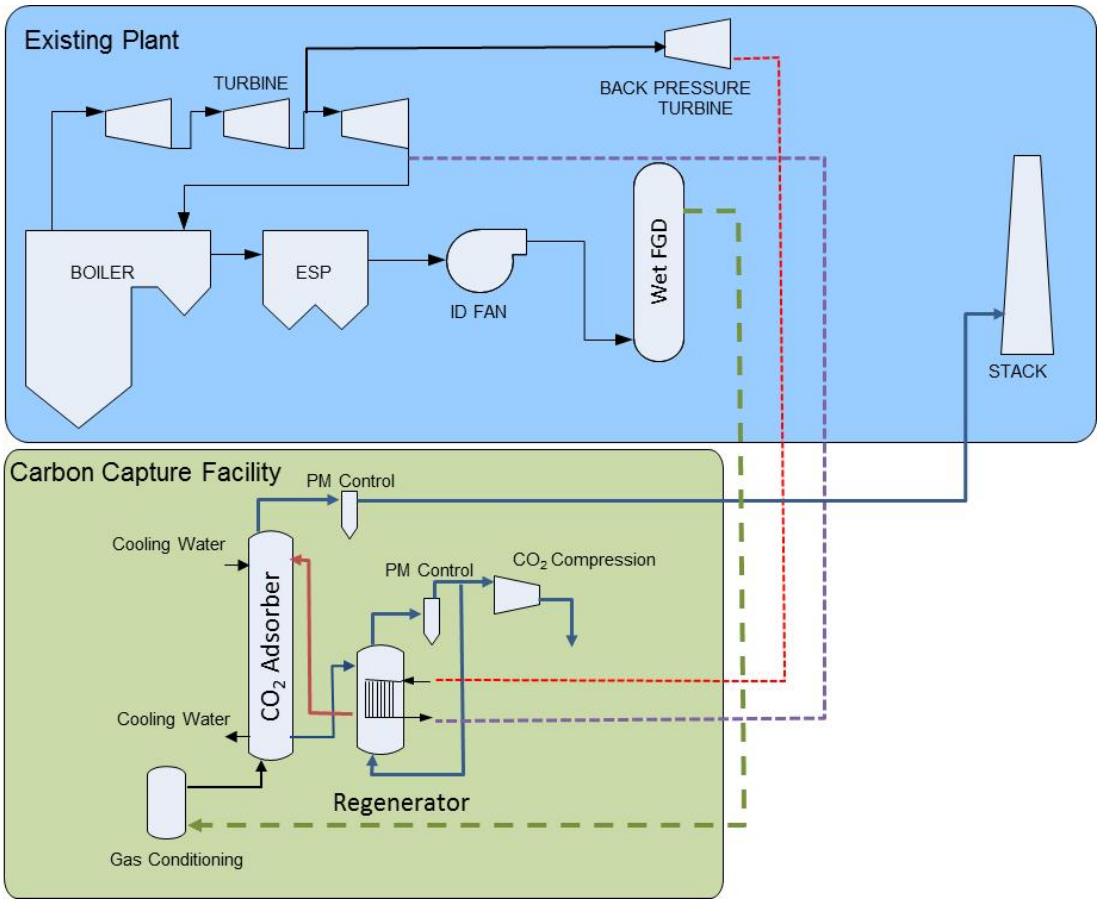

Figure 26. Process Flow Diagram of a Subcritical PC Power Plant Retrofitted with a Solid–Based CO_2 Capture Process.

A preliminary TEA model for CO_2 capture costs for the ADAsorb^{TM} CO_2 capture process for a subcritical plant, DOE Case 10, was conducted under DE-FE0004343. The TEA model was revised for a supercritical plant, Case 12 based on information provided in the NETL report "*Cost and Performance Baseline for Fossil Energy Plants - Volume 1: Bituminous Coal and Natural Gas to Electricity (Rev 2, November 2010*[25] Before this program, heat integration and process optimization had not yet been incorporated into the model. Under this task, Task 4, ADA used the results from Task 3 and input the optimal modifications into the TEA model. The output of the TEA model is the cost for CO_2 capture in terms of $/ton CO_2 avoided and levelized cost of electricity (LCOE).

3.5 Techno-Economic Analysis Elements and Approaches

Detailed approach and breakdown of the costs assumptions derived through the Techno Economic Analysis are included in the appended report "*Thermo-Economic Analysis of ADA Solid Sorbent CO_2 Capture System: Effects of Sorbent Properties and Waste Heat*". [28] This appended report derives the costs and optimization associated with:

- Capital Costs
    - Bare Erected Costs
    - Total Plant Costs
    - Total Overnight Cost
    - Total As-Spent Cost
- Existing Plant and Equipment
    - PC Plant
    - Existing ADA CO_2 Capture System
- New Equipment Construction Costs
    - Let-Down Turbine and Generator
    - Feedwater Heater for heat integration (FWH0)
    - Boiler Air Heater
    - Flue Gas Cooler (FGAS Cooler)
    - Cooling Water Circulation Pumps
    - Refrigeration Cycles
    - Cooling Towers
    - CO_2 Compression System
    - Cross Heat Exchanger (XHTX)
    - Regenerator Heater
    - Fuel Costs
    - Sorbent Costs
    - CO_2 Transportation, Storage, and Monitoring Costs (TS&M)
- Financing and Capital Costs
- Operating and Maintenance (O&M) Cost Estimates
    - Fixed O&M Costs
    - Variable O&M Costs

    - Fuel Cost Portion of Variable O&M Costs
    - Sorbent Cost Portion of Variable O&M Costs
    - CO_2 TS&M Cost Portion of Variable O&M Costs
- Cost of Electricity and Levelized Cost of Electricity
    - Cost of Electricity
    - Levelized Cost of Electricity

Table 10 summaries the equipment, fuel, and sorbent cost assumptions outlined.

Table 10. Summary of Equipment and Fuel Costs for Modified ADAsorb™ CO_2 Capture System[28]

Equipment	Units	Installed Cost	Source
Let-Down Turbine	$/kW	550	[7,8,9,16]
FWH0	$/gpm	150	[10]
Combustion Air Heater	$/$ft_{tube}$	59.34	[14]
FGAS Cooler	$/($lb_{FGAS}$/hr)	0.8 – 1.8	[6]
Cooling Water Circ. Pumps	$/gpm	4.44	[10]
Refrigeration Cycles	$/ton cooling	360	[10]
Cooling Towers	$/ton cooling	275	[10]
CO_2 Compressors	$/($lb_{CO2}$/hr)	36	[4,5]
XHTX	$/($lb_{SORB}$/hr)	3.908	Solex
Regenerator Heater	$/($lb_{SORB}$/hr)	1.954	Solex
Fuel Costs	$/klb$_{COAL}$	20.23	[15]
Sorbent Costs	$/$lb_{SORB}$	5.62	[4]
CO_2 TS&M Costs	$/klb$_{CO2}$	2.99	[4]

Table 11 details the global economic assumptions used for the analyses in this report.

Table 11. Global Economic Assumptions[28]

Parameter	Units	Value
Plant Capacity Factor	%	85
Income Tax Rate	%	38
Interest Rate	%	4
Repayment Term of Debt	Years	15
Depreciation (150% declining	Years	20
Plant Operational Life	Years	30
Duration of Construction	Years	5
Annual Inflation Rate*	%	2.95
Debt	%	45
Equity	%	55
After-tax Weighted Cost of Capital	%	7.72
Capital Charge Factor (5 Year Construction, High Risk IOU)	-	0.124
Levelization Factor (IOU @ 12% IRROE)	-	1.262

The assumptions presented in Table 10 and Table 11 were validated through comparison with results from three published sets of data for both solid sorbents and aqueous amine based CO_2 capture systems summarized in Table 12.

An aqueous amine CO_2 capture system is assumed in Case 12, cited in Table 12. Case 12 is taken from Ref. 31, "Cost and Performance Baseline for Fossil Energy Plants Volume 1: Bituminous Coal and Natural Gas to Electricity, Revision 2a". The 550 MW_{net} PC power plant, burning Illinois 6 bituminous coal, was equipped with the best available control technology (BACT) to comply with environmental targets. The flue gas desulfurization (FGD) system used for sulfur dioxide (SO_2) removal was a wet limestone forced oxidative absorber, producing gypsum as a byproduct. A fabric filter was used to control particulate matter (PM). The nitrogen oxides (NOx) concentration was reduced using a combination of low NOx burners (LNBs) and over-fire air (OFA) systems in the boiler as well as installing selective catalytic reduction (SCR) upstream of the air heater. The Econamine process was assumed to remove 90% of the CO_2 from the plant. Capital and operating costs also including the CO_2 compression system.

The sorbent based CO_2 capture process was evaluated in Ref. 30, as if it was implemented at the same power plant as the Econamine process.[32] At the time that the techno-economic analysis in Ref. 30 was

prepared, the pilot-scale data on solid sorbents was not available. Therefore, the analysis was conducted using several assumptions based on public literature and laboratory testing, including:

- Particles physically resemble polystyrene beads with respect to size
- Particle density: 36.6 lb/ft^3
- Heat of reaction is 587 Btu/lb CO_2 adsorbed
- Adsorption temperature is 104°F
- Regeneration temperature is 248°F
- Flue gas temperature after the SO_2 polishing unit is 135°F

The sorbent properties using in the Preliminary Techno-Economic Analysis (PTEA) in Ref. 30 were not the same as those of Sorbent BN, which resulted in differences between the PTEA and the TEA carried out in this project, as discussed below.

For each solid-sorbent CO_2 capture process cited in Table 12, two different approaches were used to develop cost estimate cases, referred to as Sorbent1 and Sorbent2 in the table. The first approach was based on the methodology described in a report issued by the DOE, entitled "Cost and Performance Baseline for Fossil Energy Plants – Volume 1: Bituminous Coal and Natural Gas to Electricity, Revision 2".32 The cost estimates based on the DOE methodology are referred to as the Sorbent 1 case. To develop the second cost assessment the engineering firm used vendor quotes and history of past projects from their extensive database. The cost estimates based on engineering quotes and experience are referred to as the Sorbent 2 case.

Two separate comparisons were conducted, one comparison of cost of electricity (COE) and levelized cost of electricity (LCOE) and the other comparison of capital costs. The comparison of COE and LCOE had very good agreement with variations ranging from 0% to 0.63% for Lehigh's calculations, a seen in Table 12.

Table 12. Validation Results for COE Calculations[28]

Baseline Data				
	Units	Sorbent 1 [30]	Sorbent 2 [30]	Case 12 [31]
Year		2011	2011	2007
PC Plant	$/kW$_{gross}$	1,454	1,461	1,394
CO_2 Capture	$/($lb$_{CO2}$/hr)	184.59	473.92	224.04
CO_2 Comp. System	$/($lb$_{CO2}$/hr)	30.47	30.77	29.89
Fuel Costs	$/klb$_{coal}$	20.06	20.27	19.09
CO_2 TS&M Costs	$/klb$_{comp\ flow}$	2.55	2.58	2.54
Fixed Costs	$/MWh	12.9	16.2	8.7
Variable Costs	$/MWh	16.6	14.3	13.0
COE Values				
Values Presented in Literature [30,31]				
COE	$/MWh	113.3	133.3	106.5
LCOE	$/MWh	143.6	169.0	135.2
Calculated using BASE BN Model				
COE	$/MWh	112.6	133.3	106.4
Difference	%	0.62	0.00	0.09
LCOE	$/MWh	142.7	169.0	135.0
Difference	%	0.63	0.00	0.15

Table 13 shows there are major differences in costs between the BASE BN (current ADAsorb™ system model derived for this project) model and those presented in the Preliminary Techno Economic Analysis (PTEA) [30]. The BASE BN case shows higher demand for auxiliary power from the CO_2 capture system and the CO_2 compressors. An additional 63 MW of demand is due to the inclusion of the refrigeration power required to cool the inlet flue gas as well as what is thought to be a more representative calculation of CO_2 compressor power. This required additional power increases the PC plant size and therefore its capital costs. The demand has a trickledown effect, the increase in plant size ultimately results in and increase in the flow rate of captured CO_2 resulting in higher capital costs for the CO_2 compressors.

Counter balancing this increase in capital costs is a decrease in CO_2 capture system capital cost. The cost included in the PTEA [30] was an average cost of systems utilizing two different cases, Sorbent 1 and Sorbent 2. The Sorbent 1 ADA capture system cost was approximately half that of the system cost for the Sorbent 2 case, because different methods were used for estimating capital costs. As can be seen in Table 12, the capital cost of the CO_2 capture system significantly impacts the overall cost of electricity.

The final section of Table 13 details the calculated COE and LCOE results for these two baseline cases. COE is seen to be around 13% higher for the BASE BN case, while LCOE is only around 3% higher. These results show that there is relatively close agreement between the COE and LCOE results previously presented and those calculated and presented in this report.

Table 13. Comparison between Preliminary TEA Sorbent 2 Case and the BN BASE Case

	Units	Sorbent 2 [30]	BASE BN Sorbent	Difference	Difference [%]
Gross Power	MW	690	753	63	9.1
Auxiliary Power	MW	140	203	63	45.0
CO_2 Capture Facility	MW	57.7	84.3	26.6	46.1
CO_2 Compression	MW	43.5	75.8	32.3	74.3
Other Aux. Power	MW	38.8	42.9	4.1	10.6
Net Power	MW	550	550	0	0.0
BEC	$1000	1,737,858	1,863,151	125,293	7.2
PC Plant	$1000	1,077,074	1,213,231	136,157	12.6
CO_2 Capture	$1000	620,501	449,802	170,699	27.5
CO_2 Compression	$1000	40,284	56,723	16,439	40.8
Other Costs**	$1000	0	143,395	-	-
TPC	$1000	2,319,109	2,347,848	28,739	1.2
TOC	$1000	2,865,928	2,872,792	6,864	0.2
TASC	$1000	3,267,158	3,274,983	7,825	0.2
Capital Costs	$/MWh	86.8	86.9	0.1	0.1
Fuel Costs	$/MWh	22.6	23.2	0.6	2.7
CO_2 TS&M Costs	$/MWh	6.2	8.6	2.4	38.7
Sorbent Costs	$/MWh	-	5.5	-	-
Fixed Costs	$/MWh	18.2	16.3	1.9	10.4
Variable Costs	$/MWh	16.1	14.8	1.3	8.1
COE	$/MWh	137.2	155.3	18.1	13.2
LCOE	$/MWh	189.8	195.9	6.1	3.2

*Includes price of let-down turbine and FGAS cooler

**Includes refrigeration, cooling tower, pump costs, and initial sorbent fill costs

4 Results

Thermodynamic results from the previous sections show that there are numerous modifications to the ADAsorb^{TM} system that have the potential to dramatically decrease net unit heat rate. Results from these thermodynamic models are presented in Figure 23 and Figure 24. Although all of the modeled modifications resulted in thermodynamic improvements, an economic analysis was required to determine if the improvement in performance offset the additional equipment costs. Costing for all of the proposed modifications were calculated according to the correlations presented in section 3. By adding the additional costs of these components to the PC plant and adjusting the size of the plant for the performance improvements, an estimate of capital costs was found. These costs were used to find the COE and LCOE for the configurations previously considered in the thermodynamic analyses. Figure 27 presents these COE and LCOE results for the BN sorbent.

For the BN sorbent, the addition of a cross heat exchanger (0.75 effectiveness), and each of the four heat integration options were examined independently, along with the case where all five are implemented simultaneously. From these results, it is seen that only the addition of a cross heat exchanger (XHTX 0.75 eff) and the addition of CO_2 compressor generated heat to the regenerator (HI REG) result in a lower COE or LCOE than the case where only the temperatures in the adsorber and regenerator were optimized, but no heat integration was employed (OPTI). This indicates that for these modifications the improved performance more than offsets the increase in capital costs. The reason for this seems to be the high cost of the feedwater heating options (HI FWH and HI FG FWH). For these cases, the improvement in net unit heat rate is minimal with regard to the cost of the additional feedwater heater (FWH0).

Because the inclusion of a cross heat exchanger and the addition of CO_2 compressor generated heat to the regenerator are the only modifications which resulted in improved economics, these two modifications were examined in combination. Combining the two modifications is seen to slightly improve the economics of the cross heat exchanger or regenerator heater alone, with an $8/MWh reduction in the COE and $10/MWH reduction in the LCOE from the OPTI case.

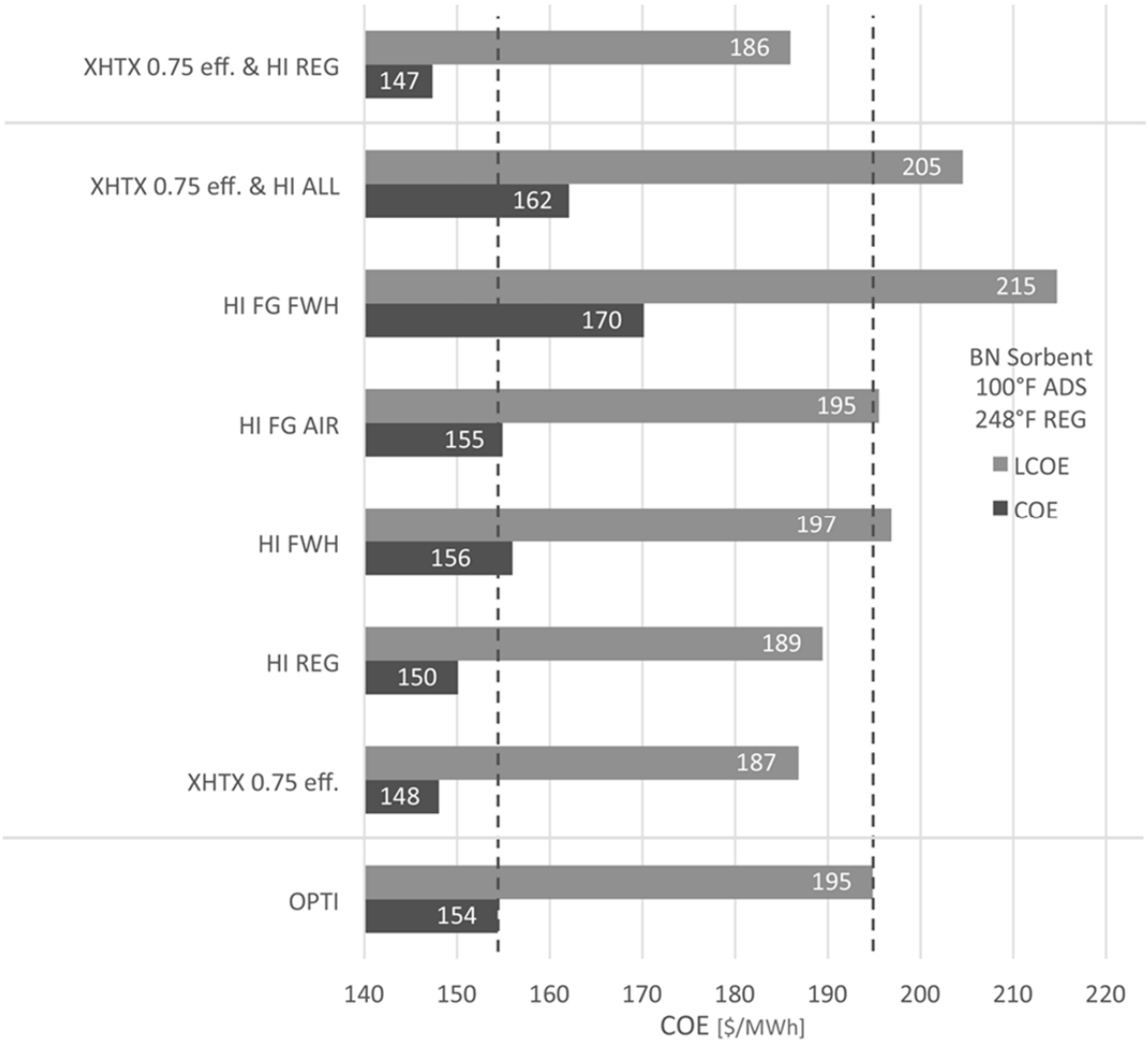

Figure 27. COE & LCOE for Various Cross Heat Exchanger & Heat Integration Cases - BN Sorbent[28]

The economic results calculated for a system where the OJ sorbent is utilized is presented in Figure 28. No modifications resulted in significant economic improvement from the OPTI. All of the thermodynamic improvements were offset by the cost of implementing the modifications.

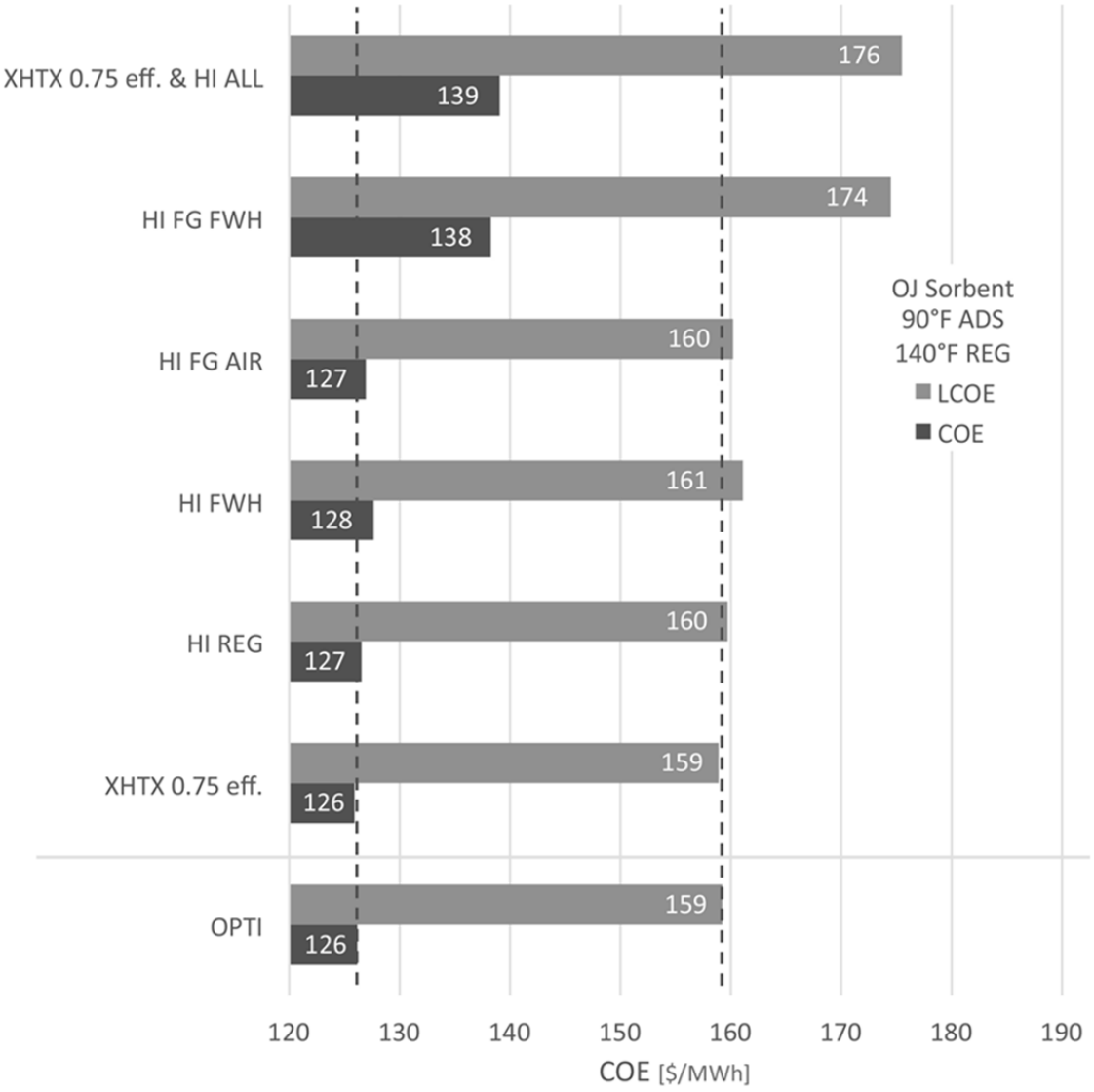

Figure 28. COE & LCOE for Various Cross Heat Exchanger & Heat Integration Cases - OJ Sorbent[28]

Another method for comparing both the BN and OJ cases is presented in Figure 29, where the COE is plotted against the net unit heat rate for the cases presented in Figure 27 and Figure 28. This plot clearly shows that the best unit performance does not directly equate to the lowest COE. It is also apparent that the OJ sorbent performs much better both thermally and economically when compared to the BN sorbent. Also plotted is the MEA 90% CO_2 capture case (Case 12 from Ref. 31 When both solid sorbents are compared to this case, it is apparent that with the improved sorbent properties of sorbent OJ, improvements can be made to the COE for CO_2 capture using solid sorbents. Given that solid sorbent CO_2 capture is only in the early stages of development, while the MEA technology is well-developed, it is expected that both net unit heat rate and COE will continue to improve with further development, particularly in the area of improved sorbents.

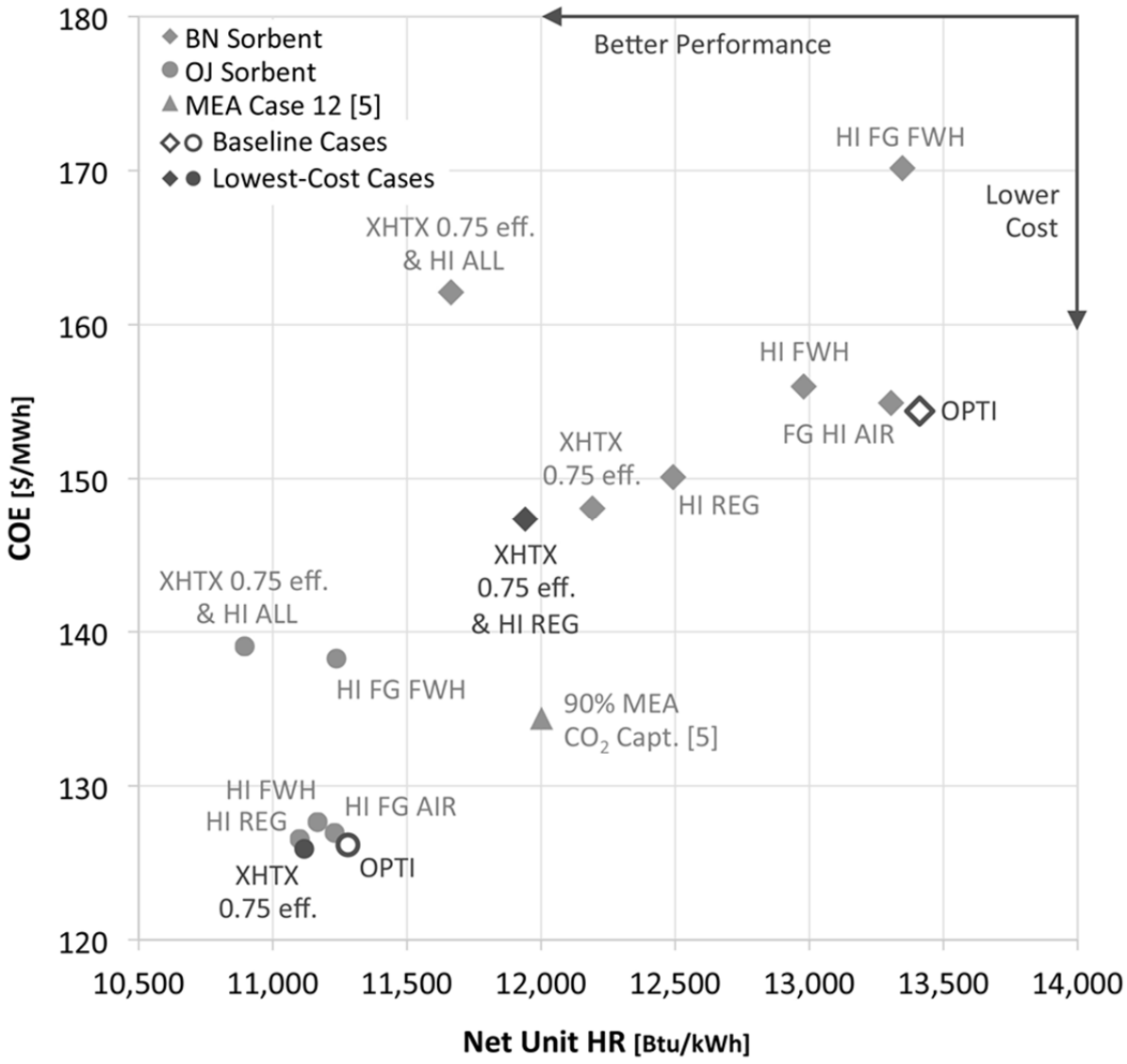

Figure 29. COE & Net Unit Heat Rate Comparison Between BN, OJ, and MEA Cases[28]

The calculated COE for six key cases is presented in Figure 30. The BN OPTI and OJ OPTI cases represent a supercritical PC power plant burning an Illinois #6 coal utilizing an ADAsorb™ CO_2 capture system without the implementation of any heat integration. These two results are presented along with the lowest-cost cases for both sorbents from Figure 27 and Figure 28. As seen, COE is reduced by \$7.1/MWh and \$0.3/MWh between the OPTI and lowest-cost cases for the BN and OJ sorbent respectively. While this is a significant improvement for the BN sorbent, the improvement for the OJ sorbent case is so minimal as to preclude the use of a cross heat exchanger. Despite this, both OJ sorbent cases are seen to result in a COE at least \$8/MWh below that of the 90% MEA CO_2 capture case (Case 12 from Ref. 31). When compared to the case without CO_2 capture, COE is seen to be around \$33/MWh higher for the OJ cases. This equates to a 36% increase in the COE due to the costs associated with CO_2 capture using the ADAsorb™ system as presented in this report.

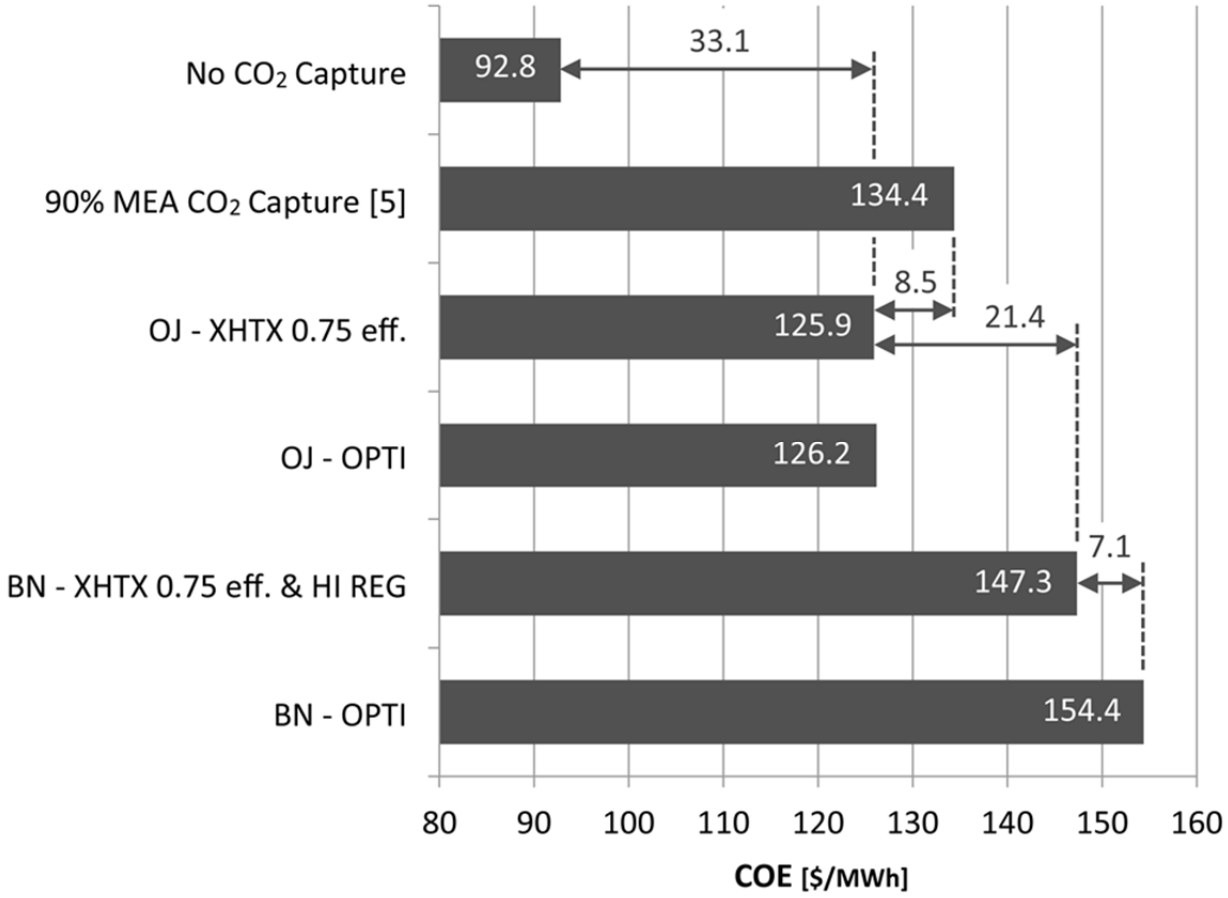

Figure 30. COE for Six Key Cases[28]

The calculated LCOE for the same six cases as Figure 30, are presented in Figure 31. The outcome of this calculation produces the same trend as the COE results and results in the same 36% increase between the no-capture and OJ OPTI cases.

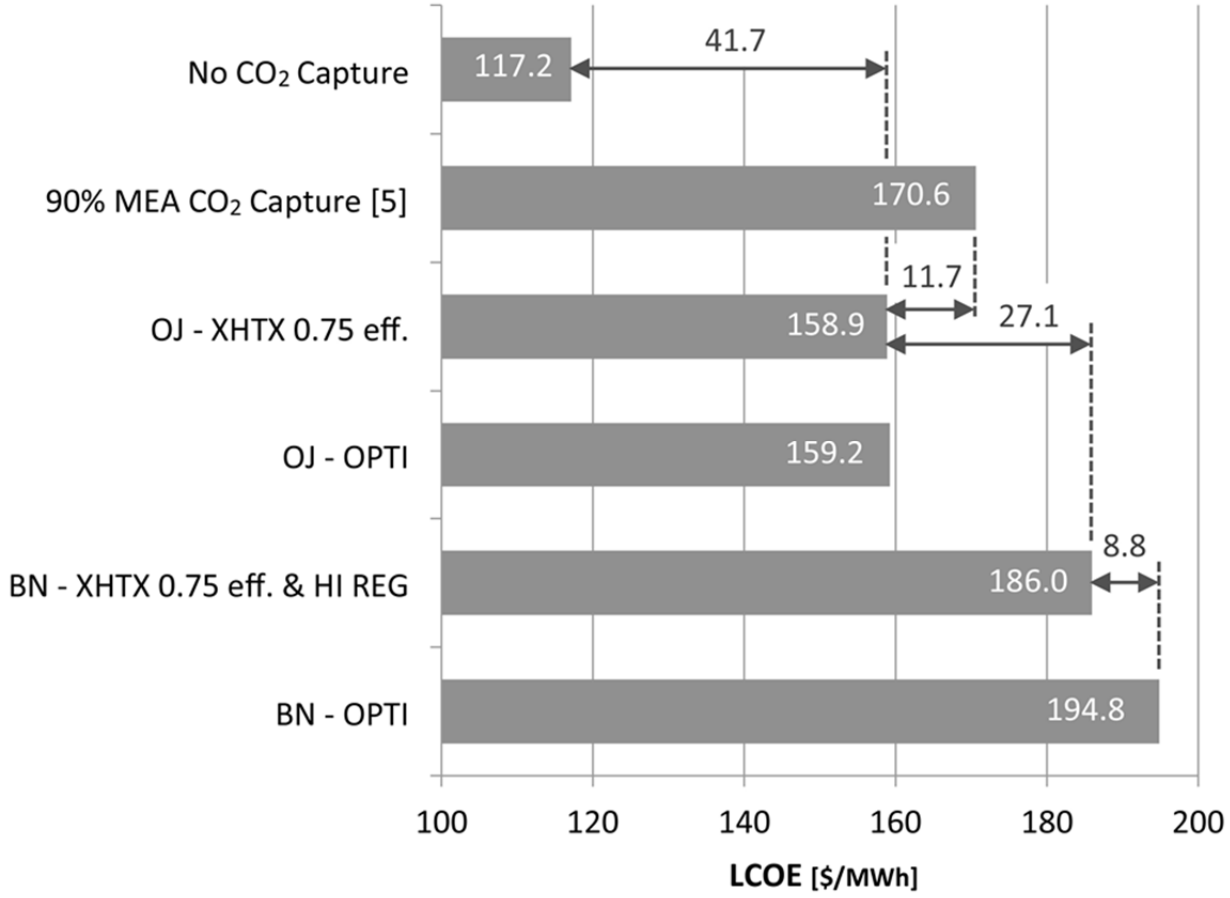

Figure 31. LCOE for Six Key Cases[28]

5 Conclusions

5.1 Thermodynamic

Analysis and modeling of the ADAsorb™ CO_2 Capture System have resulted in not only a better understanding of how the system operates, but also have suggested changes in design and process conditions, which have the potential to significantly improve the performance of a coal-fired plant equipped with the system. After development and verification of the Aspen Plus model, various operating parameters of the ADAsorb™ CO_2 Capture System were varied to determine their optimal values. Plant performance with the addition of a cross heat exchanger to cool the lean sorbent and heat the rich sorbent was also examined. Finally the utilization of waste heat from the flue gas cooler and CO_2 compressors was examined. This heat was used to heat the cold, CO_2 rich sorbent stream, the incoming boiler combustion air, and the steam cycle feedwater. Analyses of the modeling results in these areas leads to the following conclusions for the thermodynamic optimization of the ADAsorb™ solid sorbent CO_2 capture system.

5.1.1 Cross Heat Exchanger

Actual operating effectiveness of any proposed cross heat exchanger design is crucial with regard to its positive impact on the plant. As the effectiveness approaches 1, net unit heat rate is suggested to decrease by up to 14.4% for sorbent BN. As system parasitic power is reduced, overall unit efficiency increases, decreasing the coal flow rate, which results in a lower CO_2 flow rate for a 550 MWnet plant. A lower CO_2 flow rate further reduces the capture demand on the ADAsorb^{TM} CO_2 capture system, resulting in lower parasitic power for each component of the capture and compression system.

5.1.1.1 Moving Bed

Using the results from the successful bench scale testing of the Solex moving bed heat exchanger, Solex was able to develop and determine equipment size, configuration, and costing for a full scale 550 MW_{net} application.

5.1.1.2 Fluidized bed

The fluidized bed heat exchanger design developed in conjunction with Technip Stone and Webster resulted in an additional 28,000 hp of electrical load for an approximate 412,000lbs/hr reduction in steam usage. If the 412,000lbs/hr of steam were to be run through a turbine it would result in approximately 9,200 hp. The design effort and calculations performed resulted in the use of more energy than could be recovered. Despite optimization efforts performed by Technip, the fluidized bed heat exchanger design will not save process energy and make up for the increased capital costs required.

5.1.2 Heat Integration

Every heat integration option considered resulted in a reduction in net unit heat rate relative to implementing the ADAsorb^{TM} CO_2 capture system without heat integration. The best-performing case is the cross heat exchanger combined with all other modifications. Using heat from the compression system contributes most significantly to this improvement, as there is a greater quantity of high-temperature heat available from this source than from the flue gas cooling system.

5.1.3 Flue Gas Moisture

Reducing flue gas moisture and temperature through the combined use of a spray cooler and refrigeration cycle has little effect on capital costs while the power usage increases by two or three times. Development focus on sorbents with lower moisture uptake will have a much larger impact on the efficiency of the overall system than the addition of flue gas cooling.

5.1.4 Adsorber Pressure Drop Reduction

Reducing the pressure drop through the adsorber results in decreased power requirements for the flue gas blower. However, the overall heat rate decrease for 1.0 and 2.0 psia reductions is only 0.5% and

1.1% respectively. A reduction in adsorber pressure drop negatively affects the CO_2 adsorption characteristics as the partial pressure of CO_2 is reduced in the adsorber. This lowers the equilibrium loading potential of the sorbent and effectively reduces its working capacity necessitating a higher sorbent recirculation rate. For each 1 psia reduction in adsorber pressure drop, the sorbent flow rate corresponding to 90% CO_2 capture increases by approximately 1,000,000 lb/hr. This results in a larger regenerator duty, extraction steam flow, increasing the turbine cycle heat rate. As more sorbent is circulated through the system, the sensible heat loads associated with the heating and cooling of the sorbent will increase.

5.1.5 Adsorber and Regenerator Temperature Optimization

The optimal operating temperatures for the Adsorber and Regenerator for an ADAsorb^{TM} CO_2 capture system operating on sorbent BN at a supercritical PC power plant burning an Illinois #6 coal were found to be the same as the base case temperatures, 40°C (104°F) and 120°C (248°F) respectively.

The initial sorbent OJ base case adsorber and regenerator temperatures of 25°C (77°F) and 75°C (167°F) respectively were not found to provide the best overall system performance due in part to increased power requirements of flue gas chilling. Rather, adsorber and regenerator operating temperatures of 37.8°C (100°F) and 58.9°C (138°F) respectively were found to be optimal.

5.1.6 CO_2 Compression

Results show that a 1,000 psia reduction in the CO_2 discharge pressure results in a predicted 2% decrease in net unit heat rate corresponding to a 12.5% decrease in compression power. Minimizing the CO_2 compression for the required application can have a beneficial impact on heat rate.

5.1.7 Sorbent

5.1.7.1 Flue Gas Moisture Uptake

The impacts of flue gas moisture uptake on the sorbent turned out to be significant for sorbent BN. Sorbent BN's design working capacity, the delta loading between adsorption and regeneration, was measured to be 7% by weight for CO_2 and 0.9% by weight for H_2O. If the sorbent could be made to not adsorb water, the net plant heat rate for Illinois #6 coal would be reduced by 5.7%. This indicates that moisture adsorbed by the sorbent should be minimized to increase the net power plant efficiency. It also indicates that, based on the size of the possible reductions, this should clearly be a development priority and that sorbents which adsorb more than 1-2% moisture by weight are unlikely to be cost competitive unless they have an extremely high CO_2 working capacity that well exceeds 15% by weight.

5.1.7.2 CO_2 Loading & Sorbent Flow Rate

An increase in sorbent CO_2 loading, at adsorber temperatures, has a significant impact on sorbent flow rate for a given flue gas flow rate and composition. The OJ sorbent has the potential to provide three times the CO_2 loading of the BN sorbent. This can potentially cut the sorbent flow rate by around 66% if

low adsorber operating temperatures can be realized. If the OJ sorbent is used instead of the BN sorbent, net unit heat rate is reduced by between 10% and 17%.

5.1.7.3 OJ vs. BN Sorbent

A side-by side comparison of the plant using both the OJ and BN sorbents showed a dramatic improvement in predicted plant performance when the OJ sorbent was used. For sorbent optimal temperature cases without a cross heat exchanger or heat integration, the OJ sorbent was calculated to result in a 17.3% reduction in net unit heat rate and an increase in net unit efficiency from 25.6% to 30.9% when compared to the BN sorbent. As a cross heat exchanger and heat integration are added to the ADAsorb^{TM} CO_2 capture system, the heat rate benefit through use of the OJ sorbent diminishes. However, for the OPTI case with a cross heat exchanger (effectiveness of 0.75) and all four heat integration options being utilized, the use of the OJ sorbent still lowers net unit heat rate by a significant 7.95% over the BN case.

5.2 Techno-Economic

The ADAsorb^{TM} CO_2 solid sorbent CO_2 capture system has been modelled in conjunction with a supercritical pulverized coal power plant for a variety of process configurations. Two different solid sorbents were considered during modeling (the BN and OJ sorbents), the addition of a XHTX to the capture system was examined, and four opportunities for the utilization of waste heat were also considered. After a complete thermodynamic analysis of these cases, calculations were conducted to find the plant COE and LCOE for all the cases. The conclusions summarized below are drawn from these thermo-economic results as presented in the present report.

5.2.1 COE and LCOE for baseline ADAsorbTM CO_2 capture system without heat integration

The baseline ADAsorb^{TM} CO_2 capture system without heat integration (OPTI) cases designate those cases, where the capture system adsorber and regenerator temperatures were tuned to obtain the lowest net unit heat rate. These cases were considered as the baseline cases for each of the two sorbents.

For the BN sorbent, the OPTI case was found to result in a COE and LCOE of $154.4/MWh and $194.8/MWh respectively. This represents a 66% increase in the COE over the case without CO_2 capture and a 15% increase in COE over the 90% capture MEA case as presented by DOE.[5]

The OPTI OJ sorbent case performs considerably better, with a COE and LCOE of $126.2/MWh and $159.2/MWh respectively. For this case, COE is seen to be around 36% higher than the no capture case, while COE is 6% lower than the COE for the 90% capture MEA case.

5.2.2 Cross Heat Exchanger and Heat Integration Improvements

While the addition of a cross heat exchanger and heat integration was found to significantly improve net unit heat rate the additional equipment costs associated with these cases almost always outweighed the improvement in performance. The two exceptions to this are the addition of a cross heat exchanger and adding the equipment necessary to incorporate the use of waste heat into the regenerator.

5.2.3 Other Heat Integration Opportunities

For each of the other heat integration opportunities modeled, using waste heat to provide feedwater heating, combustion air heating, and a regenerator heater, for the OJ sorbent case, COE and LCOE are seen to increase. Obviously this precludes the use of any of these options as their associated costs outweigh any benefit due to their improved thermal performance.

5.2.4 Sorbent

5.2.4.1 Sorbent BN

For the BN sorbent, the addition of a cross heat exchanger with an effectiveness of 75% was found to decrease the COE by $6/MWh, or a 4% decrease in COE. By adding a regenerator heater to this case with a cross heat exchanger, COE is lowered by another $1/MWh.

5.2.4.2 Sorbent OJ

For sorbent OJ, the addition of cross heat exchanger with an effectiveness of 75% only lowers the COE by $0.3/MWh, or by 0.2%. Given this very small difference in COE between the OJ case with and without a cross heat exchanger, it is suggested that it would be best not to include a cross heat exchanger for this sorbent. The additional complexity of adding such a system will most likely outweigh the minimal improvement in COE.

5.2.4.3 BN vs. OJ Sorbent

Just as sorbent OJ has shown clear thermodynamic benefits over sorbent BN there is a clear economic advantage to using this improved sorbent. For the OPTI cases, the OJ sorbent is seen to result in a COE $28.2/MWh lower than the COE for the BN sorbent, or a reduction of 18%. When comparing the lowest-cost BN case to the lowest-cost OJ case, the OJ case comes in $21.4/MWh (15%) lower. The primary reason for this is the improved CO_2 loading capacity of the OJ sorbent. With an improvement in CO_2 loading, the OJ sorbent flow rate is reduced, which not only reduces the cost of sorbent needed to fill the capture system, but more significantly reduces the size of the entire capture system. As capture system sizes are reduced, material costs associated with the system are reduced accordingly.

5.2.5 Future Sorbent Advances

Perhaps one of the most significant points to be drawn from the COE and LCOE differences due to sorbent type is in regard to future improvements to solid sorbent CO_2 capture. ADA has supported

steady progress in developing and testing new sorbents. For instance, the BN sorbent represents a sorbent tested by prior to the initiation of this project, sorbent OJ was characterized in the year leading up to publication of this report, and improvements to the OJ sorbent are in progress. Therefore, it is suggested that solid sorbent CO_2 capture will continue to see performance gains and lower system costs as further sorbent development is conducted.

6 References

1. Ramezan M., Skone T.J., Nsakala N., Liljedahl G.N., “Carbon Dioxide Capture from Existing Coal-Fired Power Plants”, Final Report DOE/NETL-401/110907, December, 2007.

2. Birbara P.J., Filburn T.P., Nalette T.A., United Technologies Corporation. Regenerable Solid Amine Sorbent., US 5,876,488: 1999.

3. Gray M.L., Champagne K.J., Fauth D., Baltrus J.P., Pennline, H., Performance of Immobilized Tertiary Amine Solid Sorbents for the Capture of Carbon Dioxide, International Journal of Greenhouse Gas Control, **2008**, *2*, 3-8.

4. Drage T.C., Arenillas A., Smith K.M., Snape C.E., Thermal Stability of Polyethylenimine Based Carbon Dioxide Adsorbents and its Influence on Selection of Regeneration Strategies, Microporous and Mesoporous Materials, **2008**, *116*, 506-512.

5. Siriwardane R.V., The United States Department of Energy, Solid Sorbents for Removal of Carbon Dioxide from Gas Streams at Low Temperatures., US 6,908,497: 2005.

6. Harlick P.J.E., Sayari A., Applications of Pore-Expanded Mesoporous Silica. 5. Triamine Grafted Material with Exceptional CO_2 Dynamic and Equilibrium Adsorption Performance, Ind. Eng. Chem. Res., **2007**, *45*, 446-458.

7. Kim S., Ida J., Guliants V.V., Lin J.Y.S., Tailoring Pore Properties of MCM-48 Silica for Selective Adsorption of CO_2, J. Phys. Chem. B, **2005**, *109*, 6287-6293.

8. Hicks J.C., Drese J.H., Fauth D.J., Gray M.L., Qi G., Jones C.W., Designing Adsorbents for CO_2 Capture form Flue Gas - Hyperbranched Aminosilicas Capable of Capturing CO_2 Reversibility, J. Am. Chem. Soc., **2008**, *130*, 2902-2903.

9. Drage T.C., Arenillas A., Smith K.M., Pevida C., Piippo S., Snape C.E., Preparation of Carbon Dioxide Adsorbents from the Chemical Activation of Urea-Formaldehyde and Melamine-Formaldehyde Resins, Fuel, **2007**, *86*, 22-31.

10. Plaza M.G., Pevida C., Arenillas A., Rubiera F., Pis J.J., CO_2 Capture by Adsorption with Nitrogen Enriched Carbons, Fuel, **2007**, *86*, 2204-2212.

11. Radosz M., Hu X., Krutkramelis K., Shen Y., Flue-Gas Carbon Capture on Carbonaceous Sorbents: Toward a Low-Cost Multifunctional Carbon Filter for “Green” Energy Producers, Ind. Eng. Chem. Res., **2008**, *47*, 3783-3794.

12. Lu C., Bai H., Wu B., Su F., Hwang J.F., Comparative Study of CO_2 Capture by Carbon Nanotubes, Activated Carbons, and Zeolites, Energy & Fuels, **2008**, *22*, 3050-3056.

13. Nelson T., Coleman L., Anderson M., Herr J., Pavani M., *The Dry Carbonate Process: Carbon Dioxide Recovery from Power Plant Flue Gas*, Annual NETL CO_2 Capture Technology for Existing R&D Meeting, Pittsburgh, PA, March 2009.

14. Shigemoto N., Yanagihara T., Sugiyama S., Hayashi H., Material and Energy Consumption for CO_2 Recovery from Moist Flue Gas Employing K_2CO_3-on-Activated Carbon and Its Evaluation for Practical Adaptation, Energy & Fuels, 2006, 20, 721-726.

15. Siriwardane R.V., Shen M.S., Fisher E.P., Poston J.A., Adsorption of CO_2 on Molecular Sieves and Activated Carbon, Energy & Fuels, 2001, 15, 279-284.

16. H. Li, M. Eddaoudi, M. O'Keeffe, O. M. Yaghi, Nature, 1999, 402,276.

17. M. Eddaoudi, J. Kim, N. Rosi, D. Vodak, J. Wachter, M. O'Keeffe, O.M. Yaghi, Science 2002, 295, 469.

18. D. Li, K. Kaneko, Chemical Physics Letters 2001, 335, 50.

19. Y. S. Bae, K. L. Mulfort, H. Frost, P. Ryan, S. Punnathanam, L. J.Broadbelt, J. T. Hupp, R. Q. Snurr, Langmuir 2008, 24, 8592.

20. NETL, Cost and Performance Baseline for Fossil Energy Plants, Volume 1: Bituminous Coal and Natural Gas to Electricity, Revision 2, November 2010, www.netl.doe.gov, accessed September 2012.

21. Xavier, A.M., King, D.F., Davidson, J.F.., Harrison, D., Surface-bed heat transfer in a fluidized bed at high pressure, “Fluidization”, eds. J.R. Grace and J.M. Matsen, pg. 209, Plenum, New York.

22. Davidson, J.F., Clift, R., Harrison, D., Fluidization, 2nd ed., Academic Press, Orlando, FL, 1985.

23. Solex Thermal Science, *Products and Solutions: Cooling*. 2016. Web.

24. Aspen Technology Inc. *aspentech: Aspen Plus for Chemicals & Polymers*. 1994 – 2016. Web.

25. NETL, Fout, T., ESPA, Zoelle, A., Keairns, D., Turner, M., Woods, M., Kuehn, N., Shah, V., Chou, V., Pinkerton, L. *Cost and Performance Baseline for Fossil Energy Plants - Volume 1: Bituminous Coal and Natural Gas to Electricity. Rev 2, 2010*

26. Charles, J., Levy, E., Wang, X. *Aspen Plus Model of ADA Solid Sorbent CO_2 Capture System.* Lehigh University Energy Research Center, 2014

27. Lehigh University Energy Research Center. *Investigation on Flue Gas & Condensing Heat Exchanger (CHX) Cooling Water Cooling Processes and CHX Design.* 2014

28. Charles, J., Levy, E. *Thermo-Economic Analysis of ADA Solid Sorbent CO_2 Capture System: Effects of Sorbent Properties and Waste Heat Integration.* Lehigh University Energy Research Center, 2015

29. Charles, J., Levy, E., Wang, X. *Aspen Plus Modeling of ADA Solid Sorbent CO_2 Capture System:* Comparison of OJ and BN Sorbents. Lehigh University Energy Research Center, 2015

30. Krutka, H., Starns, T., Richard, M., Thitakamol, B. Evaluation of Solid Sorbents as a Retrofit Technology for CO_2 Capture: Preliminary Techno-economic Assessment of Solid Sorbents for Post-Combustion CO_2 Capture. DOE: DE-FE0004343, December 2011.

31. Cost and Performance Baseline for Fossil Energy Plants – Volume 1: Bituminous Coal and Natural Gas to Electricity. DOE/2010/1397 Revision 2a, September 2013.

32. Final report – Cost and Performance Baseline for Fossil Plants, Volume 1: Bituminous Coal and Natural Gas to Electricity, DOE/NETL-2007/1281, August 2007.

7 List of Acronyms and Abbreviations

$USD	United States Dollar
°C	degrees Celsius
°F	degrees Fahrenheit
ADA	ADA-ES Inc.
APH	air preheater
Aux	auxiliary
BASE BN	current ADAsorb™ system model derived for this project
BN	one of the two sorbents modeled
Btu	British thermal units
Cap.	Capture
Circ	circulation
CO	Colorado
CO_2	carbon dioxide
COE	cost of electricity
Comp	compression
Cond	condenser
CW	cold water
DOE	United States Department of Energy
Eff	efficiency (The effectiveness of any XHTX utilized)
ESP	electro static precioitator
FD	forced draft
FGD	flue gas desulfurization unit
FWH0	feed water heater added for heat integration
H_2O	water
HHV	higher heating value
HI ALL	All four heat integration options are considered simultaneously.
HI FG AIR	Heat integration option where heat from the flue gas cooler is used to pre-heat boiler combustion air.
HI FG FWH	Heat integration option where heat from the flue gas cooler is used to heat boiler feedwater through the addition of FWH0.
HI FWH	Heat integration option where heat from the compressors is utilized in heating the boiler feedwater through the addition of FWH0.
HI REG	Heat integration option with heat from the CO_2 compressors being utilized in heating the sorbent entering the regenerator.
Hp	horse power
hr	hour
HR	heat rate
HX	heat exchanger
HXTX	cross heat exchanger
ID	induced draft

IOU	a signed document acknowledging a debt
IP	intermediate pressure
IRROE	internal rate of return on equity
K	Kelvin
KO	knock out
kW	kilowatt
kWh	kilowatt hour
Lb	pound
LCOE	levelized cost of energy
Lean Sorbent	sorbent not loaded with CO_2
Lehigh	Energy Research Center at Lehigh University
LP	low pressure
m	meter
MEA	monoethanolamine
Mlb	million pounds
MMBtu	million British thermal units
MOFs	metal organic frameworks
MW	megawatt
MW_{net}	power plant megawatt net output
ND	North Dakota
NEPA	National Environmental Policy Act
NETL	United States National Energy Technology Labratory
O_2	oxygen
OJ	one of the two sorbents modeled
OPTI	Modeling case without XHTX or heat integration at optimal adsorber and regenerator operating temperatures.
PC	pulverized coal
PCCC	post combustion carbon capture
PM	particulate matter
PMP	project management plan
PRB	Powder River Basin cola
psia	pounds per square inch absolute
REGEN	regenerator
Rich Sorbent	sorbent which has been loaded with CO_2
SO_2	sulphur dioxide
Solex	Solex Thermal Science
TEA	Techno Economic Analysis
Technip	Technip Stone and Webster Process Technologies
TS&M	CO_2 transportation, storage, and monitoring
W	watt
ΔHR	change in heat rate
ΔP	change in pressure

8 Appendix

Thermo-Economic Analysis of ADA Solid Sorbent CO_2 Capture System: Effects of Sorbent Properties and Waste Heat Integration

Aspen Plus Model of ADA Solid Sorbent CO_2 Capture System

Investigation on Flue Gas & Condensing Heat Exchanger (CHX) Cooling Water Cooling Processes and CHX Design

Thermo-Economic Analysis of ADA Solid Sorbent CO_2 Capture System: Effects of Sorbent Properties and Waste Heat Integration

DE-FE0012914

Thermo-Economic Analysis of ADA Solid Sorbent CO_2 Capture System: Effects of Sorbent Properties and Waste Heat Integration

Prepared for:

ADA-ES, Inc.

Sharon Sjostrom
William Morris
Jayson Denney
Maryam Sayyah

Prepared by:

Joshua Charles
Edward Levy

Energy Research Center
Lehigh University
117 ATLSS Drive
Bethlehem, PA 18015

August 26, 2015

LEHIGH UNIVERSITY
ENERGY RESEARCH CENTER

Index

List of Figures

List of Tables

1. Introduction

ADA Environmental Solutions has developed a second generation CO_2 capture system for use on the backend of existing or new coal-fired generation facilities. The ADA system is based on a solid sorbent, which adsorbs CO_2 at a low temperature and is regenerated (releases CO_2) at an elevated temperature. Both the adsorber (ADS) and regenerator (REG or stripper) of this system are designed as fluidized beds, where flue gas and recycled CO_2 are the respective fluidizing fluids. Previous modeling by the Energy Research Center (ERC) has shown that through changes to this capture system, overall plant performance can be improved significantly [1,2]. The present work re-examines these results and looks at not only the thermodynamic impact of changes to the capture system but also the economics of such changes. Where possible, the methodology follows that previously set forth by NETL [3] and previously used by ADA [4]. Calculating the actual economic return of a plant (or modification to a plant) throughout its lifetime requires that not only capital costs of the plant or equipment be considered, but also labor, engineering costs, financing fees, interest, depreciation, and inflation among many other factors. This report describes the methods used to estimate the economics of a supercritical pulverized coal plant equipped with carbon capture and summarizes the results for ADA's solid sorbent CO_2 capture system. The effects of integration of waste heat and changes in sorbent characteristics are also shown.

2. Capital Costs

Capital costs refer to the construction costs of a plant or equipment added to it and their determination is the first step in any economic consideration. NETL defines the following four levels of capital costs: The Bare Erected Cost (BEC), the Total Plant Cost (TPC), the Total Overnight Capital Cost (TOC), and the Total As-Spent Capital Cost (TASC). Figure 1 illustrates these four levels of capital costs.

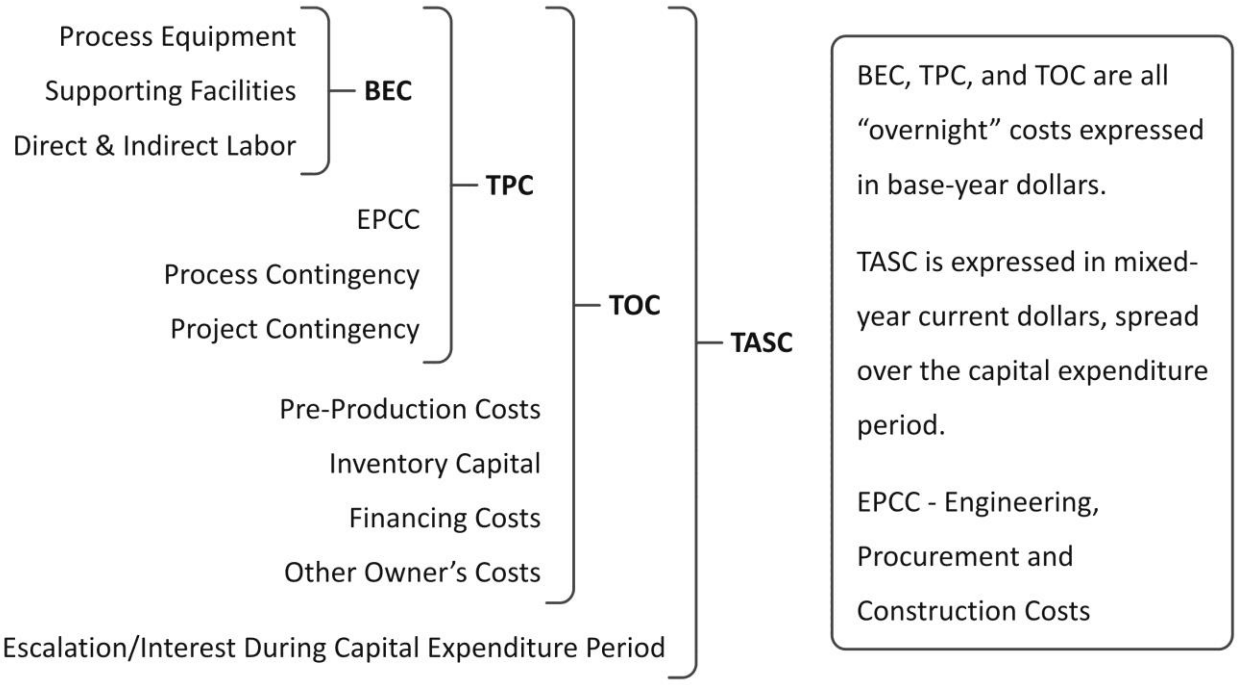

Figure 1: Capital Cost Levels as Defined by NETL [3]

Bare Erected Costs

The BEC includes the cost of equipment, facilities, and infrastructure to support the plant as well as construction and/or installation labor costs. BEC is calculated using base-year (first year of construction) dollars and does not include project contingencies or engineering costs.

Total Plant Costs

Total plant costs include the BEC plus engineering and contingency costs. Engineering, procurement, and construction costs (EPCC) are assumed as part of the TPC and are generally expressed as a function of the BEC. The EPCC includes the BEC plus engineering, procurement, design, contracting, and contractor permitting costs. For the analyses in this report, EPCC costs are assumed to be equal to 9.4% of the BEC costs.

In addition to the EPCC, the TPC includes any contingencies in base-year dollars. Contingencies are typically built into any capital intensive project to protect against significant cost overruns. DOE suggests that contingencies be separated as process contingencies and a project contingency. A process contingency is applied to a process within the scope of the project, which may require a greater level of

price margin. Typically, a process contingency is to cover unforeseen expenses in the commercial implementation of a process not previously commercially implemented. DOE guidelines for process contingency rates (as a percentage of the BEC) are presented in Table 1 for various stages of technology development. Since ADA has test data from their pilot-scale system, the process contingency for the ADA CO_2 capture system is assumed to be 20% of the BEC.

Table 1: DOE Guidelines for Process Contingencies

Technology Status	Process Contingency (% of Associated Process Capital)
New Concept with limited data	40 +
Concept with bench-scale data	30 - 70
Small pilot plant data	20 - 35
Full-sized modules have been operated	5 - 20
Process is used commercially	0 - 10

A project contingency covers the budgeting of the entire project. This contingency is typically 15 to 30% of the sum of the BEC, EPCC fees, and any process contingencies [3]. In this report, a project contingency of 15% of the sum of BEC, EPCC and ADA plant process contingency was assumed.

Total Overnight Cost

The Total Overnight Cost (TOC) includes the TPC plus any additional overnight costs, including the owner's costs. Owner's costs include project financing costs, pre-production costs, and any inventory capital needed before production begins. An overnight capital cost refers to the hypothetical cost of completing a construction project overnight. An overnight cost does not include interest incurred during construction or escalation of material and labor costs during construction.

Total As-Spent Cost

The Total As-Spent Cost (TASC) includes the TOC plus any additional expenses due to financing interest during construction as well as escalation of materials and labor costs during this period. Typically, a multiplier is applied to the TOC in calculating the TASC. For a high-risk project by an investor-owned utility where the construction period is five years, the TASC multiplier is assumed to be 1.14. This

is the assumption made for the projects outlined in this report. Table 2 presents a breakdown of the capital cost structure and basic assumptions used throughout this report.

Table 2: Breakdown of Capital Cost Structure

Level	Cost	Estimate Basis
Bare Erected Cost (BEC) Overnight Cost in Base-Year Dollars	Process Equipment Support Facilities (e.g. Offices, Labs) Total Labor for Construction and/or Installation	
Total Plant Cost (TPC) Overnight Cost in Base-Year Dollars	BEC Engineering, Procurement and Construction Cost (EPCC) Process Contingency Project Contingency	 9.4% of BEC for PC Plant 9.56% of BEC for Capture System 20% of Process Capital Cost (PCC) for Components Connected to ADA Capture System. 0.11% of PCC for Established PC Plant Processes & CO_2 Comp. 20% of Sum of BEC, EPC, and Process Contingency for Capture System. 12% for existing PC Plant components
Total Overnight Cost (TOC) Overnight Cost in Base-Year Dollars	TPC Pre-Production Costs Inventory Capital Financing Costs Other Owner's Costs	 3% of TPC 1.87% of TPC 15% of TPC
Total As-Spent Cost (TASC) Mixed-Year Current Dollars Over Capital Expenditure Period	TOC Escalation/Interest During Capital Expenditure Period	 1.140 Multiplier for High-Risk Investor-Owned Utility (IOU) Over Five-Year Capital Expenditure Period

3. Existing Plant and Equipment

This project assumes the addition of equipment to a pulverized coal (PC) plant equipped with the ADA CO_2 capture system. Therefore, the PC plant, base ADA CO_2 capture system without a cross heat exchanger (XHTX) or other form of heat integration, and CO_2 compression system are considered as existing equipment and will be priced independently of equipment added to improve the performance of the plant.

PC Plant

The PC plant described in this report is a supercritical steam cycle operating at a steam temperature of 1,000°F. A similar plant is presented by DOE in the report, Cost and Performance Baseline for Fossil Energy Plants – Volume 1, Revision 2a [5]. The plant described in Ref. 5 is connected to a MEA post-combustion CO_2 capture system and produces 550 MW_e net with a gross turbine cycle power of 663 MW. Table 3 presents cost information (BEC) for a PC Plant equipped with an MEA CO_2 capture system, where the cost of the CO_2 capture system is not included. This information, presented in 2007 dollars in Ref. 5, has been scaled by the authors of the present report to 2015 dollars at an annual inflation rate of 2.95%. Since the DOE methodology normalizes a plant's net electrical output to 550MW_e, the size of the PC plant varies with respect to the auxiliary power load of any CO_2 capture system added to the plant. As a result, in the present report, gross turbine power serves as the basis for scaling the PC plant BEC with plant size. This results in a total BEC for the bare PC plant (not inclusive of the CO_2 capture and compression system) of \$1,759/kW_{gross}.

Table 3: BEC for PC Plant Equipped With MEA Capture System, Excluding Capture System Costs [5]

Item	BEC [$1000] (2007)	BEC [$1000] (2015)	BEC [$/kW$_{gross}$] (2015)
Coal & Solvent Handling	37,517	47,341	71
Coal & Solvent Prep & Feed	17,942	22,640	34
Feedwater & Misc. Systems	80,700	101,832	154
PC Boiler & Accessories	305,822	385,904	582
Flue Gas Cleanup	135,517	171,003	258
Ductwork & Stack	30,383	38,339	58
Steam Turbine Generator	108,222	136,561	206
Cooling Water System	49,106	61,965	93
Ash/Spent Solvent Handling Systems	12,497	15,769	24
Accessory Electric Plant	66,060	83,358	126
Instrumentation & Control	20,174	25,457	38
Improvements to Site	11,921	15,043	23
Buildings & Structures	48,301	60,949	92
Total Cost	924,162	1,166,162	1,759

Existing ADA CO_2 Capture System

ADA [4] provided costing information for their base CO_2 capture system. During the present modeling effort, the ERC found that this existing ADA system did not adequately take into consideration the cooling requirements of the system. For some configurations, the flue gas is cooled to temperatures well below 100°F in both a flue gas cooler upstream of the capture system adsorber and throughout the adsorber beds. Even for the higher temperature cases considered, flue gas temperatures just above 100°F are required. Such low temperatures would necessitate the use of refrigeration systems in most locations. Figure 2 illustrates the solid sorbent capture system as presented by ADA before the addition of cooling system components, a XHTX, a regenerator heater, or a CO_2 compression system.

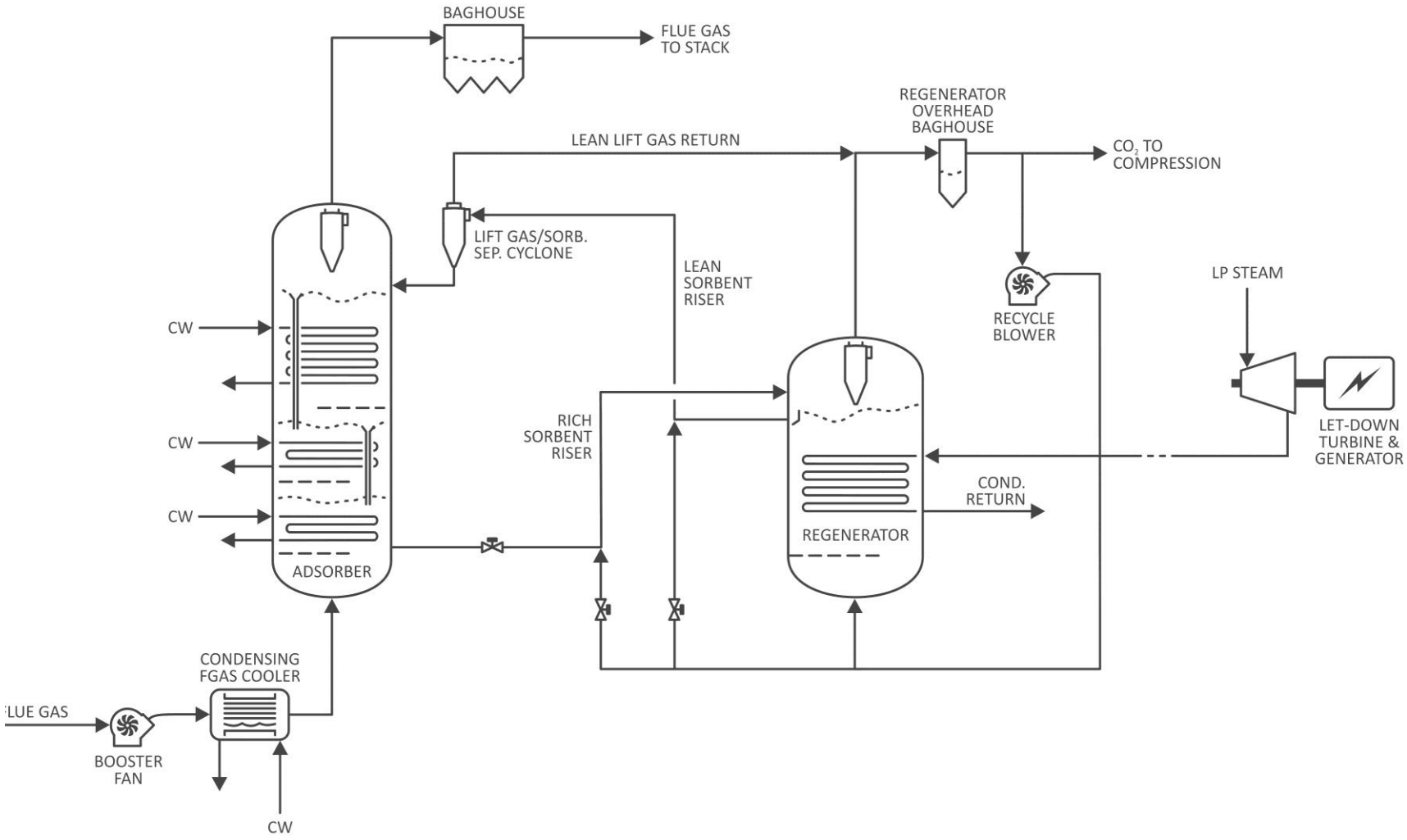

Figure 2: CO_2 Capture System as Presented by ADA

Costing information for the ADA CO_2 capture system is found in Ref. 4 for two separate cases, the Sorbent 1 and Sorbent 2 case. As seen in Figure 2, the ADA CO_2 capture system includes a flue gas cooler and let-down turbine, both of which are priced separately in this report. However, in Ref. 4 these pieces of equipment are included as part of the total system price. Therefore, the capture system BEC from Ref. 4 must be adjusted by subtracting the cost of these two pieces of equipment from the BEC as presented by ADA.

Since the flue gas cooler is sized based on the flue gas flow rate, a correlation between the coal mass flow rate and flue gas flow rate ($\dot{m}_{FGAS} = 13.625\ \dot{m}_{coal}$) was used to estimate the flue gas flow rate for the cases in the ADA report [4]. Using this correlation, an estimated flue gas mass flow rate of 7,433,541lb/hr was found. For this flow rate and a flue gas inlet temperature of 219°F, costing results by the ERC [6] suggest an installed cost of $13.37 million (2015 dollars) for the flue gas cooler.

The let-down turbine is sized based on its power generation. As will be shown, a BEC of $550/kW is suggested for pricing a let-down turbine. Since the turbine presented by ADA has a net output of 47,369kW, the BEC of this turbine-generator unit is assumed to be $26.05 million in 2015 dollars.

By subtracting the BEC's of the FGAS cooler and let-down turbine from the ADA capture system costs presented in **Error! Reference source not found.**, the BEC of the ADA capture system without these components can be found. **Error! Reference source not found.** Table 4 presents this adjusted BEC value for the ADA CO_2 capture system without a FGAS cooler and let-down turbine.

Table 4: BEC of ADA CO_2 Capture System With Adjustments

	Year	BEC [$1000]	Sorbent Flow Rate [lb/hr]
Sorbent 1 Case*	2011	215,149	
Sorbent 2 Case*	2011	552,379	16,610,220
Average & Scaled to 2015 Dollars	2015	431,092	
BEC of FGAS Cooler		13,373	
BEC of Let-Down Turbine		26,053	
BEC of ADA Capture System w/o FGAS cooler & Let-Down Turbine			
[$1000]		391,666	
[$/($lb_{SORB}$/hr)]		23.58	

*Cases from Ref. 4 in 2011 dollars

Cost information, such as that presented in Table 4, is for an ADA capture system of a particular size, which removes a specific quantity of CO_2 from the flue gas. Since the PC plant model is fixed to $550MW_{net}$, the quantity of coal fired varies as auxiliary power loads change. The flue gas flow rate varies accordingly, which changes the quantity of CO_2 needed to be captured. The sorbent flow rate is directly proportional to the CO_2 removal rate, which means that the sorbent flow rate can serve as the scaling factor for the ADA capture system. However, not all of the ADA capture system cost is directly linked to the sorbent flow rate. It is assumed in the present report that manufacturing and installation costs remain constant regardless of the size of the system. Furthermore, the assumption is made that one half of the ADA capture system costs presented in Table 5 are manufacturing and installation costs (labor), while the remaining half are variable, or material, costs. By dividing the BEC for the variable costs by the sorbent flow rate, a BEC for the variable cost portion of the ADA capture system of $\$11.79/(lb_{SORB}/hr)$ is found. The fixed cost portion of the BEC is assumed to be $195,833,000 regardless of the sorbent flow rate. Table 5 presents these calculations and the resulting BEC for the ADA CO_2 capture system.

Table 5: BEC of ADA CO_2 Capture System & Scaling Assumptions (Based on Ref. 4)

	Year	BEC [$1000]	Sorbent Flow Rate [lb/hr]	BEC [$/($lb_{SORB}$/hr)]
ADA Capture System w/o FGAS Cooler & Let-Down Turbine	2015	391,666	16,610,220	23.58
Fixed Cost (Labor)	2015	195,833	-	-
Variable Cost (Material)	2015	195,833	16,610,220	11.79

4. New Equipment Construction Costs

Determining realistic equipment and installation costs for any project is key to a useful economic assessment. In this report, various additions and re-configurations were made to the ADA solid sorbent CO_2 capture system and associated PC plant. Figure 3 illustrates all of the components assumed to be added to the PC plant and ADA capture system in the present report. New systems are shown in blue. In the steam turbine cycle, the addition of a let-down turbine and generator is considered along with the addition of a new feedwater heater (FWH0) upstream of the first existing feedwater heater. The addition of an air heater is also considered upstream of the boiler. For the ADA capture system, a flue gas cooler and its associated systems are considered. These systems include pumps to circulate cooling water, cooling towers, and a refrigeration system to further cool the cooling water. The addition of three similar cooling water and refrigeration systems is also considered for adsorber cooling. A significant portion of the thermodynamic analyses in this report centered on the addition of a cross heat exchanger (XHTX) to exchange heat between the CO_2-rich and lean streams circulating sorbent between the adsorber and regenerator. The addition of a heat exchanger in the CO_2-rich stream upstream of the regenerator (Regen. Heater) is also considered as this has been shown to be a viable destination for waste heat from the CO_2 compression system. The entire CO_2 compression and cooling system is also considered, complete with associated pumps and cooling towers.

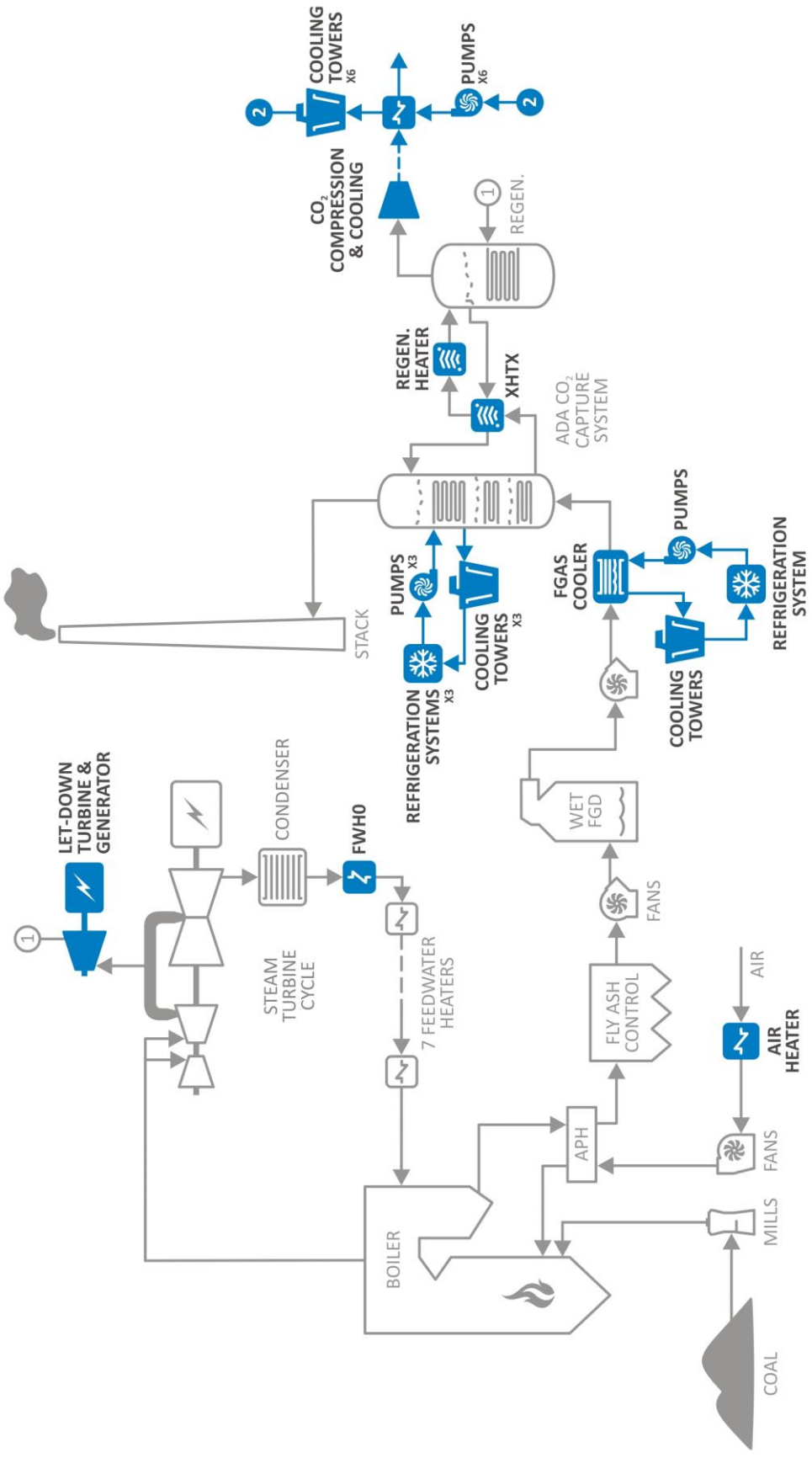

Figure 3: PC Plant with ADA CO_2 Capture System and Additional Equipment Considered

Let-Down Turbine and Generator

The let-down turbine is used to extract useful heat from the low pressure steam before it is sent to the regenerator. Not only does this allow for a greater net power generation, but it also helps to control the steam temperature, which can damage the sorbent at high temperatures. This turbine is known as a back-pressure turbine as superheated steam exits the turbine at a pressure above the condensation pressure. Table 6 presents costing information for a back-pressure turbine scaled to 2015 dollars. Installed costs (equivalent to the BEC) are assumed to be equal to equipment costs plus 75% as recommended by Ref. 7. From the broad range of installed costs suggested in Table 6, a BEC of $550/kW is assumed as the let-down turbine and generator installed cost.

Table 6: Let-Down Turbine Cost Estimate

Year	Equipment Costs [$/kW]	BEC [$/kW]	Turbine Size [MW]	Source
2004	200.00	350.00	-	[7]
2006	216.24	378.41	45	[8]
2015	392.00	686.00	15	[9]
2015*	218.23	481.90	-	[7]
2015*	280.91	491.59	45	[8]

*Scaled at 2.95% annual increase in material cost.

FWH0

It is assumed that any feedwater heating by waste heat takes place through the addition of a feedwater heater (FWH0) upstream of the existing seven feedwater heaters in the supercritical cycle. The existing steam cycle feedwater heaters are steam/water heat exchangers, while this new feedwater heater uses hot water to heat the feedwater. The RSMeans online equipment cost estimation database (Costworks) [10] was not able to provide costing information for a shell and tube water/water heat exchanger at the required flow rates, but it did supply costing information for a shell and tube heat exchanger at lower flow rates as well as a plate-type heat exchanger at higher water flow rates. Figure 4 presents total installed cost for both of these heat exchangers with respect to the water flow rate. These costs are the O&P values (Total installed costs with contractor overhead and profit included) taken from the RSMeans Costworks database [10]. It is suggested that total installed cost (BEC) will lie somewhere

between the costs for these two heat exchangers due to the high cost of the copper tubes for the shell and tube heat exchanger and the lower cost of plate-type heat exchangers. To provide some pricing margin due to these uncertainties, a BEC at the top of the pricing range, $150/gpm, is assumed for the new FWH0.

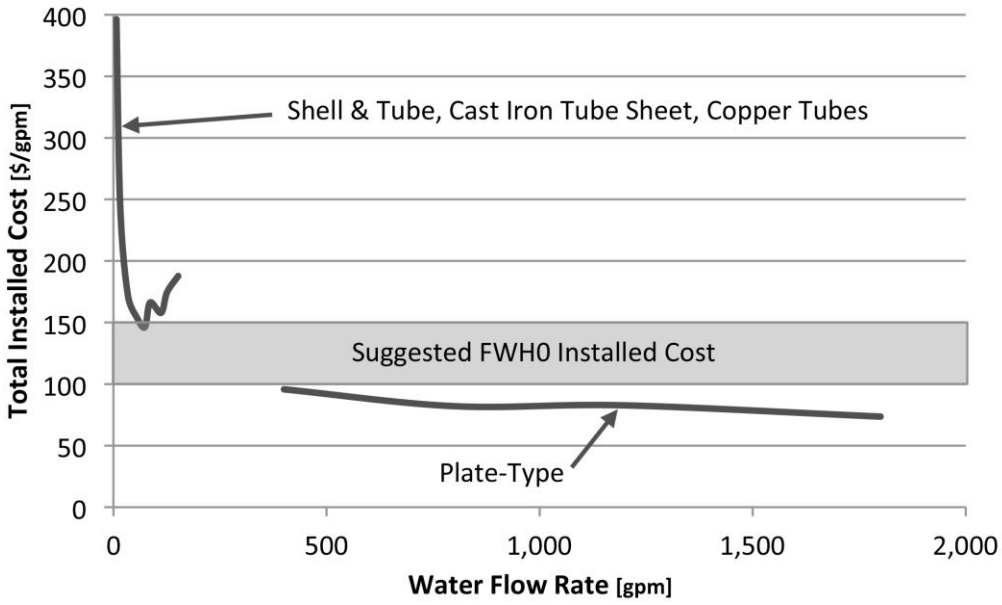

Figure 4: Estimated Costing for New FWH0 [10]

Air Heater

One destination for waste heat from the FGAS cooler is a combustion air heater added upstream of the boiler. This heat exchanger is assumed to be a tubular liquid/gas heat exchanger operating in a counter-flow arrangement. The tubes are located inside of an existing air duct upstream of the forced-draft fans. Figure 5 shows a side view of the proposed air heater. Cool air enters the duct with a temperature T_{a1} and leaves at an elevated temperature of T_{a2}. The hot water enters at the hot end of the heat exchanger at a temperature T_{w1} and leaves at the cool end at a temperature of T_{w2}. A 10°F temperature approach between T_{w1} and T_{a2} is assumed at the hot end as well as between T_{w2} and T_{a1} at the cold end.

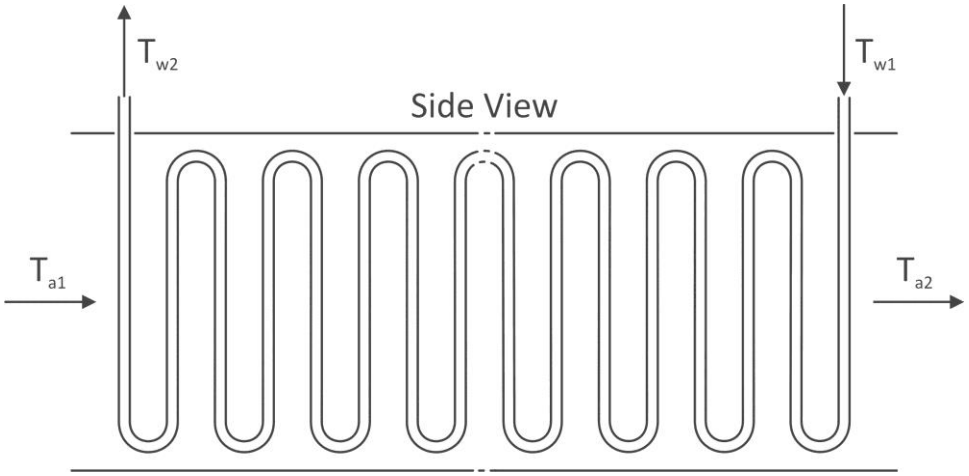

Figure 5: Side View of Proposed Combustion Air Heater

The temperatures of both water and air entering and leaving the air heater can be used to find the log-mean temperature difference (ΔT_{LMTD}) through the following equation:

$$\Delta T_{LMTD} = \frac{(T_{w2} - T_{a1}) - (T_{w1} - T_{a2})}{ln\left(\frac{T_{w2} - T_{a1}}{T_{w1} - T_{a2}}\right)}$$

This ΔT_{LMTD} value is used to find the heat transfer area of the heat exchanger through the following simplified heat transfer equation:

$$q = U\ A\ F\ \Delta T_{LMTD}$$

Where q is the heat duty of the heat exchanger, U is the overall heat transfer coefficient, A is the heat transfer surface area, and F is an arrangement factor (assumed to be 1 for this case [11]). U is calculated by using the convective heat transfer coefficients of both the water (h_i) and air (h_o) as well as the inside (i) and outside (o) diameters (d) of the tubes [11]:

$$U = \frac{h_i h_o}{h_i + h_o \frac{d_o}{d_i}}$$

Calculation of the heat transfer coefficients is not as straight forward, but can still be estimated relatively easily. In order to make these calculations, several assumptions must be made about the air heater. First, a square tube arrangement is assumed, as seen in the top-down view of the heat exchanger in Figure 6. Not only does Figure 6 show the top-down configuration of the heat exchanger, but also the critical parameters needed to determine the gas-side heat transfer coefficient, h_o.

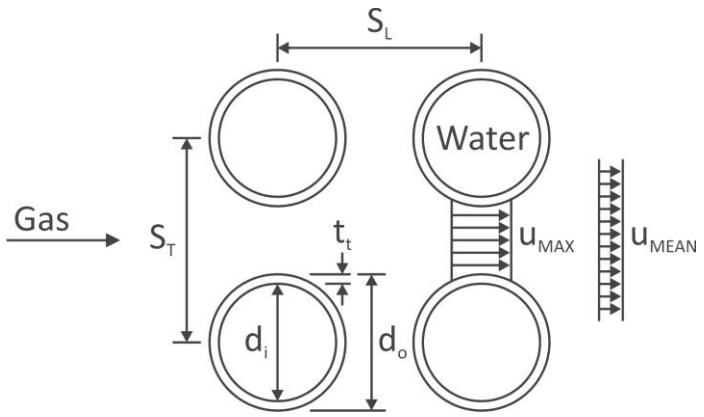

Figure 6: Top View of Proposed Combustion Air Heater

The heat-transfer characteristics of a gas flowing through a tube bundle with greater than 10 rows of tubes can be calculated from [12]:

$$Nu = \frac{h_o d_o}{k} = C\left(\frac{u_{MAX} d_o}{v}\right)^n Pr^{1/3}$$

where Nu is the Nusselt number for the gas flow, k is the thermal conductivity of the gas, C and n are constants, which depend on tube configuration, u_{MAX} is the gas velocity in the gap between tubes, v is the kinematic viscosity, and Pr is the gas Prandtl number. u_{MAX} is a function of u_{MEAN} and the values of d_o and S_T through the following equation:

$$u_{MAX} = u_{MEAN}\frac{S_T}{S_T - d_o}$$

Table 7 shows the assumptions used to calculate the heat transfer coefficient on the air (gas) side of the combustion air heater. The National Institute of Standards and Technology (NIST) have

compiled fluid transport and thermodynamic information in their Refprop database. Refprop was used to find v, Pr, and k values for air at the inlet (77°F) and outlet (118°F) temperatures of the heat exchanger. Average values of these inlet and outlet values were used to approximate the value across the entire heat exchanger. Using these assumptions and the equations above for heat transfer across tubes in a tube bank, an h_o value of 33.7 Btu/hr°F ft^2 was calculated.

Table 7: Assumptions for Calculation of Air-Side Heat Transfer Coefficient

	Units	Value
d_o	in	2.375
t_t	in	0.154
S_T	in	3.5625
S_L	in	3.5625
u_{MEAN}	ft/s	50
u_{MAX}	ft/s	150
$v_{77°F}$	ft^2/s	1.6762×10^{-4}
$v_{118°F}$	ft^2/s	1.9106×10^{-4}
v_{AVG}	ft^2/s	1.7934×10^{-4}
$Pr_{77°F}$	-	0.70730
$Pr_{118°F}$	-	0.70462
Pr_{AVG}	-	0.70596
$k_{77°F}$	Btu/hr°F ft	0.015175
$k_{118°F}$	Btu/hr°F ft	0.016144
k_{AVG}	Btu/hr°F ft	0.015660
C	-	0.278
n	-	0.620

For the flow of water through the tube, a fully-developed turbulent flow is assumed. Reference 13 presents the following equation for calculating the heat transfer of a fully-developed turbulent flow in a pipe:

$$Nu = \frac{h_i d_i}{k} = C\left(\frac{u d_i}{v}\right)^{0.8} Pr^n$$

u is not given directly, but is instead calculated from the mass flow rate of water, the density of water entering the heat exchanger, the inner tube dimensions, and the number of tubes:

$$u = \frac{\dot{m}_{water}}{\rho \, A_{xs\,tube} \, n_{tubes}}$$

where $\dot{m}_{water}$ is the total mass flow rate of water used for combustion air heating, ρ is the water density entering the heat exchanger, $A_{xs\,tube}$ is the interior cross-sectional area of a single tube, and n_{tubes} is the number of tubes. Using the dimensions previously shown in Figure 6, and assuming a duct width of 40 feet, a total of 134 tubes would be needed to cover the width of the duct. An average mass flow rate was found using previously calculated Aspen Plus results. Table 8 presents all of the assumptions used with the heat transfer equations in calculating the heat transfer coefficient for the water-side of the tubes.

The assumptions in Table 8 are used along with the water-side heat transfer equations to arrive at a h_i value of 528.9 Btu/hr°F ft^2. With h_o and h_i known, the overall heat transfer coefficient, U can be easily calculated as 31.4 Btu/hr°F ft^2. Using this overall heat transfer coefficient, the heat exchanger heat transfer surface area (A) can be found if the heat duty and ΔT_{LMTD} are known:

$$A = \frac{q}{U \, \Delta T_{LMTD}}$$

This area is assumed to be equal to the outside surface area of the tubes in the heat exchanger and it can be used to find the length of steel tubing needed in the heat exchanger. Previous work by the ERC [13] has shown that the installed cost (fabrication and installation labor costs plus the material costs) of a similar heat exchanger can be estimated as a function of the tube material cost. As the size of a heat exchanger increases, the ratio of material costs rises relative to the labor costs. Eventually, for a standard carbon steel heat exchanger, the costs plateau where labor costs are approximately three times greater than the tubing material costs. Reference 14 added an extra 30% to this factor, bringing the total manufacturing and installation labor costs to 3.90 times the tube material costs.

Table 8: Assumptions for Calculation of Water-Side Heat Transfer Coefficient

	Units	Value
d_i	in	2.047
$A_{xs\ tube}$	in^2	3.291
w_{duct}	ft	40
n_{tubes}	-	134
$\dot{m}_{water}$	lb/hr	1,482,286
$\rho_{128°F}$	lb/ft^3	61.585
$v_{128°F}$	ft^2/s	5.6443×10^{-6}
$v_{87°F}$	ft^2/s	8.5192×10^{-6}
v_{AVG}	ft^2/s	7.0818×10^{-6}
$Pr_{128°F}$	-	3.3580
$Pr_{87°F}$	-	5.3527
Pr_{AVG}	-	4.3554
$k_{128°F}$	Btu/hr°F ft	0.37250
$k_{87°F}$	Btu/hr°F ft	0.35571
k_{AVG}	Btu/hr°F ft	0.36411
C	-	0.023
n	-	0.4

Prices for steel tubing were obtained from Columbia Pipe & Supply Company [14]; effective May 2015. It is assumed that a galvanized steel tube is more appropriate for this application than black steel. The estimated cost per foot for 2" schedule 40 pipe (2.375" OD, 2.047" ID) with plain ends is $12.11. If T-304 stainless steel were used instead, the price would rise to $32.02/ft or 2.64 times the carbon steel price. This is consistent with a suggested cost ratio between carbon steel and stainless steel of 2.8 [13]. Since the combustion air heater is operating in an environment with little corrosive potential, the galvanized steel price of $12.11/ft is used. After, multiplying by 3.9 to find the manufacturing and installation labor costs and adding this number to the tube cost, a total installed cost of $59.34/ft results.

FGAS Cooler – Condensing FGAS Heat Exchanger

The Energy Research Center's (ERC) condensing flue gas heat exchanger model was used to calculate the operating characteristics of a flue gas cooler. This model not only calculates the required surface area of the heat exchanger, but also provides a cost estimate for it. These results are presented in the previous report for ADA, Investigation on Flue Gas & Condensing Heat Exchanger (CHX) Cooling Water Cooling Processes and CHX Design [6]. Figure 7 presents these FGAS cooler cost results (equivalent to BEC) for three different FGAS cooler inlet temperatures. Below a temperature of 100°F, the cost is seen to drop significantly. This is the result of a decrease in heat exchanger surface area due to a decrease in the cooling water temperature below 100°F. Since the typical FGAS inlet temperature is 219°F, total installed cost for the FGAS cooler lies between \$0.8/(lb_{FGAS}/hr) and \$1.8/(lb_{FGAS}/hr).

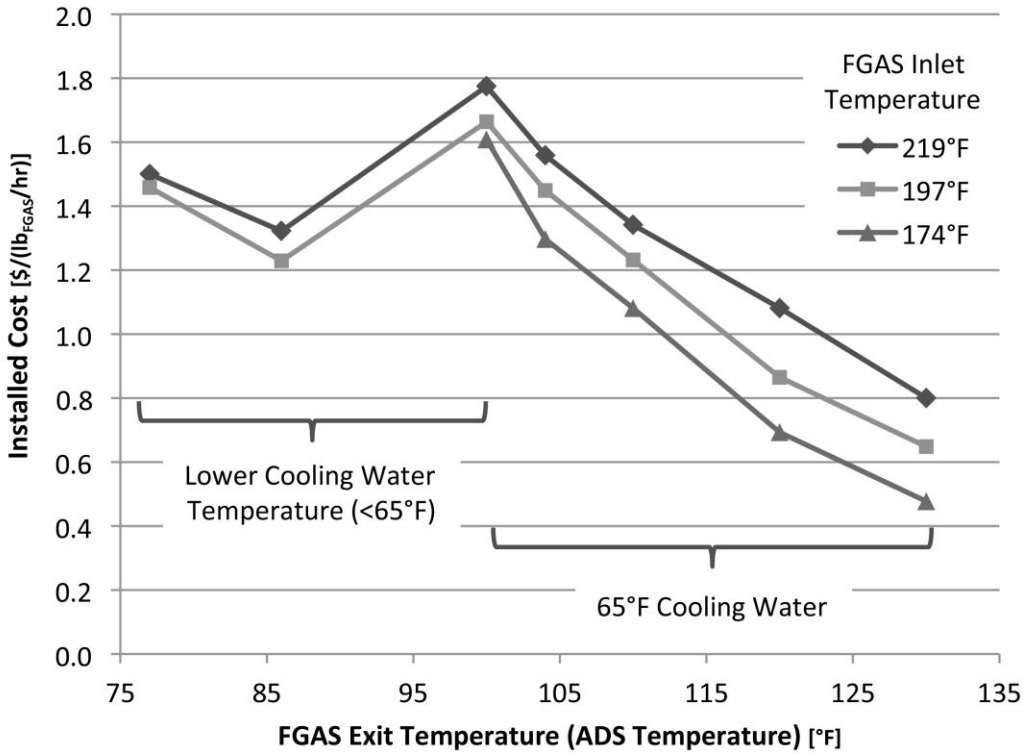

Figure 7: FGAS Cooler Installed Cost vs. ADS Operating Temperature [6]

Cooling Water Circulation Pumps

Pumps are used to circulate cooling water in the flue gas cooling system, the adsorber cooling systems, and through the CO_2 compression intercoolers and cooling towers. Figure 8 presents total

installed cost (BEC) for cast iron turbine pumps across varying fluid flow rates. These costs are the O&P values taken from the RSMeans Costworks database [10]. At flow rates greater than 1,000 gpm, total installed cost approaches $8/gpm, and as the flow rate increases to 10,000 gpm the BEC drops to $4.44/gpm.

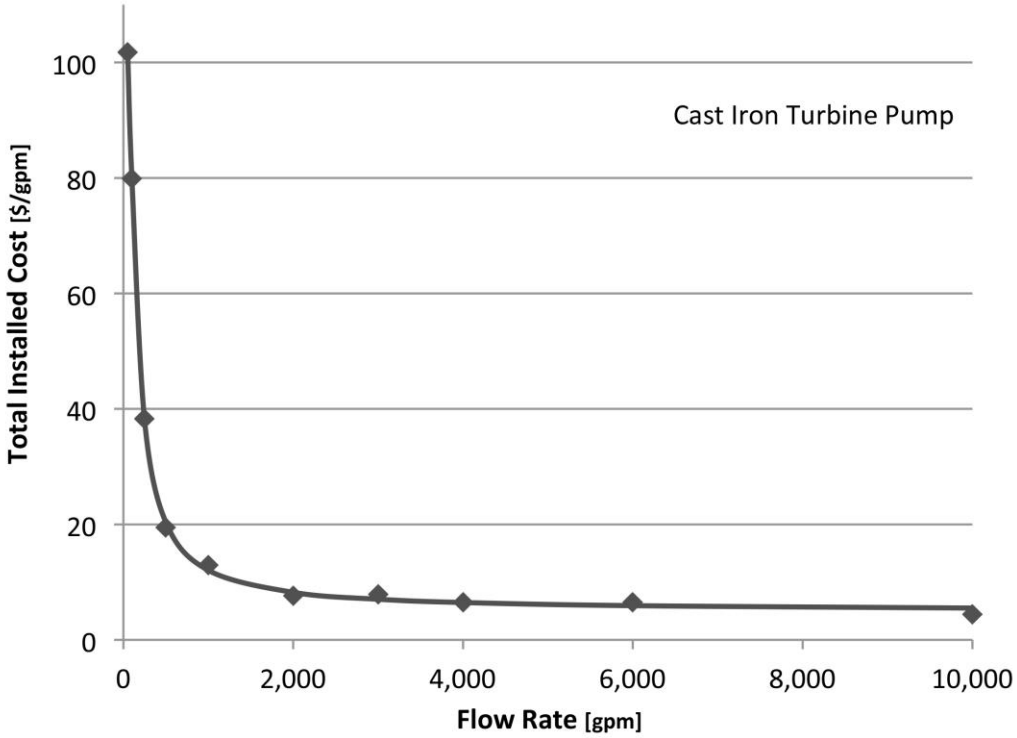

Figure 8: Cast Iron Turbine Pump Total Installed Cost [10]

Refrigeration Cycles

Refrigeration cycles are used to cool the cooling water entering both the flue gas cooler as well as the adsorber cooling water loops. For cost estimation purposes, a centrifugal type water chiller cycle was assumed. Figure 9 presents total installed costs for this type of refrigeration cycle with respect to tons of cooling. As was the case with the pumps, these prices are the O&P estimates from the RSMeans Costworks database [10]. A typical installed cost of $360/ton cooling was assumed for the refrigeration cycles.

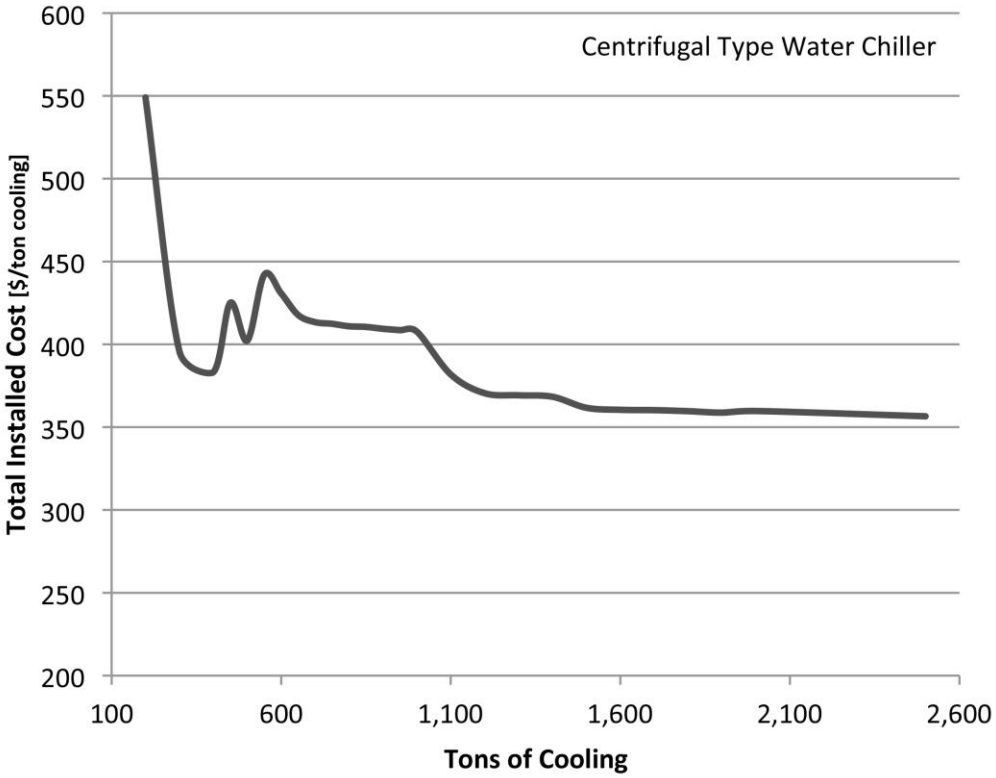

Figure 9: Centrifugal Type Water Chiller Total Installed Cost [10]

Cooling Towers

As Figure 3 illustrates, cooling towers are required to cool the cooling water loops for the flue gas cooler, the three adsorber beds, and CO_2 compressor intercoolers. The RSMeans Costworks database [10] was utilized in finding O&P costs for a galvanized steel, induced draft, axial fan cooling tower. Total installed costs (BEC) are assumed to be equal to the Costworks O&P costs and are presented in Figure 10. As the cooling load of the tower increases above 400 tons of cooling, total installed costs with pumps and piping is seen to average around $275/ton cooling.

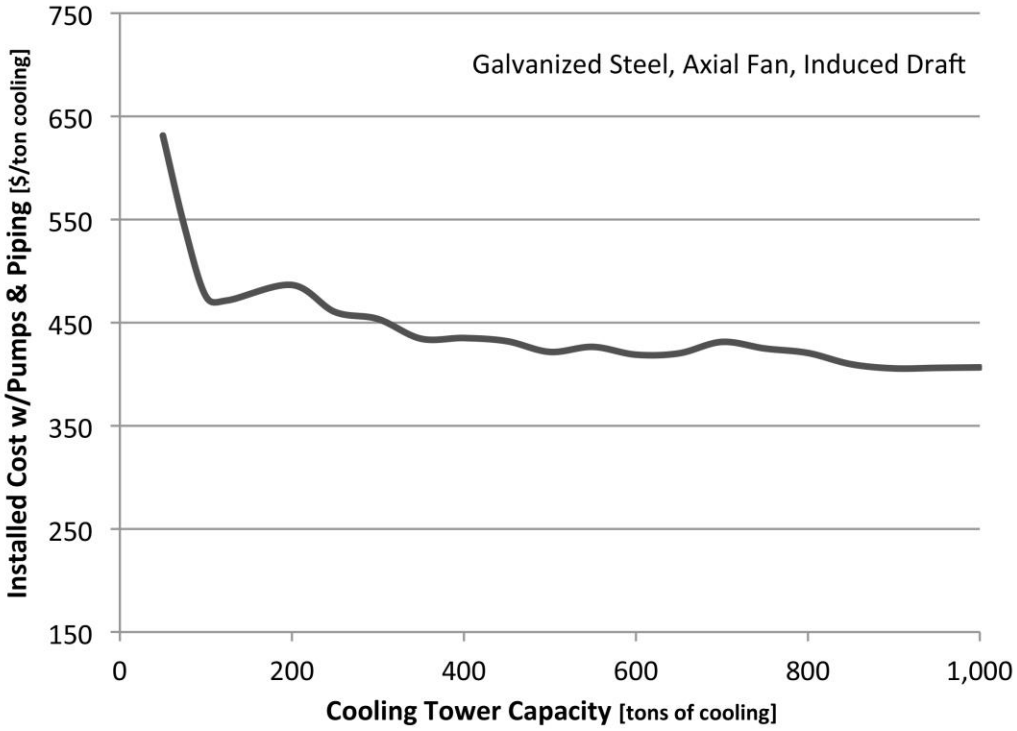

Figure 10: Induced Draft, Axial Fan, Cooling Tower Total Installed Cost [10]

CO_2 Compression System

Cost estimates of the CO_2 compression system were obtained from both the previous ADA solid sorbent report [4] and the DOE's Cost and Performance Baseline for Fossil Energy Plants – Volume 1 [5]. Table 9 presents these costing estimates for the CO_2 compression system along with their values scaled to 2015 dollars. As seen, the BEC varies between \$34.22/(lb_{CO2}/hr) and \$37.72/(lb_{CO2}/hr). An average value of \$36/(lb_{CO2}/hr) is assumed for this report.

Table 9: CO_2 Compression System Cost Estimates

Year	BEC [$/($lb_{CO2}$/hr)]	Compressor CO_2 Flow [lb/hr]	Source
2007	29.89	1,211,096	[5]
2011	30.47	1,165,561	[4] – DOE Methods
2011	30.77	1,165,561	[4] – Experience
2015*	37.72	1,211,096	[5]
2015*	34.22	1,165,561	[4] – DOE Methods
2015*	34.56	1,165,561	[4] – Experience

*Scaled at 2.95% annual increase in material cost.

XHTX

A XHTX was designed and priced for ADA by Solex Thermal Technologies. Solex specializes in bulk solids heating and cooling. A plate-type solid to liquid heat exchanger was designed to transfer heat from the hot CO_2-lean sorbent to a liquid water loop. This heated water is used to heat the coldl CO_2-rich sorbent in a second plate-type liquid to solids heat exchanger. This system of two heat exchangers and an intermediate water loop is the complete XHTX system as presented by Solex.

Table 10 presents XHTX design and costing information (BEC) from Solex. Since the sorbent capacity per unit is well below the total sorbent flow rate of sorbent in the ADA system, it is assumed that multiple Solex XHTX systems (units) would be required to handle the entire sorbent flow rate.

Table 10: Solex Cross Heat Exchanger Design Information

Sorbent Heating Heat Exchanger		
Sorbent Capacity per Unit	lb/hr	2,634,524
Sorbent Temp. In	°F	104
Sorbent Temp. Out	°F	204.08
Water Capacity per Unit	lb/hr	662,710
Water Temp. In	°F	225.5
Water Temp. Out	°F	126.5
Sorbent Cooling Heat Exchanger		
Sorbent Capacity per Unit	lb/hr	2,634,524
Sorbent Temp. In	°F	248
Sorbent Temp. Out	°F	147.92
Water Capacity per Unit	lb/hr	662,710
Water Temp. In	°F	126.5
Water Temp. Out	°F	225.5
XHTX Effectiveness	frac.	0.695
Pump Power per Unit	kW	51.27
BEC per Unit (2 HTX)	$ millions	10.295
BEC per Sorbent Flow	$/($lb_{SORB}$/hr)	3.908

Regenerator Heater

During the heat integration analyses, the addition of a regenerator heater to heat the CO_2-rich sorbent upstream of the regenerator was considered. It is assumed that such a heater would utilize the same design as the liquid to solid Solex XHTX. However, this heater would only consist of a single plate heat exchanger with hot water supplied from a waste heat source. Table 11 presents flow rate and cost information for the regenerator heater designed by Solex. As was the case with the XTHX, as the sorbent and/or water capacity per unit are exceeded, additional units would be added to handle the flow rate.

Table 11: Flow Rate and Cost Information for Regenerator Heater

Sorbent Capacity per Unit	lb/hr	2,634,524
Water Capacity per Unit	lb/hr	662,710
BEC per Unit (1 HTX)	$ millions	5.148
BEC per Sorbent Flow	$/($lb_{SORB}$/hr)	1.954

Fuel Costs

Since a coal-fired plant relies on coal to generate heat, the cost of fuel is critical to any economic analysis. As of May 29, 2015, the U.S. Energy Information Administration [15] quoted the price of a 11,800 Btu/lb Illinois #6 coal at $40.45/ton, or $20.23/klb. This is the price of coal used for all economic analyses in this report.

Sorbent Costs

The costs of the solid sorbent are important not only in pricing the initial fill for the ADA system, but also in accounting for any sorbent leakage or attrition during operation. In their previous report, ADA suggested a sorbent price of $5.62/lb (scaled to 2015 dollars). No sorbent leakage is assumed. However, a sorbent attrition rate of 0.0025% per cycle is taken into account.

Total sorbent fill is not directly equivalent to the sorbent flow rate, but is also a function of the time it takes for the sorbent to make one complete cycle of the system. This cycle time is dependent on the residence times of the adsorber and regenerator as well as that of any XHTX or regenerator heater, which may be added to the cycle. If both the sorbent fill quantity and flow rate are known, an estimate of the time required for the sorbent to complete one circuit of the system can be found. Table 12 presents sorbent fill and flow rates as provided by ADA and Solex and the corresponding cycle times. It can be seen that for the ADA CO_2 capture system without a XHTX or heat integration, a cycle time of only 8.6 minutes was found. It is assumed that for the majority of this time the sorbent is contained in the adsorber and regenerator. Table 12 shows that the addition of a Solex XHTX adds 18.4 minutes to the total cycle time, bringing it to 27 minutes. The further addition of a regenerator heater adds an additional 9.2 minutes to the total cycle time.

Table 12: System Cycle Times With and Without Solex Heat Exchanger Units

ADA System w/o XHTX or Heat Integration	
Sorbent Fill in System [lb]	2,384,000
Sorbent Flow Rate [lb/hr]	16,610,220
System Total Cycle Time [min]	8.6
Sorbent Flow in Solex Heat Exchanger Units	
Sorbent in 16 Solex Units [ft^3]	198,000
Sorbent Density [lb/ft^3]	29.59
Sorbent Fill [lb]	5,858,820
Sorbent Flow Rate [lb/hr]	19,120,000
Time Through Both Sides of XHTX [min]	18.4
System Total Cycle Time [min]	27
Sorbent Flow in Regen. Heater Solex Units (With XHTX)	
Time Through Regen. Heater [min]	9.2
System Total Cycle Time [min]	36.2

With cycle times known, sorbent fill can be calculated from the sorbent flow rate using the following equation:

$$Sorbent\ Fill\ (lb)\ =\ \frac{Cycle\ Time\ (min)}{60\ \left(\frac{min}{hr}\right)}\ \cdot\ \dot{m}_{SORB}\left(\frac{lb}{hr}\right)$$

CO_2 Transportation, Storage, and Monitoring Costs

CO_2 captured by the capture system is assumed to be compressed to a pipeline pressure of 2,215 psia before being piped to an underground sequestration site. There are certain costs surrounding the transport, storage, and continued monitoring of the stored CO_2 (TS&M costs). TS&M costs are assumed to be directly proportional to the quantity of CO_2 captured, with Table 13 showing TS&M costs as presented by ADA and DOE. Two different TS&M costs were presented, with the first based on DOE estimating practice and the second based on experience. By averaging these two values and scaling to 2015 dollars, a TS&M cost of \$2.99/lb_{CO2} was found.

Table 13: TS&M Costs as Presented by ADA & DOE

Year	CO_2 Mass Flow [lb/hr]	CO_2 TS&M [$/klb]	Source	Notes
2007	1,209,902	2.54	[5]	Case 12
2011	1,165,561	2.55	[4]	Sorbent 1 Case
2011	1,165,561	2.58	[4]	Sorbent 2 Case
2015*		2.99		Average value

*Scaled at annual inflation rate of 2.95%

Summary of Costing Assumptions

Table 14 summaries the equipment, fuel, and sorbent cost assumptions outlined above.

Table 14: Summary of Equipment and Fuel Costs for Modified ADA CO_2 Capture System

Equipment	Units	Installed Cost	Source
Let-Down Turbine Generator	$/kW	550	[7,8,9,16]
FWH0	$/gpm	150	[10]
Combustion Air Heater	$/$ft_{tube}$	59.34	[14]
FGAS Cooler	$/($lb_{FGAS}$/hr)	0.8 – 1.8	[6]
Cooling Water Circ. Pumps	$/gpm	4.44	[10]
Refrigeration Cycles	$/ton cooling	360	[10]
Cooling Towers	$/ton cooling	275	[10]
CO_2 Compressors	$/($lb_{CO2}$/hr)	36	[4,5]
XHTX	$/($lb_{SORB}$/hr)	3.908	Solex
Regenerator Heater	$/($lb_{SORB}$/hr)	1.954	Solex
Fuel Costs	$/$klb_{COAL}$	20.23	[15]
Sorbent Costs	$/$lb_{SORB}$	5.62	[4]
CO_2 TS&M Costs	$/$klb_{CO2}$	2.99	[4]

5. Financing & Capital Costs

The industry standards used to account for the costs associated with generating electricity at a power generation facility are generally referred to as the cost of electricity (COE) and levelized cost of electricity (LCOE). COE is a measure of a plant's revenue per net megawatt-hour (MWh) during the first year of operation. It is assumed that COE escalates throughout each successive operating year at a nominal rate equal to the general inflation rate. In other words, the COE remains "constant" throughout the life of the plant, if it is adjusted for inflation. LCOE represents the revenue per net megawatt-hour for the plant during its first year of operation, assuming that the COE escalates at a nominal annual rate of 0% throughout the life of the plant. There are numerous assumptions that must be made in calculating the COE and LCOE. These assumptions include the plant capacity factor, financing terms, tax rates, plant depreciation, construction and operation times, and the annual inflation rate. Table 15 details the global economic assumptions used for the analyses in this report.

Table 15: Global Economic Assumptions

Parameter	Units	Value
Plant Capacity Factor	%	85
Income Tax Rate	%	38
Interest Rate	%	4
Repayment Term of Debt	Years	15
Depreciation (150% declining balance)	Years	20
Plant Operational Life	Years	30
Duration of Construction	Years	5
Annual Inflation Rate*	%	2.95
Debt	%	45
Equity	%	55
After-tax Weighted Cost of Capital	%	7.72
Capital Charge Factor (5 Year Construction, High Risk IOU) [3]	-	0.124
Levelization Factor (IOU @ 12% IRROE)	-	1.262

*Taken from the Producer's Price Index for Finished Goods – 1947 to 2015

The percentage of debt to equity for any project is largely set by the lender and is dependent on the risk associated with the project. CO_2 capture projects are generally considered on a high-risk financing structure. In the 2008 NETL report, "Recommended Project Finance Structures for the Economic Analysis of Fossil-Based Energy Projects" [17], high risk projects are suggested to have a debt/equity ratio (D/E ratio) of up to 45/55. However, it is also stated that, "high risk, first-of-a-kind projects, may include requirements for loan guarantees, guarantees from project owners, fixed price turnkey EPC contracts with performance guarantees, subsidies, direct federal funding or municipal or state sources of funding, along with product off take contracts or federal price guarantees" [17]. For the analysis in this report, a D/E ratio of 45/55 is assumed.

Further details of the financial structure assumed for a high-risk investor owned utility (IOU) are seen in Table 16. The current (nominal) dollar cost (α) on the debt-funded portion of the project is simply the annual interest rate (2.95%), while the cost of the equity-funded portion of the project is a desired annual rate of return (profit) on the equity. The weighted current (nominal) cost (β) is obtained by multiplying these values by their cost fraction of the project., These values can be used along with the annual tax rate (R) to calculate the after tax weighted cost of capital:

$$After\ Tax\ Weighted\ Cost\ of\ Capital\ =\ \beta_{Equity}\ +\ \beta_{Debt}\ (1\ -\ R)$$

Table 16: Financial Structure for High Risk IOU

Parameters	%	Current (Nominal) Dollar Cost [α]	Weighted Current (Nominal) Cost [β]	After Tax Weighted Cost of Capital
Debt	45	4%	1.8%	
Equity	55	12%	6.6%	
Total	100		8.4%	7.72%

6. Operating and Maintenance Cost Estimates

Estimates of operating and maintenance costs (O&M) are needed to complete the COE calculations described above. The following assumptions were made in estimating these costs:

Fixed O&M Costs

Fixed O&M costs include annual labor costs of the plant and other similar costs that do not scale with production. ADA had previously estimated the labor costs of a PC Plant equipped with their CO_2 capture system at between 1.29 and 1.62¢/kWh [4]. It is assumed that fixed operating costs do not vary with respect to changes in the ADA solid sorbent CO_2 capture system. It is also assumed that fixed O&M costs are scaled from 2011 dollars to 2015 dollars at an annual inflation rate of 2.95%. An average fixed O&M operating cost of 1.63¢/kWh was obtained after scaling to 2015 dollars. Since fixed O&M costs do not scale with the plant capacity factor, the following equation is used to determine annual fixed O&M costs:

$$O\&M_{FIX}\left(\frac{\$}{yr}\right) = \frac{1.64\left(\frac{¢}{kWh}\right)}{100} \cdot kW_{net} \cdot 8{,}766\left(\frac{hr}{yr}\right)$$

where kW_{net} is plant net power output in kW and 8,766 hr/yr is annual plant operation time at a capacity factor of 100%.

Variable O&M Costs

Variable O&M costs are costs which scale with respect to the net generation of the plant. ADA has suggested variable O&M costs of between 1.21 and 1.41¢/kWh in 2011 dollars [4]. When scaled to 2015 dollars, average variable O&M cost are assumed to be 1.48¢/kWh. The following equation is used to convert this ¢/kWh value to an annual dollar value:

$$O\&M_{VAR}\left(\frac{\$}{yr}\right) = \frac{1.48\left(\frac{¢}{kWh}\right)}{100} \cdot kW_{net} \cdot 8{,}766\left(\frac{hr}{yr}\right)$$

where kW_{net} is plant net power output in kW and 8,766 hr/yr is annual plant operation time at a capacity factor of 100%.

Fuel Cost Portion of Variable O&M Costs

While fuel costs are a variable O&M cost, they are included as a separate line item. A coal cost of $20.23/(klb/hr) is used with the following equation being used to calculate annual fuel O&M costs:

$$O\&M_{Fuel}\left(\frac{\$}{yr}\right) = \$20.23\left(\frac{1}{klb}\right) \cdot \frac{\dot{m}_{coal}\left(\frac{lb}{hr}\right)}{1000} \cdot 8{,}766\left(\frac{hr}{yr}\right)$$

where $\dot{m}_{coal}$ is the mass flow rate of coal in lb/hr and 8,766 hr/yr is the plant operation time at a capacity factor of 100%.

Sorbent Cost Portion of Variable O&M Costs

The bulk of sorbent costs are in the initial fill of the ADA CO_2 capture system. An estimated sorbent cost of $5.62/lb is assumed. ADA has suggested a sorbent attrition rate of 0.0025% per cycle of the solid sorbent system [4]. Further testing by ADA with their pilot project should help determine the accuracy of this number. Using this sorbent attrition rate, annual O&M costs due to sorbent attrition can be found through the following equation:

$$O\&M_{SORB}\left(\frac{\$}{yr}\right) = \$5.62\left(\frac{1}{lb}\right) \cdot \dot{m}_{SORB}\left(\frac{lb}{hr}\right) \cdot R(\%\, loss) \cdot 8{,}766\left(\frac{hr}{yr}\right)$$

where $\dot{m}_{SORB}$ is the mass flow rate of sorbent in lb/hr, R is the attrition rate as a % per cycle, and 8,766 hr/yr is the plant annual operation time at a capacity factor of 100%.

CO_2 TS&M Cost Portion of Variable O&M Costs

TS&M costs are included as part of the O&M variable costs as they vary with respect to the CO_2 flow being captured and sequestered, which varies with plant load. It was previously shown in this report that a TS&M cost of $2.99/klb$_{CO2}$ is assumed. The following equation is used to calculate the O&M costs due to TS&M:

$$O\&M_{TS\&M}\left(\frac{\$}{yr}\right) = \$2.99\left(\frac{1}{klb}\right) \cdot \frac{\dot{m}_{CO2}\left(\frac{lb}{hr}\right)}{1000} \cdot 8{,}766\left(\frac{hr}{yr}\right)$$

where $\dot{m}_{CO2}$ is the mass flow rate of captured CO_2 in lb/hr and 8,766 hr/yr is annual operation time of a plant operating at a capacity factor of 100%.

7. Cost of Electricity and Levelized Cost of Electricity

Cost of Electricity

The cost of electricity (COE) is a measure of the plant's total annual revenue per net megawatt-hour (MWh) during the first year of operation. The following equation is used to calculate COE:

$$COE = \frac{(CFF)(TOC) + OC_{FIX} + (CF)(O\&M_{Fuel} + O\&M_{SORB} + O\&M_{TS\&M} + OC_{VAR})}{(CF)(kWh)}$$

where

COE: Annual cost per kWh (expressed in base-year dollars) of electricity produced.

CCF: Capital charge factor. The CCF is assumed to be 0.124 for a high risk capital investment by an investor owned utility (IOU) and a five-year construction period.

TOC: Total overnight cost in base-year dollars.

OC_{FIX}: Total of all fixed annual O&M costs in base-year dollars ($/yr at CF of 100%).

OC_{VAR}: Total of all variable annual O&M costs – including fuel – expressed in base-year dollars ($/yr at CF of 100% for all costs).

CF: Plant capacity factor.

kWh: Annual net kilowatt-hours of net generation at a capacity factor of 100%.

Levelized Cost of Electricity

Calculation of the levelized cost of electricity (LCOE) involves the addition of a levelization factor (LF) to the COE. The LCOE is expressed in operational year (first year of operation) dollars, which means that any LCOE costs expressed in base-year dollars (throughout construction period) must be scaled to operational year dollars using an inflation rate. After operation begins, the LCOE does not escalate with inflation during the life of the plant. The following equation presents LCOE as a function of COE and the LF:

$$COE = COE \cdot LF$$

The levelization factor is calculated using the following equations:

$$LF = \frac{A\,(1 - K^{LP})}{(D - N_r)}$$

$$K = \frac{1 + N_r}{1 + D}$$

$$A = \frac{D\,(1 + D)^{LP}}{(1 + D)^{LP} - 1}$$

where

LF: Levelization factor.

LP: Levelization period in years (operational period of plant). An operational lifespan of 30 years is assumed.

D: Discount rate. Assumed to be the internal rate of return on equity (IRROE). For these analyses an IRROE of 12% is assumed.

N_r: Nominal escalation rate, which is assumed to be equal to the annual inflation rate – assumed to be 2.95% for these analyses.

Using these equations and assumptions above, a levelization factor of 1.262 was found.

8. Validation of Costing Assumptions and Calculations

The costing assumptions and calculations outlined above were validated by re-calculating values presented in the literature. In particular, results presented in the previous ADA report [4] and DOE report detailing baseline cost and performance data for pulverized coal plants [5] were examined. There are two cases presented in Ref. 4, which are referred to as Sorbent 1 and Sorbent 2. Table 17 presents a comparison of the COE values presented in the Ref. 4 and 5 against those calculated by the authors using baseline data from these references. It can be seen that there is very good agreement between the COE and LCOE values presented by Ref. 4 and 5 and those calculated here.

Table 17: Validation Results for COE Calculations

Baseline Data				
	Units	Sorbent 1 [4]	Sorbent 2 [4]	Case 12 [5]
Year		2011	2011	2007
PC Plant	$/kW$_{gross}$	1,454	1,461	1,394
CO_2 Capture System	$/(lb$_{CO2}$/hr)	184.59	473.92	224.04
CO_2 Comp. System	$/(lb$_{CO2}$/hr)	30.47	30.77	29.89
Fuel Costs	$/klb$_{coal}$	20.06	20.27	19.09
CO_2 TS&M Costs	$/klb$_{comp\ flow}$	2.55	2.58	2.54
Fixed Costs	$/MWh	12.9	16.2	8.7
Variable Costs	$/MWh	16.6	14.3	13.0
COE Values				
Values Presented in Literature [4,5]				
COE	$/MWh	113.3	133.3	106.5
LCOE	$/MWh	143.6	169.0	135.2
Calculated by Authors				
COE	$/MWh	112.6	133.3	106.4
Difference	%	0.62	0.00	0.09
LCOE	$/MWh	142.7	169.0	135.0
Difference	%	0.63	0.00	0.15

A second method of validation is to compare the calculated capital costs for the system being modeled with those presented in the literature. The Sorbent 2 case from Ref. 4 was selected as the reference case, with the BEC, TPC, TOC, and TASC being scaled to 2015 dollars. Reference year dollars were scaled at an assumed inflation rate of 2.95%. These Sorbent 2 results are scaled to 2015 dollars and are compared in Table 18 to the BASE BN sorbent case calculated by the authors. The BASE BN case refers to the case where the ADA system without a XHTX or heat integration utilizes the sorbent referred to as the BN sorbent.

Table 18: Comparison Between Ref. 4 Sorbent 2 Case and the BN BASE Case by the Authors

	Units	Sorbent 2 [4]	BASE BN Sorbent	Difference	Difference [%]
Gross Power	MW	690	753	63	9.1
Auxiliary Power	MW	140	203	63	45.0
CO_2 Capture Facility	MW	57.7	84.3	26.6	46.1
CO_2 Compression	MW	43.5	75.8	32.3	74.3
Other Aux. Power	MW	38.8	42.9	4.1	10.6
Net Power	MW	550	550	0	0.0
BEC	$1000	1,737,858	1,863,151	125,293	7.2
PC Plant	$1000	1,077,074	1,213,231	136,157	12.6
CO_2 Capture Facility*	$1000	620,501	449,802	170,699	27.5
CO_2 Compression	$1000	40,284	56,723	16,439	40.8
Other Costs**	$1000	0	143,395	-	-
TPC	$1000	2,319,109	2,347,848	28,739	1.2
TOC	$1000	2,865,928	2,872,792	6,864	0.2
TASC	$1000	3,267,158	3,274,983	7,825	0.2
Capital Costs	$/MWh	86.8	86.9	0.1	0.1
Fuel Costs	$/MWh	22.6	23.2	0.6	2.7
CO_2 TS&M Costs	$/MWh	6.2	8.6	2.4	38.7
Sorbent Costs	$/MWh	-	5.5	-	-
Fixed Costs	$/MWh	18.2	16.3	1.9	10.4
Variable Costs	$/MWh	16.1	14.8	1.3	8.1
COE	$/MWh	137.2	155.3	18.1	13.2
LCOE	$/MWh	189.8	195.9	6.1	3.2

*Includes price of let-down turbine and FGAS cooler
**Includes refrigeration, cooling tower, pump costs, and initial sorbent fill costs

Table 18 shows there are major differences between the current ADA capture system model and that previously presented in Ref. 4. The first major difference is in auxiliary power demands. It can be seen that the difference in auxiliary power is primarily due to the greater power demands of the ADA capture system and CO_2 compressors for the BN sorbent case. Auxiliary power is seen to increase by 63MW, which results in a similar increase in gross power. An increase in gross power increases overall

PC plant size, driving its capital costs higher. The reason for this is that the BASE BN case includes both the refrigeration power required to cool the ADA system as well as what is thought to be a more representative calculation of CO_2 compressor power.

The second section of Table 18 details the BEC, TPC, TOC, and TASC for these two cases. PC plant costs are seen to be higher for the BN case, CO_2 capture facility costs are lower for the BN case, and CO_2 compression system costs are higher for the BN case. The reason for the higher plant and compression system costs is primarily due to the increase in plant size, which increases the flow rate of captured CO_2. The lower capture system cost is not surprising since the ADA system cost was assumed to be equal to the average of the system costs for both the Sorbent 1 and Sorbent 2 cases in Ref. 4. The Sorbent 1 ADA capture system cost was approximately half that of the system cost for the Sorbent 2 case. Therefore, the costing factor used by the authors of this report suggest a capture system cost somewhat less than that for the Sorbent 2 case. Interestingly, the BEC, TPC, TOC, and TASC show very good agreement between the two cases as these increases and decreases in costs balance each other out.

The final section of Table 18 details the calculated COE and LCOE results for these two cases. COE is seen to be around 13% higher for the BN case, while LCOE is only around 3% higher. These results show that there is relatively close agreement between the COE and LCOE results previously presented and those calculated and presented in this report.

9. Thermo-Economic Results

Thermodynamic results from previous reports [1,2] show that there are numerous modifications to the ADA solid sorbent capture system that have the potential to dramatically decrease net unit heat rate (HR). Results from these thermodynamic models are presented in Figure 11, which plots net unit HR for the two sorbents examined (BN and OJ) and for cases with a XHTX and the four heat integration options examined.

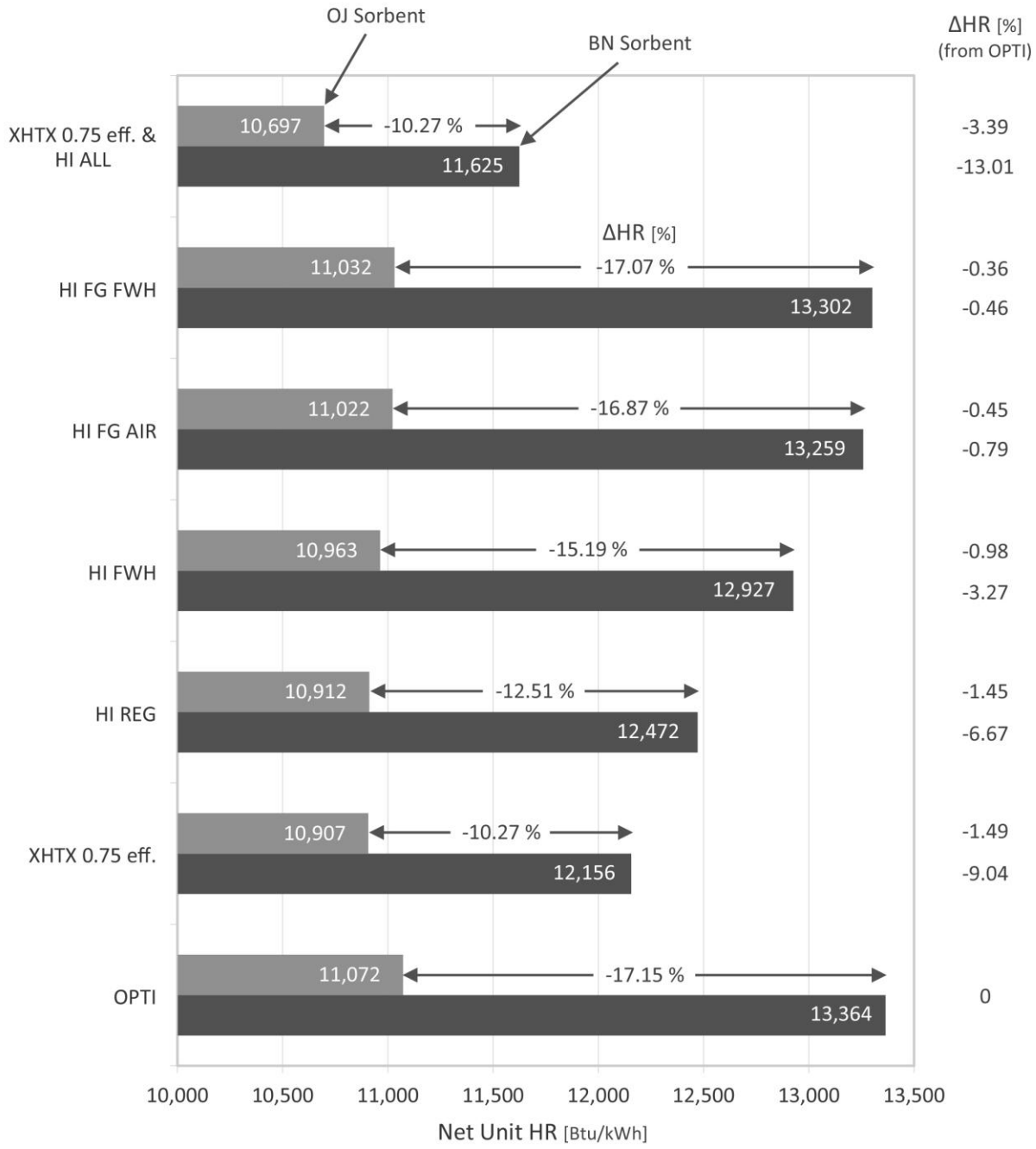

Figure 11: Net Unit HR for Both Sorbents & for XHTX & Heat Integration Cases

The abbreviations seen in Figure 11 are defined as follows:

OPTI: Case without XHTX or heat integration at optimal adsorber and regenerator operating temperatures.

eff: The effectiveness of any XHTX utilized.

HI REG: Heat integration option with heat from the CO_2 compressors being utilized in heating the sorbent entering the regenerator.

HI FWH: Heat integration option where heat from the compressors is utilized in heating the boiler feedwater through the addition of a feedwater heater (FWH0) upstream of the existing FWH1.

HI FG AIR: Heat integration option where heat from the flue gas cooler is used to pre-heat boiler combustion air.

HI FG FWH: Heat integration option where heat from the flue gas cooler is used to heat boiler feedwater through the addition of FWH0.

HI ALL: All four heat integration options are considered simultaneously.

Figure 11 clearly shows that every XHTX and/or heat integration option considered results in a reduction in net unit heat rate relative to the OPTI cases. The best-performing case is the XHTX 0.75 eff. & HI ALL configuration, which results in a 13.01% reduction in net unit HR for the BN sorbent and a 3.39% reduction in net unit HR (from the OPTI case) for the OJ sorbent. The case with the smallest HR improvement is the HI FG FWH case, which only reduces net unit HR by 0.46% for the BN sorbent and 0.36% for the OJ sorbent. The reason for the small performance improvement for this case is the low quantity of low quality heat, which is available from the flue gas cooler for feedwater heating. It's interesting to note that cases utilizing compressor heat for regenerator and/or feedwater heating perform better, with heat rate reductions between 3.3% and 6.7% for the BN sorbent and 1% and 1.5% for the OJ sorbent.

If the OJ sorbent is used instead of the BN sorbent, net unit HR is reduced by between 10.27% and 17.15%. This reduction is partially due to a reduction in the sorbent flow rate (due to higher CO_2 loading capacity of the OJ sorbent). A lower sorbent flow rate reduces the energy needed to heat and cool the sorbent in the regenerator and adsorber. Another factor promoting the enhanced thermodynamic performance of the OJ sorbent is the optimal operating temperatures of the adsorber and regenerator. For the BN sorbent, optimal adsorber and regenerator temperatures of 104°F and 248°F respectively were found. However, for the OJ sorbent, optimal adsorber and regenerator temperatures were found to be 100°F and 140°F respectively. With a lower temperature difference

between the adsorber and regenerator, heating and cooling demands by the sorbent in the adsorber and regenerator are further reduced.

Although the XHTX 0.75 eff. & HI ALL case is seen to result in the best unit performance, an economic analysis must be conducted to determine if the improvement in performance offsets the additional equipment costs. For instance, the XHTX 0.75 eff. & HI ALL case includes the addition of the following: a XHTX, the regenerator heater, FWH0 with capacity for both heat from compressors and flue gas cooler, a combustion air heater, and all other associated equipment. Costing for all of these components was examined according to the correlations presented above. By adding the additional costs of these components to the PC plant and adjusting the size of the plant for the performance improvements, an estimate of capital costs can be found. These costs were used to find the COE and LCOE for the configurations previously considered in the thermodynamic analyses [1,2]. Figure 12 presents these COE and LCOE results for the BN sorbent.

Figure 12 shows how the thermodynamic analyses differ widely from the economic analyses. For the BN sorbent, the addition of a XHTX (0.75 effectiveness), and each of the four heat integration options were examined independently, along with the case where all five are implemented simultaneously. From these results, it is seen that only the XHTX 0.75 eff. and HI REG cases result in a lower COE or LCOE than the OPTI case. This indicates that for these cases the improved performance more than offsets the increase in capital costs. While the XHTX 0.75 eff. & HI All case was found to be the best-performing case thermodynamically, it is second to last economically. The reason for this seems to be the high cost of the feedwater heating options (HI FWH and HI FG FWH). For these cases, the improvement in net unit heat rate is minimal with regard to the cost of the additional feedwater heater (FWH0).

At the top of Figure 12 is a case considering the implementation of the two best-performing cases (XHTX 0.75 eff. & HI REG). This case is seen to slightly outperform either of the individual cases, with an $8/MWh reduction in the COE and $10/MWH reduction in the LCOE from the OPTI case.

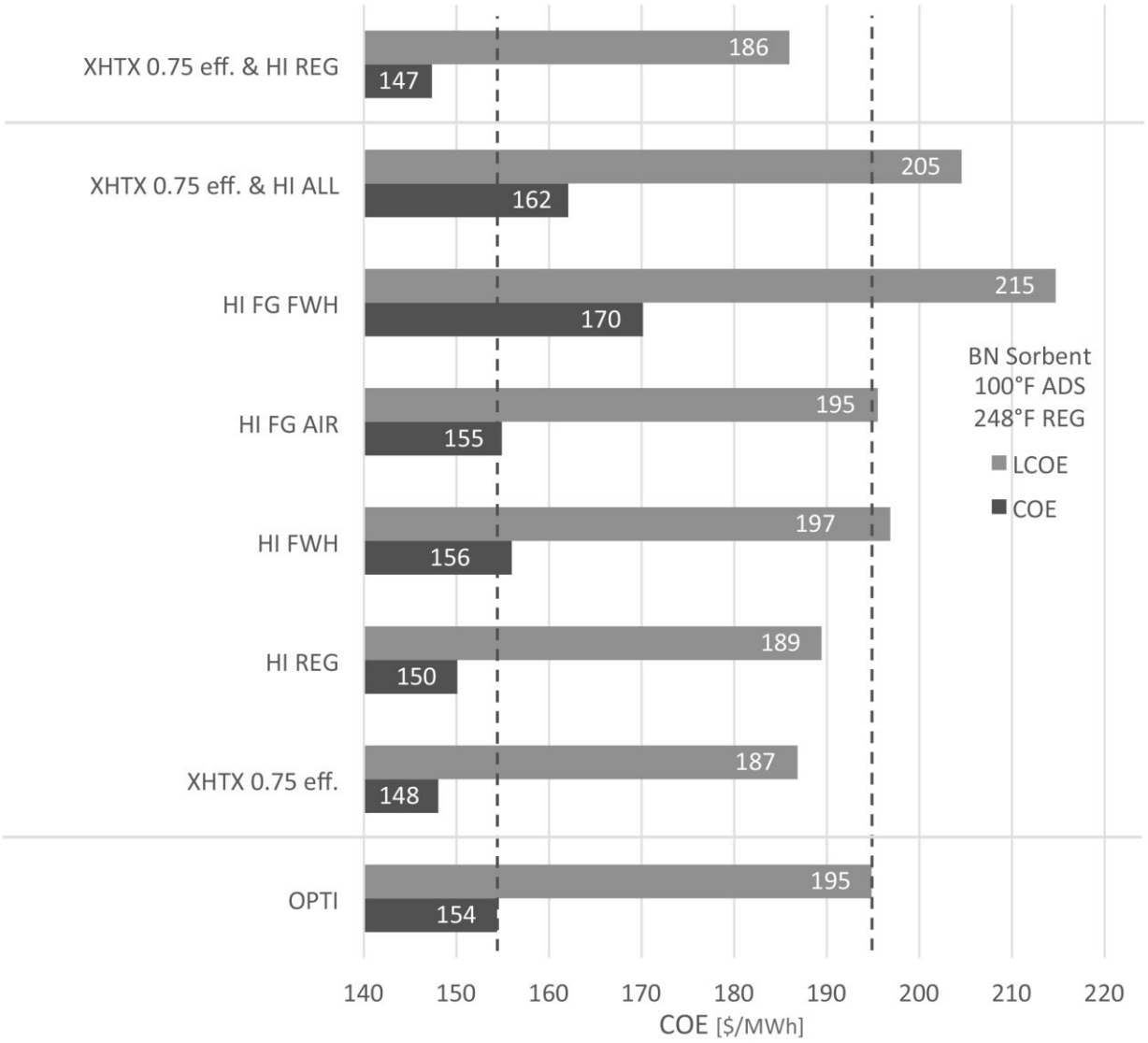

Figure 12: COE & LCOE for Various XHTX & Heat Integration Cases - BN Sorbent

Figure 13 presents similar economic results, but for the case where the OJ sorbent is utilized. For the OJ sorbent, only the XHTX 0.75 eff. case is seen to result in a lower COE than the OPTI case. However, the improvement in cost is minimal. The reason for the small improvement through use of a XHTX is the small thermal improvement of this case (See Figure 11). With such a small thermal improvement, the addition cost is just covered by the improvement in performance. As with the BN sorbent, OJ cases utilizing feedwater heating tend to have the highest COE.

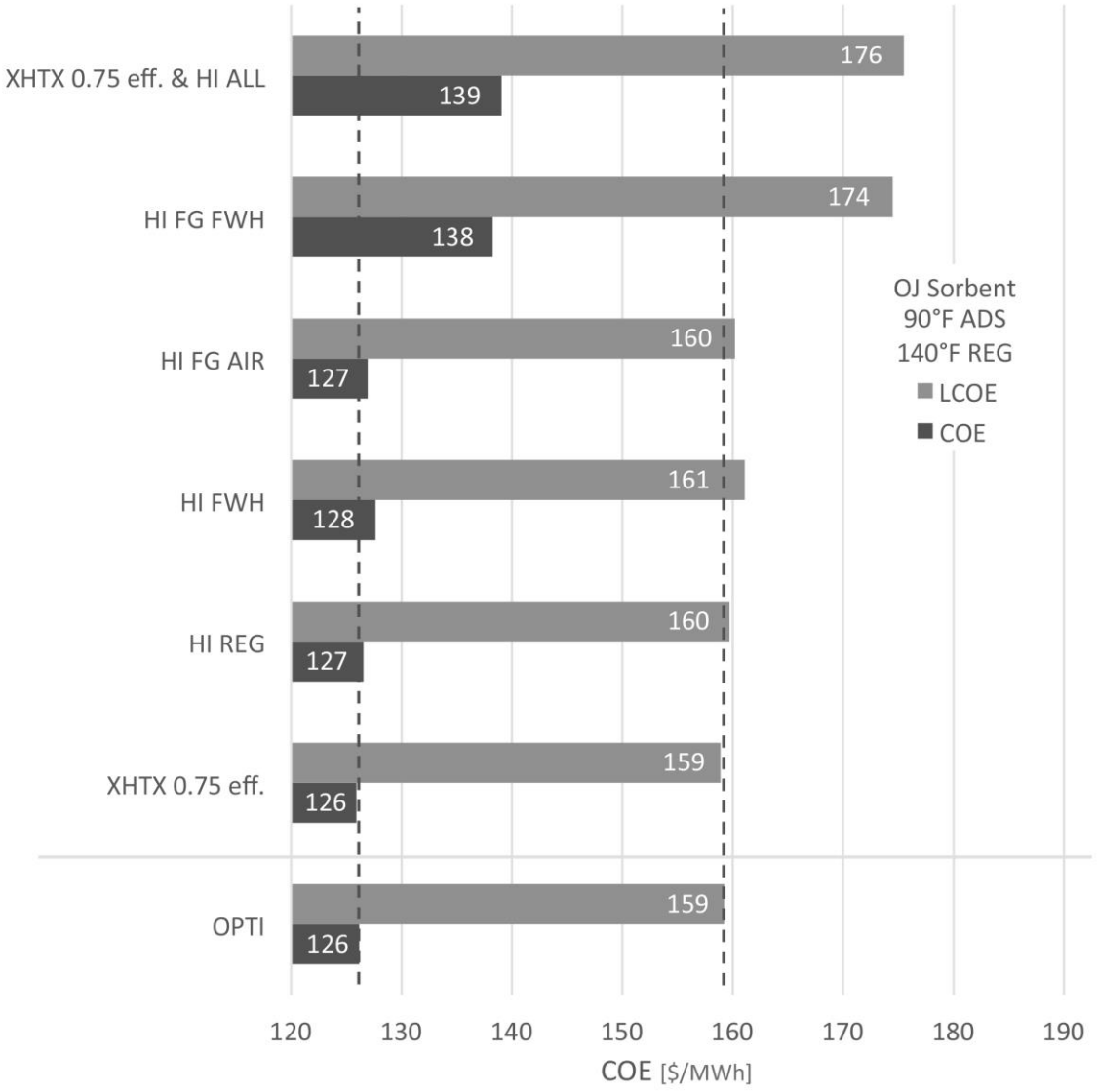

Figure 13: COE & LCOE for Various XHTX & Heat Integration Cases - OJ Sorbent

Another method for comparing both the BN and OJ cases is presented in Figure 14, where COE is plotted vs. net unit HR for the cases presented in Figure 12 and Figure 13. Here it can be clearly seen that the best unit performance does not directly equate to the lowest COE. It is also apparent that the OJ sorbent performs much better both thermally and economically when compared to the BN sorbent. Splitting the difference between these two cases is the MEA 90% CO_2 capture case (Case 12 from Ref. 5). Given that the ADA CO_2 capture system is only in the early stages of development, while the MEA technology is well-developed, it is expected that both net unit HR and COE will continue to improve with further development, particularly in the area of improved sorbents.

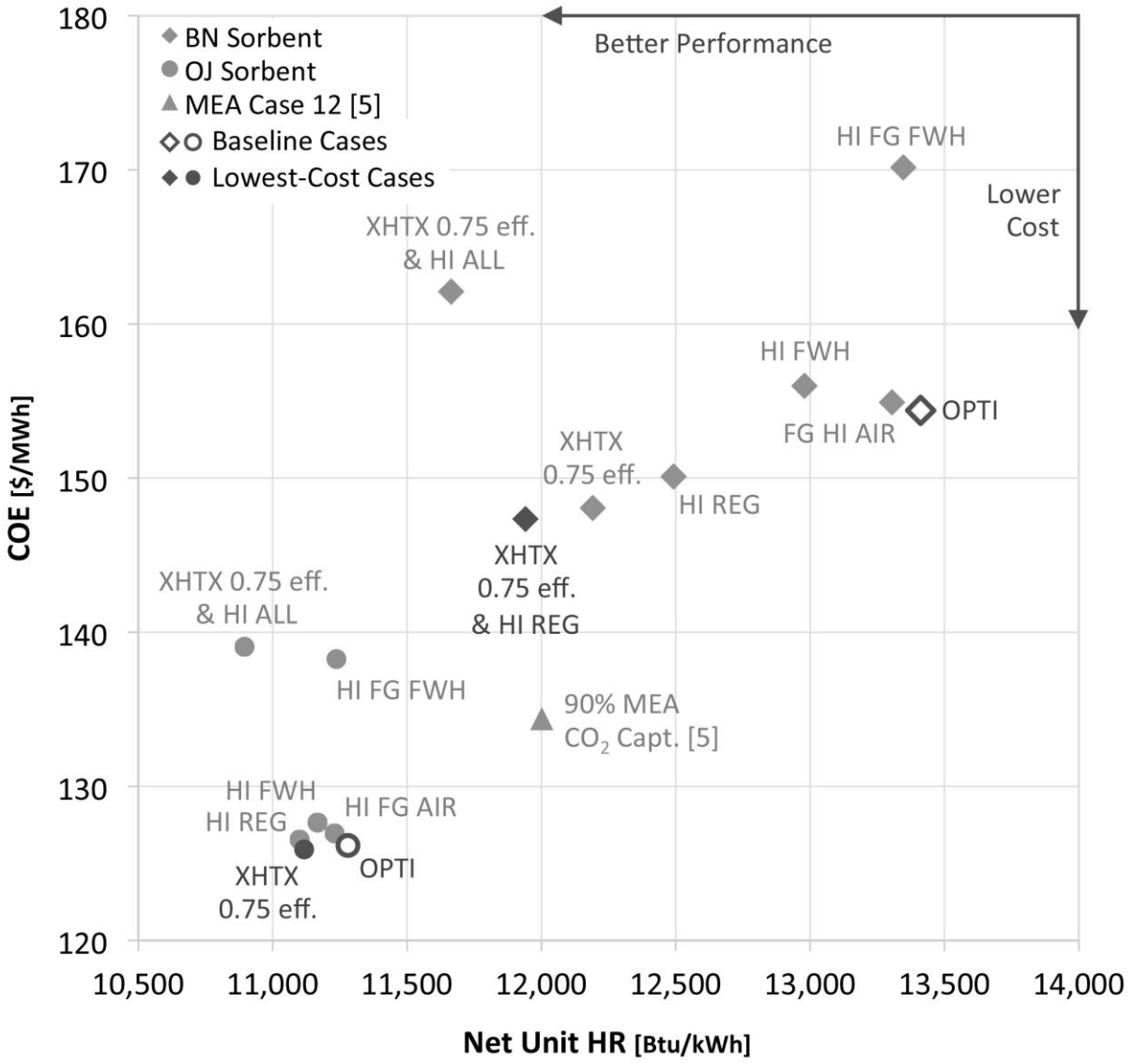

Figure 14: COE & Net Unit HR Comparison Between BN, OJ, and MEA Cases

Figure 15 presents COE results for six key cases. The BN and OJ OPTI cases are presented along with the lowest-cost cases for both sorbents from Figures 12 and 13. As seen, COE is reduced by \$7.1/MWh and \$0.3/MWh between the OPTI and lowest-cost cases for the BN and OJ sorbent respectively. While this is a significant improvement for the BN sorbent, the improvement for the OJ sorbent case is so minimal as to preclude the use of a XHTX. Despite this, both OJ sorbent cases are seen to result in a COE at least \$8/MWh below that of the 90% MEA CO_2 capture case (Case 12 from Ref. 5). When compared to the case without CO_2 capture, COE is seen to be around \$33/MWh higher for the OJ

cases. This equates to a 36% increase in the COE due to the costs associated with CO_2 capture using the ADA system as presented in this report.

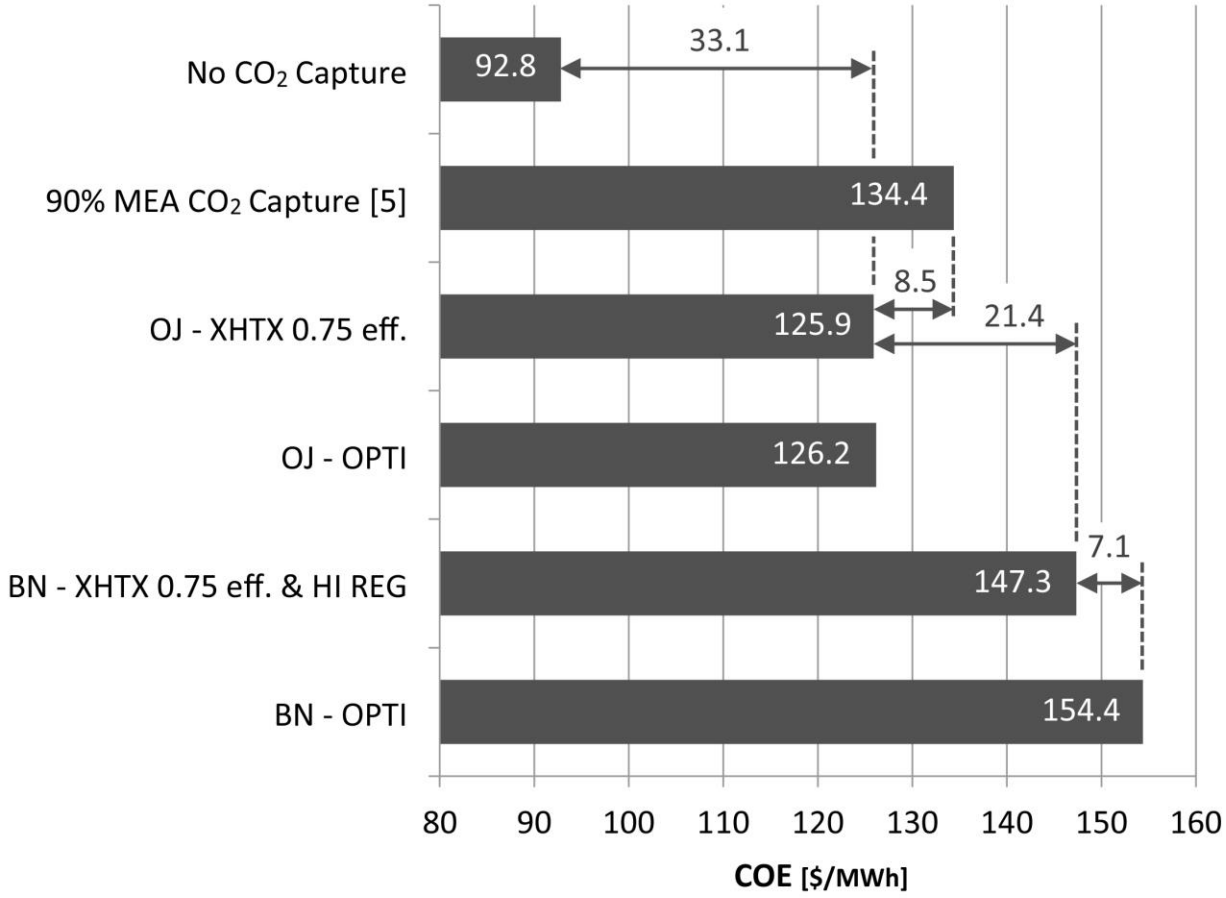

Figure 15: COE for Six Key Cases

Figure 16 presents LCOE results for the same six cases as Figure 15. These results track very well with those presented for the COE. One key value to note is the $41.7/MWh increase in LCOE from the case with no CO_2 capture to the OJ – XHTX 0.75 eff. case. This shows that the increase in LCOE is 36%, which is equivalent to the increase in COE.

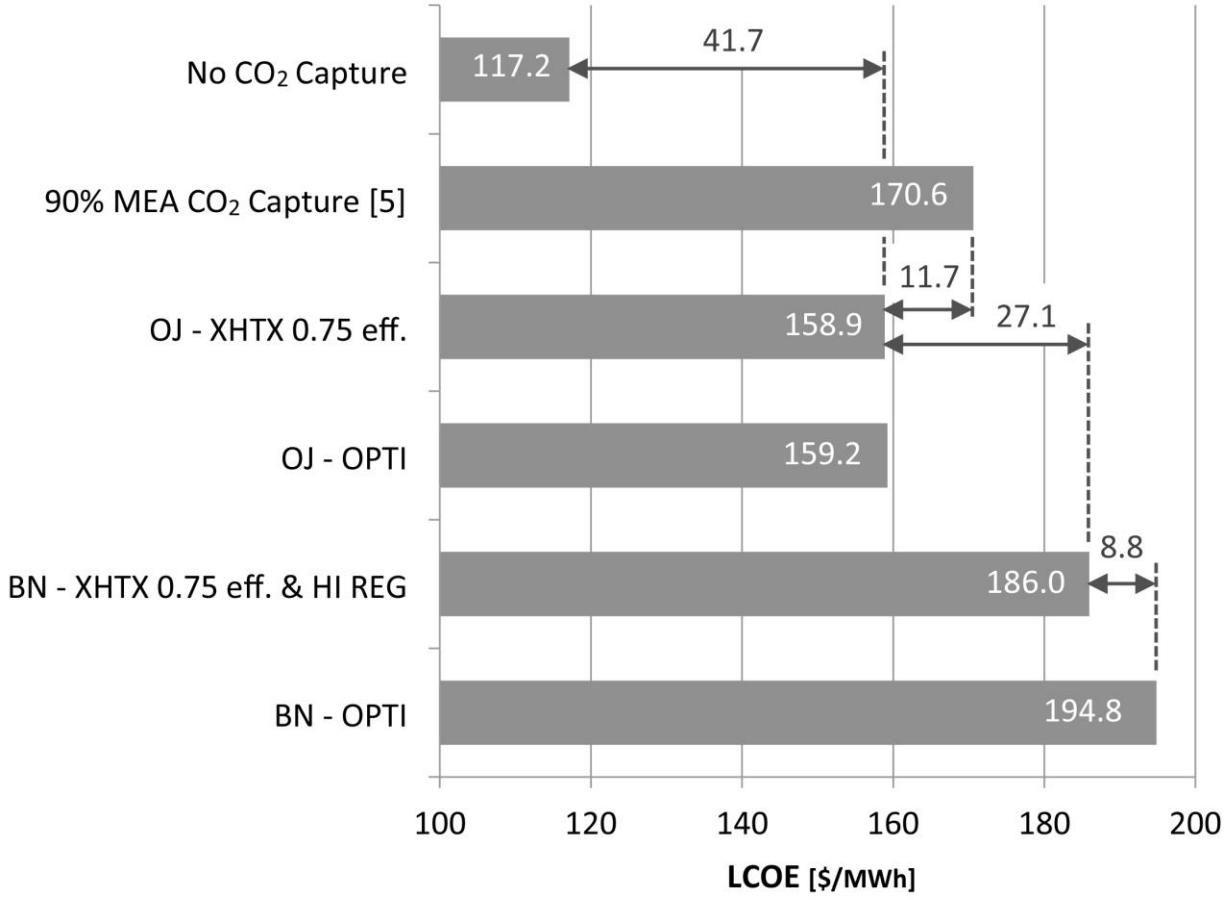

Figure 16: LCOE for Six Key Cases

10. Conclusions

The ADA solid sorbent CO_2 capture system has been fully modelled in conjunction with a supercritical pulverized coal power plant for a variety of process configurations. Two different solid sorbents were considered during modeling (the BN and OJ sorbents), the addition of a XHTX to the capture system was examined, and four opportunities for the utilization of waste heat were also considered. After a complete thermodynamic analysis of these cases, calculations were conducted to find the plant COE and LCOE for all the cases. The following conclusions are drawn from these thermo-economic results as presented in the present report:

COE and LCOE for OPTI Cases

The OPTI cases designate those cases, where the capture system adsorber and regenerator temperatures were tuned to obtain the lowest net unit HR. These cases were considered as the baseline cases for each of the two sorbents.

For the BN sorbent, the OPTI case was found to result in a COE and LCOE of $154.4/MWh and $194.8/MWh respectively. This represents a 66% increase in the COE over the case without CO_2 capture and a 15% increase in COE over the 90% capture MEA case as presented by DOE [5]. The OPTI OJ sorbent case performs considerably better, with a COE and LCOE of $126.2/MWh and $159.2/MWh respectively. For this case, COE is seen to be around 36% higher than the no capture case, while COE is 6% lower than the COE for the 90% capture MEA case.

XHTX and Heat Integration Improvements

While the addition of a cross heat exchanger and heat integration was found to significantly improve net unit HR in the preceeding reports [1,2], the present report found that the additional equipment costs associated with these cases almost always outweighed the improvement in performance. The two exceptions to this are the addition of a XHTX and a regenerator heater. For the BN sorbent, the addition of a XHTX with an effectiveness of 75% was found to decrease the COE by $6/MWh, or a 4% decrease in COE. By adding a regenerator heater to this case with a XHTX, COE is lowered by another $1/MWh. However, the story is different for the OJ sorbent. For this sorbent, the addition of XHTX with an effectiveness of 75% only lowers the COE by $0.3/MWh, or by 0.2%. Given this very small difference in COE between the OJ case with and without a XHTX, it is suggested that it would be best not to include a XHTX for this sorbent. The additional complexity of adding such a system will most likely outweigh the minimal improvement in COE.

Other Heat Integration Opportunities

For each of the other heat integration opportunities modeled (the addition of a FWH0 for feedwater heating, combustion air heating, and a regenerator heater for the OJ sorbent case), COE and LCOE are seen to increase. Obviously this precludes the use of any of these options as their associated costs outweigh any benefit due to their improved thermal performance.

BN vs. OJ Sorbent

Just as the previous study [2] has shown clear thermodynamic benefits through use of the OJ sorbent instead of the BN sorbent, the current work shows that there is a clear economic advantage to using this improved sorbent. For the OPTI cases, the OJ sorbent is seen to result in a COE $28.2/MWh lower than the COE for the BN sorbent, or a reduction of 18%. When comparing the lowest-cost BN case to the lowest-cost OJ case, the OJ case comes in $21.4/MWh (15%) lower. The primary reason for this is the improved CO_2 loading capacity of the OJ sorbent. With an improvement in CO_2 loading, the OJ sorbent flow rate is reduced, which not only reduces the cost of sorbent needed to fill the capture system, but more significantly reduces the size of the entire capture system. As capture system sizes are reduced, material costs associated with the system are reduced accordingly.

Future Sorbent Advances

Perhaps one of the most significant points to be drawn from the COE and LCOE differences due to sorbent type is in regard to future improvements to the ADA CO_2 capture system. ADA has shown steady progress in developing and testing new sorbents. For instance, the BN sorbent represents a sorbent tested by ADA prior to the initiation of this project two years ago, the OJ sorbent was characterized in the year leading up to publication of this report, and improvements to the OJ sorbent are in progress. Therefore, it is suggested that the solid sorbent CO_2 capture system developed by ADA will continue to see performance gains and lower system costs as further sorbent development is conducted.

References

[1] Charles, J., Levy, E., Xingchao, W. "Aspen Plus Modeling of ADA Solid Sorbent CO_2 Capture System." Prepared for ADA-ES, Inc. by the Energy Research Center, November 2014.

[2] Charles, J., Levy, E., Xingchao, W. "Aspen Plus Modeling of ADA Solid Sorbent CO_2 Capture System: Comparison of OJ and BN Sorbents" Prepared for ADA-ES, Inc. by the Energy Research Center, May 2015.

[3] *Cost Estimation Methodology for NETL Assessments of Power Plant Performance*. DOE/NETL-2011/1455 Final Report, August 2011.

[4] Krutka, H., Starns, T., Richard, M., Thitakamol, B. *Evaluation of Solid Sorbents as a Retrofit Technology for CO_2 Capture: Preliminary Techno-economic Assessment of Solid Sorbents for Post-Combustion CO_2 Capture*. DOE: DE-FE0004343, December 2011.

[5] *Cost and Performance Baseline for Fossil Energy Plants – Volume 1: Bituminous Coal and Natural Gas to Electricity.* DOE/2010/1397 Revision 2a, September 2013.

[6] *Investigation on Flue Gas & Condensing Heat Exchanger (CHX) Cooling Water Cooling Processes and CHX Design.* Energy Research Center. Prepared for ADA-ES, Inc. September 2014.

[7] EERE Information Center. *Energy Tips – Steam. Steam Tip Sheet #22*, DOE/GO-102004-2006, September 2004.

[8] *Carbon Dioxide Capture from Existing Coal-Fired Power Plants.* DOE/NETL-401/110907 Final Report, November 2007.

[9] *Catalog of CHP Technologies: Section 4 – Technology Characterization – Steam Turbines*. U.S. EPA Combined Heat and Power Partnership, March 2015.

[10] RS Means Construction Cost Data. RS Means Online 6.2 (2015). Retrieved June 2015 from <http://rsmeansonline.com/SearchData>

[11] Kitto, J., Stultz, S. (eds). *Steam* (41st ed.). The Babcock & Wilcox Company, Barberton, Ohio, 2005.

[12] Holman, J. *Heat Transfer.* McGraw-Hill Publishing Company, New York, 1986.

[13] Hazell, D. *Modeling and Optimization of Condensing Heat Exchangers for Cooling Boiler Flue Gas.* M.S. Thesis, Lehigh University, Bethlehem, PA. 2011.

[14] Columbia Pipe & Supply Company. *Steel Pipe Price List.* Retrieved June 2015 from <http://www.columbiapipe.com/documents/0/2015%20June%2015.aspx>

[15] Independent Statistics & Analysis, U.S. Energy Information Administration. *Coal News and Markets.* Retrieved June 2015 from <http:// http://www.eia.gov/coal/news_markets>

[16] Pauschert, D. *Study of Equipment Prices in the Power Sector.* ESMAP Technical Paper 122/09, December 2009.

[17] *Recommended Project Finance Structures for the Economic Analysis of Fossil-Based Energy Projects.* DOE/NETL-401/090808, September 2008.

Aspen Plus Model of ADA Solid Sorbent CO_2 Capture System

Aspen Plus Modeling of ADA Solid Sorbent CO_2 Capture System

Prepared for:

ADA-ES, Inc.

Sharon Sjostrom
William Morris
Jayson Denney

Prepared by:

Joshua Charles
Edward Levy
Xingchao Wang

Energy Research Center
Lehigh University
117 ATLSS Drive
Bethlehem, PA 18015

Nov. 5, 2014

Index

List of Figures

List of Tables

Executive Summary

ADA Environmental Services, Inc. has developed a solid-sorbent CO_2 capture system to remove CO_2 from the flue gas of a pulverized coal (PC) power plant. CO_2 rich flue gas interacts with the sorbent in a fluidized bed adsorber operating at 104°F. The sorbent adsorbs CO_2 from the gas before exiting the adsorber and being conveyed to a separate fluidized bed, where the sorbent is heated to 248°F. At this temperature, CO_2 is released from the sorbent, which is then conveyed back to the adsorber, where the process of adsorption is repeated. CO_2 released from the sorbent in the regenerator is compressed to the pressure required for sequestration.

The Energy Research Center (ERC) used the Aspen Plus process modeling software package to model the ADA system and the CO_2 compressors. Models of a PC plant boiler and steam cycle were also constructed in Aspen before being connected to the ADA system and CO_2 compression models. After these models were created, connected, and their operation verified, changes were made in the CO_2 capture system's process conditions. The following process conditions were varied across a range of values:

Adsorber operating temperature
Regenerator operating temperature
Sorbent water adsorption characteristics
Adsorber pressure drop
CO_2 discharge pressure

For each of these changes in process condition, net unit heat rate information was examined along with system information relating to the particular parameter being examined. A key aspect of the analysis centered around the addition of a cross heat exchanger (XHTX) to the ADA system. A XHTX improves system performance by using heat from the hot, CO_2 lean sorbent to heat the cold, CO_2 rich sorbent. To study the impact of a XHTX on the plant, a simple XHTX was added to the Aspen model, where effectiveness values of the XHTX could be varied between 0 and 1.

A significant quantity of heat is rejected from both the flue gas cooler upstream of the adsorber and the CO_2 compressors. It was determined that the quality of this heat was sufficient to accomplish heating of boiler combustion air, steam cycle feedwater, and the cold CO_2 rich sorbent entering the regenerator. The following four heat integration cases were examined in depth using the Aspen model:

HI REG – Heat from the compressors used to heat sorbent entering the regenerator
HI FWH – Heat from the compressors used to heat steam cycle feedwater
HI FG AIR – Heat from the flue gas cooler used to heat boiler combustion air
HI FG FWH – Heat from the flue gas cooler used to heat steam cycle feedwater

Combinations of these four cases were also analyzed. For instance, HI ALL is a case where all four heat integration cases are examined simultaneously.

Analyses were also performed where the concentration of CO_2 entering the adsorber column was increased by recirculating a portion of the CO_2 entering the compressors. However, the results show that recirculation of CO_2 increased both net unit HR and sorbent circulation rate.

Figure E.1 presents a summary of the major findings of this report for an Illinois #6 coal. Maximum changes in net unit HR are shown for all process condition changes, the addition of the XHTX, all individual heat integration cases, and cases where heat integration was combined with a XHTX (with an idealized effectiveness of 1.0). Also shown at the top of Figure E.1 is a case where HI ALL, a XHTX (with effectiveness of 1), and zero sorbent water adsorption are combined. This case is considered an idealized best-case scenario for the sorbent analyzed here and it shows the maximum improvement in net unit HR due to the system improvements presented in this report.

In conclusion, it was found that changes in the operating conditions of the ADA CO_2 capture system, the addition of XHTX, and heat integration can all have a major positive impact on net unit HR – especially when the various changes are combined. Decreases in net unit HR of up to 16.6, 20.2, and 19.3 percent were found for an Illinois #6, PRB, and ND Lignite coals respectively.

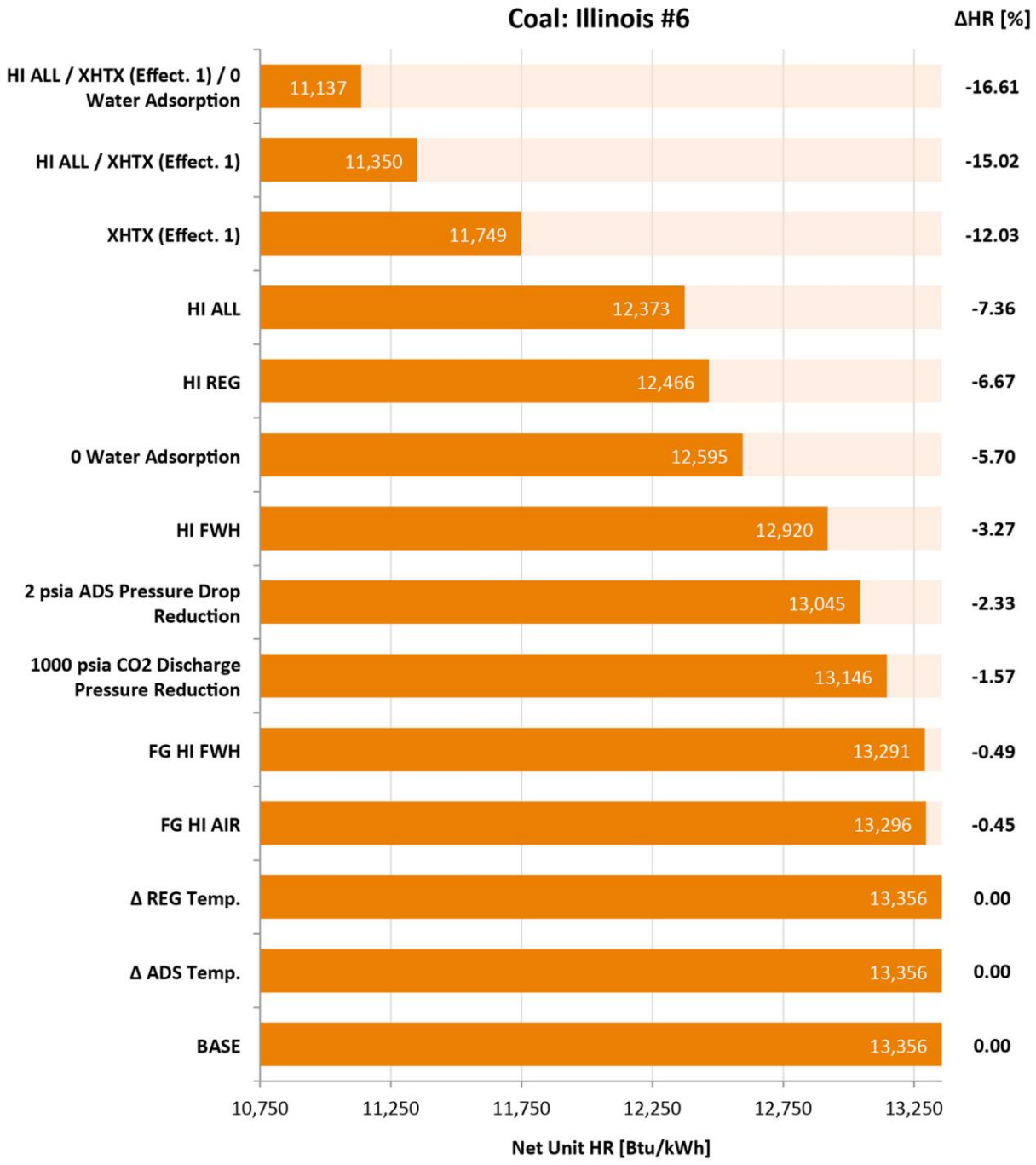

Figure E.1: Summary of Report HR Findings for Illinois #6

Introduction

ADA Environmental Solutions has designed a second generation CO_2 capture system for use on the backend of existing or new coal-fired generation facilities. The ADA system is based on a solid sorbent, which adsorbs CO_2 at a low temperature and is regenerated (releases CO_2) at an elevated temperature. Both the adsorber and regenerator (or stripper) of this system are designed as fluidized beds, where flue gas and recycled CO_2 are the respective fluidizing fluids. Figure 1.1 presents the ADA solid sorbent capture system as provided by ADA, with Table 1.1 containing supplied stream information. For the purposes of this report, any time information from Table 1.1 is referenced it is referred to by the designation “ADA”.

1.0 CO_2 Adsorption

The baseline ADA system adsorbs CO_2 at 104°F and regenerates the CO_2 at 248°F. Figure 1.2 shows CO_2 loading on the sorbent with respect to temperature and the partial pressure of CO_2 in the fluidizing gas. An attempt was made to fit the data in Figure 1.2 using a 3D curve fit, where temperature and the CO_2 partial pressure were the independent variables and sorbent loading was the dependent variable. After several attempts, it was found that this method did not provide the needed accuracy. As an alternative, separate 2D curve fits were made for each of the temperatures shown.

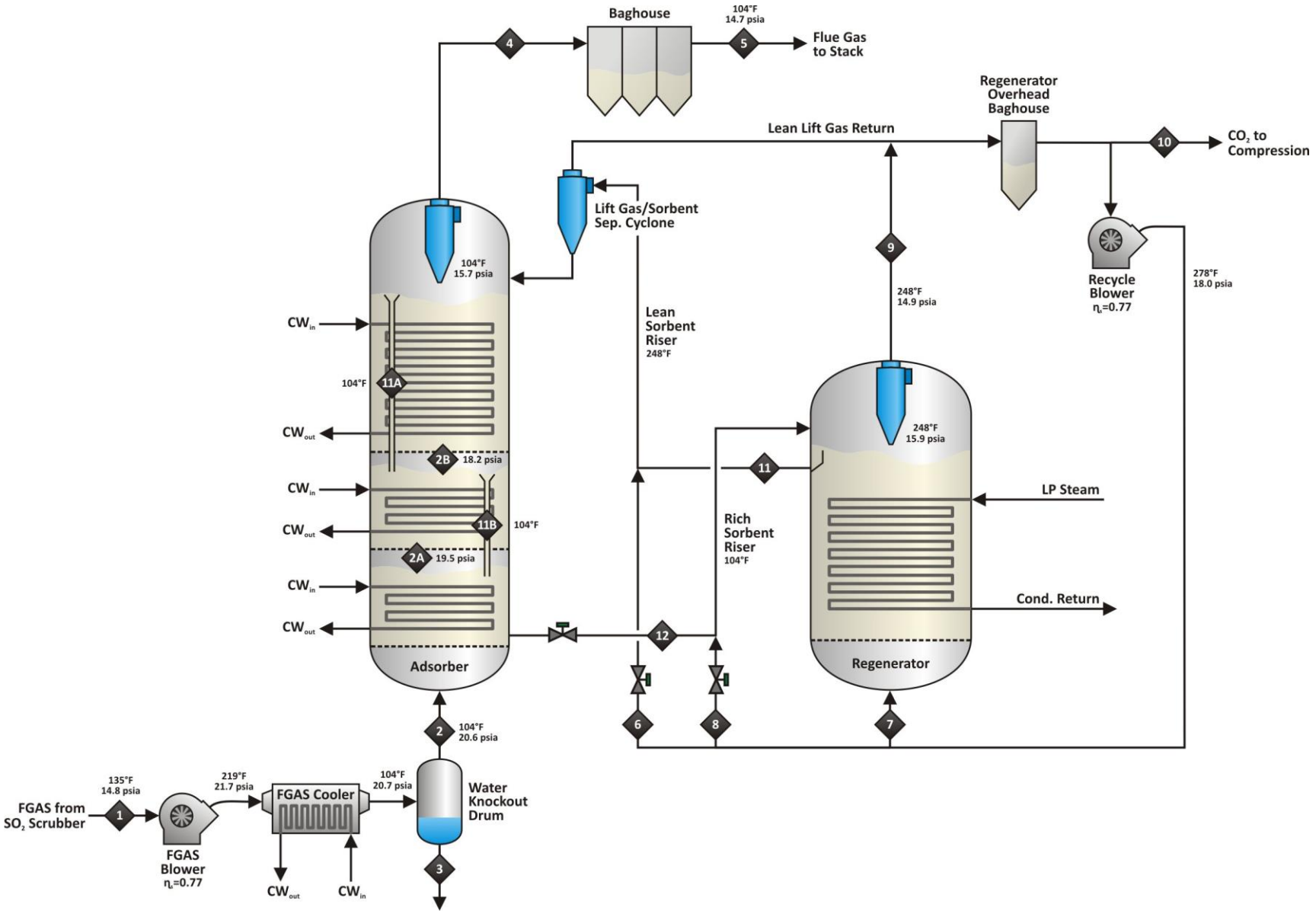

Figure 1.1: Baseline ADA CO_2 Capture System

Table 1.1: Baseline ADA CO_2 Capture System Stream Information (Data Provided by ADA)

Stream Number		1	2	2A	2B	3	4	5	6	7	8	9	10	11	11A	11B	12
		Flue Gas	FG to ADS-1	FG from ADS-1	FG from ADS-2	FG Condensate	FG from ADS-3	Clean FG	Sorbent Lift Gas	Regen Fluidized Gas	Regen Lift Gas	Regen CO2	CO2 Prod	Regen Sorbent	Sorbent from ADS-3	Sorbent from ADS-2	Sorbent from ADS-1
Substream: MIXED	**M**																
Mass Flow [lb/hr]																	
Argon	39.95	57,268	57,258	57,240	57,188	10	64,732	56,787	7,945	320	18	809	471	405	402	453	471
Carbon Dioxide	44.01	1,038,700	1,036,750	722,046	408,743	1,950	117,765	103,311	14,454	634,068	34,871	1,602,370	933,429	736	731	3,239	5,945
Water	18.02	477,785	145,406	145,360	145,229	332,379	164,385	144,209	20,176	813	45	2,054	1,197	1,028	1,020	1,151	1,197
Nitrogen	28.01	3,334,210	3,333,700	3,332,650	3,329,650	505	3,768,830	3,306,260	462,567	18,639	1,025	47,103	27,439	23,563	23,383	26,387	27,440
Oxygen	32.00	135,940	135,914	135,872	135,749	25	153,655	134,796	18,859	760	42	1,920	1,119	961	953	1,076	1,119
Sulfur Dioxide	64.06	0	0	0	0	0	0	0	0	0	0	0	0	0	0	0	0
Total Fluid [lb/hr]		5,043,903	4,709,028	4,393,168	4,076,559	334,869	4,269,367	3,745,363	524,000	654,600	36,000	1,654,257	963,655	26,693	26,489	32,306	36,173
Molar Flow [lbmol/hr]																	
Argon	39.95	1,434	1,433	1,433	1,432	0	1,620	1,422	199	8	0	20	12	10	10	11	12
Carbon Dioxide	44.01	23,602	23,557	16,406	9,288	44	2,676	2,347	328	14,407	792	36,409	21,210	17	17	74	135
Water	18.02	26,521	8,071	8,069	8,061	18,450	9,125	8,005	1,120	45	2	114	66	57	57	64	66
Nitrogen	28.01	119,022	119,004	118,966	118,859	18	134,536	118,024	16,512	665	37	1,681	980	841	835	942	980
Oxygen	32.00	4,248	4,247	4,246	4,242	1	4,802	4,213	589	24	1	60	35	30	30	34	35
Sulfur Dioxide	64.06	0	0	0	0	0	0	0	0	0	0	0	0	0	0	0	0
Total Fluid [lbmol/hr]		174,826	156,313	149,120	141,882	18,513	152,759	134,010	18,749	15,150	833	38,285	22,302	955	948	1,124	1,228
Mol-Frac																	
Argon		0.0082	0.0092	0.0096	0.0101	0.0000	0.0106	0.0106	0.0106	0.0005	0.0000	0.0005	0.0005	0.0105	0.0105	0.0098	0.0098
Carbon Dioxide		0.1350	0.1507	0.1100	0.0655	0.0024	0.0175	0.0175	0.0175	0.9510	0.9508	0.9510	0.9510	0.0178	0.0179	0.0658	0.1099
Water		0.1517	0.0516	0.0541	0.0568	0.9966	0.0597	0.0597	0.0597	0.0030	0.0024	0.0030	0.0030	0.0597	0.0601	0.0569	0.0537
Nitrogen		0.6808	0.7613	0.7978	0.8377	0.0010	0.8807	0.8807	0.8807	0.0439	0.0444	0.0439	0.0439	0.8806	0.8808	0.8381	0.7980
Oxygen		0.0243	0.0272	0.0285	0.0299	0.0001	0.0314	0.0314	0.0314	0.0016	0.0012	0.0016	0.0016	0.0314	0.0316	0.0302	0.0285
Sulfur Dioxide		0.0000	0.0000	0.0000	0.0000	0.0000	0.0000	0.0000	0.0000	0.0000	0.0000	0.0000	0.0000	0.0000	0.0000	0.0000	0.0000
Substream: SOLIDS																	
Mass Flow [lb/hr]																	
Sorbent (pure)														13,320,900	13,320,900	13,320,900	13,320,900
Carbon Dioxide (adsorbed)														461,729	766,355	1,077,211	1,389,196
Water (adsorbed)														0	0	0	
Total Solid [lb/hr]														13,782,629	14,087,255	14,398,111	14,710,096
Mass-Frac [% of pure sorb.]																	
Sorbent (pure)														100	100	100	100
Carbon Dioxide (adsorbed)														3.47	5.75	8.09	10.43
Water (adsorbed)														0.00	0.00	0.00	0.00
Substream: TOTAL																	
Total Mass Flow [lb/hr]		5,043,903	4,709,028	4,393,168	4,076,559	334,869	4,269,367	3,745,363	524,000	654,600	36,000	1,654,257	963,655	13,809,322	14,113,744	14,430,417	14,746,269
Properties: Mixed																	
Temperature [°F]		135	104	104	104	104	104	104	139	289	289	248	248		104	104	104
Pressure [psia]		14.8	20.6	19.5	18.2	20.6	14.7	14.7	17.2	18	18	14.7	14.7		14.7	18.2	19.5
Average MW		28.85	30.13	29.46	28.73	18.09	27.95	27.95	27.95	43.21	43.21	43.21	43.21				
Density [lb/cuft]		0.067	0.103	0.095	0.086	61.177	0.068	0.068	0.075	0.097	0.097	0.084	0.084				
Heat Capacity [Btu/lb°F]		0.257	0.243			0.94	0.252	0.252	0.252	0.23	0.23	0.226	0.226		0.252	0.249	0.246
Thermal Cond. [Btu/hrft°F]		0.015	0.014			0.279	0.015	0.015	0.016	0.015	0.015	0.014	0.014		0.015	0.015	0.014
Properties: Solid																	
Heat Capacity [Btu/lb°F]														0.251	0.251	0.251	0.251
Utility		Regenerator	ADS-1	ADS-2	ADS-3	Flue Gas Cooler	Flue Gas Comp.	Lift Gas Comp.	CO2 Recycle Comp.	Total							
30 psig Steam [lb/hr]		1,128,150								1,128,150							
CW (20°F rise) [gpm]			18,233	18,123	66,437	49,946				152,739							
Electric Power [BHP]							47,600	2,000	2,300	51,900							

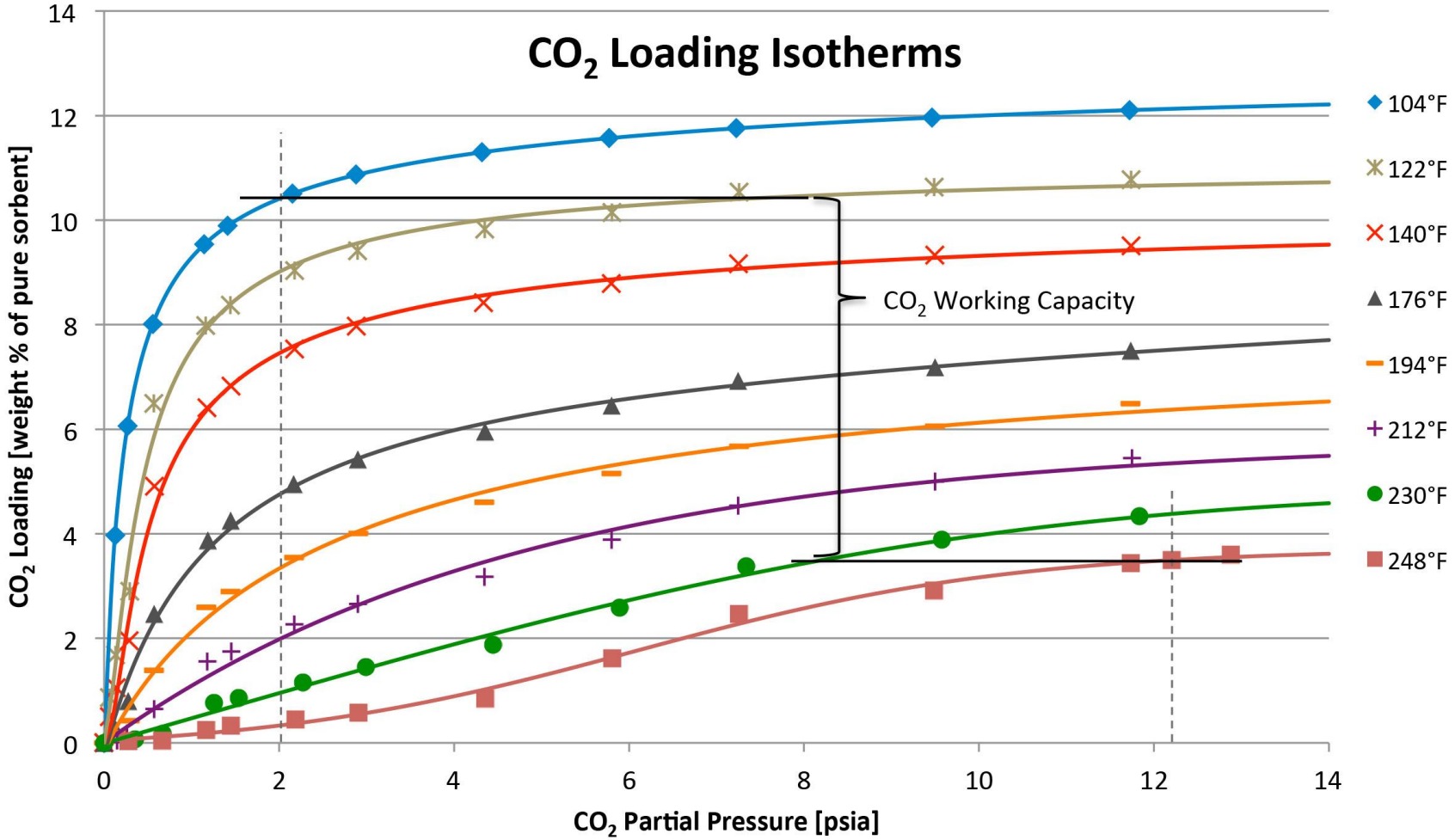

Figure 1.2: CO_2 Loading Isotherm Data and Curve Fits

2.0 H_2O Adsorption

Information from ADA suggests that the H_2O loading on the sorbent leaving the adsorber is 0.013 $lbm_{H2O}/lbm_{sorbent}$ and that the change in loading across the adsorber (H_2O working capacity) is 0.009 $lbm_{H2O}/lbm_{sorbent}$. This implies that the H_2O loading leaving the regenerator, or entering the adsorber, is 0.004 $lbm_{H2O}/lbm_{sorbent}$. While it is expected that H_2O loading also depends on the partial pressure of H_2O in the gas, no information was provided on H_2O loading vs. H_2O pressure and temperature. It was thus assumed that H_2O is adsorbed in much the same fashion as CO_2. With this assumption in place, the CO_2 loading curves of Figure 1.2 were used as the starting point for finding appropriate H_2O adsorption characteristics. First, the x-axis was assumed to designate H_2O partial pressure instead of CO_2 partial pressure. Next, both the 104°F and 248°F curves were multiplied by H_2O loading multipliers. These multipliers were selected such that a rich H_2O loading value of 0.013 $lbm_{H2O}/lbm_{sorbent}$ and a lean H_2O loading value of 0.004 $lbm_{H2O}/lbm_{sorbent}$ (as presented in the information from ADA) result for the H_2O partial pressures typically found in both the adsorber and regenerator. The resulting H_2O loading multipliers are as follows:

For the adsorber (104°F):
H_2O Loading Multiplier = 0.13955

For the regenerator (248°F):
H_2O Loading Multiplier = 0.39983

Figure 2.1 presents the assumed H_2O loading isotherms (after applying the H_2O loading multipliers) along with the rich and lean loading values and the resulting H_2O working capacity of the sorbent. Note that these loading values correlate with the rich and lean H_2O loading values of 0.013 $lbm_{H2O}/lbm_{sorbent}$ and 0.004 $lbm_{H2O}/lbm_{sorbent}$ respectively. These values agree with the information provided by ADA.

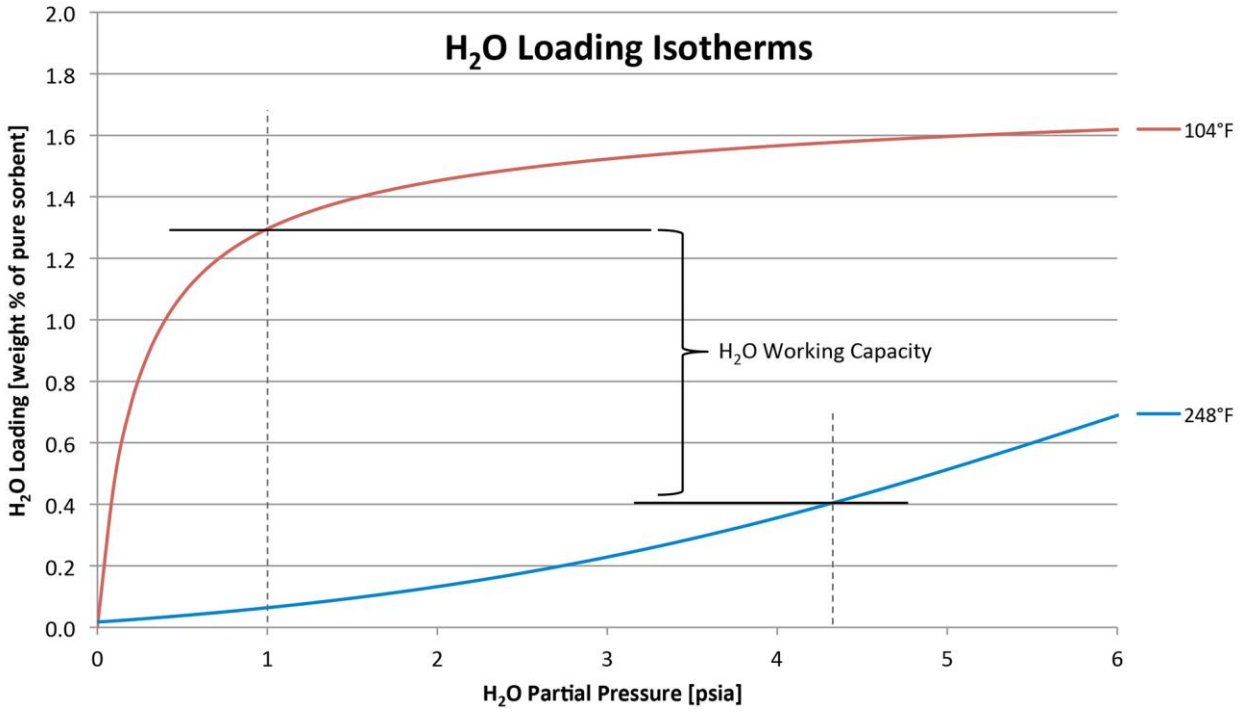

Figure 2.1: Assumed H_2O Loading Isotherms

3.0 Three-Section Adsorber Model

As seen in Figure 1.1, the ADA adsorber is divided into three separate fluidized beds, with the solids entering the uppermost bed and being cascaded through the lower two beds. The uppermost (3rd) bed is the largest because of the need for increased cooling surface area. The sorbent enters this bed at around 248°F and needs to be cooled to 104°F to maximize CO_2 adsorption. Cooling is also required in each bed section to maintain a constant temperature of 104°F throughout the adsorber. CO_2 adsorption is a highly exothermic reaction at 587 Btu/lbm$_{CO2\ adsorbed}$. For H_2O adsorption, the heat released is assumed to be equal to the latent heat of water (~1,035 Btu/lbm$_{H2O\ adsorbed}$).

Since the overall bed sorbent and gas flows are countercurrent to each other, the three-bed model must be solved iteratively. For each bed, it is assumed that the gas and sorbent are well-mixed within a short distance from the gas-inlet (bottom) end of the bed. The gas and sorbent leaving each bed section are thus assumed to be equal to their composition in the well-mixed bed. Figure 3.1 presents a graphical illustration of the 3-bed adsorber model developed for this project. Both the gas and sorbent

inlet streams are specified as well as the gas pressure of each bed and an adsorber temperature of 104°F in all three beds. For each of the three iteration loops, an initial guess of the gas composition is used to calculate the CO_2 and H_2O loading by use of the 2D loading curve fits. CO_2 and H_2O capture rates for each bed are calculated using these loading values. If these capture rates correlate with the guessed gas compositions, the iteration is complete. Otherwise, the initial guesses of the gas CO_2, and H_2O flows are adjusted and the entire process is repeated. The capture rate of either CO_2 or H_2O in each bed section must correlate with an equal change in gas composition for that compound.

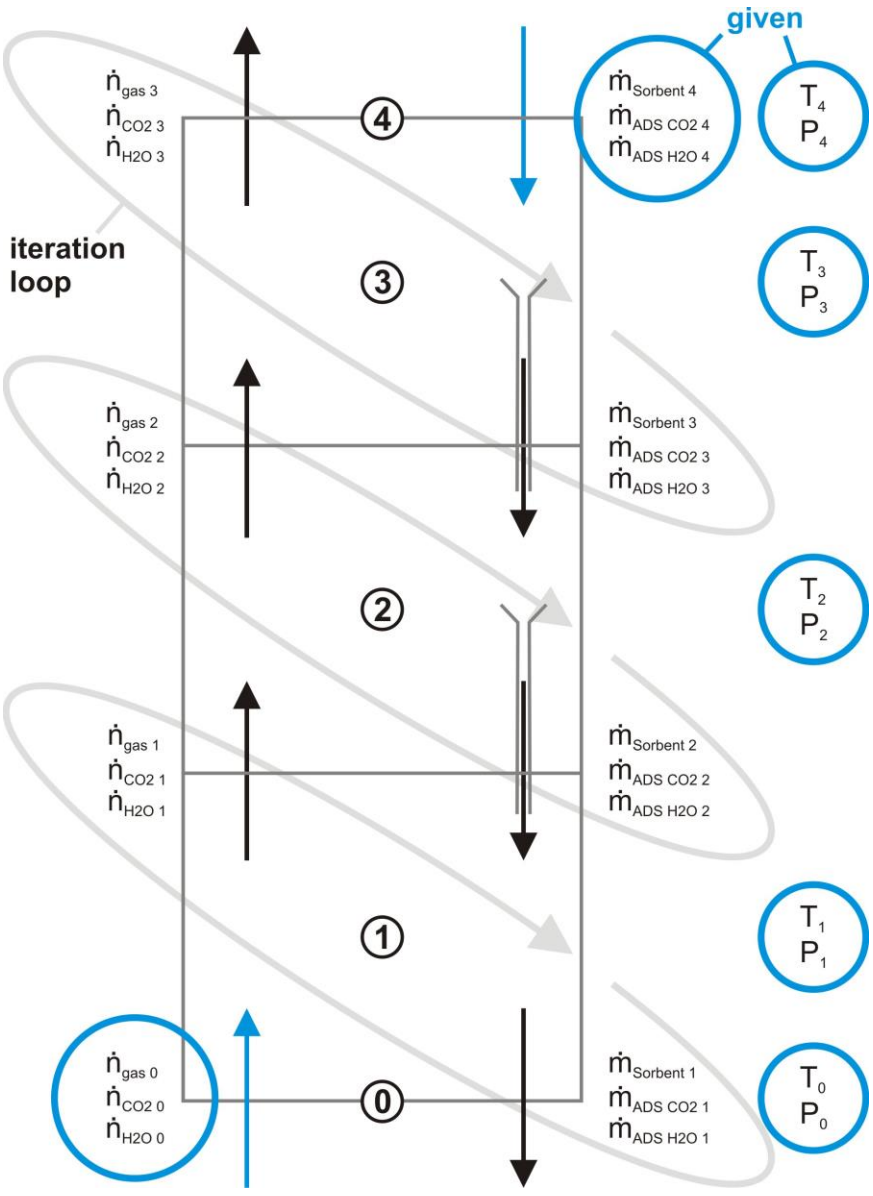

Figure 3.1: Iterative 3-Section Adsorber Model

When this model was first implemented in Microsoft Excel to test its operation, it was found to provide an accurate, converging solution. However, since the aim of this project was to use Aspen Plus to model the ADA solid sorbent capture system, this model was implemented in an Aspen Plus calculator block using Fortan code. Also integrated into the code was another iteration loop to adjust the sorbent flow rate until 90 percent CO_2 capture across the entire adsorber was attained.

4.0 Regenerator Model

A similar iterative model was constructed for the regenerator. However, since the regenerator consists of a single fluidized bed, the model is considerably simpler. Figure 4.1 presents the iterative regenerator model, which iterates CO_2 and H_2O gas composition guesses until they converge with the rate of CO_2 and H_2O calculated to be released in the stripper. The 2D loading curve fits were utilized to find the CO_2 and H_2O loadings on the sorbent leaving the stripper. As with the adsorber model, the stripper model was implemented in Excel before being built into a calculator block in Aspen Plus.

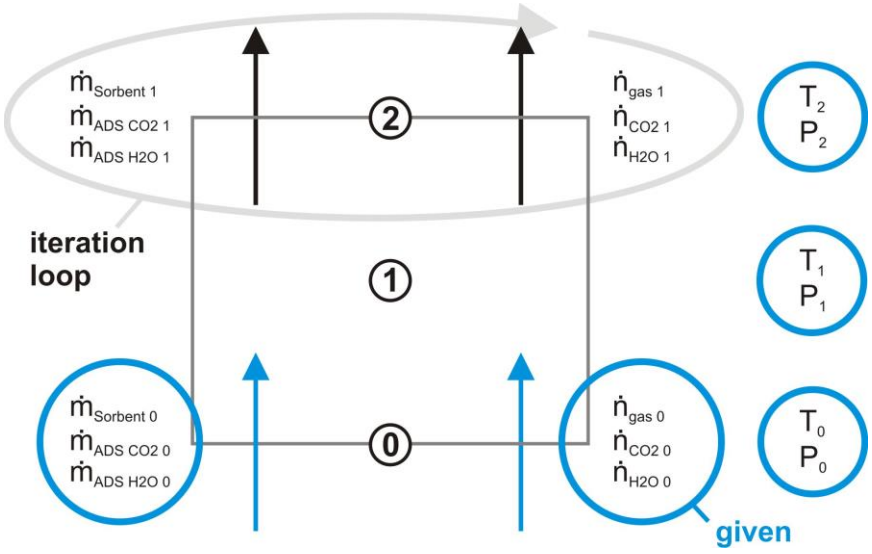

Figure 4.1: Iterative Stripper Model

5.0 ADA System Model Validation

The Excel and Aspen Plus results were validated by using the stream input values presented in Table 1.1. For this validation, the sorbent was assumed to not adsorb water since this was the assumption for the ADA results in Table 1.1. Table 5.1 presents these validation results for key streams in the system design. It can be seen that the Excel and Aspen results closely agree with one another. However, there is considerable discrepancy between these results and the ADA results for the CO_2 adsorbed in the individual bed sections. This is also illustrated in Figure 5.1, which shows the CO_2 adsorbed in each bed section.

Table 5.1: Model Validation Results

Stream		ADA [mol/hr]	Diff [%]	Excel [mol/hr]	Diff [%]	Aspen [mol/hr]	Diff [%]	ADA [mol/hr]
	Gas	124,685	0.0	124,685	0.0	124,704	0.0	124,685
2	CO2	23,557	0.0	23,557	-0.2	23,602	-0.2	23,557
	H2O	8,071	0.0	8,071	-2.0	8,230	-2.0	8,071
	Gas	124,645	0.8	123,658	0.0	123,677	0.8	124,645
2A	CO2	16,406	-25	20,529	-0.3	20,585	-25	16,406
	H2O	8,069	0.8	8,005	-2.0	8,163	-1.2	8,069
	Gas	124,533	0.7	123,658	0.0	123,676	0.7	124,533
2B	CO2	9,288	-10	10,234	-0.4	10,273	-11	9,288
	H2O	8,061	0.7	8,005	-2.0	8,163	-1.3	8,061
	Gas	123,658	0.0	123,658	0.0	123,677	0.0	123,658
5	CO2	2,347	-0.4	2,356	-0.2	2,360	-0.6	2,347
	H2O	8,005	0.0	8,005	-2.0	8,163	-2.0	8,005
	Gas	1,762	-1.4	1,787	0.2	1,784	-1.3	1,762
9	CO2	36,409	-1.3	36,896	0.0	36,904	-1.4	36,409
	H2O	114	-1.8	116	-1.5	118	-3.3	114
	Gas	1,026	-0.1	1,027	0.0	1,027	-0.1	1,026
10	CO2	21,210	0.0	21,210	-0.1	21,241	-0.1	21,210
	H2O	66	0.0	66	-2.7	68	-2.7	66
		[lb/hr]	[%]	[lb/hr]	[%]	[lb/hr]	[%]	[lb/hr]
	Sorb	13,320,900	2.2	13,031,199	-0.1	13,046,300	2.1	13,320,900
11	ADS C	461,729	-4	479,965	0.1	479,654	-4	461,729
	ADS W	0	-	0	-	0	-	0
	Sorb	13,320,900	2.2	13,031,199	-0.1	13,046,300	2.1	13,320,900
11A	ADS C	766,355	-7.9	826,696	-0.1	827,870	-8.0	766,355
	ADS W	0	-	0	-	0	-	0
	Sorb	13,320,900	2.2	13,031,199	-0.1	13,046,300	2.1	13,320,900
11B	ADS C	1,077,211	-19	1,279,749	-0.2	1,281,710	-19	1,077,211
	ADS W	0	-	0	-	0	-	0
	Sorb	13,320,900	2.2	13,031,199	-0.1	13,046,300	2.1	13,320,900
12	ADS C	1,389,196	-1.2	1,405,528	-0.1	1,406,950	-1.3	1,389,196
	ADS W	0	-	0	-	0	-	0

Figure 5.1: Comparison of CO_2 Capture Results Across Adsorber

It can be seen that the Excel and Aspen models suggest the bulk of CO_2 adsorption takes place in the middle adsorber bed (ADS2), followed closely by the uppermost bed (ADS3). This is in contrast to the ADA results, which show close to equal adsorption in all three beds. Figure 1.2 clearly shows that CO_2 capture is driven by the partial pressure of gaseous CO_2 in each bed. However, Figure 1.2 also clearly illustrates a non-linear correlation between CO_2 partial pressure and CO_2 loading. At lower CO_2 partial pressures (ADS2 and ADS3) and 104°F, small changes in partial pressure result in large changes in CO_2 loading, while at higher partial pressures values (ADS1), large changes in partial pressure results in relatively small changes in CO_2 loading. Despite these differences between the ADA results and the Excel and Aspen results, Figure 5.1 and Table 5.1 show that all of the results have virtually the same total CO_2 capture rate.

Model Mass & Energy Balances

In order to further validate the Excel and Aspen Plus results, mass and energy balances were conducted for both models. Separate control volumes were assumed around both the adsorber and stripper as seen in Figure 5.2 and Figure 5.3.

Mass Balance Governing Equations

Equations were assumed, which summarize the mass flows into and out of the adsorber and stripper control volumes.

Adsorber Inlet Streams:

2. $\dot{m}_{gas\ in}$
13. $\dot{m}_{SORB} + \dot{m}_{ADS\ CO2\ lean} + \dot{m}_{ADS\ H2O\ lean}$
14. $\dot{m}_{ADS3\ CWin}$
16. $\dot{m}_{ADS2\ CWin}$
18. $\dot{m}_{ADS1\ CWin}$

Adsorber Outlet Streams:

4. $\dot{m}_{gas\ out}$
12. $\dot{m}_{rich\ gas\ lk} + \dot{m}_{SORB} + \dot{m}_{ADS\ CO2\ rich} + \dot{m}_{ADS\ H2O\ rich}$
15. $\dot{m}_{ADS3\ CWout}$
17. $\dot{m}_{ADS2\ CWout}$
19. $\dot{m}_{ADS1\ CWout}$

Regenerator Inlet Streams:

7. $\dot{m}_{recycle\ gas}$
23. $\dot{m}_{rich\ gas\ lk} + \dot{m}_{rich\ lift\ gas} + \dot{m}_{SORB} + \dot{m}_{ADS\ CO2\ rich} + \dot{m}_{ADS\ H2O\ rich}$
24. $\dot{m}_{LP\ Steam}$

Regenerator Outlet Streams:

9. $\dot{m}_{CO2\ prod\ gas}$
11. $\dot{m}_{lean\ gas\ lk} + \dot{m}_{SORB} + \dot{m}_{ADS\ CO2\ lean} + \dot{m}_{ADS\ H2O\ lean}$

25. $\dot{m}_{Condensed\ Steam}$

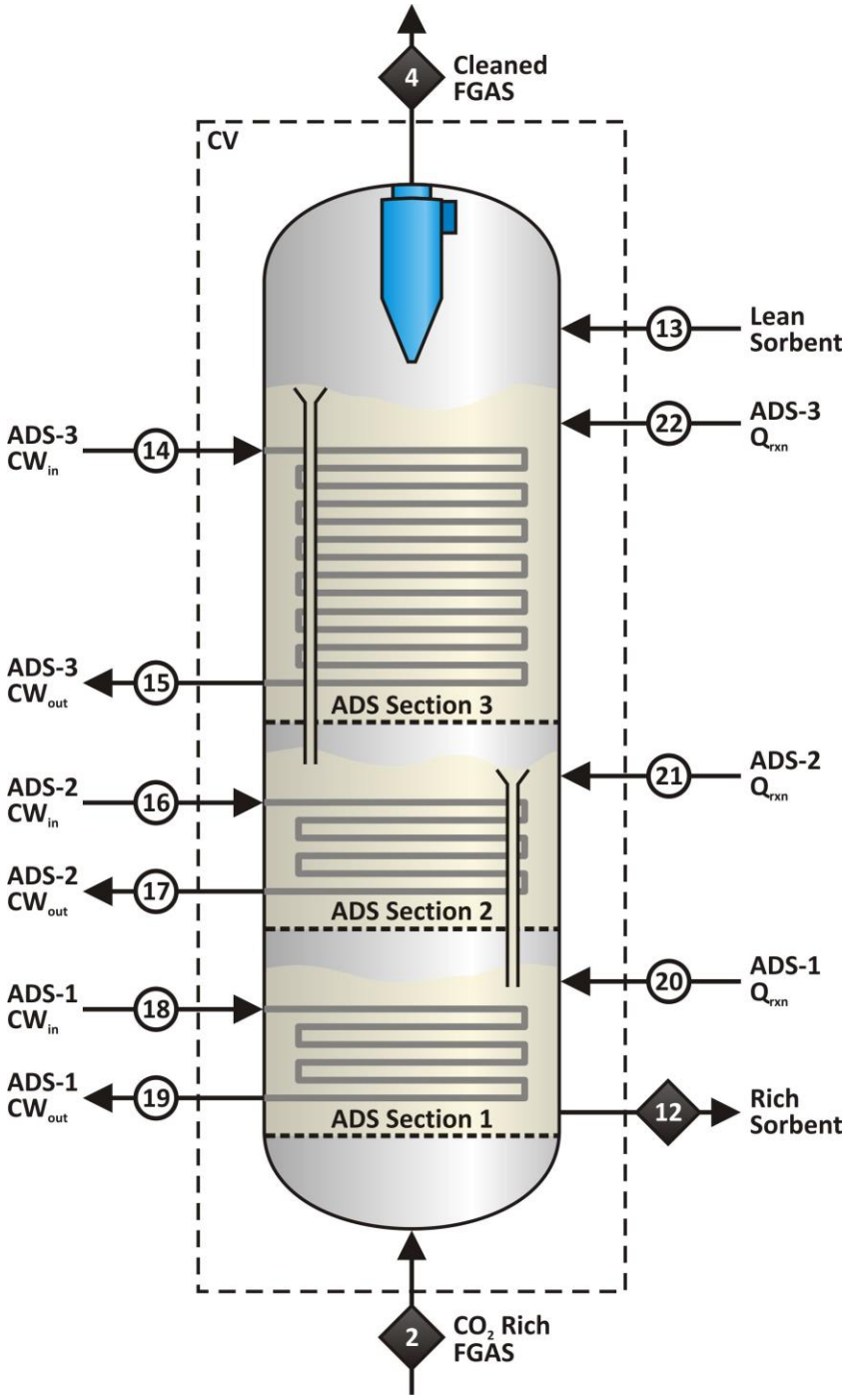

Figure 5.2: Adsorber Mass & Energy Balance

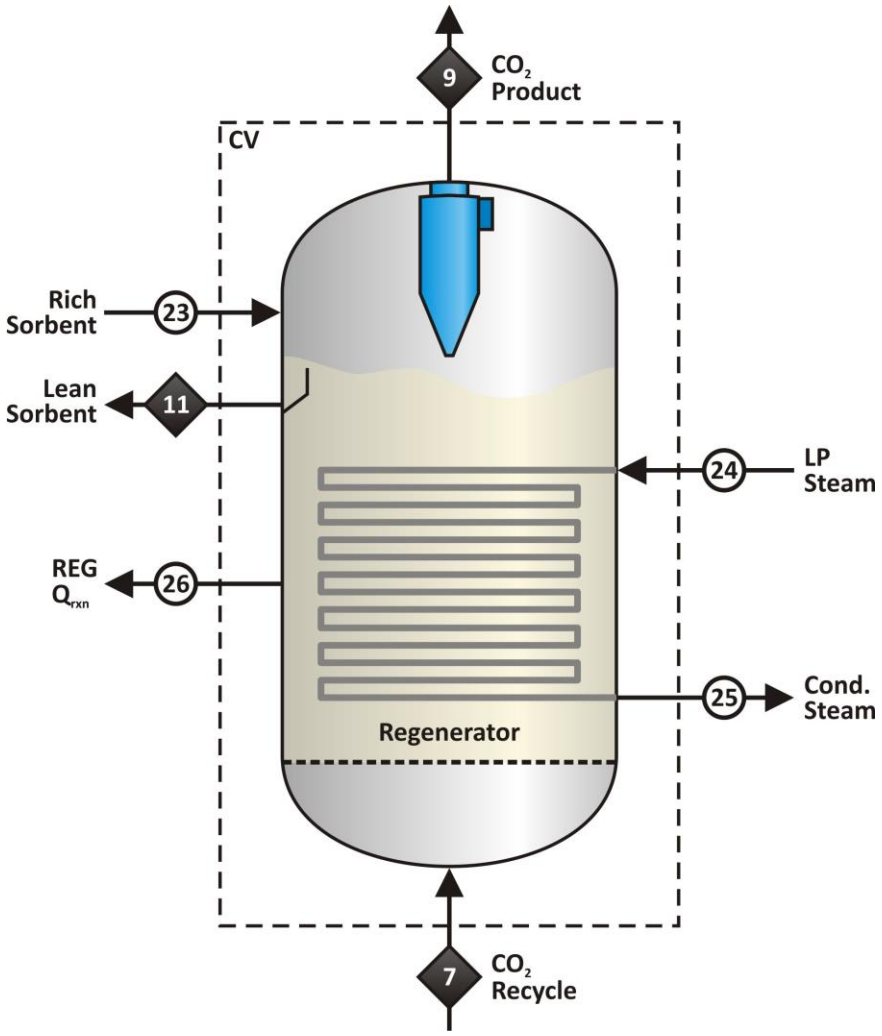

Figure 5.3: Stripper Mass & Energy Balance

Energy Balance Governing Equations

The following equations were assumed to summarize the energy flows into and out of the adsorber and stripper control volumes:

Adsorber Inlet Streams:

2. $\dot{m}_{gas\ in}\left[h_g\left(T_{(2)}\right) - h_g\left(T_{77°F}\right)\right]$

13. $\dot{m}_{SORB}0.251\frac{Btu}{lbm°F}\left(T_{(13)} - T_{77°F}\right) + \dot{m}_{ADS\ CO2\ lean}0.222\frac{Btu}{lbm°F}\left(T_{(13)} - T_{77°F}\right) + \dot{m}_{ADS\ H2O\ lean}0.998\frac{Btu}{lbm°F}\left(T_{(13)} - T_{77°F}\right)$

14. $\dot{m}_{ADS3\ CWin}\left[h_l\left(T_{(14)}\right) - h_l\left(T_{(77°F)}\right)\right]$

16. $\dot{m}_{ADS2\ CWin}\left[h_l\left(T_{(16)}\right) - h_l\left(T_{(77°F)}\right)\right]$

18. $\dot{m}_{ADS1\ CWin}\left[h_l\left(T_{(18)}\right) - h_l\left(T_{(77°F)}\right)\right]$

20. $\dot{m}_{ADS1\ CAP\ CO2}\ 587\frac{Btu}{lbm} + \dot{m}_{ADS1\ CAP\ H2O}\ L\left(T_{(20)}\right)$

21. $\dot{m}_{ADS2\ CAP\ CO2}\ 587\frac{Btu}{lbm} + \dot{m}_{ADS2\ CAP\ H2O}\ L\left(T_{(21)}\right)$

22. $\dot{m}_{ADS3\ CAP\ CO2}\ 587\frac{Btu}{lbm} + \dot{m}_{ADS3\ CAP\ H2O}\ L\left(T_{(22)}\right)$

Adsorber Outlet Streams:

4. $\dot{m}_{gas\ out}\left[h_g\left(T_{(4)}\right) - h_g(T_{77°F})\right]$

12. $\dot{m}_{rich\ gas\ lk}\left[h_g\left(T_{(12)}\right) - h_g(T_{77°F})\right] + \dot{m}_{SORB}0.251\frac{Btu}{lbm°F}\left(T_{(12)} - T_{77°F}\right) +$
$\dot{m}_{ADS\ CO2\ rich}0.222\frac{Btu}{lbm°F}\left(T_{(12)} - T_{77°F}\right) + \dot{m}_{ADS\ H2O\ rich}0.998\frac{Btu}{lbm°F}\left(T_{(12)} - T_{77°F}\right)$

15. $\dot{m}_{ADS3\ CWout}\left[h_l\left(T_{(15)}\right) - h_l\left(T_{(77°F)}\right)\right]$

17. $\dot{m}_{ADS2\ CWout}\left[h_l\left(T_{(17)}\right) - h_l\left(T_{(77°F)}\right)\right]$

19. $\dot{m}_{ADS1\ CWout}\left[h_l\left(T_{(19)}\right) - h_l\left(T_{(77°F)}\right)\right]$

Regenerator Inlet Streams:

7. $\dot{m}_{recycle\ gas}\left[h_g\left(T_{(7)}\right) - h_g(T_{77°F})\right]$

23. $\dot{m}_{rich\ gas\ lk}\left[h_g\left(T_{(23)}\right) - h_g(T_{77°F})\right] + \dot{m}_{rich\ lift\ gas}\left[h_g\left(T_{(23)}\right) - h_g(T_{77°F})\right] +$
$\dot{m}_{SORB}0.251\frac{Btu}{lbm°F}\left(T_{(23)} - T_{77°F}\right) + \dot{m}_{ADS\ CO2\ rich}0.222\frac{Btu}{lbm°F}\left(T_{(23)} - T_{77°F}\right) +$
$\dot{m}_{ADS\ H2O\ rich}0.998\left(T_{(23)} - T_{77°F}\right)$

24. $\dot{m}_{LP\ Steam}\left[h_g\left(T_{(24)}\right) - h_l(T_{77°F})\right]$

Regenerator Outlet Streams:

9. $\dot{m}_{CO2\ prod\ gas}\left[h_g\left(T_{(9)}\right) - h_g(T_{77°F})\right]$

11. $\dot{m}_{lean\ gas\ lk}\left[h_g\left(T_{(11)}\right) - h_g(T_{77°F})\right] + \dot{m}_{SORB}0.251\frac{Btu}{lbm°F}\left(T_{(11)} - T_{77°F}\right) +$
$\dot{m}_{ADS\ CO2\ lean}0.222\frac{Btu}{lbm°F}\left(T_{(11)} - T_{77°F}\right) + \dot{m}_{ADS\ H2O\ lean}0.998\frac{Btu}{lbm°F}\left(T_{(11)} - T_{77°F}\right)$

25. $\dot{m}_{Condensed\ Steam}\left[h_l\left(T_{(25)}\right) - h_l(T_{77°F})\right]$

26. $\dot{m}_{REG\ REL\ CO2}\ 587\frac{Btu}{lbm} + \dot{m}_{REG\ REL\ H2O}\ L\left(T_{(26)}\right)$

It should be noted that the value of 587 Btu/lbm$_{CO2}$ in streams 20 through 22 and stream 26 is the heat released during the adsorption of CO_2 or the heat adsorbed during the desorption of CO_2. 0.251

Btu/lbm°F is the specific heat of the pure sorbent, 0.222 Btu/lbm°F is the specific heat of CO_2 adsorbed into the sorbent, and 0.998 Btu/lbm°F is the specific heat of liquid water adsorbed by the sorbent. L is the latent heat of vaporization of water in these equations and Cp is the specific heat of the cooling water.

Mass & Energy Balance Results

For both the mass and energy balance equations, the difference in the sum of inlet and outlet steams divided by the sum of inlet streams provide mass and energy balance results for the system.

$$Balance\ Results\ [\%] = \frac{\sum Inlet\ Streams - \sum Outlet\ Streams}{\sum Inlet\ Streams} 100\%$$

Using the equation above, the following results were found for the mass and energy balances of both the Excel and Aspen Plus models:

Excel Adsorber Mass Balance:	0.0001%
Excel Stripper Mass Balance:	-0.0002%
Aspen Adsorber Mass Balance:	0.0000%
Aspen Stripper Mass Balance:	0.0000%

Excel Adsorber Energy Balance:	-1.7867%
Excel Stripper Energy Balance:	0.8751%
Aspen Adsorber Energy Balance:	-0.8816
Aspen Stripper Energy Balance:	0.1977

Table A.1 through Table A.4 in the Appendix summarize the calculations behind these mass and energy balance results. It can be seen that all of the results are consistent from a mass and energy balance standpoint, with a largest discrepancy of only around 1.8 percent. This helps to confirm that the Excel and Aspen models of the ADA capture system are producing well-behaved results.

6.0 ADA Capture System Components

Capture System Fans

Fans are an integral part of the ADA solid sorbent capture system. The primary purpose of the largest of these (the Booster Fan) is to overcome the pressure drop of the flue gas as it passes through the three adsorber beds. Before entering the adsorber, the flue gas also experiences lesser, but still significant, pressure drops in the flue gas cooler. In total, the Booster Fan must increase the flue gas pressure by around 6 psia. A blower efficiency of 77 percent was assumed based on the temperature of the gas leaving the fan in Table 1.1. Another fan, the CO_2 Recycle Blower, pressurizes the CO_2 used to fluidize the regenerator bed and lift both the rich and lean sorbent streams. As before, a fan efficiency of 77 percent is assumed.

CO_2 Recycle and Sorbent Lift Gases

Table 1.1 was used to determine the flow rate of recycled CO_2 required to fluidize the regenerator and lift both the rich and lean sorbent streams. The following correlations were found with respect to the mole flow rate of gas ($lbmol_{gas}$) required per mass flow rate of sorbent and adsorbed CO_2 and H_2O (lbm_{sorb}):

Regenerator Fluidizing Gas:	1.03×10^{-3} $lbmol_{gas}/lbm_{sorb\ RICH}$
Rich Lift Gas:	5.66×10^{-5} $lbmol_{gas}/lbm_{sorb\ RICH}$
Lean Lift Gas:	5.66×10^{-5} $lbmol_{gas}/lbm_{sorb\ LEAN}$

Note that the lean lift gas in Table 1.1 is recycled scrubbed flue gas, while recycled CO_2 is utilized in the Aspen Plus model. Also, the flow rate of this lift gas was much higher than the rich lift gas flow in Table 1.1. Therefore, it was assumed that a lean lift gas flow rate equal to the rich lift gas flow rate could be used.

In addition to the rich lift gas, the rich sorbent stream also contains 0.82 percent of the flue gas flow leaving the first (bottom) adsorber bed. This gas is assumed to be entrained in the CO_2 rich sorbent stream and is carried along with the sorbent into the regenerator.

Flue Gas Cooling

It is assumed that the flue gas entering the adsorber column is first cooled to the adsorber operating temperature (104°F for the BASE ADA case) in a condensing heat exchanger (flue gas cooler) upstream of the adsorber. This heat exchanger is called a condensing heat exchanger because it not only cools the flue gases, but also condenses water vapor from the flue gas. The flue gas leaving the cooler at 104°F is saturated with H_2O. Xingchao Wang conducted detailed calculations to find the optimal flue gas cooler specifications and operating conditions [1]. With his design, flue gas enters the cooling system at an average temperature of 223°F, and before entering the condensing heat exchanger is cooled to an average temperature of 177°F by a spray of cold water (Figure 6.1).

Cooling water is fed to the condensing heat exchanger and heated to a nominal temperature of 130°F. Wang calculated results for cooling water temperatures of 65°F and 80°F entering the cooler. The cooling water was assumed to be cooled by a cooling tower to 80°F, while if it was further cooled to 65°F a refrigeration cycle was needed. If the cooling water is cooled to 65°F instead of 80°F, the cooling water mass flow rate is reduced, heat exchanger surface area is reduced, and power required to operate water circulation pumps and flue gas fans is reduced. However, these benefits are partially offset by the additional power required for the refrigeration system. Ultimately, it was found that for adsorber operating temperatures below 110°F, cooling the water to 65°F with a refrigeration system is more economical than only cooling it to 80°F in a cooling tower. Therefore, the Aspen Plus model of the flue gas cooler was constructed with a refrigeration system to cool the cooling water to 65°F. Figure 6.1 shows the complete flue gas cooling system as modeled.

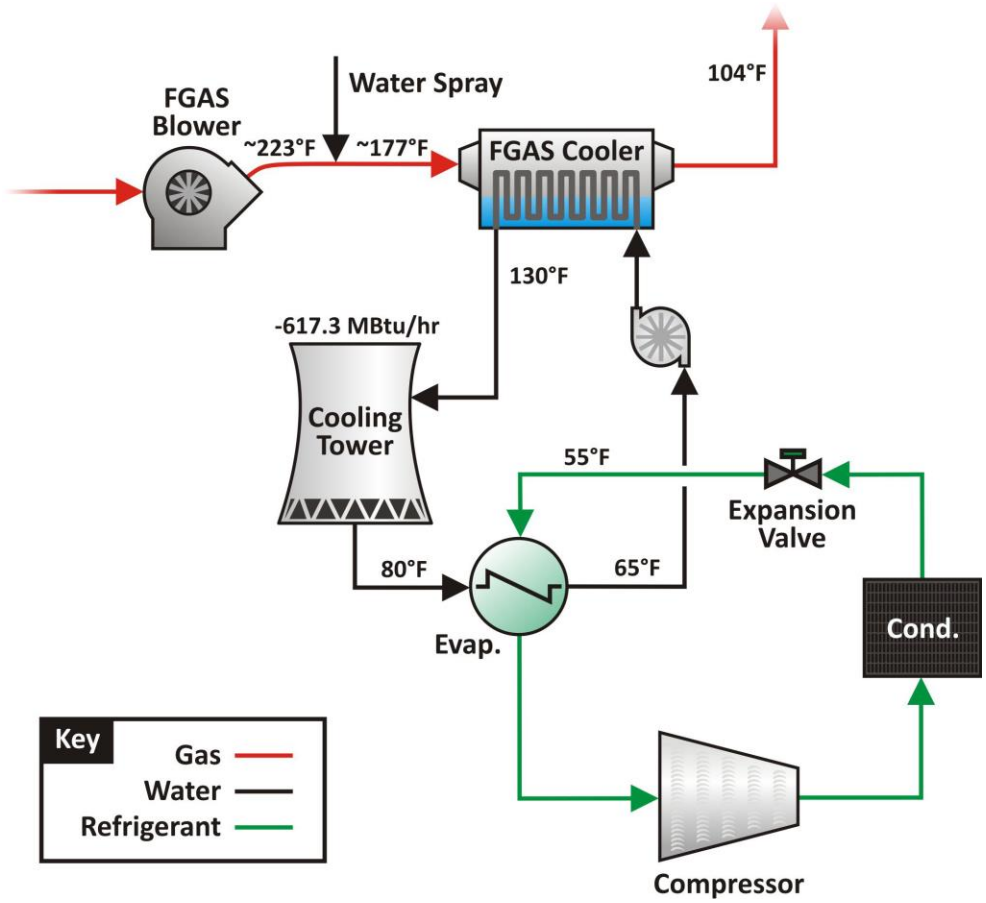

Figure 6.1: Flue Gas Cooler System

As seen, 65°F cooling water absorbs heat in the flue gas cooler and is assumed to be heated to 130°F before being cooled to 80°F in a cooling tower. After leaving the cooling tower, the cooling water passes through the refrigeration cycle evaporator, where it evaporates the refrigerant while being cooled to 65°F. The refrigeration cycle operates at a cold-side temperature of 55°F and compressor discharge pressure of 101.4 psia.

Adsorber Cooling

Not only is a cooling system required for the flue gas stream upstream of the adsorber, but internal cooling of each adsorber bed section is required to remove the heats of adsorption of CO_2 and H_2O as well as cool the lean sorbent from 248°F to 104°F in the ADS3 bed. As in the case of the flue gas cooler, cooling water at 65°F is pumped through coils placed throughout the fluidized beds. This water is heated to nearly 100°F in the adsorber before being cooled in a cooling tower to 80°F. A heat exchanger

coupling the cooling water to a refrigeration cycle completes the cooling of the water to 65°F. Figure 6.2 illustrates an adsorber cooling system for a single bed. In total, three of these cooling loops are required to cool all three adsorber beds.

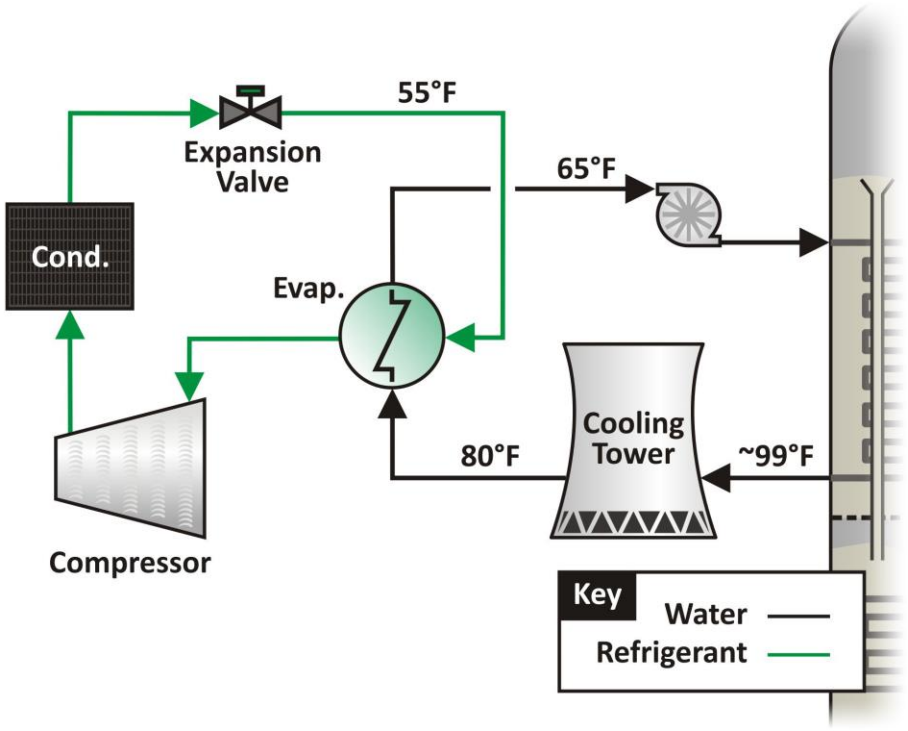

Figure 6.2: Adsorber Cooling System

Low Pressure Steam

Low pressure steam from the steam cycle provides the heat necessary to maintain the stripper at its operating temperature of 248°F. The mass flow of steam required not only depends on the mass of sorbent to be heated, but also on the mass of CO_2 and H_2O released from the sorbent. Release of CO_2 or H_2O by the sorbent is endothermic, while the adsorption process was exothermic. The heat of desorption for both fluids is assumed to be equal in magnitude, but opposite in sign, to their heats of adsorption. The low pressure steam is extracted from the crossover between the intermediate and low pressure turbines of the supercritical steam cycle. This steam is expanded through a back pressure (BP) turbine to a pressure of 45 psia. ADA has stated that it is necessary to lower the steam pressure (lower stream saturation temperature) in this fashion in order to prevent thermal damage to the amines impregnated in the solid sorbent. In addition, power produced by the BP turbine can help offset the

turbine generation losses due to the steam extraction. Steam entering the regenerator is superheated vapor and it is completely condensed within the regenerator. Figure 6.3 illustrates the connection of the regenerator to the supercritical steam cycle.

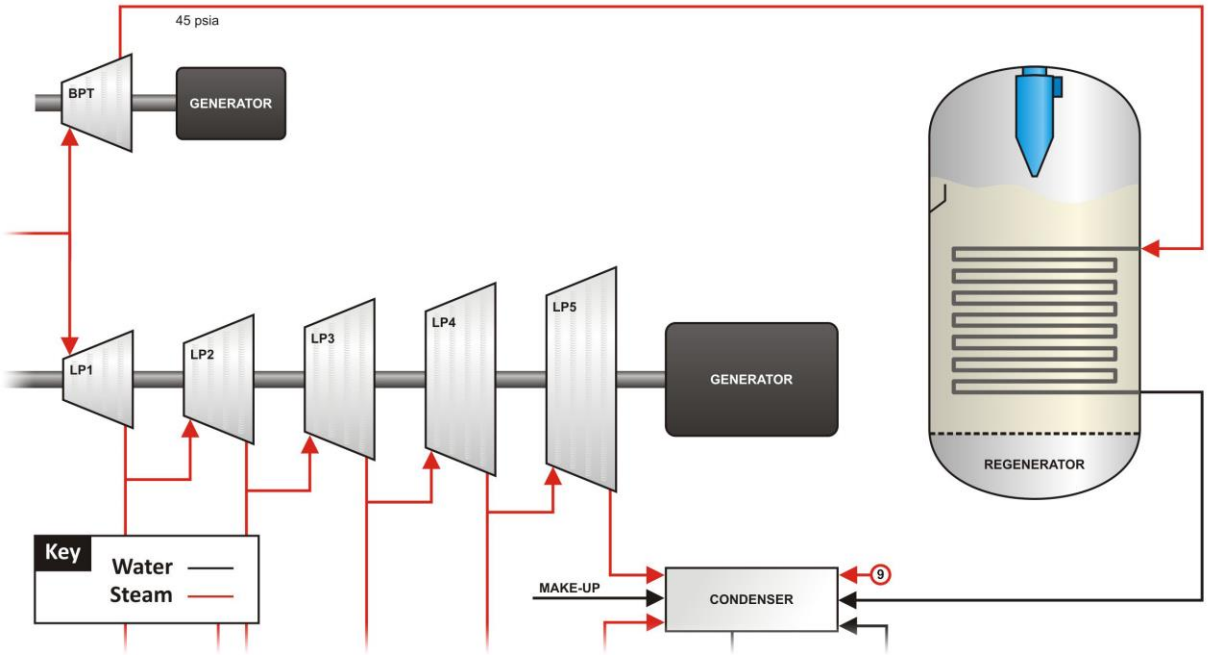

Figure 6.3: Connection of Supercritical Steam Cycle to Regenerator

7.0 PC Plant Without Carbon Capture

A pulverized coal power plant was modeled in Aspen Plus. At the heart of this model is the combustion or boiler model, which contains such axillary components as forced draft (FD), primary air (PA), and induced draft (ID) fans, mills, an air preheater (APH), electrostatic precipitator (ESP), and wet flue gas desulfurization unit (FGD). This combustion and boiler model was connected to a supercritical stream cycle. Figure 7.1 presents the turbine kit for this cycle, while Figure 7.2 shows the Aspen Plus model with both the boiler and steam cycle models connected.

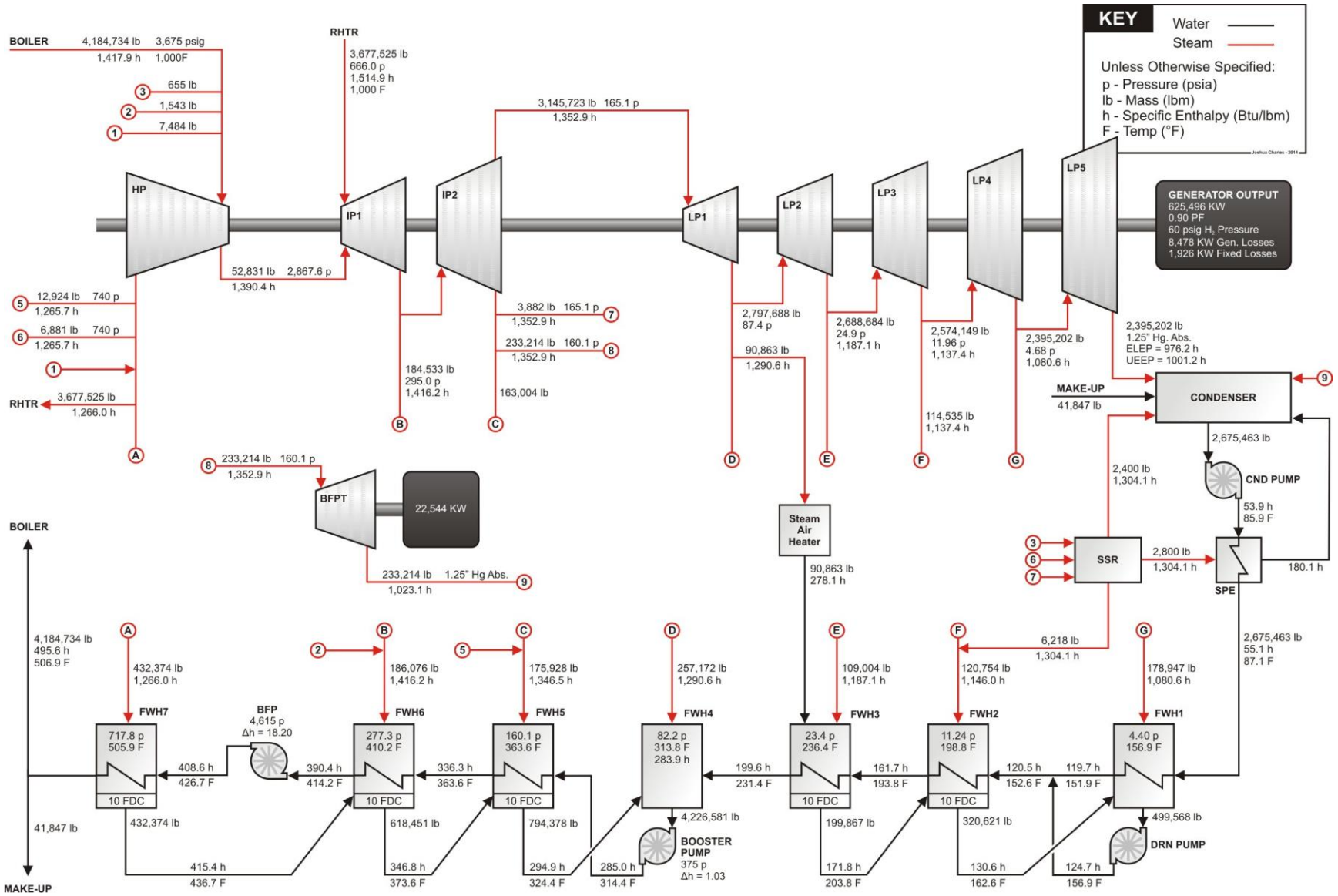

Figure 7.1: Supercritical Steam Cycle Used for Model Analyses

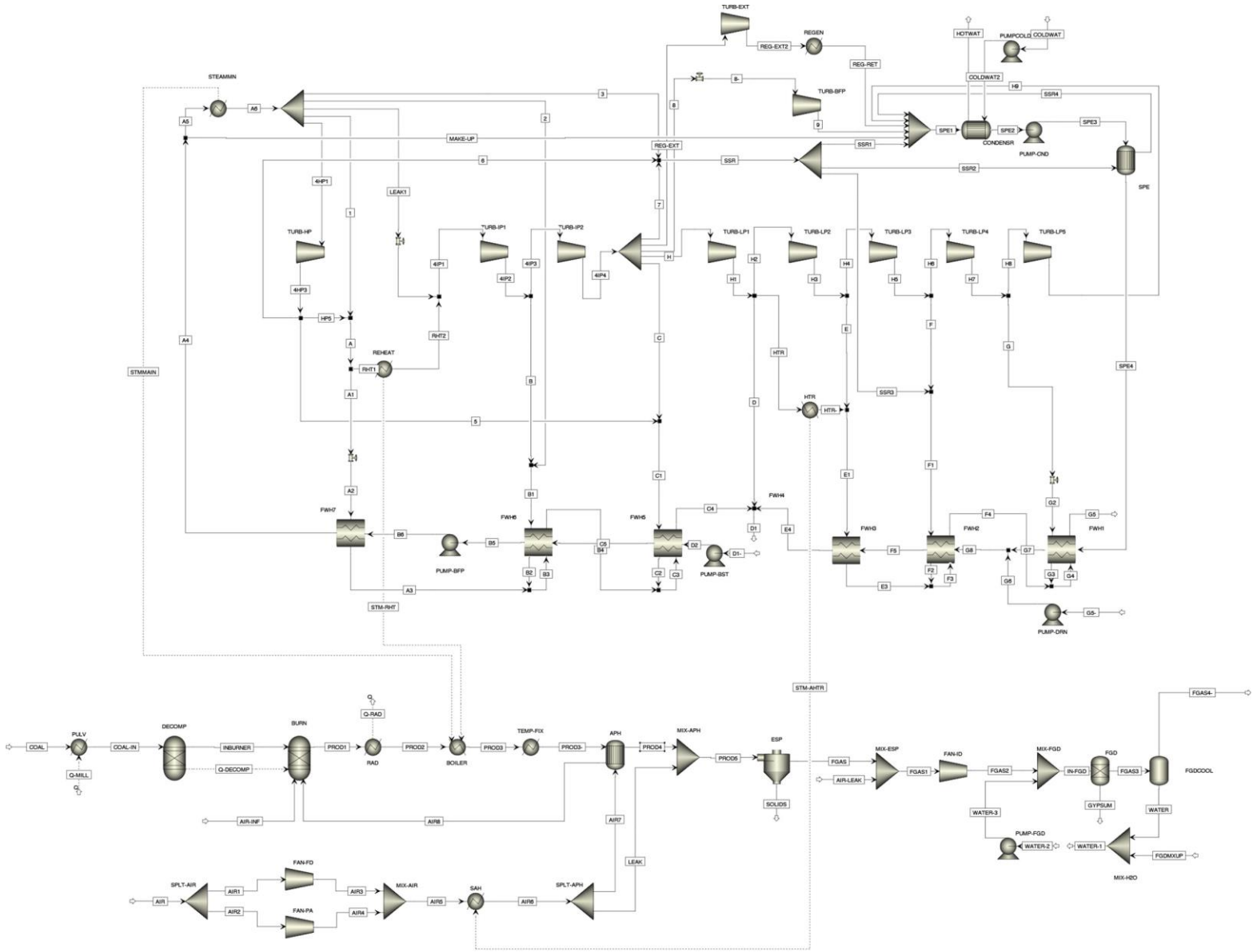

Figure 7.2: Aspen Plus Model of Combined Boiler and Steam Cycles

Flue Gas Desulfurization Model

A wet FGD operates by spraying a limestone and water slurry into the flue gas in vertical adsorber columns. This slurry is collected in a tank at the bottom of the adsorber columns and is recirculated back into the columns through spray nozzles. By varying the flow rate of slurry to flow rate of flue gas, called the liquid to gas ratio (L/G ratio), the capture rate of SO_2 can be controlled. Water and limestone are either added or removed from this cycle to vary this L/G ratio. Figure 7.3 presents the L/G ratio required for 98 percent SO_2 capture across varying coal sulfur levels. This plot was constructed utilizing data from both Walsh and Sargent and Lundy [2,3].

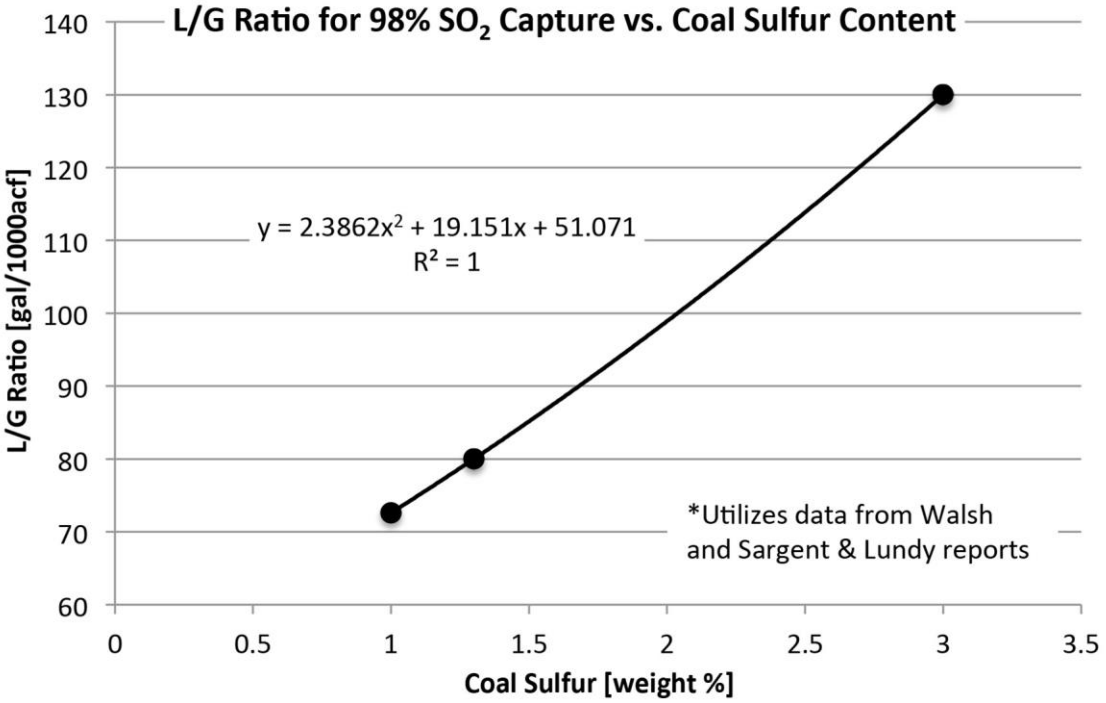

Figure 7.3: L/G Ratio For 98 Percent SO_2 Capture With Respect to Coal Sulfur Content [**2**,**3**]

FGD gas exit temperatures vary with respect to the coal being burnt, and more specifically with regard to the sulfur content of the coal. The wet FGD model in Aspen assumes the flue gas leaves the FGD at a nominal temperature of 135°F and is saturated with water vapor.

The curve fit found in Figure 7.3 was used in Aspen Plus to specify the target L/G ratio for a particular coal sulfur content. As the specified L/G ratio is varied (for higher or lower coal sulfur), the water circulated in the FGD is varied, which in turn changes the exit temperature of the FGD. Table 7.1

summarizes the operating characteristics of the Aspen Plus FGD model for four different coals. It should be noted that not only does the sulfur content of the coal affect the FGAS exit temperature, but also the coal moisture level, which directly impacts FGAS moisture. The FGD model results in Table 7.1 agree well with FGD characteristics at actual power plants.

Table 7.1: Coal Composition and FGD Model Results

Coal	ILL #6	PRB	ND Lignite
	AR Proximate Analysis [weight %]		
Fixed Carbon	44.19	32.98	21.87
Volatile Matter	34.99	32.17	27.33
Ash	9.70	6.31	12.30
HHV [Btu/lb]	11,666	8,426	6,406
	AR Ultimate Analysis [weight %]		
Moisture	11.12	28.09	38.50
Carbon	63.75	49.21	34.03
Hydrogen	4.50	3.51	2.97
Nitrogen	1.25	0.73	0.72
Chlorine	0.29	0.02	0.00
Sulfur	2.51	0.45	0.51
Ash	9.70	6.31	12.30
Oxygen	6.88	11.67	10.97
	FGD Results		
L/G Ratio [gal/Macf]	124.1	64.1	68.6
FGAS Exit T [°F]	127.8	134.4	142.3

Pulverized Coal (PC) Plant Model Results

The supercritical steam cycle in Figure 7.1 was modified in Aspen Plus in such a way that the steam flow rate could be varied in order to meet a desired net electric power output. As the steam flow rate was varied, the heat duty on the boiler changed accordingly. Coal flow rate was then adjusted to meet the condition where flue gas exits the economizer at 600°F. The air feed to the boiler was also adjusted to result in an O_2 mole-fraction of 3.5 percent at the economizer exit. Air was assumed to leak into the boiler at a rate of 8 percent of the flue gas (FGAS) flow rate, the APH seals are assumed to leak at a rate equal to 6 percent of the FGAS mass flow rate, and the ductwork downstream of the APH is assumed to leak air into the duct at a rate equal to 5 percent of the FGAS mass flow rate.

The model was run using the three coals presented in Table 7.1. For each of the coals, net plant electric output was specified at 550 MW, while the steam and coal flow rates were allowed to vary accordingly. Table 7.2 presents the PC plant results for these three coals without CO_2 capture.

Table 7.2: BASE PC Plant Aspen Model Results Without CO_2 Capture

		Illinois #6	PRB	ND Lignite
Generator Power	MW	581	578	580
TC Net Power	MW	574	571	573
Net $Power_e$	MW	550	550	550
Cond. Pump Power	kW	263	262	263
Drain Pump Power	kW	62	62	62
Boost Pump Power	kW	1,264	1,258	1,262
Cond. Circ. Pump Power	kW	5,078	5,056	5,073
TC Pump Pow.	kW	6,667	6,637	6,659
Main Steam Flow	lb/hr	3,882,313	3,865,288	3,878,071
Main Steam Q	Btu/hr	3.574E+09	3.559E+09	3.570E+09
Reheat Steam Q	Btu/hr	8.608E+08	8.570E+08	8.599E+08
TC Q	Btu/hr	4.435E+09	4.416E+09	4.430E+09
TCHR	Btu/kWh	7,728	7,728	7,728
FD Fan Power	kW	1,784	1,895	1,841
PA Fan Power	kW	2,724	2,893	2,811
ID Fan Power	kW	7,338	7,315	7,566
Total Fan Power	kW	11,846	12,103	12,218
Mill Power	kW	2,200	3,145	4,289
ESP Power	kW	663	734	752
FGD Power	kW	6,225	2,426	3,056
Other Aux Power	kW	3,007	2,994	3,004
Total SS Power	kW	30,607	28,040	29,979
Coal Flow	lb/hr	415,651	594,347	810,377
Coal HHV	Btu/lb	11,666	8,426	6,406
Coal Q (Combustion)	Btu/hr	4,849,147,920	5,007,790,350	5,191,144,760
Boiler Efficiency	%	91.5	88.2	85.3
Unit Heatrate	Btu/kWh	8,817	9,105	9,439
Unit Efficiency	%	38.7	37.5	36.2

8.0 CO_2 Compression Model

It is assumed that CO_2 captured from the exhaust of a coal-fired plant will need to be pressurized to around 2,215 psia before being transported for underground storage. This compression process comes at a high energy penalty due to the large flow rate of CO_2 being compressed. Previous work by the ERC found that an integrally-geared (IG) type compressor was the best choice for minimizing compression power. Figure 8.1 presents the IG CO_2 compression system as modeled in Aspen Plus.

Figure 8.1 shows the addition of a precooler, PRE, upstream of the first compression stage. This precooler is necessary due to the CO_2 stream leaving the regenerator being at a temperature approaching 248°F. Also, a post cooler, PST, is seen to be added after the final compression stage. While such a cooler may not be needed in most situations, it provides an additional source of waste heat for cases where the utilization of waste heat is desired.

CO_2 compression power is higher for the ADA solid sorbent capture system than for an Econamine-type capture system since the CO_2 leaving the capture system and entering the compression train is at a lower pressure: 13.7 psia for the ADA system vs. approximately 44 psia for an Econamine system. This difference in pressure leads to overall CO_2 compressor compression ratios (discharge pressure/inlet pressure) of 161.7 and 50.3 respectively.

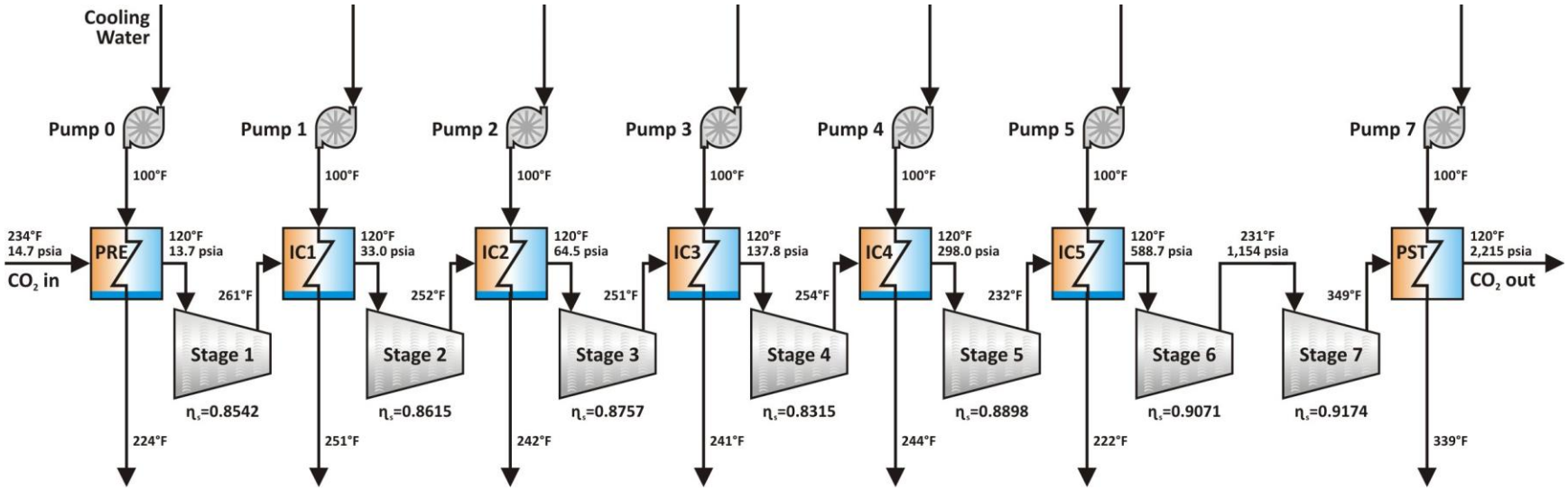

Figure 8.1: IG CO_2 Compression System as Modeled in Aspen Plus

9.0 PC Plant with ADA Solid Sorbent CO_2 Capture

The ADA solid sorbent CO_2 capture system model, the PC plant model, and the CO_2 compression models were combined in Aspen Plus to form a complete model of a PC plant equipped with the ADA solid sorbent capture system. Steam, which provides the heat to the regenerator, is extracted from the steam cycle between the IP and LP turbines before passing through a back pressure turbine, which reduces the steam pressure to 45 psia. Total steam flow in the turbine cycle is varied in order to maintain a net plant electric output of 550 MW_e. Since net electric output is maintained, the coal flow rate increases with the addition of the capture system, which increases overall CO_2 emissions, resulting in a larger steam extraction to the regenerator. Therefore, the Aspen Plus model iterates until the steam extraction rate is not changing for a given net electric output. Note that net electric output is calculated after all plant electric loads (included CO_2 compressors and their associated pumps) are subtracted.

The Aspen Plus model results can be compared to previous plant and ADA capture system model results. The most comprehensive plant and capture system results are presented in the Preliminary Techno-Economic Assessment Results [4]. Table 4-1 from Reference 4 compares a plant equipped with the ADA capture system with a model of a plant equipped with an Econamine CO_2 capture system.

Net Unit Heat Rate and Efficiency

Before undertaking a detailed look at a PC plant equipped with ADA CO_2 capture, a clarification should be made with regard to the definitions of net unit heat rate (HR) and unit efficiency. Net unit HR is defined as the energy contained in the fuel (as specified by the higher heating value [HHV] of the fuel) over the net electric output:

$$Net\ Unit\ HR = \frac{\dot{m}_{coal}\ HHV}{Net\ Power_e}$$

The units of net unit HR are Btu/kWh. Net $Power_e$ can be expressed as the gross turbine power minus the station service power, where station service power refers to the auxiliary power loads of the plant, such as fans, pulverizers, pumps, CO_2 compressors, and refrigerant compressors.

$$Net\ Unit\ HR = \frac{\dot{m}_{coal}\ HHV}{Gross\ Power_e - SS\ Power}$$

Unit efficiency is defined as the net electric power output divided by the fuel energy. In other words, unit efficiency is the reciprocal of the net unit HR. The following defines unit efficiency, where 3412.14 Btu/kWh is a multiplier to convert the efficiency into a dimensionless parameter.

$$Unit\ Efficiency = \frac{1}{Net\ Unit\ HR\ \cdot 3{,}412.14\frac{Btu}{kWh}}$$

PC Plant With CO_2 Capture Results

Table 9.1 of the present report compares the Aspen Plus model results to those presented in the Preliminary Techno-Economic Assessment [4] as well as scaled results from the ADA CO_2 Capture Study Preliminary Flow Sketch. All of these results are for Illinois #6 coal as presented in Table 7.1. The rightmost column of results were originally presented for a lower inlet CO_2 flow rate and were thus scaled to match the CO_2 flow rate entering the ADA capture system in the Aspen Plus model. In all of these cases, it is assumed that the sorbent does not adsorb any moisture from the flue gas.

The top few rows of Table 9.1 present the coal and combustion information for the cases examined. Moving down the table, generated power, net power, and auxiliary power loads are tabulated for the boiler and supercritical steam cycle. Two values in this section warrant further explanation. Boiler Feed Pump Power refers to the power requirement of the boiler feed pump (BFP) in the steam cycle. This pump is assumed to be steam driven by a dedicated turbine and thus this power load is not included in the calculation of PC Plant Station Service (SS) Power. Secondly, Fixed Aux Power refers to additional plant power loads that are not modeled in the Aspen Plus model. Examples would include such things as plant lighting, heating, and control system power requirements. Fixed Aux Power is assumed to be ½ percent (0.005) of gross power. Gross power is defined as the sum of all steam turbine power terms.

Table 9.1: Aspen Plus Model Results vs. Previous ADA Results

			Aspen ADA Capture (No Water Capture)	Sorbent1*	Stream Table ADA Sys. (Scaled)**
	Coal Flow Rate	lb/hr	571,396	545,581	-
	HHV	Btu/lb	11,666	11,666	-
	Q_{coal} (Combustion)	Btu/hr	6.666E+09	6.365E+09	-
PC Plant	Generated Power	MW	706	703	-
	Net Power	MW	550	550	-
	Boiler Feed Pump Power	kW	45,725	47,369	-
	Turb. Cycle Pump Power	kW	6,972	-	-
	FD Fan Power	kW	2,453	-	-
	PA Fan Power	kW	3,745	-	-
	ID Fan Power	kW	10,061	-	-
	Pulv. Power	kW	3,024	-	-
	ESP Power	kW	908	-	-
	FGD Power	kW	8,532	-	-
	Fixed Aux Power	kW	3,673	-	-
	PC Plant SS Power	kW	39,368	50,280	-
CO_2 Capture System	Boost Fan Power (a)	kW	48,429	-	45,749
	Recirc. Fan Power (b)	kW	2,214	-	4,133
	SO_2 Polisher Power	kW	-	2,230	-
	CO_2 Capture System Power (a+b)	kW	50,643	57,744	49,881
	CO_2 Compressor Power (c)	kW	66,064	42,858	-
	Total CO_2 Capture Power (a+b+c)	kW	116,707	100,602	-
	Sorbent Flow Rate	lb/hr	16,038,315	16,610,220	17,168,863
	CO_2 Captured	lb/hr	1,189,792	1,165,561	1,195,381
	CO_2 Entering Capture Sys.	lb/hr	1,332,520	1,295,067	1,331,541
	CO_2 Emissions	lb/hr	133,254	129,507	133,154
	CO_2 Capture Rate	%	90	90	-
	Regenerator Heat Duty	Btu/hr	-1.327E+09	-1.328E+09	-1.352E+09
	Total Plant Auxiliary Power	kW	156,075	153,534	-
	Turb. Cycle HR	Btu/kWh	8,666	-	-
	Net Unit HR	Btu/kWh	12,122	11,573	-
	Unit Efficiency	%	28.1	29.5	-

*Preliminary Techno-Economic Assessment (Dec. 2011) [4]

**ADA CO_2 Capture Study Preliminary Flow Sketch Sorbent BN (Scaled with respect to CO_2 flow into the Aspen Plus Model with no water capture and no CO_2 lift gas)

For the most part the Aspen Plus Model and the previous ADA results (Sorbent1) agree very closely. Two notable differences are in the PC plant station service power and the CO_2 compression power. The differences in station service power are most likely due to the methods by which station service power is estimated. More significant is a 23 MW difference in CO_2 compressor power despite similar mass flow rates of CO_2 being captured. Compressor power calculated using the Aspen Plus model is consistent with results previously found by the ERC for comparable CO_2 flow rates and pressure ratios [5].

Despite the differences described above in specific power parameters, overall, the two sets of results agree closely. Both models show similar coal flow rates, similar sorbent flow rates, similar rates of CO_2 capture, similar regenerator duties, and comparable capture system station service powers (ADA System SS Power). It is assumed that the bulk of this station service power is due to the flue gas blower located upstream of the adsorber column. The flue gas blower power requirements cannot be directly compared to the Sorbent1 results. However, the scaled ADA system results in the last column show comparable fan loads to the Aspen Plus results. These results in Table 9.1 provide a degree of confidence in the Aspen Plus model results.

PC Plant with ADA Capture System BASE Results

A series of cases were run to determine the performance of the PC plant equipped with the ADA solid sorbent CO_2 capture system (BASE Case). These BASE case results are presented in Table 9.2 for all three coals in Table 7.1.

Table 9.2: PC Plant With ADA Solid Sorbent Capture System (BASE Case)

			Illinois #6	PRB	ND Lignite
	Coal Flow Rate	lb/hr	629,785	969,749	1,307,881
	HHV	Btu/lb	11,666	8,426	6,406
PC Plant	Generated Power	MW	752	793	795
	Turb. Cycle Net Power	MW	745	786	788
	Net Power	MW	550	550	550
	Turb. Cycle Pump Power	kW	7,072	7,261	7,399
	FD Fan Power	kW	2,703	3,091	2,971
	PA Fan Power	kW	4,128	4,721	4,537
	ID Fan Power	kW	11,083	11,898	12,174
	Pulv. Power	kW	3,333	5,132	6,921
	ESP Power	kW	1,001	1,194	1,210
	FGD Power	kW	9,397	3,916	4,893
	Fixed Aux Power	kW	3,919	4,135	4,144
	PC Plant SS Power	kW	42,636	41,348	44,249
CO_2 Capture System	Boost Fan Power	kW	54,979	70,396	71,585
	Recirc. Fan Power	kW	2,945	3,458	3,257
	ADA Sys. Pump Power	kW	7,584	15,217	18,930
	ADA Sys. Refrig. Power	kW	18,458	22,847	23,226
	CO_2 Compressor Power	kW	75,802	89,958	84,099
	Total CO_2 Capture Power	kW	159,769	201,875	201,097
	Sorbent Flow Rate	lb/hr	21,531,480	25,252,683	23,805,052
	CO_2 Captured	lb/hr	1,311,738	1,560,069	1,454,985
	CO_2 Entering Capture Sys.	lb/hr	1,468,730	1,747,076	1,629,203
	CO_2 Emissions	lb/hr	146,867	174,701	162,913
	CO_2 Capture Rate	%	90	90	90
	Regenerator Heat Duty	Btu/hr	-1.832E+09	-2.159E+09	-2.026E+09
	Total Plant Auxiliary Power	kW	202,404	243,223	245,346
	Turb. Cycle HR	Btu/kWh	8,943	9,086	8,999
	Net Unit HR	Btu/kWh	13,358	14,855	15,233
	Unit Efficiency	%	25.5	23.0	22.4

These BASE results form the initial case where the ADA capture system is assumed to be operating in a state before any process conditions have been changed to improve performance. As the model is updated with varying process conditions, BASE shall refer to these initial model results.

10.0 Effects of Changes in ADA Capture System Process Conditions

The ADA Solid Sorbent CO_2 Capture System is designed according to numerous operating conditions, which may or may not be optimal. A summary of the more significant conditions are as follows:

Adsorber operating temperature
Regenerator operating temperature
Sorbent water adsorption characteristics
Adsorber bed pressure drop
CO_2 compressor discharge pressure

Parametric analyses were carried out individually for each of the above process conditions to find the optimal operating points. It is important to note that these analyses only consider the effects of varying single parameters on unit operation. Therefore, these results may not hold true when changes of multiple parameters are considered simultaneously or when additional equipment is added to the capture system.

Changes in Adsorber Operating Temperature

The first parameter to be examined was the operating temperature of the adsorber. For the BASE case the adsorber is operated at a uniform temperature of 104°F. Figure 1.2 presented the sorbent CO_2 loading for an adsorber operating at 104°F and a curve fit of the data was created and used in the numerical adsorption model. In order to operate at adsorber temperatures other than 104°F, the curves of Figure 1.1 were interpolated (or extrapolated to 100°F) to find the following curves in Figure 10.1. Curve fits were produced for each of these temperatures and implemented into the Aspen Plus model. If an adsorber temperature in Aspen is specified between two of these temperature curves, the CO_2 loading for both temperature curves is calculated at the specified CO_2 partial pressure. These two temperature curve results are then linearly interpolated to find the CO_2 loading at the desired temperature and partial pressure.

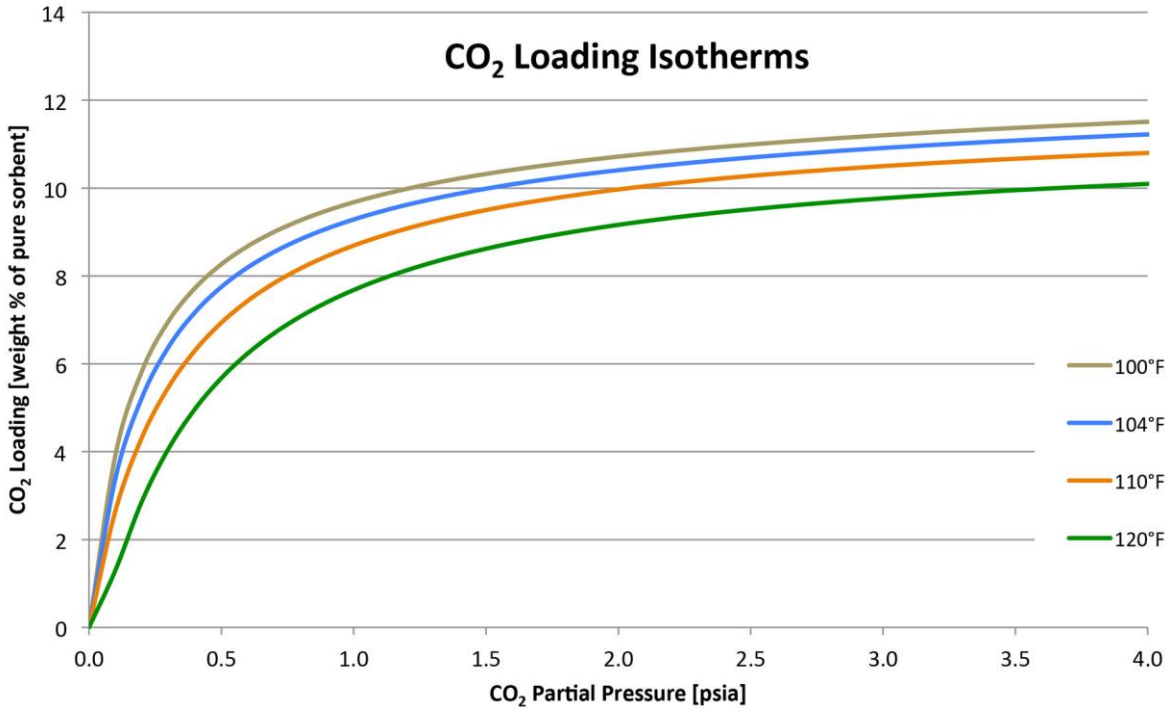

Figure 10.1: CO_2 Loading Isotherms for Varying Adsorber Temperatures

The Aspen Plus model was found to operate well at adsorber temperatures between 100°F and 118°F, which was broad enough to determine optimal operating temperatures. Figure 10.2 presents the results of varying adsorber temperature on the change in net unit HR and corresponding sorbent flow rate.

Figure 10.2 shows that the overall net unit heat rate results vary from coal to coal as well as by temperature as was expected. For the Illinois #6 an adsorber temperature of 104°F is assumed to be ideal. For this coal, the net unit heat rate is seen to remain virtually constant across the temperature range between 104°F and 108°F. However, since the sorbent flow rate is lower at the low end of this range, 104°F was selected as the optimal temperature. The same logic carried over into the selection of 108°F as the ideal adsorber operating temperature for both the PRB and ND Lignite coals. Overall, changes in net unit heat rate are not dramatic for these temperature changes, with the largest change in heat rate (-51 Btu/kWh) being for PRB when the adsorber temperature is increased to 108°F. Table 10.1 shows the results in Figure 10.2 in tabular form.

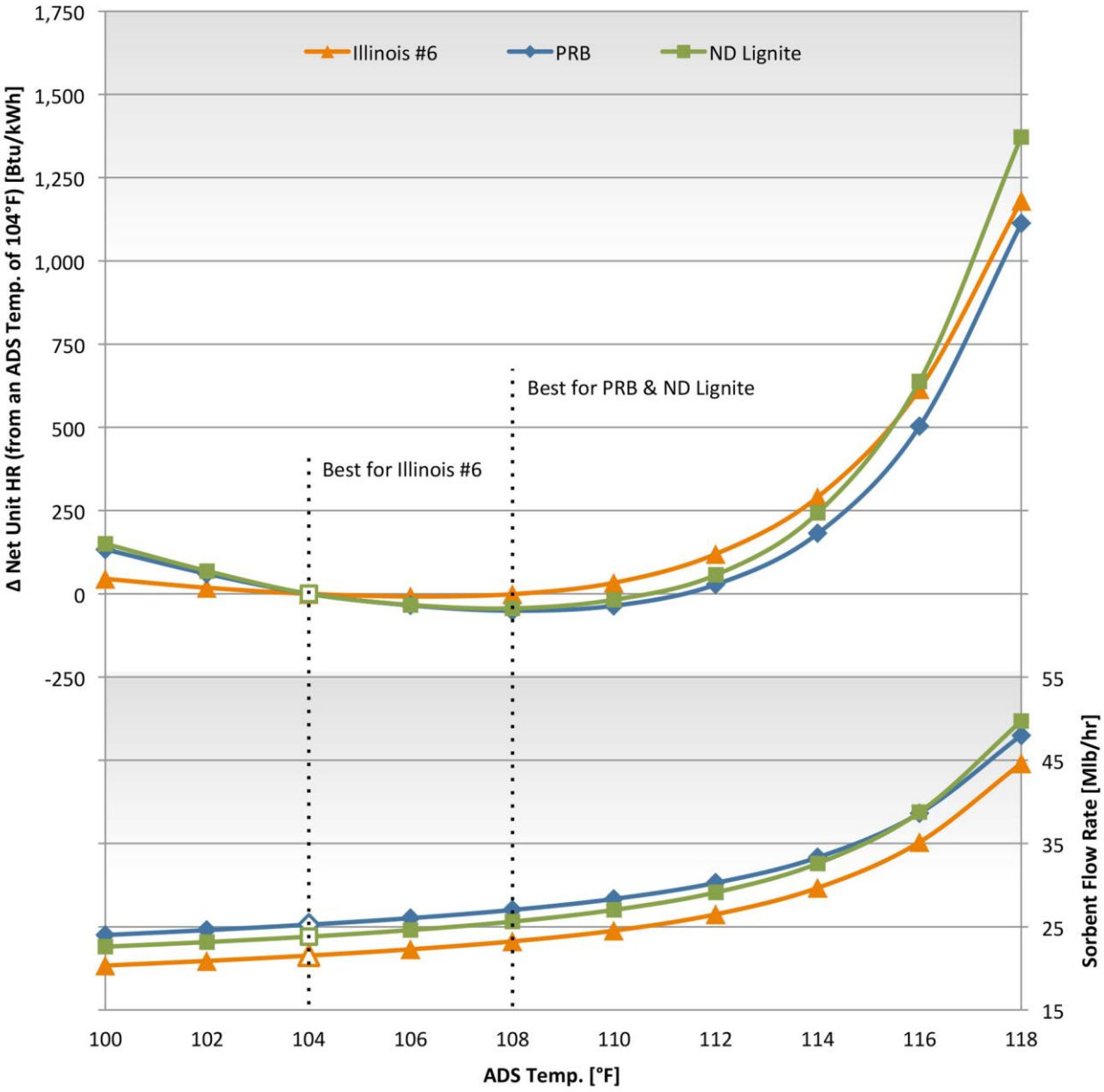

Figure 10.2: Impact of Adsorber Temperature on Net Unit HR and Sorbent Flow Rate

Table 10.1: Impact of Adsorber Temperature on Net Unit HR and Sorbent Flow Rate

	Illinois #6	PRB	ND Lignite
ADS Temperature [°F]	Δ Net Unit HR [Btu/kWh]		
100	45	134	150
102	18	60	68
104	0	0	0
106	-8	-35	-33
108	-1	-51	-44
110	33	-36	-18
112	120	28	57
114	291	181	243
116	615	503	638
118	1,181	1,112	1,372
ADS Temperature [°F]	Sorbent Flow Rate [Mlb/hr]		
100	20.3	24.0	22.6
102	20.9	24.6	23.2
104	21.5	25.3	23.8
106	22.3	26.0	24.6
108	23.2	27.0	25.6
110	24.5	28.3	27.0
112	26.5	30.3	29.1
114	29.7	33.3	32.6
116	35.2	38.6	38.8
118	44.6	48.0	49.7

Changes in Regenerator Operating Temperature

The second parameter to be examined was the operating temperature of the regenerator. For the BASE case, the adsorber is operated at a constant temperature of 248°F. As with the adsorber, additional curve fits were produced for a range of regenerator operating temperatures. Figure 10.3 presents the CO_2 loading isotherms associated with these temperatures. These temperature curves are used to either directly find the CO_2 loading in the regenerator or if the temperature lies between two of the curves, a linear interpolation is used to find the loading at the intermediate temperature.

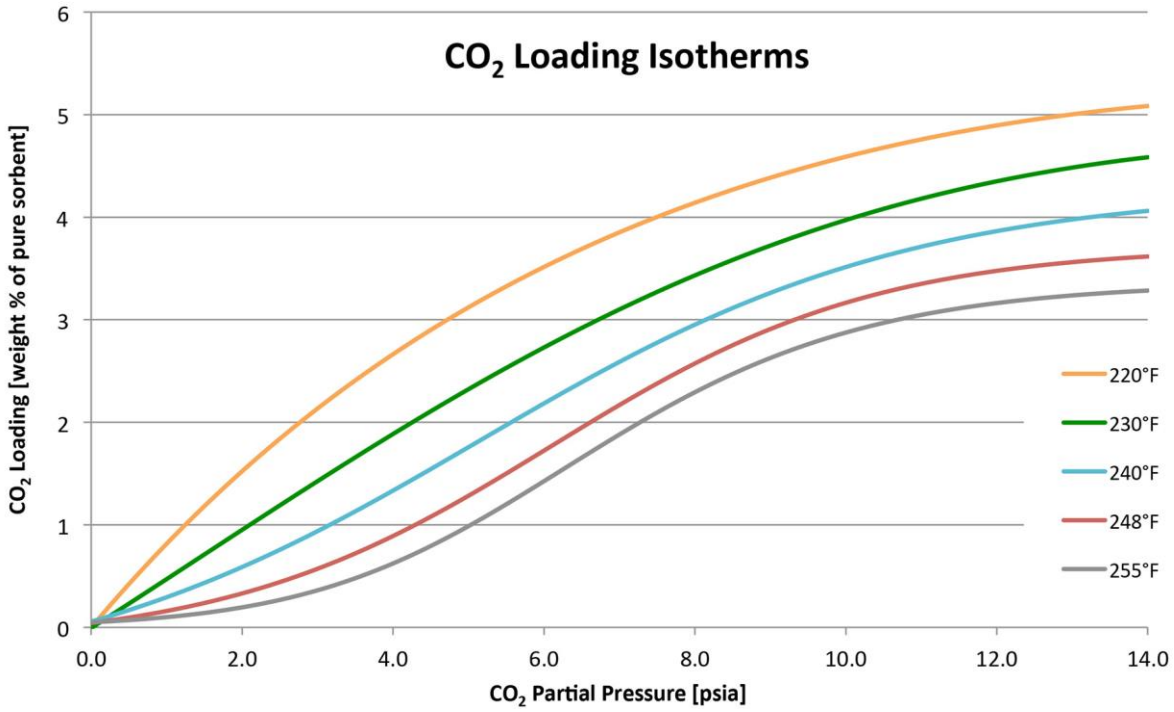

Figure 10.3: CO_2 Loading Isotherms for Varying Regenerator Temperatures

The Aspen Plus model was found to operate well at regenerator temperatures between 224°F and 255°F. This temperature range was found to be broad enough to determine optimal regenerator temperatures. Figure 10.4 presents the results of varying regenerator temperature on the change in overall plant heat rate and the corresponding sorbent flow rate. Table 10.2 presents these results in tabular form.

For the Illinois #6 coal, the optimal regenerator temperature appears to be 248°F, as this corresponds to the lowest sorbent flow rate in the low (flat) range of the net unit HR curve. An ideal temperature of 244°F is suggested as best for the ND Lignite, while a temperature of 240°F appears to be better for the PRB. However, the overall change in net unit HR is quite small, with the largest drop in HR (-12 Btu/kWh) occurring with the change from 248°F to 240°F for PRB coal. Also, it should be noted than any small gain in net unit HR due to a reduction in regenerator temperature comes at the expense of a significantly higher sorbent flow rate.

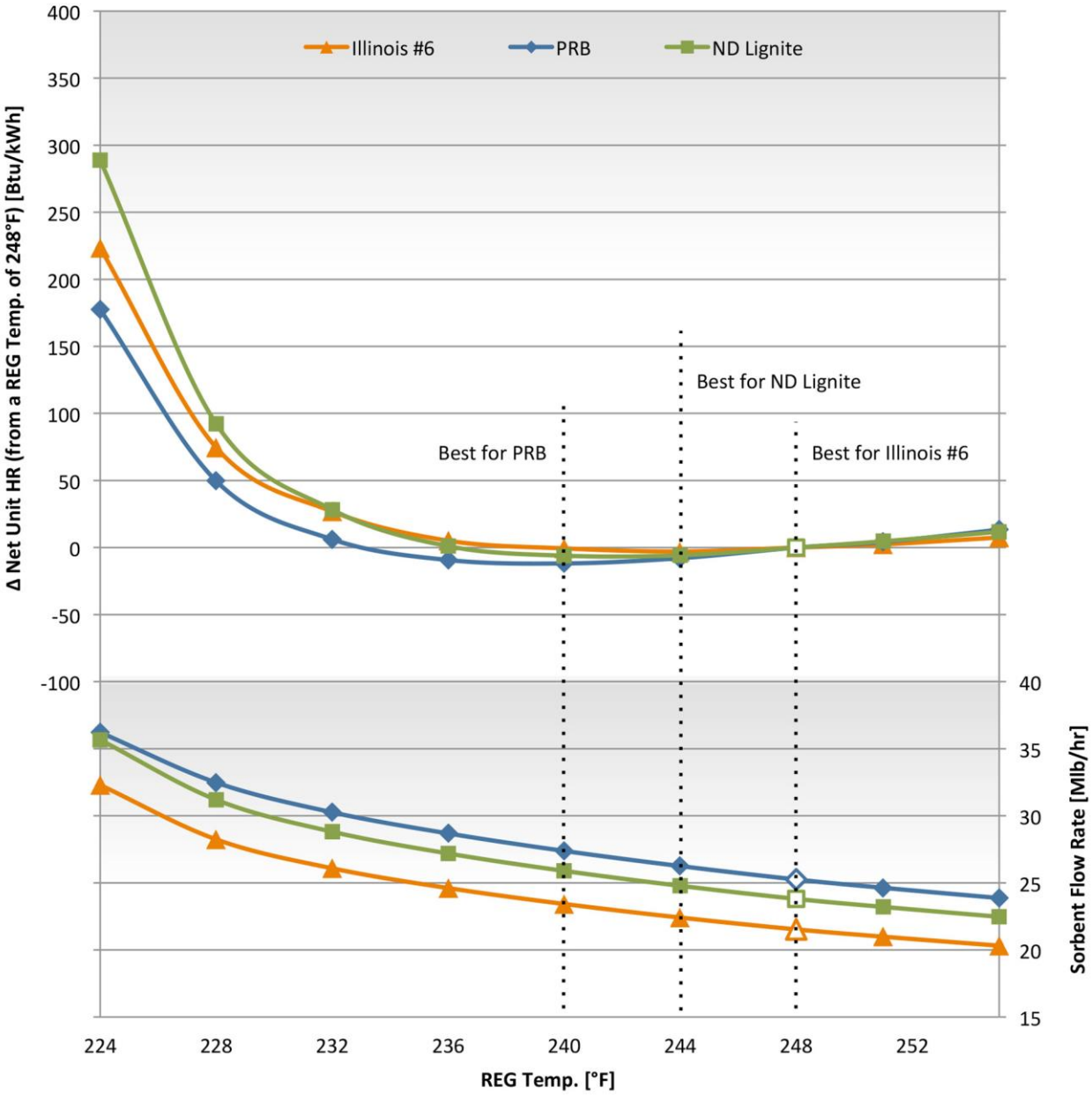

Figure 10.4: Impact of Regenerator Temperature on Net Unit HR and Sorbent Flow Rate

Table 10.2: Impact of Regenerator Temperature on Net Unit HR and Sorbent Flow Rate

	Illinois #6	PRB	ND Lignite
REG Temperature [°F]	Δ Net Unit HR [Btu/kWh]		
255	8	13	12
251	2	4	5
248	0	0	0
244	-3	-8	-6
240	-1	-12	-6
236	5	-9	1
232	27	6	28
228	74	50	92
224	223	177	289
REG Temperature [°F]	Sorbent Flow Rate [Mlb/hr]		
255	20.3	23.9	22.5
251	21.0	24.6	23.2
248	21.5	25.3	23.8
244	22.4	26.3	24.8
240	23.4	27.4	25.9
236	24.6	28.7	27.2
232	26.1	30.3	28.8
228	28.2	32.5	31.2
224	32.3	36.2	35.7

Sorbent Water Adsorption Characteristics

The solid sorbent utilized in the ADA capture system analyses is known to adsorb moisture as well as CO_2. This is considered to be an area of concern for several reasons. First, it is assumed that any moisture adsorbed by the sorbent will proportionally decrease the effective CO_2 loading of the sorbent. In other words, as more water is adsorbed by the sorbent, less CO_2 is able to be adsorbed. The Aspen Plus model takes this effect into account when calculating the CO_2 adsorption rate in the adsorber. The other major impact of increased water adsorption by the sorbent is that any water adsorbed in the adsorber must be released from the sorbent in the regenerator. This results in a higher regenerator duty

since driving off the water is assumed to require heat input equal to the heat of vaporization of water. Also, since the water is evaporated into the product CO_2 stream, the mass flow entering the cooler upstream of the first CO_2 compression stage is increased. Not only does this necessitate a higher cooling water flow rate to condense the water vapor from the CO_2 stream, but the compressor power of the first few stages is increased since all of the excess water vapor is not condensed upstream of the compressors.

In order to study to impact of sorbent water uptake on plant performance, a multiplier was added to the water adsorption and desorption curves. This allows the water adsorption rate to be scaled across the entire range of H_2O partial pressures. For instance, a water multiplier of 1 corresponds to the original water adsorption curve, while a water multiplier of 1.5 specifies a 50 percent increase in water adsorption and a multiplier of zero specifies zero water adsorption.

For all three coals, the water multiplier was varied between 0 and 1.5 at 0.25 increments. These results are presented in Figure 10.5 and Table 10.3 below. The rate of water adsorption was seen to have a very large impact on net unit heat rate (up to a 6.9 percent reduction for PRB) and an even larger impact on sorbent flow rate (up to a 23.1 percent reduction for ND Lignite). As the water multiplier rises above 1, both the net unit HR and sorbent flow rate curves are seen to begin to flatten, which implies a reduced impact on HR and flow rate with changes in water adsorption in this region.

While the sorbent water adsorption characteristics that the Aspen Plus model is built on are quite rudimentary, these results show that anything that can be done to reduce the uptake of moisture by the sorbent will pay large dividends in both reducing net unit HR and sorbent flow rate.

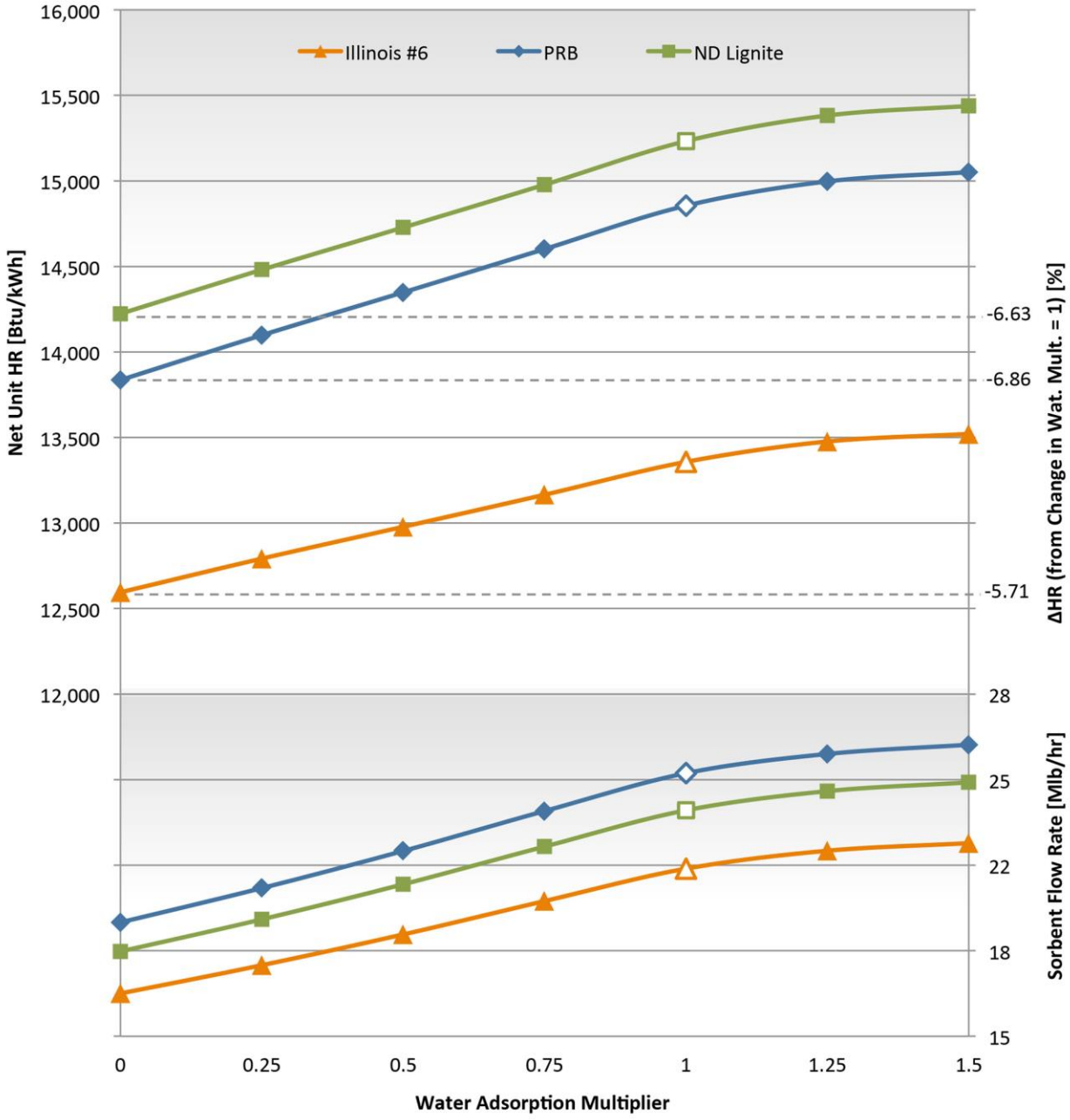

Figure 10.5: Impact of Water Adsorption Multiplier on Net Unit HR and Sorbent Flow Rate

Table 10.3: Impact of Water Adsorption Multiplier on Net Unit HR and Sorbent Flow Rate

	Illinois #6		PRB		ND Lignite	
Water Multiplier	Net Unit HR [Btu/kWh]					
0	12,595	-5.7%	13,836	-6.9%	14,223	-6.6%
0.25	12,792	-4.2%	14,098	-5.1%	14,481	-4.9%
0.5	12,978	-2.8%	14,348	-3.4%	14,728	-3.3%
0.75	13,165	-1.4%	14,602	-1.7%	14,978	-1.7%
1	13,358	-	14,855	-	15,233	-
1.25	13,477	0.9%	14,997	1.0%	15,382	1.0%
1.5	13,521	1.2%	15,051	1.3%	15,438	1.3%
Water Multiplier	Sorbent Flow Rate [Mlb/hr]					
0	16.7	-22.6%	19.4	-23.0%	18.3	-23.1%
0.25	17.8	-17.5%	20.8	-17.7%	19.6	-17.8%
0.5	19.0	-11.9%	22.2	-12.0%	20.9	-12.1%
0.75	20.3	-5.9%	23.8	-5.8%	22.4	-5.9%
1	21.5	-	25.3	-	23.8	-
1.25	22.2	3.2%	26.0	3.0%	24.6	3.1%
1.5	22.5	4.6%	26.4	4.4%	24.9	4.6%

Adsorber Pressure Drop Reduction

The flue gas booster fan upstream of the adsorber contributes to the heat rate penalty due to the ADA capture system (Booster fan power accounts for nearly 20 percent of the increase in heat rate due to the CO_2 capture system). Since the primary purpose of this fan is to overcome the pressure drop in the adsorber bed, any reduction in bed pressure drop should result in a reduction in fan power. Although the specifics of lowering overall adsorber pressure drop are not discussed here, two models were completed with the overall pressure drop used in the Aspen calculations being reduced by 1 psia and then 2 psia.

Since the top bed of the adsorber (ADS3) is the deepest, its pressure drop as supplied by ADA is more than twice as large as that of either of the lower beds (2.3 psia vs. ~1 psia). Therefore, for the 1 psia reduction in pressure drop, the pressure drop across this top bed section was simply reduced by 1

psia, which resulted in a 1 psia reduction in fan discharge pressure. For the case with a 2 psia reduction in pressure drop, each of the beds were given equal pressure drops (~0.77 psia). Figure 10.6 and Table 10.4 shows the results for these reductions in adsorber bed pressure drop.

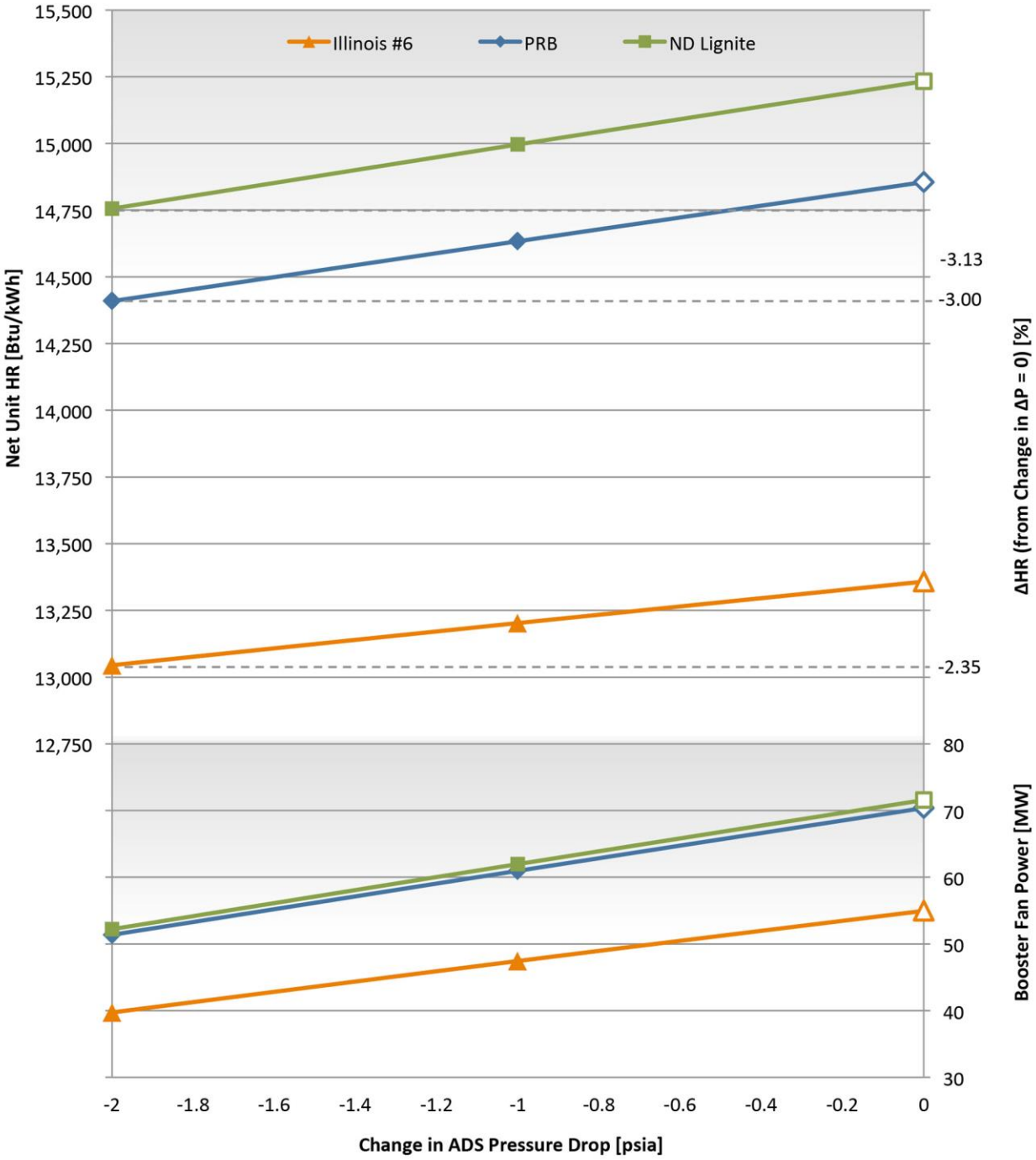

Figure 10.6: Effect of Change in ADS Pressure Drop on Unit HR and Booster Fan Power

Table 10.4: Effect of Change in ADS Pressure Drop on Unit HR, Booster Fan Power, and Sorbent Flow

	Illinois #6		PRB		ND Lignite	
ADS Change in ΔP [psia]	Net Unit HR [Btu/kWh]					
0	13,358	-	14,855	-	15,233	-
-1	13,203	-1.2%	14,633	-1.5%	14,996	-1.6%
-2	13,045	-2.3%	14,409	-3.0%	14,756	-3.1%
ADS Change in ΔP [psia]	Booster Fan Power [MW]					
0	55.0	-	70.4	-	71.6	-
-1	47.4	-13.7%	61.0	-13.4%	62.0	-13.4%
-2	39.7	-27.7%	51.4	-27.0%	52.2	-27.1%
ADS Change in ΔP [psia]	Sorbent Flow Rate [lb/hr]					
0	21,531,480	-	25,252,683	-	23,805,052	-
-1	21,650,566	0.6%	25,297,863	0.2%	23,857,836	0.2%
-2	21,770,851	1.1%	25,332,829	0.3%	23,893,062	0.4%

For the Illinois #6, it is seen that the 1 and 2 psia reductions in adsorber pressure drop correspond to net unit heat rate drops of 1.2 and 2.3 percent respectively. The reason for this is that booster fan power is reduced from 55 MW to 47 MW and then 40 MW.

It should be noted that reducing the adsorber pressure drop also reduces the CO_2 partial pressure in the adsorber (particularly toward the bottom of the adsorber). Because of this, sorbent CO_2 loading is reduced according to the curves presented in Figure 1.2. As sorbent CO_2 loading is reduced, the sorbent flow rate must increase to meet the 90 percent CO_2 capture target. This is reflected in the sorbent flow rate results of Table 10.4. These results suggest that the operating pressure of the adsorber beds has a direct impact on the adsorption characteristics of the sorbent. Further testing with the sorbent would need to be conducted to determine if this is indeed the case.

Reduction in CO_2 Compressor Discharge Pressure

A CO_2 discharge pressure of 2,215 psia was assumed for the results shown up to this point. This is a typical CO_2 pressure discussed in literature. However, depending on the wellhead pressure requirements of the CO_2 sequestration process, it may be possible to use a lower discharge pressure. In order to determine the effect of CO_2 discharge pressure on net unit HR, the discharge pressure was decreased by 200 psia increments to 1,215 psia. In order to lower the discharge pressure, the compression ratio of the final compression stage (Stage 7) was decreased. This process continued until the Stage 7 compression ratio reached 1.0. For larger reductions in final discharge pressure, the compression ratio of Stage 6 was then lowered. Table 10.5 and Figure 10.7 show the reductions in net unit HR and compression power for this range of CO_2 pressures.

These results show that a 1,000 psia reduction in the CO_2 discharge pressure results in a predicted 2 percent decrease in net unit HR with something like a 12.5 percent decrease in compression power.

Table 10.5: Effect of CO_2 Pressure on Net Unit HR and Compression Power

	Illinois #6		PRB		ND Lignite	
CO_2 Pressure [psia]	Net Unit HR [Btu/kWh]					
2215	13,358	-	14,855	-	15,233	-
2015	13,321	-0.3%	14,802	-0.4%	15,182	-0.3%
1815	13,282	-0.6%	14,747	-0.7%	15,129	-0.7%
1615	13,240	-0.9%	14,689	-1.1%	15,072	-1.1%
1415	13,195	-1.2%	14,625	-1.5%	15,010	-1.5%
1215	13,146	-1.6%	14,557	-2.0%	14,943	-1.9%
CO_2 Pressure [psia]	CO_2 Compression Power [MW]					
2215	75.8	-	90.0	-	84.1	-
2015	74.2	-2.1%	88.0	-2.2%	82.2	-2.2%
1815	72.4	-4.4%	85.8	-4.6%	80.3	-4.5%
1615	70.6	-6.9%	83.6	-7.1%	78.2	-7.0%
1415	68.6	-9.5%	81.1	-9.8%	75.9	-9.7%
1215	66.4	-12.4%	78.5	-12.8%	73.4	-12.7%

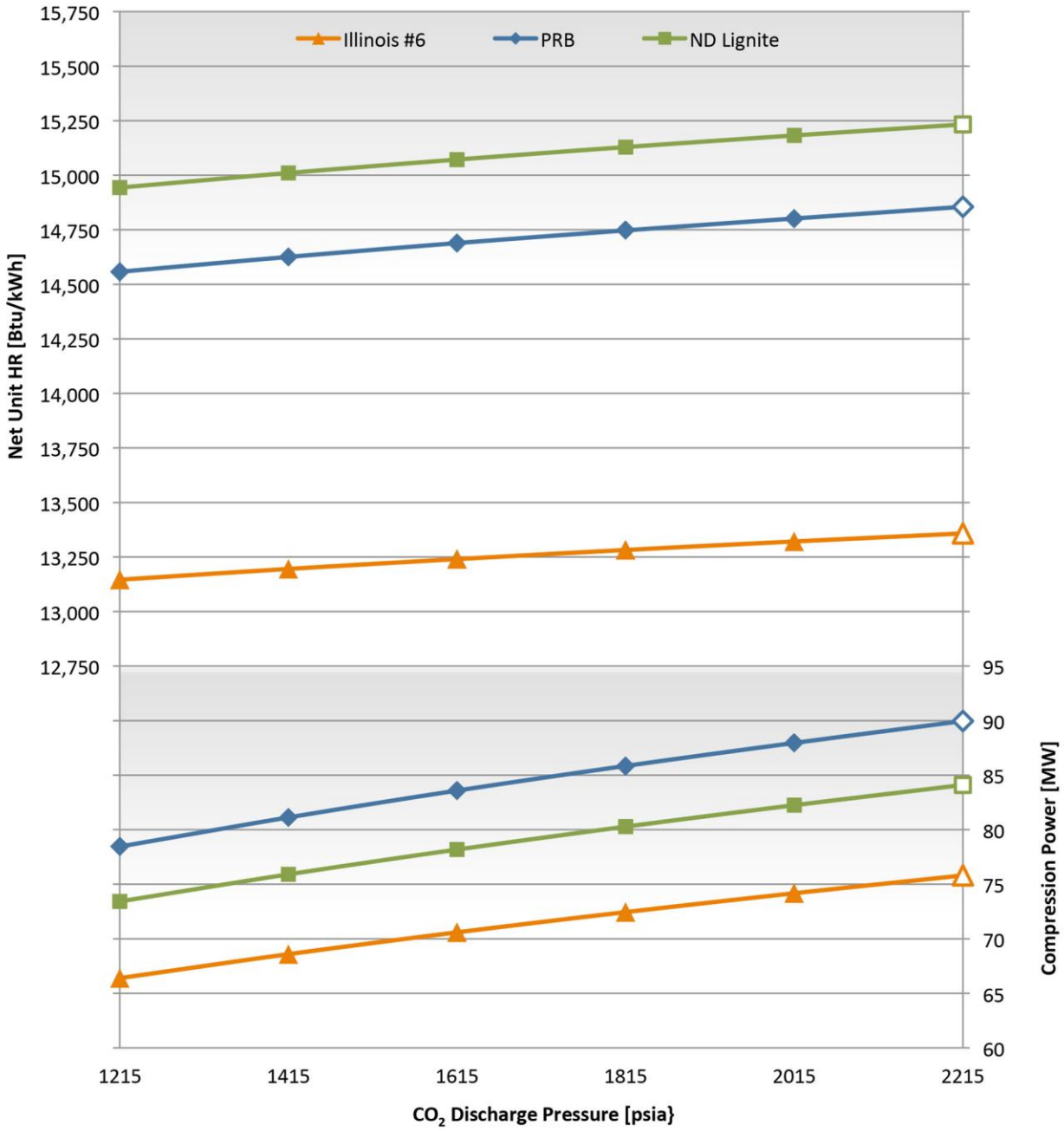

Figure 10.7: Effect of CO_2 Pressure on Net Unit HR and Compression Power

11.0 ADA Capture System With Cross Heat Exchanger

In the ADA system as shown in Figure 1.1, the cold, rich sorbent stream is lifted by recirculated CO_2 and subsequently fed into the top of the regenerator. After entering the regenerator bed, the sorbent is heated from 104°F to 248°F. The reverse is true for the hot, lean sorbent stream, which is fed into the top of the adsorber. After entering the top of the adsorber, the lean sorbent is cooled from 248°F to 104°F. The heating of the rich sorbent requires extra steam to be extracted from the steam cycle, and the cooling of the lean sorbent requires additional cooling of the adsorber. A heat exchanger which exchanges heat between these two streams (a cross heat exchanger [XHTX]) would help to reduce these heating and cooling loads, reducing the power losses associated with the CO_2 capture system.

In order to quickly examine the energy impact of such a XHTX, two separate heater blocks were added to the Aspen Plus model of the PC plant with ADA's CO_2 capture system. One heater was inserted in the lean sorbent stream, with a heat stream linking it to a similar block placed in the rich sorbent stream. It is assumed that in practice two fluidized or moving beds (one for each sorbent stream) would be linked with an intermediate fluid stream to transfer the heat. Figure 11.1 shows the ADA CO_2 capture system with the idealized heat transfer setup as modeled.

The ADA capture system model was also modified to account for the decrease in adsorber pressure drop associated with cooling of the CO_2 lean sorbent stream. The uppermost bed of the adsorber is assumed to be more than twice as deep as the lower two beds in order to provide room for the additional heat exchanger elements used to reduce the sorbent temperature from 248°F to 104°F. An examination of the pressure drop in each bed section shows that the bottom beds each account for around 1 psia of the total gas pressure drop, while the top bed accounts for 2.3 psia of the total pressure drop. Therefore, it was assumed that if the lean sorbent were cooled to 104°F prior to entering the adsorber, the pressure drop of the top bed would also be approximately 1 psia (a reduction in pressure drop of 1.3 psia). Assuming a linear correlation between the lean sorbent temperature and the top bed (ADS3) pressure drop, the following equation was used to predict the pressure drop in this bed:

$$\Delta P_{ADS3} = 9.028\ x\ 10^{-3}\ T_{Lean} + 0.061111$$

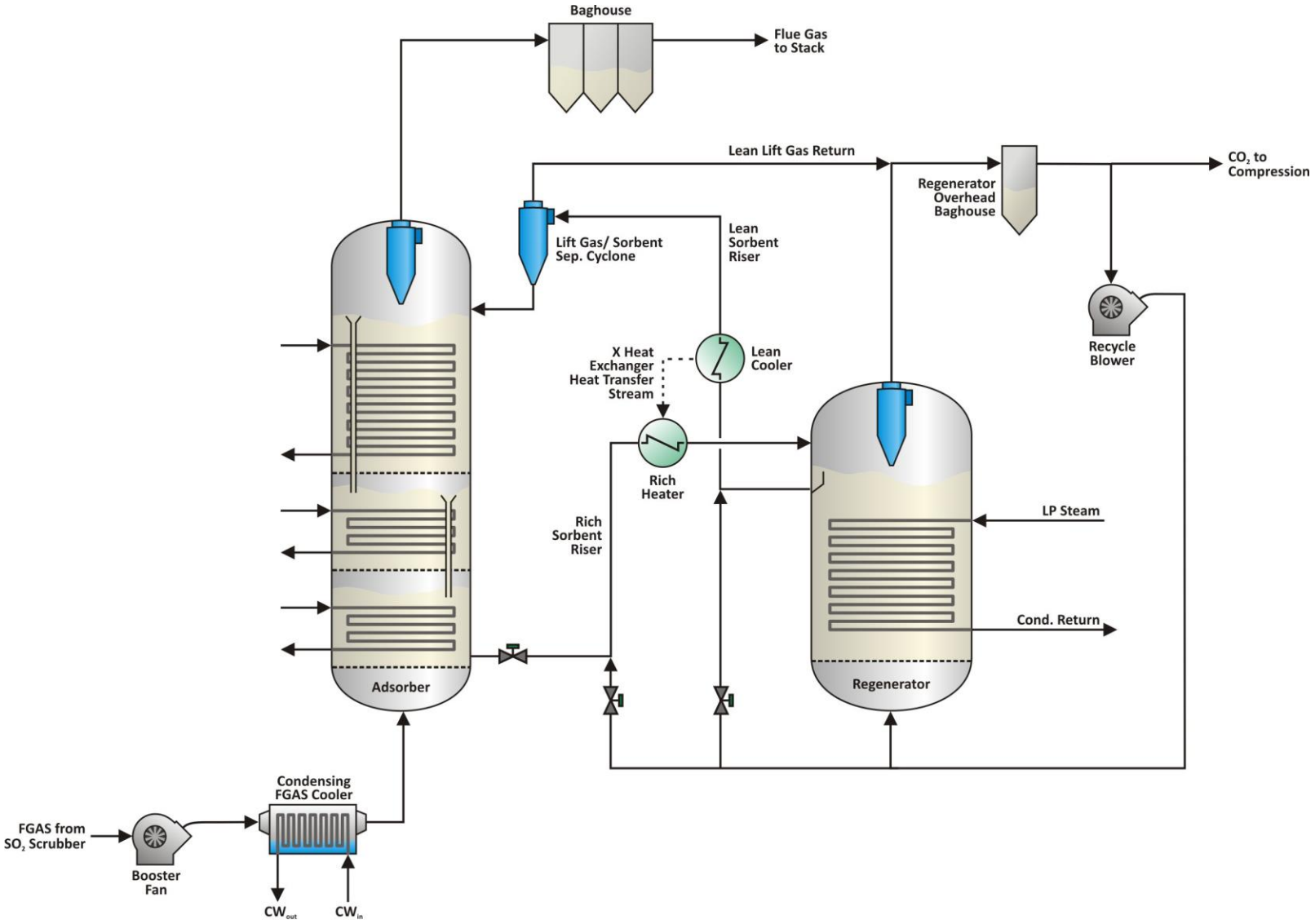

Figure 11.1: ADA CO_2 Capture System With XHTX as Modeled

Heat exchanger effectiveness was used to express the performance of the XHTX system. At a cross heat exchanger effectiveness of 1, the lean sorbent stream is cooled to its minimum temperature (the adsorber operating temperature), while the rich sorbent stream is heating accordingly. The lean sorbent temperature reaches its lower temperature limit before the rich stream reaches its upper temperature limit (the regenerator operating temperature), because the flow rate of sorbent plus adsorbed CO_2 and water is lower for the lean stream than the rich stream. Note that an effectiveness of 0 equates to the case without a XHTX. Figure 11.2 and Table 11.1 present the XHTX results as modeled in Aspen Plus. Figure 11.3 shows the sorbent temperatures leaving the XHTX for effectiveness values between 0 and 1.

These results show that addition of a XHTX would improve the heat rate of the ADA solid sorbent capture system. It is also clear that the actual operating effectiveness of any proposed XHTX design is crucial with regard to its positive impact on the plant. As the effectiveness approaches 1, net unit HR is suggested to decrease by 12.0 to 14.4 percent depending on the coal.

It is known that both the ADA solid sorbent capture system and the CO_2 compressors require electric power for their operation. In addition, LP steam extracted from the steam cycle and used to regenerate the sorbent is no longer available to generate electricity in the steam turbines. These electricity and steam requirements of the CO_2 capture and compression system are referred to here as the system's Parasitic Power (See Figure 11.2 and Table 11.1). It should be noted that when referencing the parasitic power due to lost generation in the LP turbines, an estimate of lost electrical generation is used.

Figure 11.4 presents a breakdown of the parasitic power of the CO_2 capture system for XHTX effectiveness values between 0 and 1. It can be seen that the largest contributor to parasitic power is lost electrical generation, followed by compression power and the blower or fan power. Pump and refrigeration power only account for a small percentage of the total parasitic power. Figure 11.4 shows that the addition of a XHTX primarily decreases the overall parasitic power through decreasing the lost electrical generation. The reason for this is that the XHTX adds heat to the rich sorbent stream that otherwise would come from the LP steam. Blower/fan power is slightly reduced by the use of a XHTX as fewer cooling water tubes are required in the ADS3 bed, resulting in a shallower bed and lower bed pressure drop. As system parasitic power is reduced, overall unit efficiency increases, decreasing the

coal flow rate, which results in a lower CO_2 flow rate for a 550MW_{net} plant. A lower CO_2 flow rate further reduces the capture demand on the ADA capture system, resulting in lower parasitic power for each component of the capture and compression system.

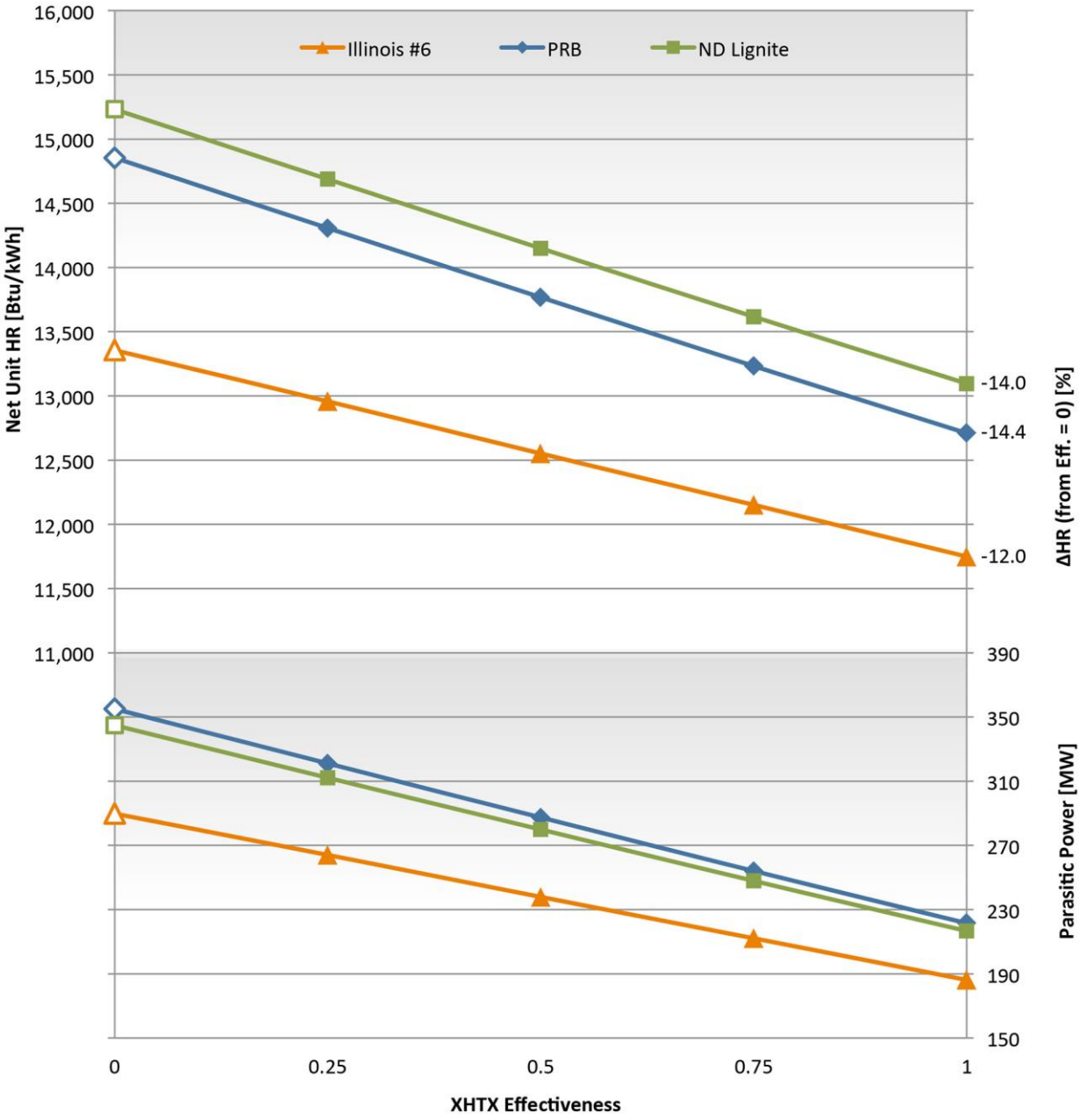

Figure 11.2: Effect of XHTX on Net Unit HR and Parasitic Power

Table 11.1: Effect of XHTX on Net Unit HR and Parasitic Power

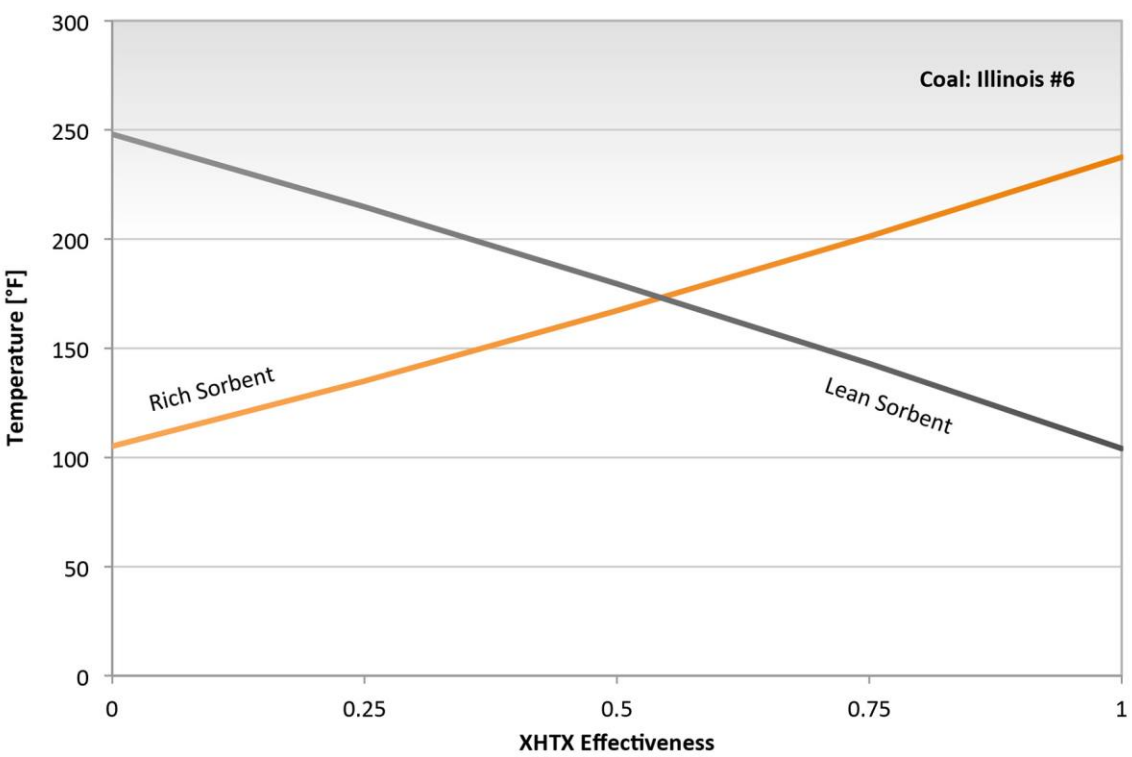

Figure 11.3: Rich and Lean Sorbent Temperatures Leaving a XHTX at Varying Effectiveness Values

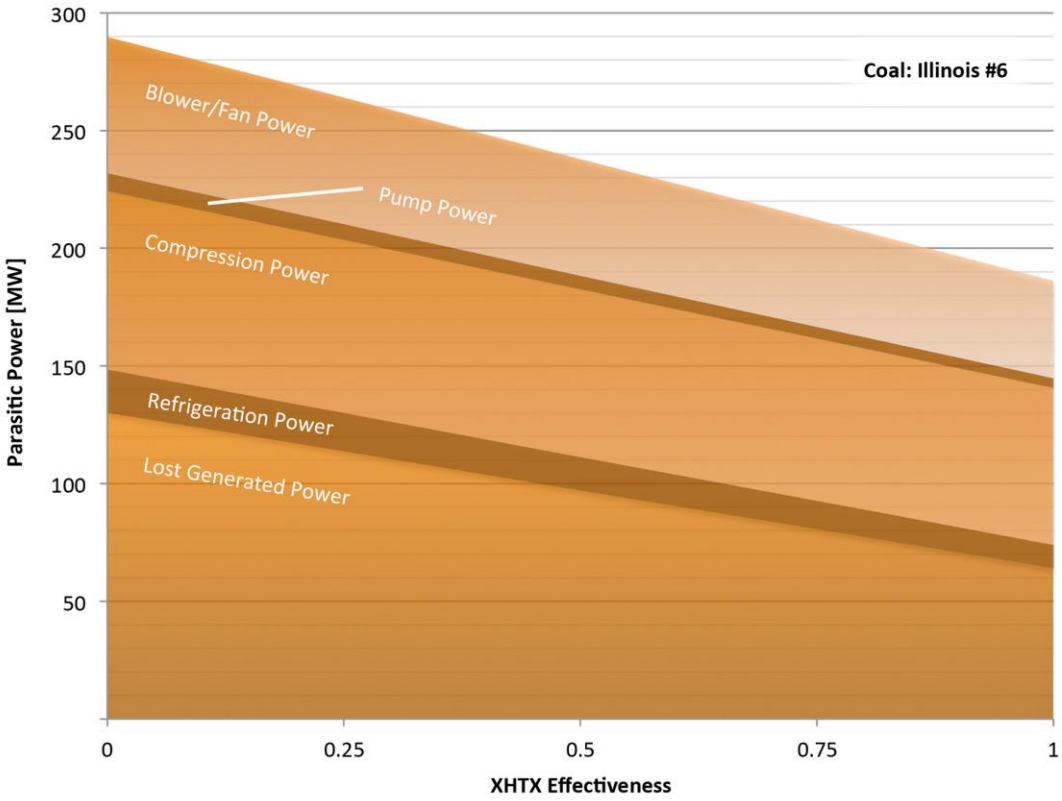

Figure 11.4: Parasitic Power Breakdown vs. XHTX Effectiveness

12.0 Utilization of Waste Heat Generated in the ADA Capture System

One of the distinguishing features of the ADA solid sorbent CO_2 capture system is that a large quantity of heat is rejected throughout the system, with some of the rejected heat being at a high temperature. The two primary locations where high-temperature heat is rejected is in cooling the CO_2 during compression (in the compressor pre cooler, intercoolers, and post cooler) and in cooling flue gas upstream of the adsorber (in the flue gas cooler).

Figure 12.1 illustrates these sources of heat (enclosed by the green boxes) and possible locations or heat sinks where it could be used to offset heat demands elsewhere in the plant (red circles).

CO_2 Compressors as a Source of Waste Heat

Figure 12.2 illustrates the heat available from the IG-1 CO_2 compression system for the Illinois #6 BASE case. Cooling water at 100°F is assumed to enter each cooler, with the water exit temperature

specified as 10°F below the hot CO_2 inlet temperature. All of the water exit temperatures are in excess of 222°F, with the highest water temperature being for the post cooler, where the water reaches 339°F. The cooling water mass flow rates were selected such that the CO_2 temperature leaving each cooler is 120°F. If all of these cooling water streams were cooled to 100°F in a cooling tower, 444.5 MBtu/hr of heat would be rejected to the atmosphere. This shows that the compressor intercooler heat has the potential to provide significant heating potential at relatively high temperatures.

Flue Gas Cooler as a Source of Waste Heat

The second significant source of heat is found in the flue gas (FGAS) cooler located upstream of the adsorber. This cooler was previously illustrated in Figure 6.1, for the Illinois #6 BASE case. Figure 6.1 shows that 617.3 MBtu/hr of heat is rejected to the atmosphere in the cooling tower used to cool the cooling water from 130°F to 80°F. This shows that the FGAS Cooler is a significant source of relatively low temperature heat that could be utilized elsewhere in the plant.

Regenerator as a Destination for Waste Heat

The regenerator is an ideal destination for waste heat as this heat could potentially offset a portion of the heat supplied by the LP steam. This would result in a lower steam extraction flow rate, allowing more LP steam to pass through the turbines and generate power. There are two methods by which hot water could be utilized in the regenerator. First, tubes for the hot water could be added alongside the LP steam tubes, as shown in Figure 12.3. However, since the regenerator operates at a temperature of 248°F, the temperature of the hot water would need to be in excess of this temperature. A second method for the utilization of waste heat involves the addition of a rich sorbent water heat exchanger upstream of the regenerator. This case is illustrated in Figure 12.4 below. If this heat exchanger operates in a counter flow arrangement, the water temperature only needs to be higher than the temperature of the sorbent entering the heat exchanger. In the case where a XHTX is not utilized, this temperature would be equal to the adsorber operating temperature; 104°F for the BASE case. Since this second method provides the potential for better utilization of waste heat, it was the one selected for further analysis.

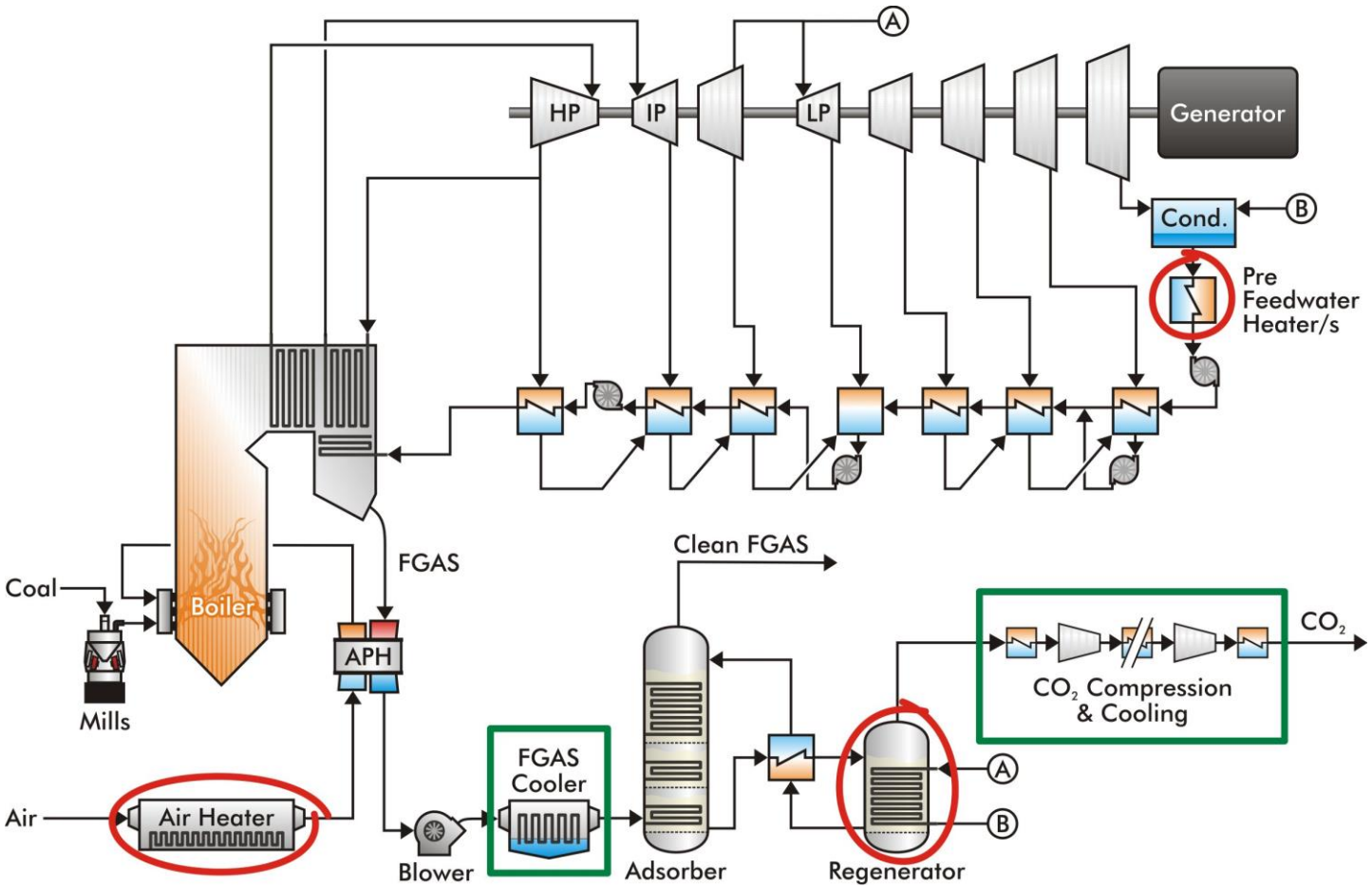

Figure 12.1: Sources and Possible Destinations for Waste Heat Generated in the ADA Capture System

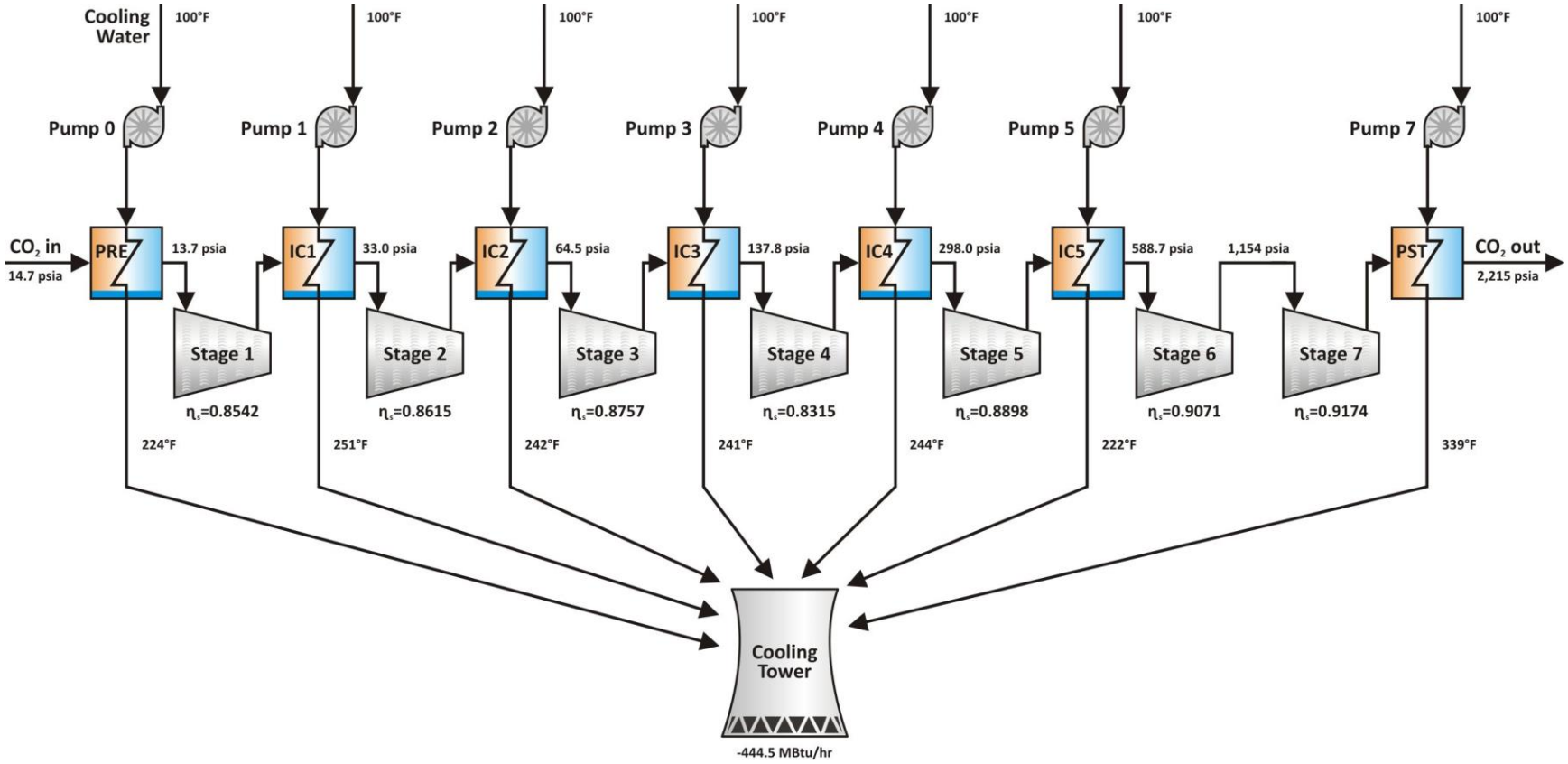

Figure 12.2: CO_2 Compression System for Illinois #6 BASE Case

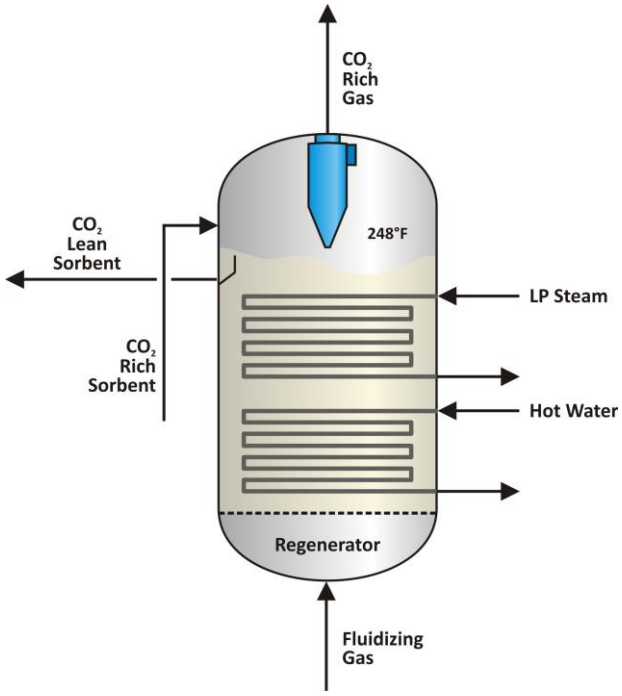

Figure 12.3: First Method for Utilizing Waste Heat to Offset Regenerator Steam Duty

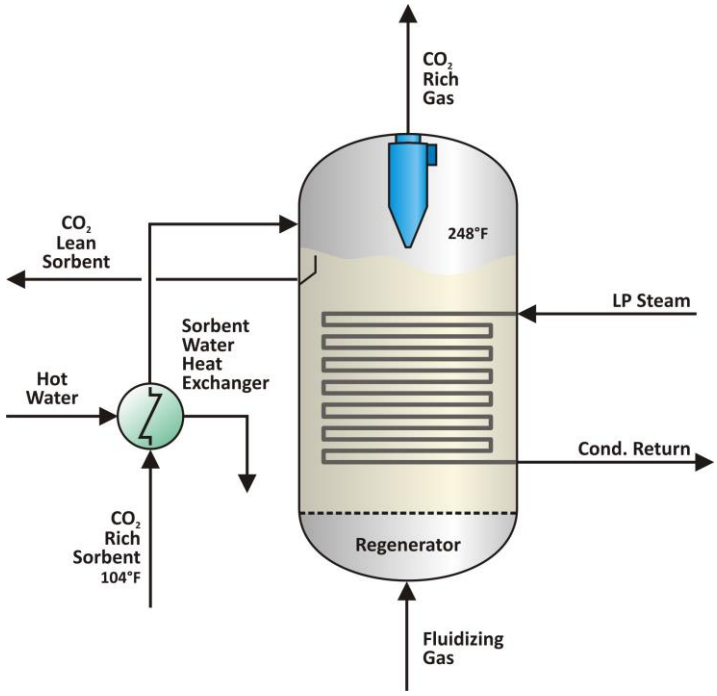

Figure 12.4: Method Selected for Utilizing Waste Heat to Offset Regenerator Steam Duty

Air Heater as a Destination for Waste Heat

A potential destination for low-temperature waste heat is in heating the combustion air. In the BASE case Aspen Plus model, 77°F ambient air is assumed with the air passing through both FD and PA fans before being heated by a steam air heater. Steam for this air heater is extracted after the first LP turbine stage. Air exiting the fans is at approximately 89°F before entering the heater. Figure 12.5 illustrates the configuration of this air heater downstream of the fans and upstream of the regenerative air preheater (APH). If instead of steam, waste heat were to be utilized in heating the incoming combustion air, the extraction from the LP turbine could be reduced or eliminated. For the purposes of the analyses in this report, when hot water is used to heat the incoming air, the steam extraction is entirely cut off.

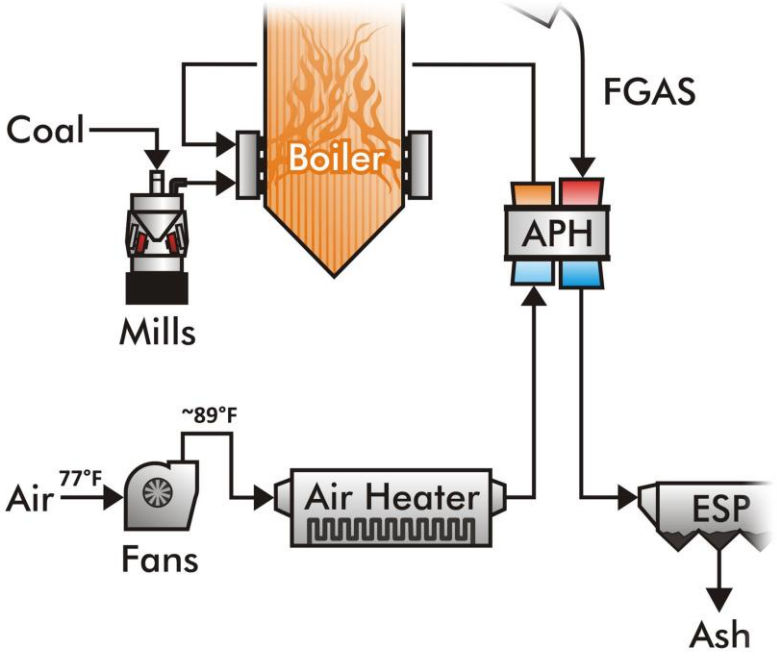

Figure 12.5: Configuration of Air Heater Upstream of APH

Feedwater Heaters as Destination for Waste Heat

The final location selected as a potential destination for waste heat is in heating the steam cycle feedwater. Figure 12.6 presents the first four feedwater heaters of the supercritical steam cycle modeled. Looking at these feedwater heaters, there are several important considerations to be made. First, superheated vapor is extracted from the turbines and enters the feedwater heaters. This vapor

always exits the feedwater heaters as a saturated liquid. Secondly, the steam cycle is designed in such a way that the temperature of this saturated liquid is exactly 10°F above the temperature of the feedwater entering the heater. The exceptions to this are FWH1, where the liquid is coming from the condenser and has only been slightly heated in the SPE heat exchanger, and FWH4, which is an open-type feedwater heater.

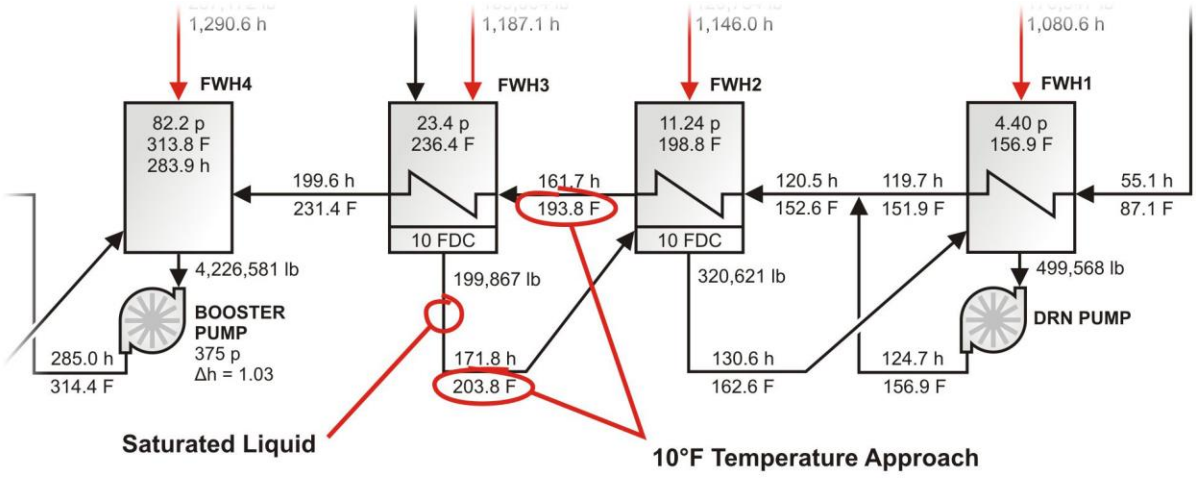

Figure 12.6: First Four Feedwater Heaters of Supercritical Steam Cycle

If waste heat is to be used in heating the feedwater, it was determined that the simplest and most effective way of accomplishing this is through the addition of a feedwater heater upstream of FWH1 (FWH0). Since, for the particular steam cycle process conditions used in this analysis, the feedwater at the FHW0 location is 87.1°F, relatively low-temperature heat can be utilized effectively (Figure 12.7).

FWH0 can also be utilized as a sink for high-temperature heat. The steam extraction outlet pressure for FWH1 dictates a liquid saturation temperature of 156.9°F, which limits the incoming feedwater temperature to 10°F below this (146.9°F). If FWH0 increases the feedwater temperature to above 146.9°F, extraction G to FWH1 is entirely cut off. In this case, the feedwater temperature leaving FWH1 is equal to that entering FWH1. Furthermore, if this feedwater heater temperature is in excess of 152.6°F (10°F above the temperature of the saturated liquid extraction leaving FWH2), extraction F to FWH2 is also cut. This principle carries over to FWH3 as well. Figure 12.7 illustrates a case where feedwater heating in FWH0 results in the extractions to FWH1, FWH2, and FWH3 being cut off. The

outlet flow from the Steam Air Heater was also redirected from FWH3 to the condenser, and the flow from the SSR to FWH2 was directed to the condenser. With extractions E, F, and G being cut, the DRN Pump is no longer necessary and was removed. Since the feedwater temperature entering FWH4 is lower than the design condition, extraction D is increased slightly to meet the design feedwater temperature of 313.8°F in FWH4. If the feedwater temperature leaving FWH0 were lower, perhaps fewer extractions would be shut off, with the condensed steam being pumped to pressure by the DRN Pump before being combined with the feedwater.

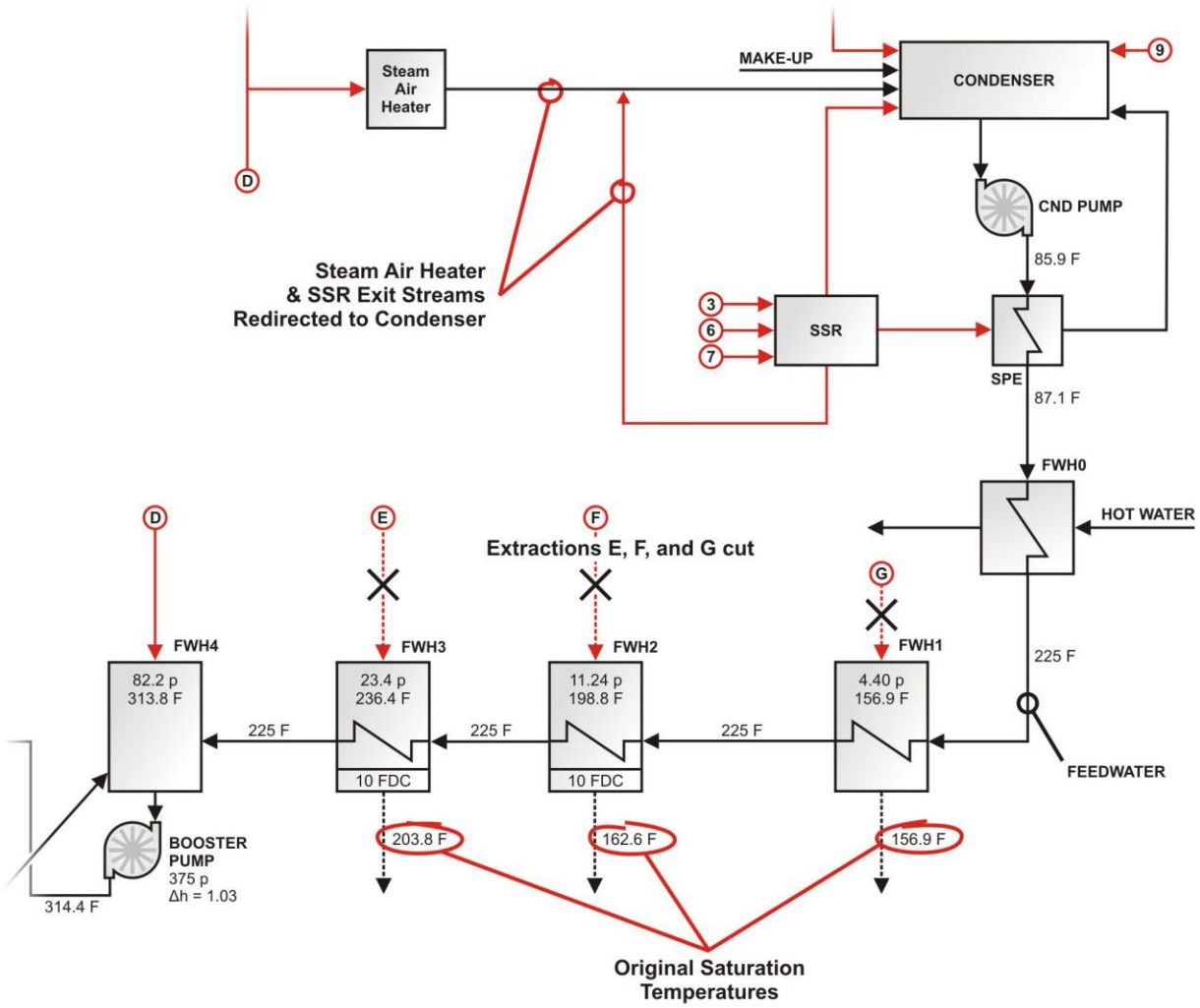

Figure 12.7: High-Temperature Waste Heat Feedwater Heating Example

In some cases, waste heat from two different sources can be used to heat the feedwater. An example of this is where heat from both the compression coolers and flue gas cooler is available for

feedwater heating. In such a case, two feedwater heaters are added upstream of FWH1 as illustrated in Figure 12.8. Hot water from the one heat source is directed through FWH0-1, while the hot water from the other source is directed through FWH0-2. Hot water being fed to FWH0-1 should be at a lower temperature than the water to FWH0-2 as this will allow the feedwater to be heated to the highest possible temperature.

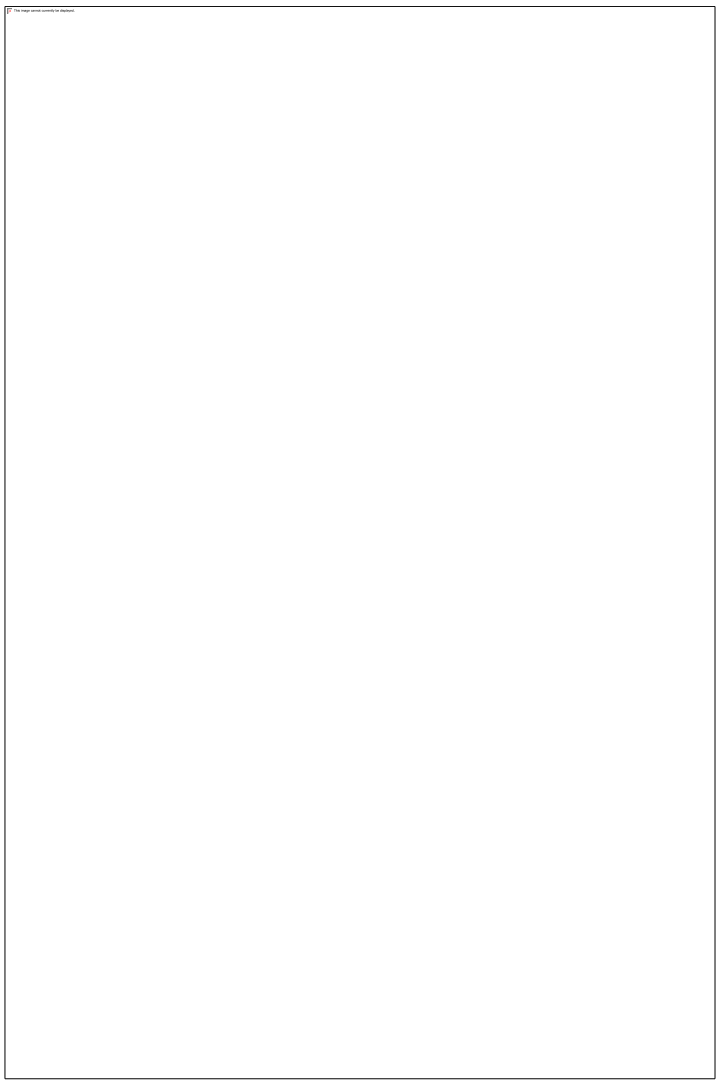

Figure 12.8: Using Waste Heat From Two Sources for Feedwater Heating

13.0 Connection of Waste Heat Sources and Sinks

For the analyses in this report, waste heat from the two sources above (CO_2 compression coolers and flue gas cooler) was directed to the three destinations, both individually and in various

combinations. Since the connections for these cases vary from case to case, they will be summarized briefly.

Compressor Cooler Heat to Regenerator

It was shown in Section 12.0 that hot water exiting the seven coolers in the CO_2 compression train is a significant source of waste heat. If a heat exchanger were to be added to heat the cold, rich sorbent entering the regenerator, hot water from the compressor coolers could be used to heat the sorbent. To be used successfully, the water temperature leaving each cooler needs to exceed the cold sorbent temperature by a value equal to or greater than the temperature approach between the cold sorbent and cold water in the heat exchanger. In the case where a cross heat exchanger is added to the system, the heat exchanger for transferring heat from the compressors, could be incorporated into the cross heat exchanger itself to further heat the sorbent. After leaving the rich sorbent heater, the cooling water is cooled to 100°F in a cooling tower (or towers) before returning to the compression coolers. Figure 13.1 illustrates the cooling water circuit between the compression coolers and the rich sorbent heat exchanger and cooling towers. In figures and tables, this case is designated as “HI REG”.

The approach temperature in the sorbent heater is important to the performance of this waste heat integration scenario. Approach temperature is defined as the minimum temperature difference between the hot water and cold sorbent at any given point in the heat exchanger. Figure 13.3 illustrates this concept and shows that for the rich sorbent heat exchanger, the approach temperature is at the sorbent inlet / water outlet end of the heat exchanger. The heat exchanger is assumed to operate in a counter-flow arrangement. If the approach temperature is low, more waste heat can be utilized in heating the sorbent. However, a closer approach temperature necessitates a larger heat transfer surface area, increasing both heat exchanger size and capital cost. In order to examine the impact of the approach temperature on the HI REG scenario, calculations were performed in which the temperature approach was varied between 2°F and 35°F. These results are presented in Figure 13.3. Heat exchanger approach temperature is seen to affect heat rate, but more information with regards to heat exchanger sizing and cost is needed before a conclusion on the ideal approach temperature can be reached. For the time being, an approach temperature of 10°F is used.

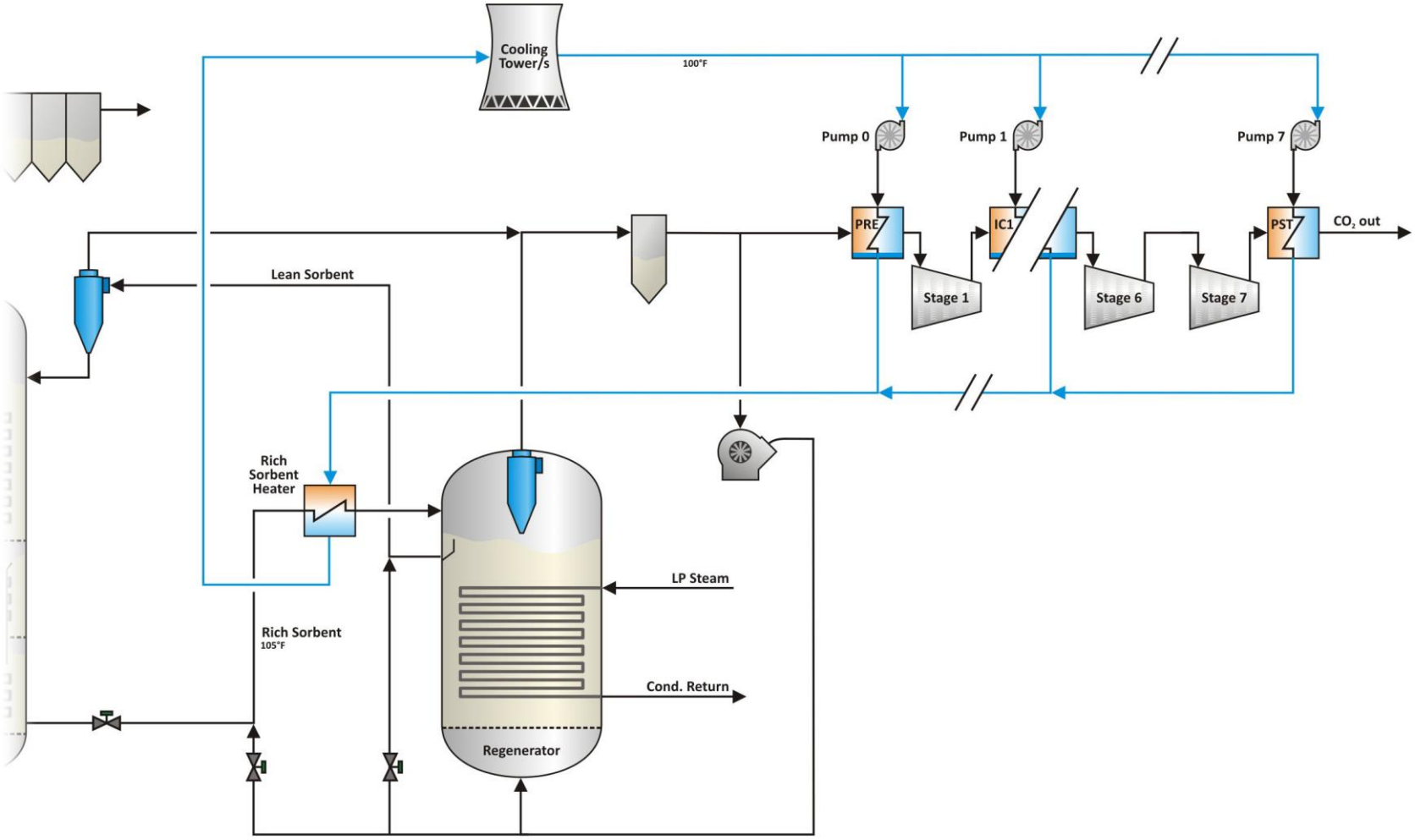

Figure 13.1: Cooling Water Circuit for the HI REG Case

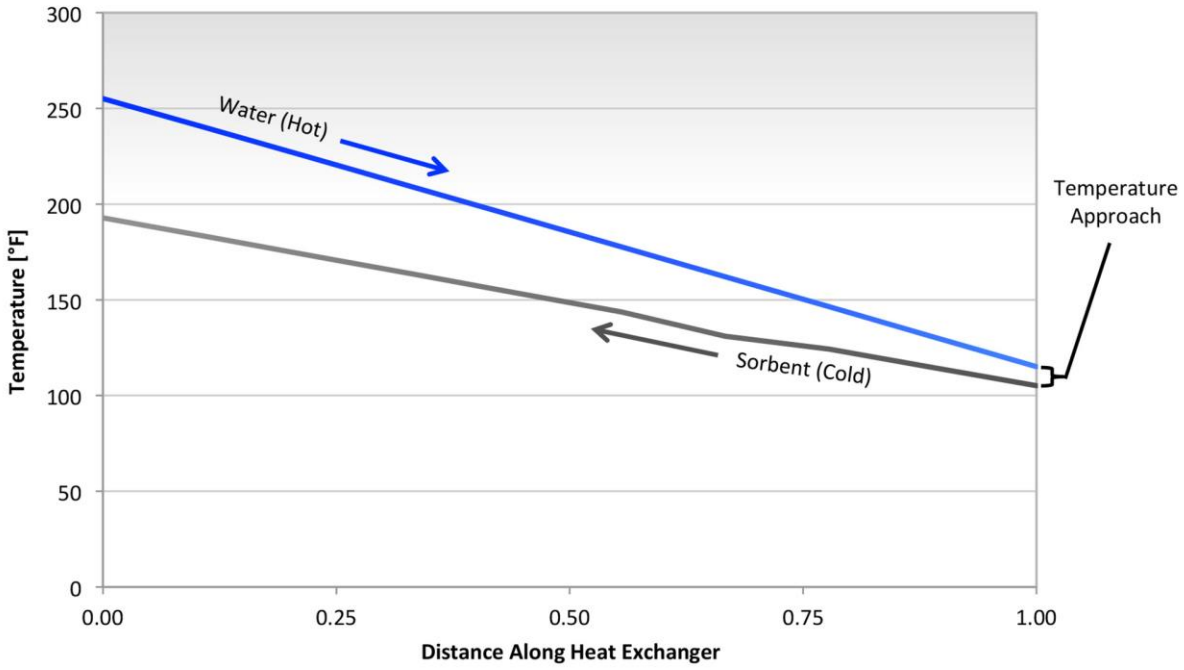

Figure 13.2: Temperature Approach Throughout Length of Rich Sorbent Heater

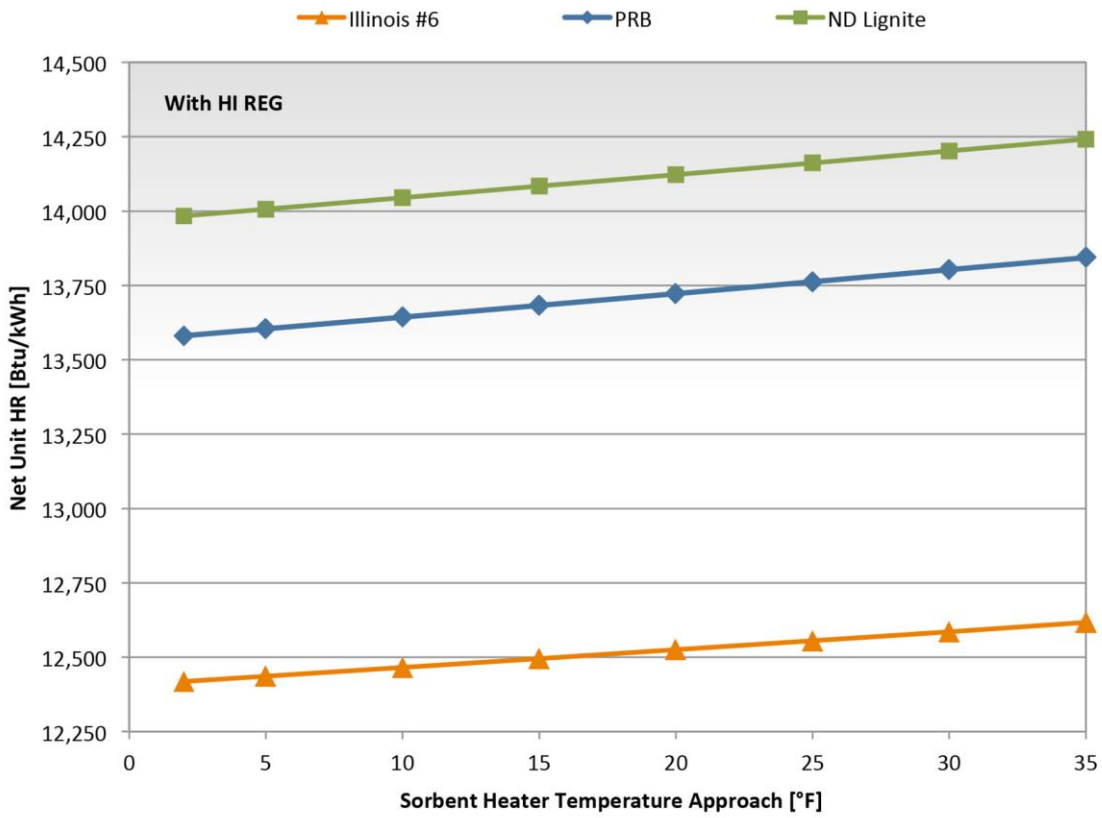

Figure 13.3: Net Unit HR Results for Variations in Sorbent Heat Exchanger Approach Temperature

Compressor Cooler Heat to Feedwater Heating

Feedwater heating is the second destination for heat generated during CO_2 compression (HI FWH). As was shown in Figure 12.7, an additional feedwater heater (FWH0) is added upstream of FWH1. If the water temperature exiting any of the seven compression train coolers is greater than the feedwater temperature entering FWH0, this water stream can be directed through FWH0 (Figure 13.4). For the BASE case with only HI FWH, the feedwater enters FWH0 at 87.1°F. Since the minimum approach temperature of FWH0 was assumed to be 10°F, the water can be directly cooled to 100°F without the need for additional cooling towers.

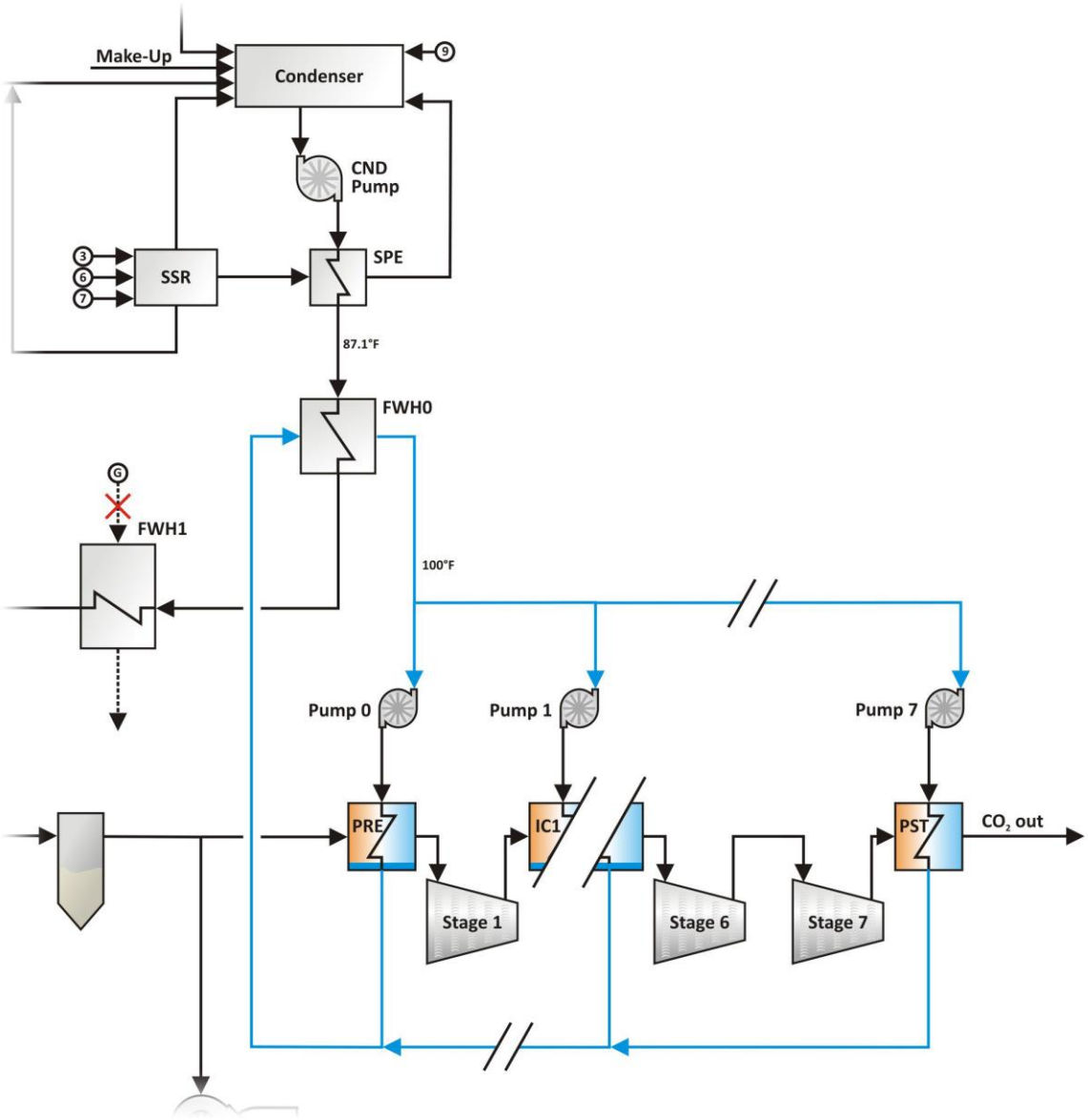

Figure 13.4: Cooling Water Circuit for the HI FWH Case

Compressor Cooler Heat to Both Regenerator and Feedwater Heating

A final method for utilizing compression cooler heat is to direct the hot water to both heat the sorbent entering the regenerator and the feedwater. Since the cold sorbent temperature exceeds the temperature of feedwater entering FWH0, hot water from the compressors is utilized to heat the sorbent before being used to heat the feedwater. This allows the utilization of nearly all of the heat that would otherwise have been rejected in cooling towers. The cooling water circuit for this HI REG / HI FWH case is detailed in Figure 13.5 below.

Flue Gas Cooler Heat for Heating Combustion Air

It was previously mentioned in a separate ERC study looking at the design of a condensing flue gas cooler [1], that hot cooling water exits the flue gas cooler at a nominal temperature of 130°F. Although this water is at a relatively low temperature, the temperature is still sufficient high to heat the boiler combustion air. This hot water is piped to a water-air heat exchanger that replaces the steam-air heat exchanger downstream of the FD and PA fans. For all figures and tables, this case is designated as "FG HI AIR". Figure 13.6 shows the cooling water circuit as modeled for this case. Before entering the air heater, a portion of the hot cooling water is bypassed and fed directly to the cooling tower. The bypass flow rate is varied such that a 10°F approach temperature at the cold end of the air heater is achieved. A 10°F approach temperature at the hot end of the heater is a design specification for the heater. Cooling water is cooled in a cooling tower to 80°F and then cooled to 65°F through the use of a refrigeration cycle.

Flue Gas Cooler Heat for Feedwater Heating

130°F water from the flue gas cooler can also be effectively used to heat feedwater through the addition of a FWH0. After being cooled in FWH0, the water is passed through a cooling tower before being cooled to 65°F by way of a refrigeration cycle as shown in Figure 13.7. This case is designated as "FG HI FWH".

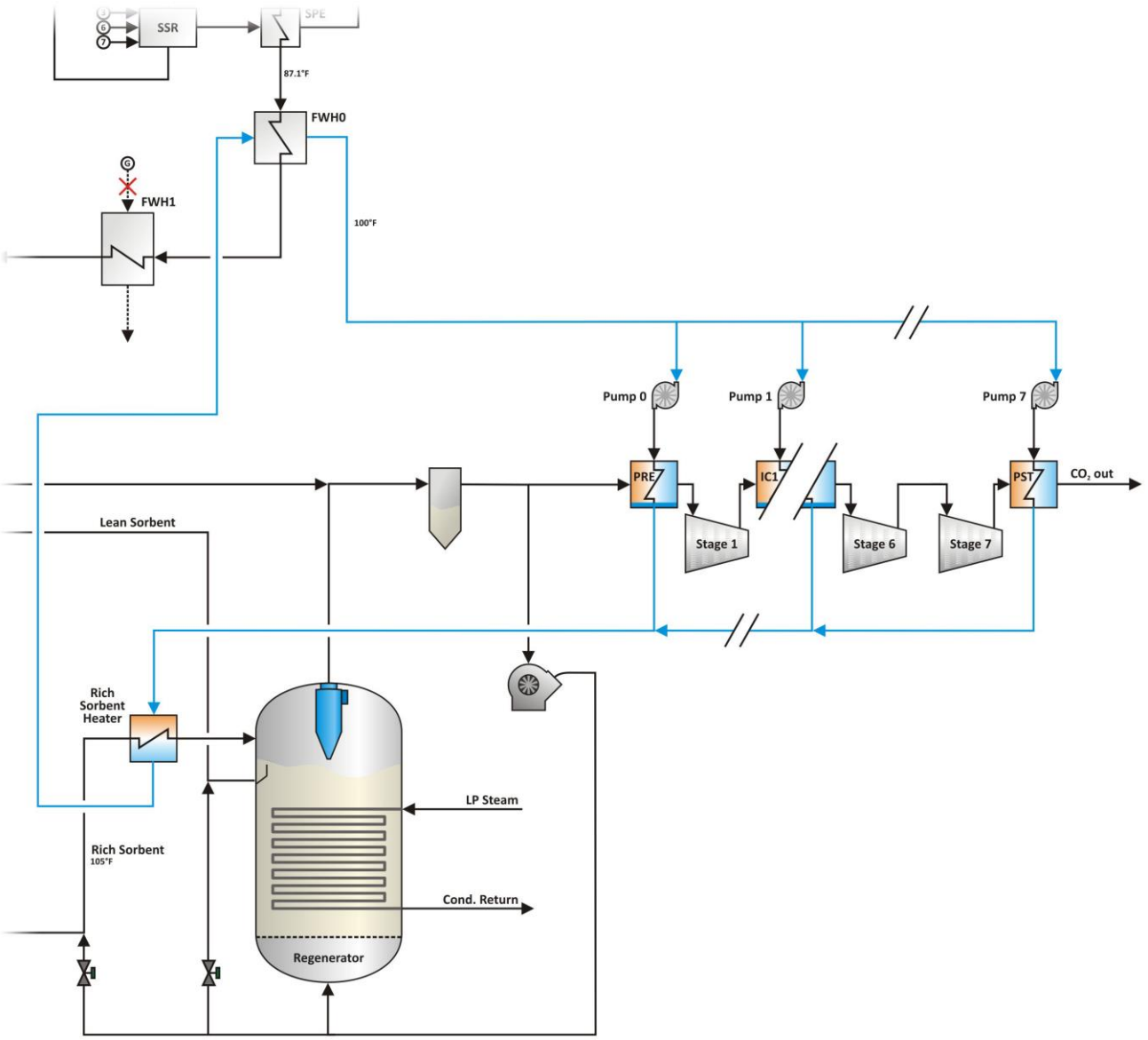

Figure 13.5: Cooling Water Circuit for the HI REG / HI FWH Case

Figure 13.6: Cooling Water Circuit for the FG HI AIR Case

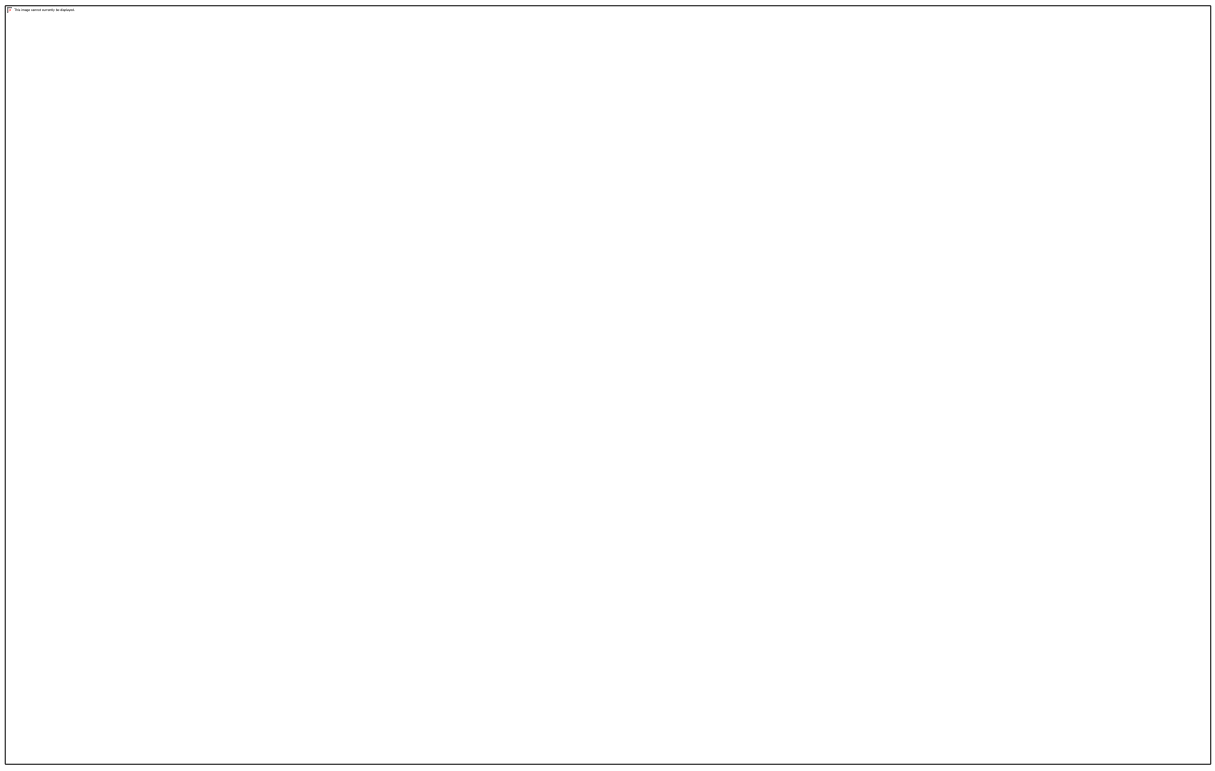

Figure 13.7: Cooling Water Circuit for the FG HI FWH Case

Flue Gas Cooler Heat for Both Combustion Air and Feedwater Heating

The hot water exiting the flue gas cooler, can be used to heat both the incoming boiler air and the feedwater simultaneously. First, the hot water flow is split, with part of the flow being directed to the air heater and the remainder flowing to FWH0. As mentioned above, the flow through the air heater is selected such that a 10°F temperature approach results at the cold end of the heater. Cold water from both the air heater and FWH0 are further cooled by a cooling tower and refrigeration cycle before returning to the flue gas cooler at 65°F. Figure 13.8 illustrates this FG HI AIR / FG HI FWH case.

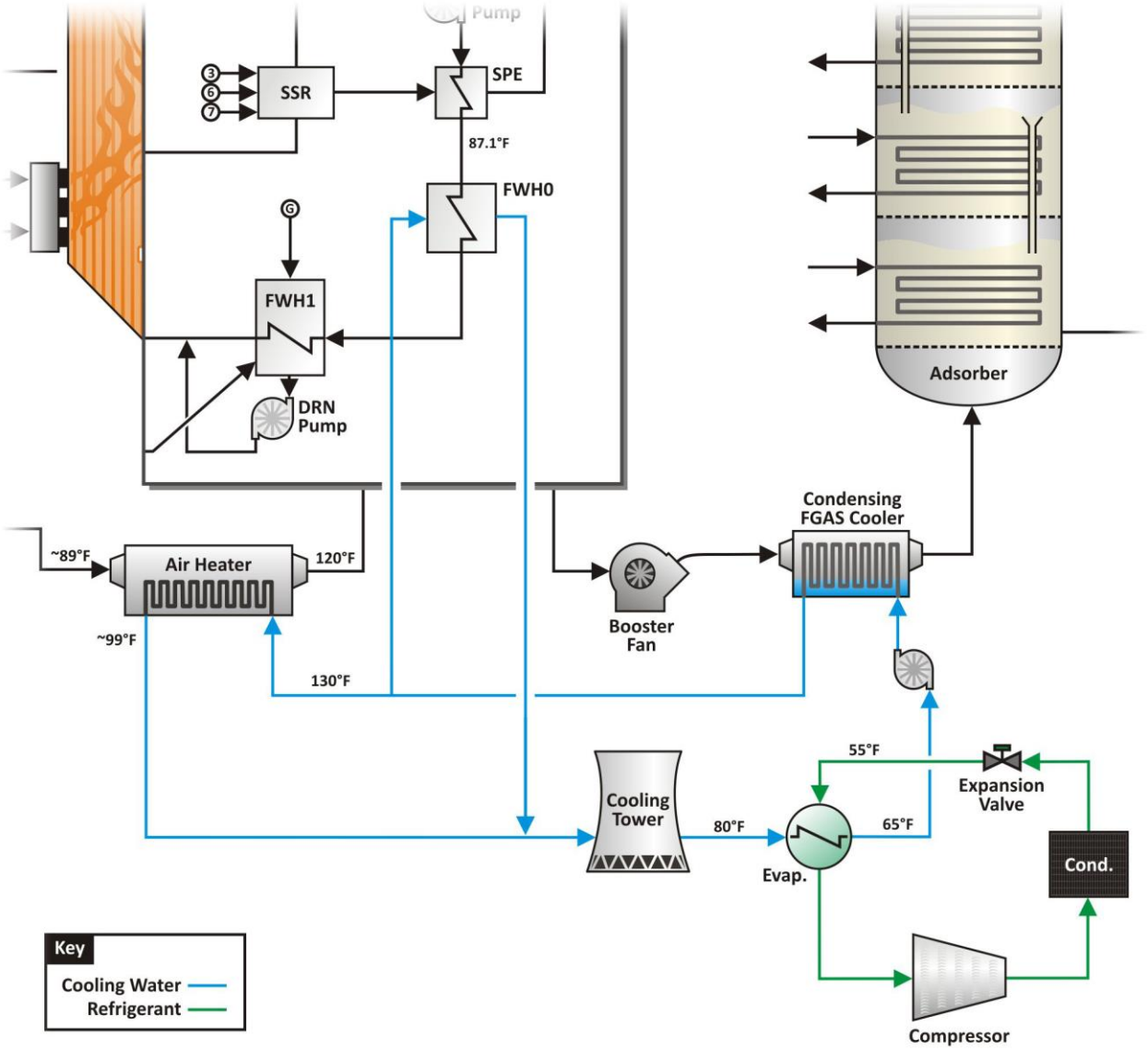

Figure 13.8: Cooling Water Circuit for the FG HI AIR / FG HI FWH Case

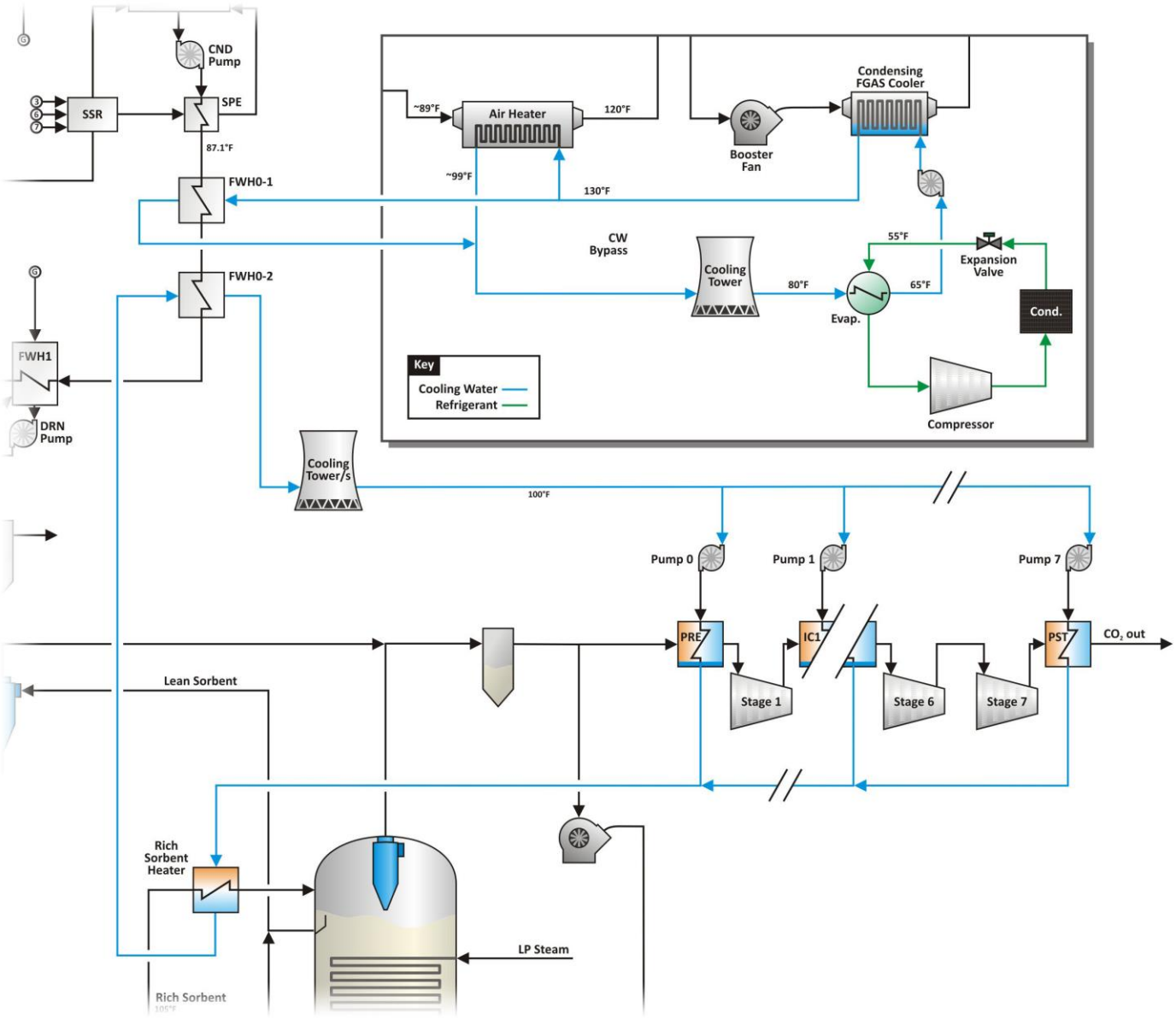

Figure 13.9: Cooling Water Circuit for the HI ALL Case

Compressor and Flue Gas Cooler Heat for Combustion Air, Regenerator, and FWH

For the HI ALL case, cases HI REG, HI FWH, FG HI AIR, and FG HI FWH are all used simultaneously (Figure 13.9) The major consideration in this case is that two feedwater heaters are added upstream of FWH1 (FWH0-1 and FWH0-2). The order of these heaters depends on the water temperature from the compression coolers. If this water temperature is greater than the 130°F water from the flue gas cooler, the first feedwater heater receives the 130°F water. This is the condition illustrated below in Figure 13.9. However, if the water temperature from the rich sorbent heater/compression coolers is below 130°F, the first feedwater heater receives this water instead.

14.0 Waste Heat Integration Results

Figures 14.1 through Figure 14.3 present net unit heat rate results for combinations of the heat integration connections mentioned above.

Starting with the bottom row of Figure 14.1 through Figure 14.3 we see the BASE case with the ADA capture system. As previously mentioned, this case operates at an adsorber temperature of 104°F, a regenerator temperature of 248°F, a water sorption multiplier of 1, and there is no XHTX (effectiveness = 0). Above this row we find the cases where heat from the flue gas cooler is used in heating combustion air and feedwater. To the right of these rows are labels, which display the decrease in net unit HR from the BASE case. Moving up the charts, the next cases are using heat from the compressor coolers to heat the sorbent entering the regenerator and the feedwater. Above these three is the case (HI ALL) where heat is utilized from both sources in heating all four destinations for the heat. For this case, it can be seen that for the Illinois #6, PRB, and ND Lignite the predicted decreases in net unit HR from the BASE case are 7.4 percent, 9.0 percent and 8.6 percent.

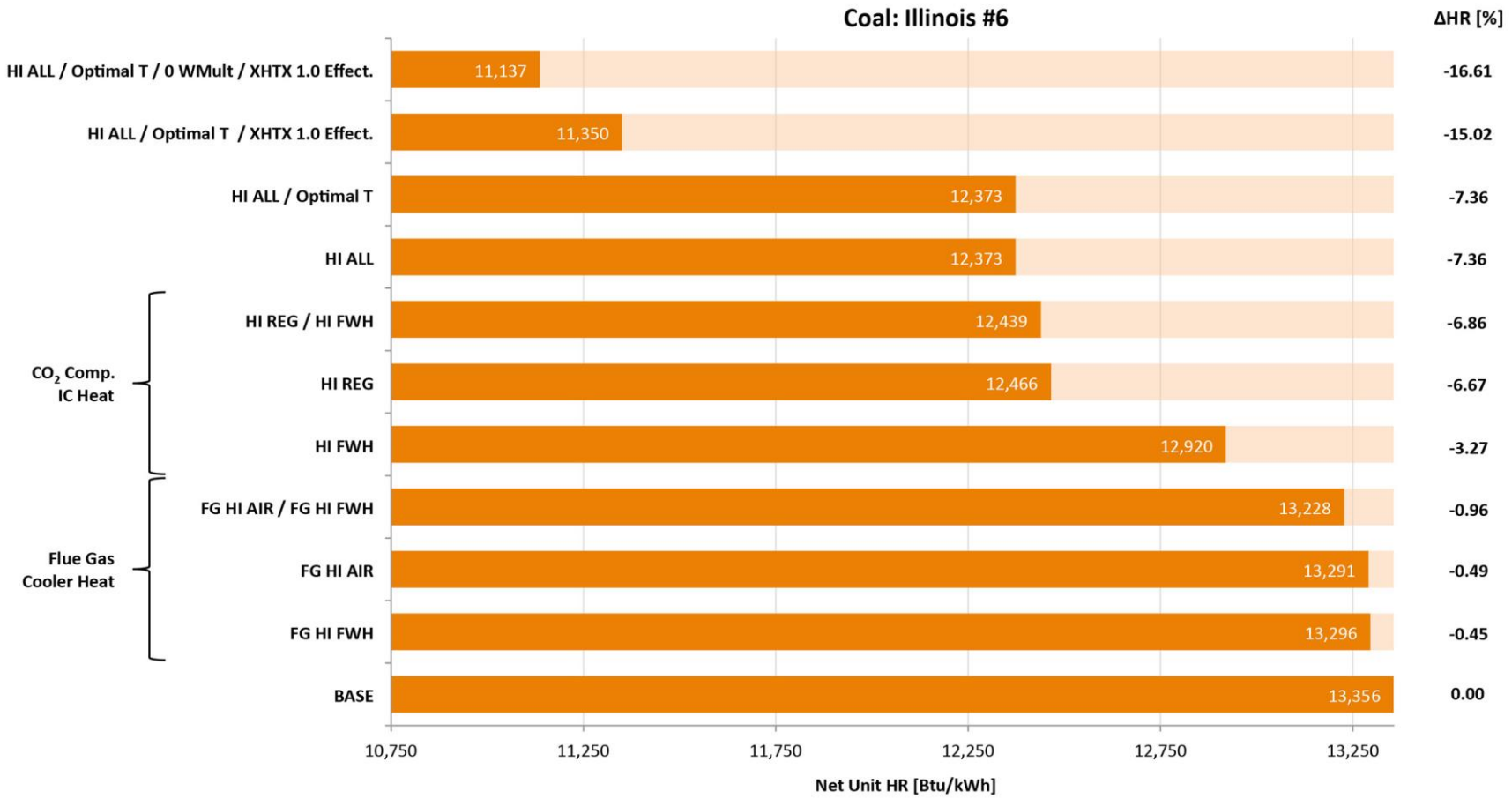

Figure 14.1: Waste Heat Integration Results for Illinois #6

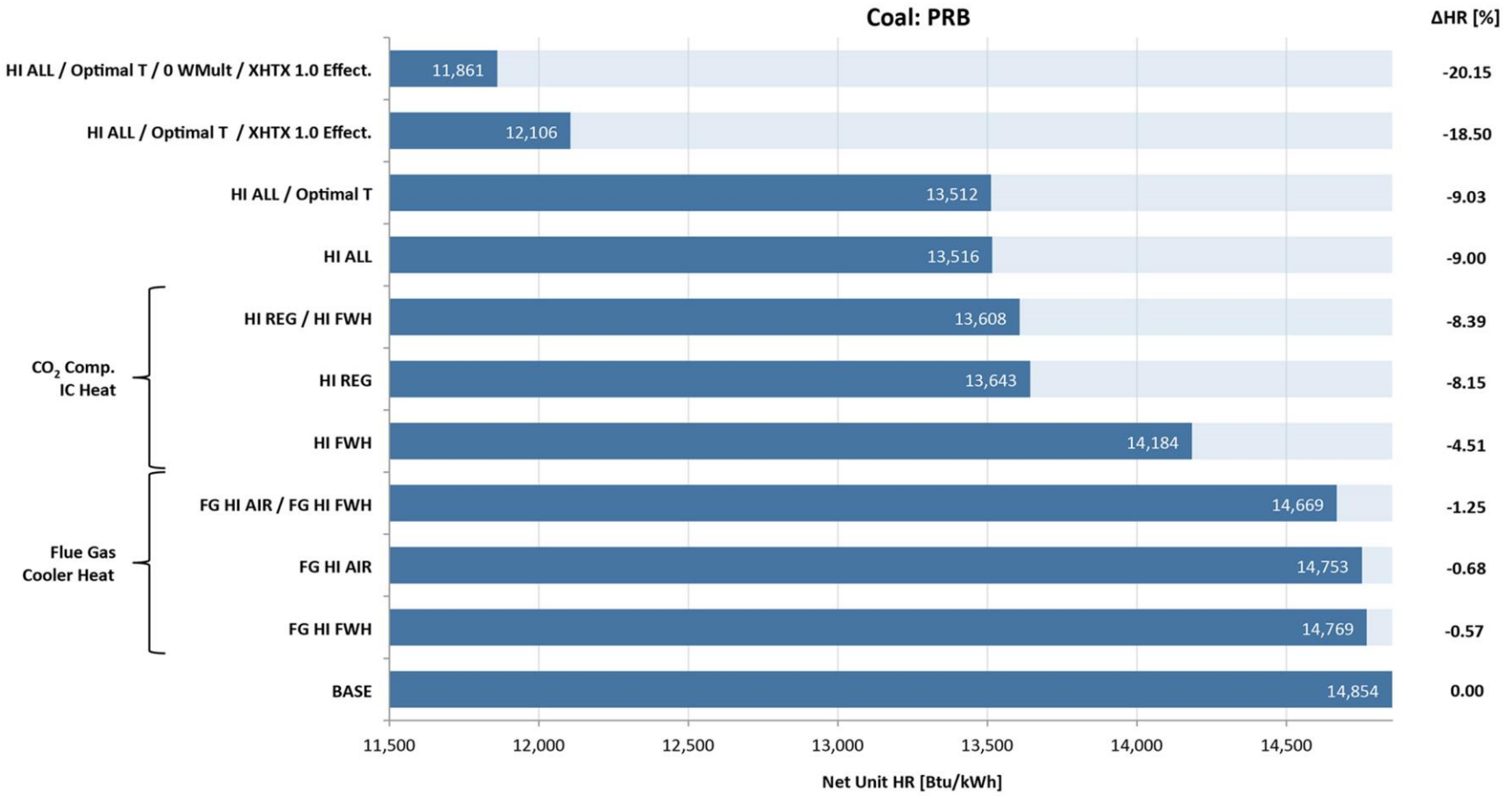

Figure 14.2: Waste Heat Integration Results for PRB

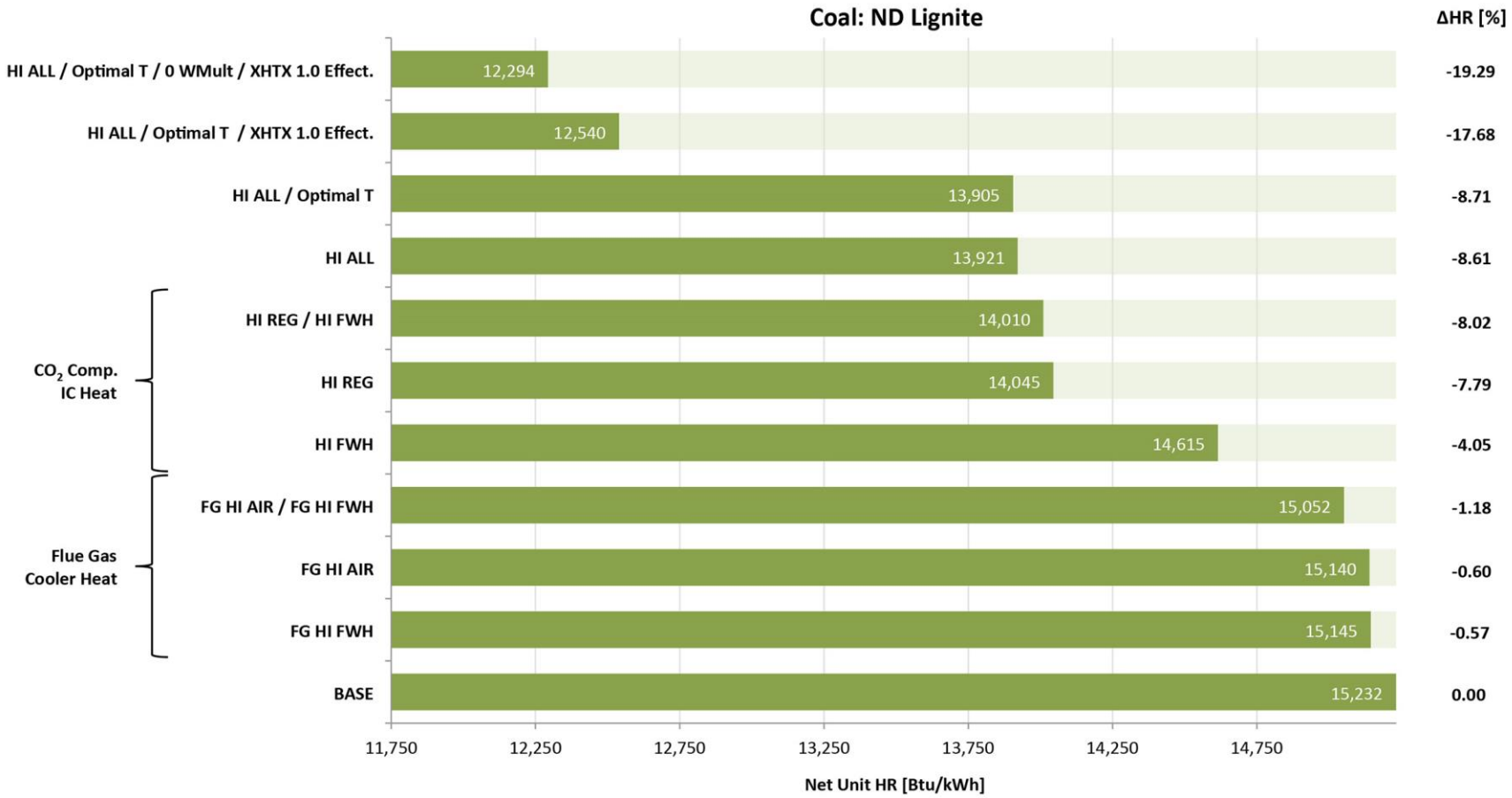

Figure 14.3: Waste Heat Integration Results for ND Lignite

Figure 10.2 and Figure 10.4 showed that the optimal operating temperatures of the adsorber and regenerator are not always 104°F and 248°F respectively. A series of analyses were conducted where regenerator temperature was varied across a range of adsorber temperatures, while full waste heat integration was also conducted. Figure 14.4 through Figure 14.6 show these results for the three coals. It should be noted that for these results, a higher regenerator temperature always results in better unit performance and a lower sorbent flow rate for a given adsorber operating temperature. For these analyses, the regenerator temperature was caped at 255°F. It is known that elevated sorbent temperatures can degrade the sorbent and reliable desorption curves were not available for temperatures above 248°F. Therefore, 248°F was selected as the ideal regenerator temperature for all of the coals. The ideal adsorber temperature is the one that results in the lowest net unit HR at this regenerator temperature. For the three coals, the ideal adsorber temperatures are as follows: 104° for the Illinois #6, and 108°F for the PRB, and 106°F for the ND Lignite. Heat Rate results for HI ALL at these temperatures are presented in Figure 14.1 through Figure 14.3 as "HI ALL / Optimal T."

Two results are presented at the top of each of the heat integration figures (Figure 14.1 through Figure 14.3). For both of these cases, HI ALL and the optimal adsorber and regenerator temperatures were used. In addition, a XHTX with a theoretical effectiveness of 1 is introduced into the mix with dramatic reductions in HR. For the uppermost case, a theoretical sorbent with 0 moisture uptake is also assumed. These cases are presented to illustrate the theoretical upper limits of the modeled improvements to the ADA solid sorbent CO_2 capture system. Reductions in net unit HR (from the BASE case) for these cases are in the 15 to 18 percent range, depending on the coal.

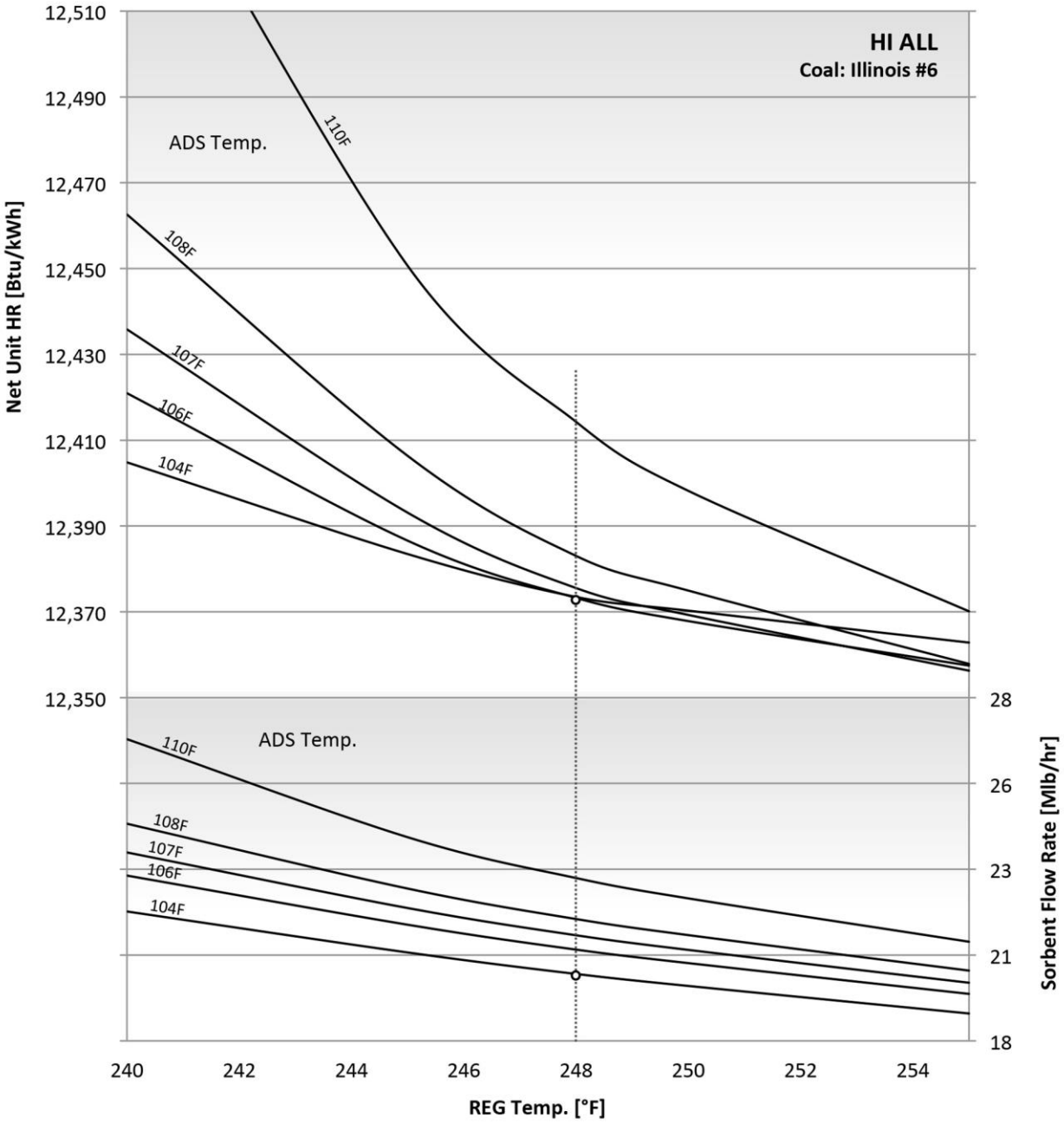

Figure 14.4: Variations in Adsorber and Regenerator Temperature for HI ALL and Illinois #6

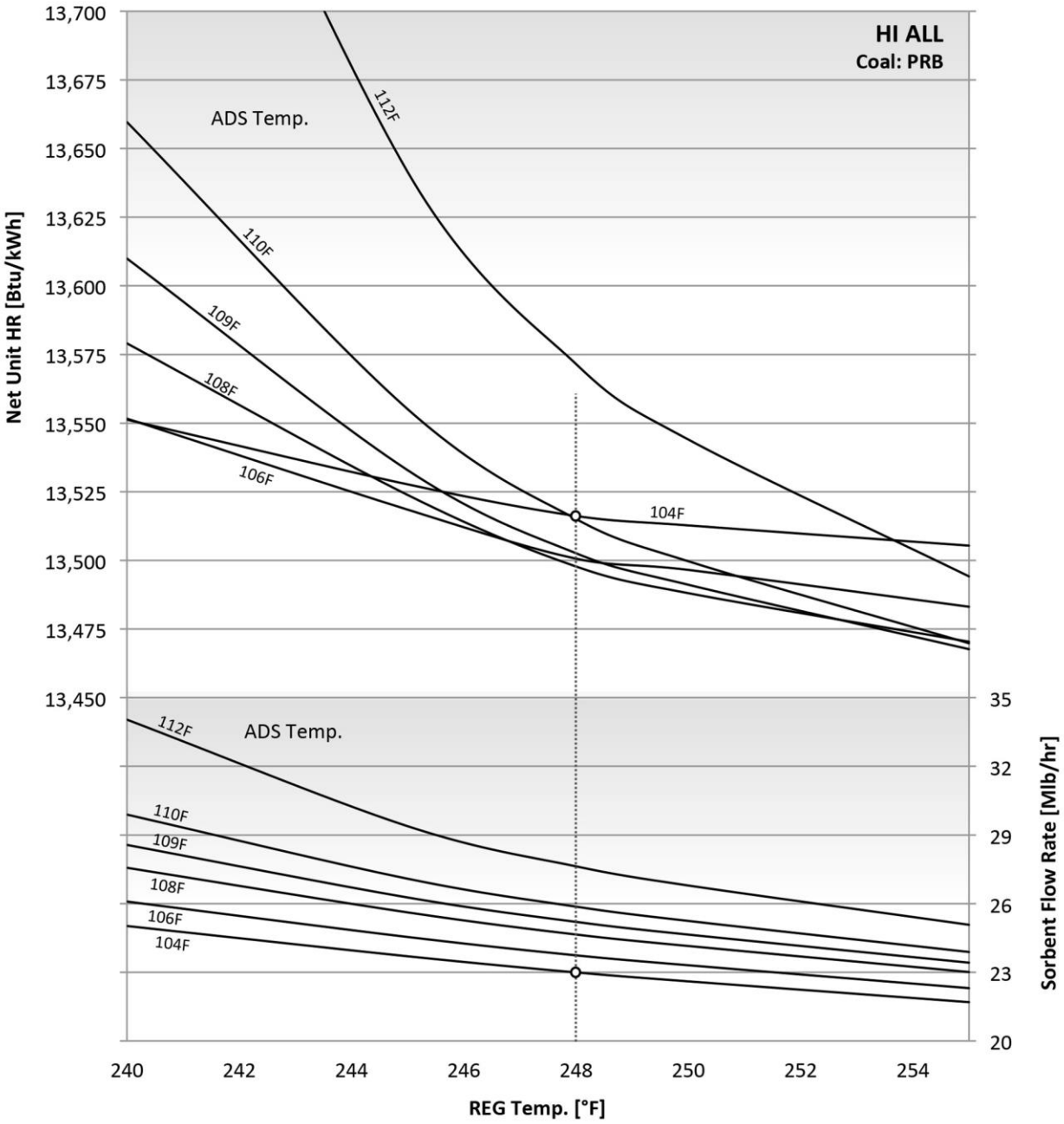

Figure 14.5: Variations in Adsorber and Regenerator Temperature for HI ALL and PRB

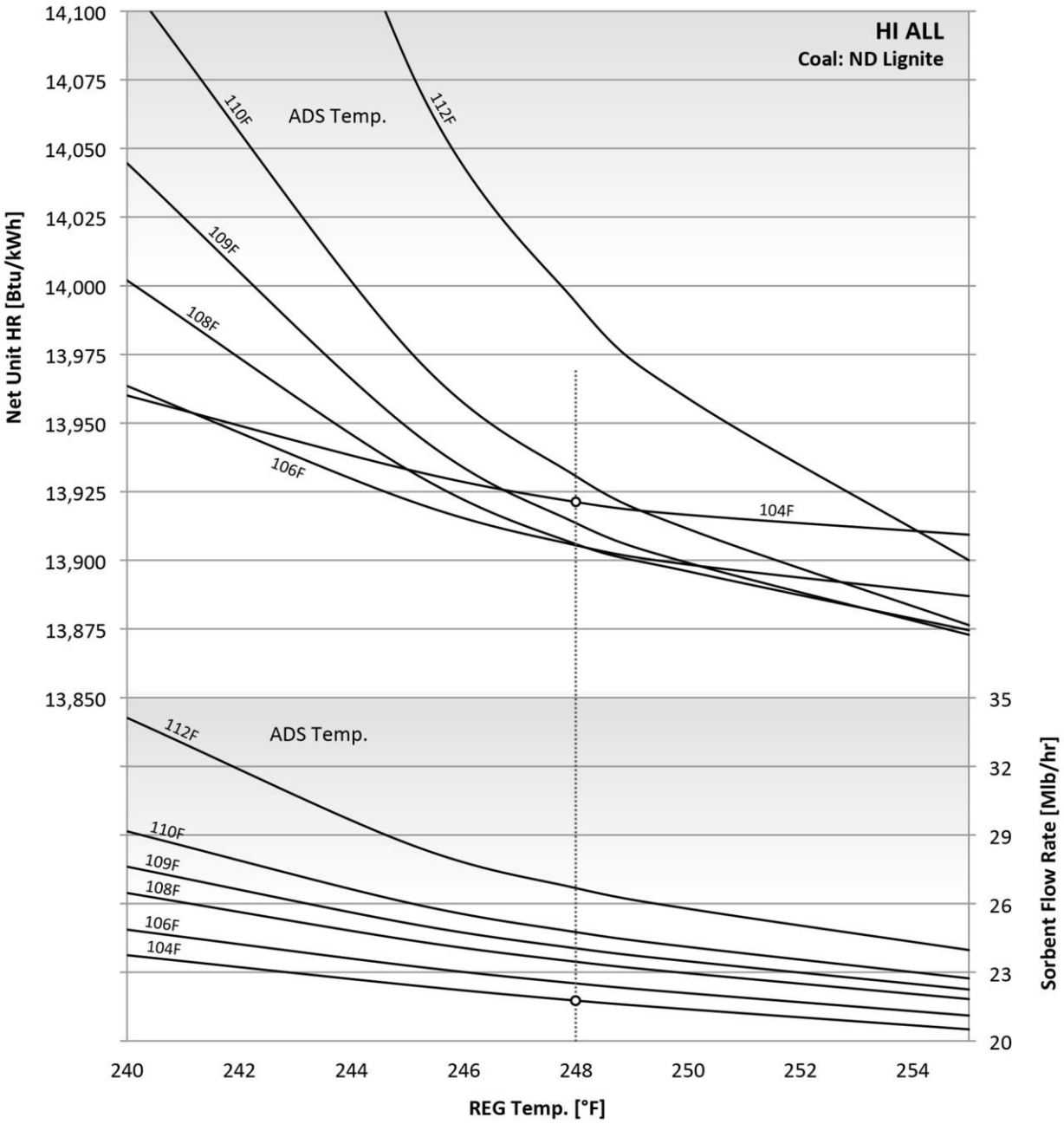

Figure 14.6: Variations in Adsorber and Regenerator Temperature for HI ALL and ND Lignite

Heat Integration and a XHTX: Effects of XHTX Effectiveness

The results above mention the result of adding a XHTX to the case with HI ALL, however, they do not detail the effects of this across a range of XHTX effectiveness values. Figure 14.7 and Table 14.1 present net unit HR for all three coals where HI ALL is in place and the XHTX effectiveness is varied between 0 and 1. These results show that utilizing a XHTX in combination with waste heat integration can result in significant improvements in net unit HR. Note that these results are for the original adsorber and regenerator temperatures of 104°F and 248°F respectively.

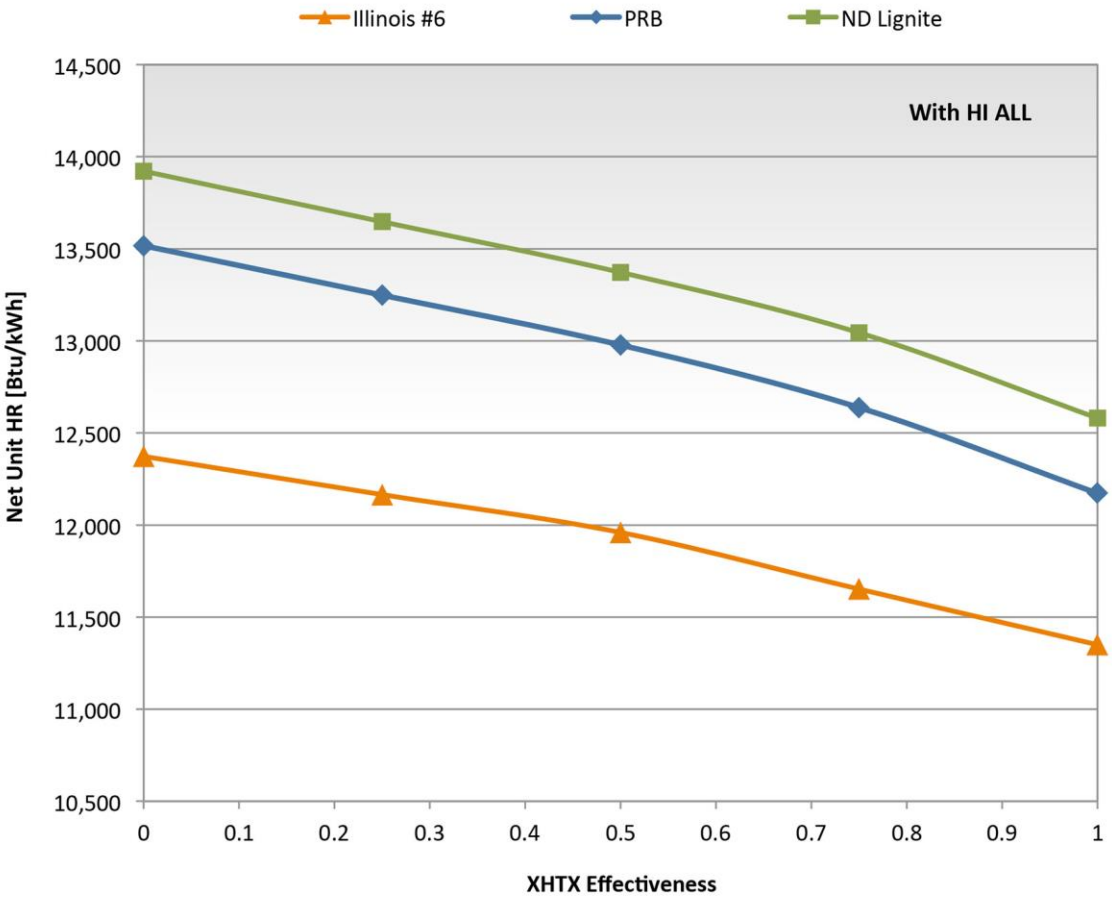

Figure 14.7: Net Unit HR for HI ALL with Varying XHTX Effectiveness

Table 14.1: Net Unit HR for HI ALL with Varying XHTX Effectiveness

	Illinois #6		PRB		ND Lignite	
XHTX Effectiveness	Net Unit HR [Btu/kWh]					
0	12,373	-	13,516	-	13,921	-
0.25	12,165	-1.7%	13,248	-2.0%	13,647	-2.0%
0.5	11,960	-3.3%	12,978	-4.0%	13,372	-3.9%
0.75	11,652	-5.8%	12,638	-6.5%	13,045	-6.3%
1	11,350	-8.3%	12,172	-9.9%	12,581	-9.6%

15.0 ADA Capture System With CO_2 Recycle

It has been suggested [6] that the performance of a sorbent capture system might be improved if the concentration of CO_2 in the flue gas entering the adsorber were increased. At a higher CO_2 partial pressure, the sorbent will be more fully loaded with adsorbed CO_2, which has the potential to reduce the sorbent flow rate and perhaps improve overall system and plant performance. One method for increasing the CO_2 concentration of the gas entering the adsorber is to recycle a portion of the CO_2 being sent through the compression train into the flue gas entering the adsorber. Figure 15.1 illustrates this updated system with CO_2 recycle being extracted from the CO_2 stream downstream of the compression pre-cooler. The moisture content of the CO_2 is significantly reduced downstream of this cooler, which provides a higher purity CO_2 stream for recycling.

The Aspen Plus plant model, for the case without a XHTX, was run at CO_2 recycle rates ranging from 0 to 25 percent. Figure 15.2 and Table 15.1 present these results, which predict that CO_2 recycle would have a negative impact on overall plant performance.

.

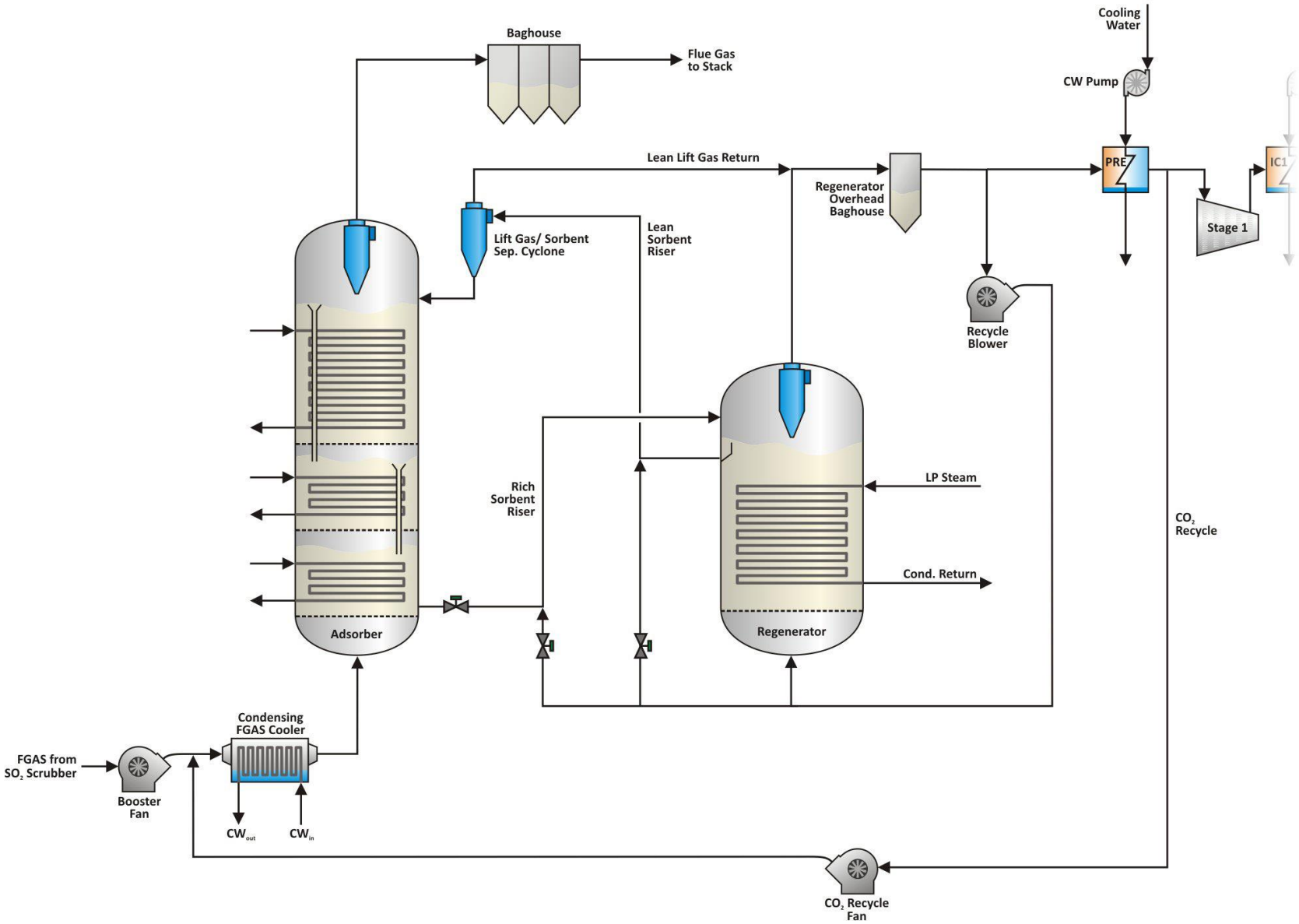

Figure 15.1: ADA Solid Sorbent CO_2 Capture Syste m With CO_2 Recycle

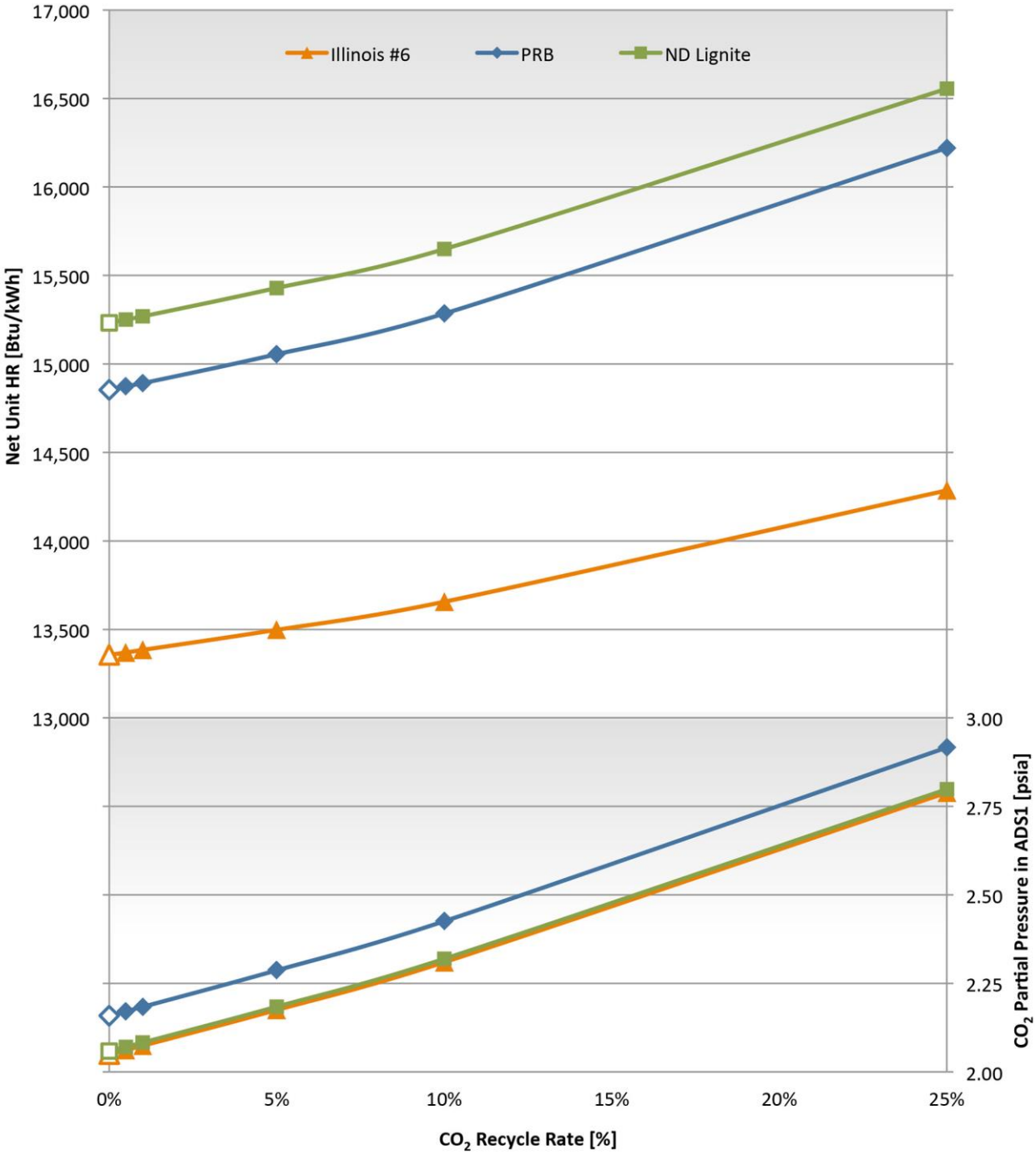

Figure 15.2: Effect of CO_2 Recycle on Net Unit HR and CO_2 Partial Pressure in ADS1

Table 15.1: Effect of CO_2 Recycle on HR, CO_2 Partial Pressure, Sorbent Loading, and Sorbent Flow

	Illinois #6		PRB		ND Lignite	
CO_2 Recycle [%]	Net Unit HR [Btu/kWh]					
0.0%	13,356	-	14,854	-	15,232	-
0.5%	13,369	0.1%	14,874	0.1%	15,251	0.1%
1.0%	13,384	0.2%	14,891	0.3%	15,269	0.2%
5.0%	13,498	1.1%	15,055	1.4%	15,429	1.3%
10.0%	13,656	2.2%	15,284	2.9%	15,649	2.7%
25.0%	14,286	7.0%	16,220	9.2%	16,555	8.7%
CO_2 Recycle [%]	CO_2 Partial Pressure in ADS1 [psia]					
0.0%	2.05	-	2.16	-	2.06	-
0.5%	2.06	0.6%	2.17	0.6%	2.07	0.6%
1.0%	2.07	1.2%	2.18	1.2%	2.08	1.2%
5.0%	2.18	6.1%	2.29	5.9%	2.18	6.1%
10.0%	2.31	13%	2.43	12%	2.32	13%
25.0%	2.79	36%	2.92	35%	2.80	36%
CO_2 Recycle [%]	CO_2 Loading in ADS1 [% of pure Sorbent weight]					
0.0%	9.57	-	9.66	-	9.59	-
0.5%	9.58	0.1%	9.66	0.1%	9.60	0.1%
1.0%	9.59	0.2%	9.67	0.2%	9.61	0.2%
5.0%	9.66	0.9%	9.73	0.8%	9.67	0.9%
10.0%	9.74	1.7%	9.82	1.7%	9.76	1.7%
25.0%	9.99	4.3%	10.1	4.3%	10.01	4.4%
CO_2 Recycle [%]	Sorbent Flow Rate [Mlb/hr]					
0.0%	21.5	-	25.2	-	23.8	-
0.5%	21.6	0.4%	25.4	0.5%	23.9	0.4%
1.0%	21.7	0.8%	25.5	0.9%	24.0	0.9%
5.0%	22.5	4.4%	26.4	4.8%	24.9	4.7%
10.0%	23.5	9.4%	27.8	10.2%	26.2	9.9%
25.0%	27.8	29%	33.3	32%	31.2	31%

Table 15.1 shows that at a recycle rate of 25 percent for the Illinois #6 coal, the predicted net unit HR is increased by over 34 percent. It is thought that the reason for this is that an increase in CO_2 partial pressure does not result in a large enough increase in CO_2 loading to offset the increase in sorbent flow rate required to scrub the additional CO_2. It can be seen in Table 15.1 that, although CO_2 partial pressure in ADS1 increases from 2.1 to 2.8 for the Illinois #6 coal with recycle increased from 0 to 25 percent, the CO_2 loading only increases from 9.6 to 10 weight percent. A 30 percent increase in sorbent flow rate indicates that this increase in loading does not offset the increase in CO_2 flow in the gas entering the adsorber. From these results it is concluded that CO_2 recycle would have an overall harmful effect on plant performance.

A second set of CO_2 recycle analyses were conducted where CO_2 recycle was combined with both HI ALL and a XHTX with an effectiveness of 1.0. Figure 15.3 shows these CO_2 recycle results for cases where ALL HI and a XHTX effectiveness of 1 are assumed.

As seen in Figure 15.2 for the previous CO_2 recycle cases without HI or a XHTX, an increase in CO_2 recycle is shown to still negatively impact unit HR. However, Figure 15.3 shows that increasing CO_2 recycle has a diminished negative effect on unit performance. That being said, it should still be noted that the best performance is always for the case without CO_2 recycle. Therefore, the conclusion can be drawn that, for the sorbent used here, CO_2 recycle of any kind results in a decrease in unit efficiency.

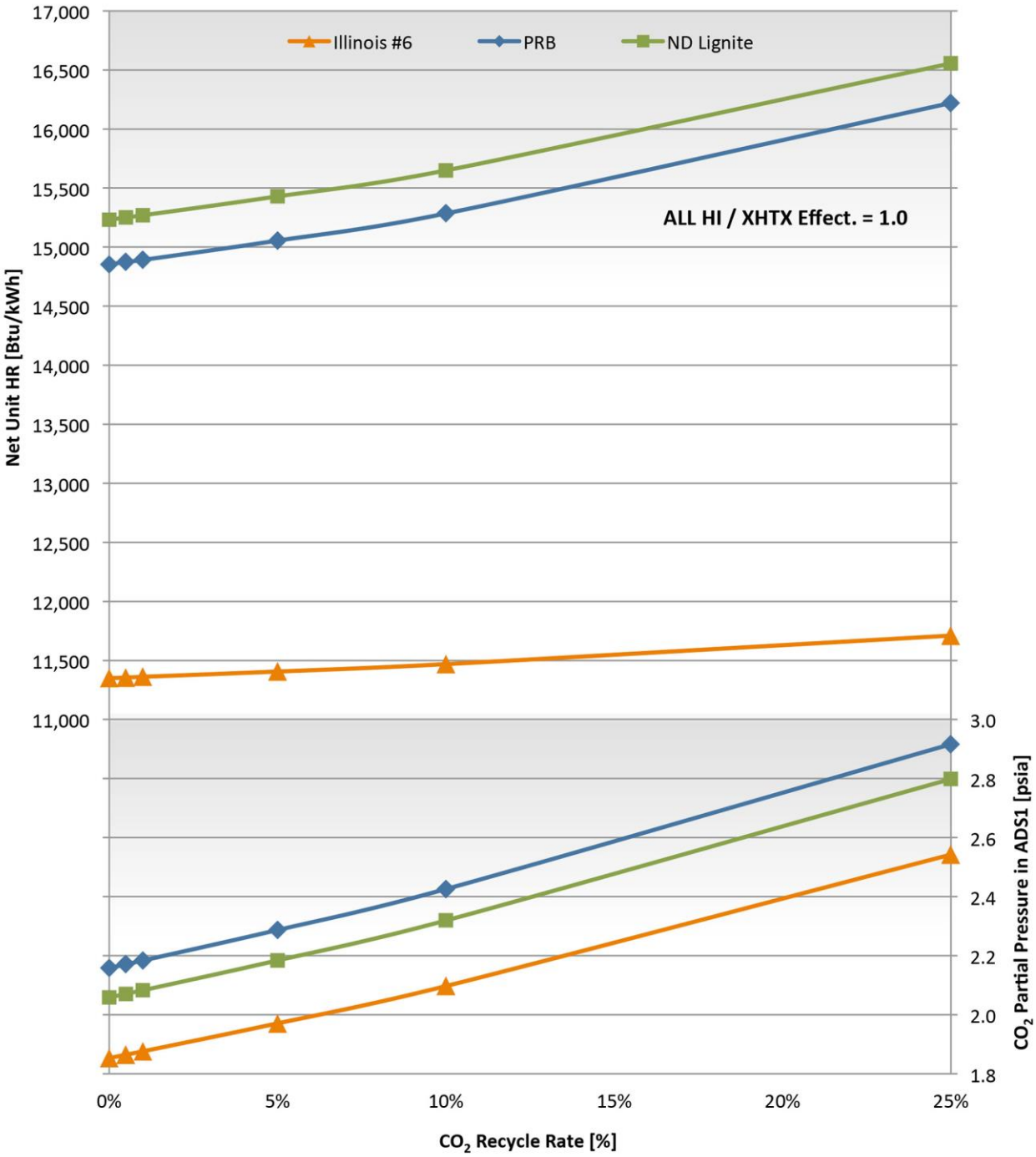

Figure 15.3: Effect of CO_2 Recycle for HI ALL and XHTX Effect. = 1 on Unit HR and CO_2 Partial Pres.

16.0 Conclusions

Analysis and modeling of the ADA Solid Sorbent CO_2 Capture System have resulted in not only a better understanding of how the system operates, but also have suggested changes in design and process conditions, which have the potential to significantly improve the performance of a coal-fired plant equipped with the system. After development and verification of the Aspen Plus model, various operating parameters of the ADA Capture System were varied to determine their optimal values. Plant performance with the addition of a XHTX to cool the lean sorbent and heat the rich sorbent was also examined. Finally the utilization of waste heat from the flue gas cooler and CO_2 compressors was examined. This heat was used to heat the cold, CO_2 rich sorbent stream, the incoming boiler combustion air, and the steam cycle feedwater. Analyses of the modeling results in these three areas leads to the following conclusions for the optimization of the ADA solid sorbent CO_2 capture system:

- Changes in adsorber and regenerator operating temperature were found to result in relatively small changes in net unit HR. In fact, for the Illinois #6 coal, the design adsorber and regenerator temperatures of 104°F and 248°F respectively result in the best unit performance. For the PRB and ND Lignite coals, raising the adsorber temperature to 108°F, decreased net unit HR by around 0.3 percent (See Figure 16.1).

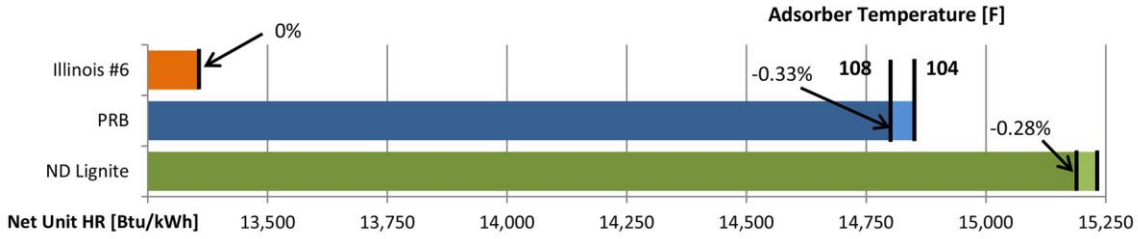

Figure 16.1: Effect of Adsorber Temperature on Net Unit HR Results

- The moisture adsorption characteristics of the sorbent were found to have a dramatic impact on ADA capture system performance. If it was assumed that the sorbent does not adsorb any water, predicted net unit HR was found to decrease by 5.7, 6.9 and 6.6 percent (from the BASE case) (Figure 16.2) for the Illinois #6, PRB, and ND Lignite coals, respectively.

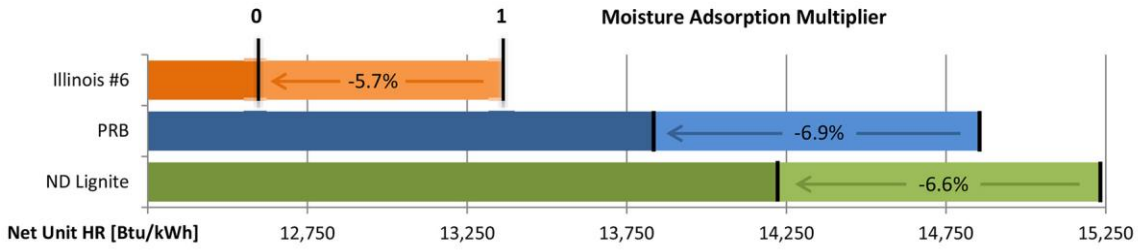

Figure 16.2: Effect of Sorbent Moisture Adsorption on Net Unit HR Results

- The gas-side pressure drop across the adsorber beds has a direct correlation with the power requirement of the booster fan power used to overcome this pressure drop. The booster fan accounts for between 25 to 28 percent of the parasitic power of the ADA system. It was found that a 2 psia reduction in adsorber bed pressure drop results in a 2.3, 3.0, and 3.1 percent drop in net unit HR for the Illinois #6, PRB and ND Lignite coals, respectively (Figure 16.3).

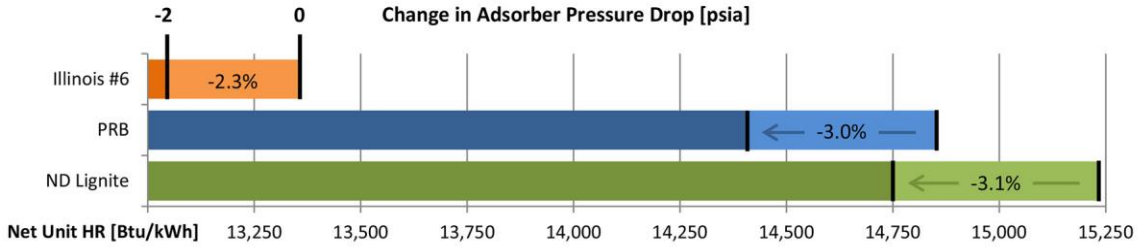

Figure 16.3: Effect of Change in Adsorber Pressure Drop on Net Unit HR Results

- CO_2 compressor discharge pressure depends on the requirements for CO_2 sequestration. A lower CO_2 pressure results in a lower overall compression ratio for the compression train, resulting in lower compressor power. If CO_2 discharge pressure were reduced from 2,215 psia to 1,215 psia, the predicted net unit HR was found to decrease by 1.6, 2.0, and 1.9 percent for the Illinois #6, PRB, and ND Lignite coals, respectively (Figure 16.4).

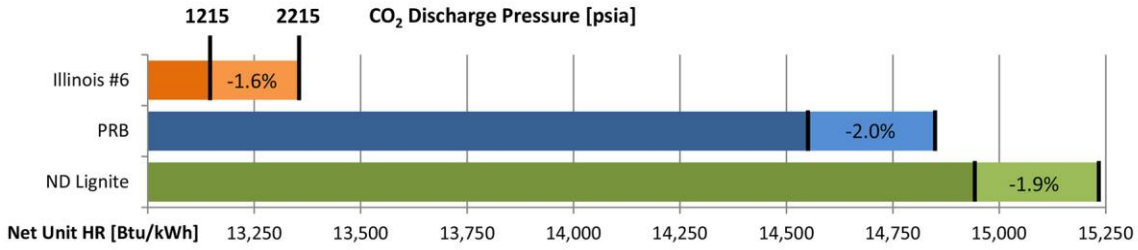

Figure 16.4: Effect of CO_2 Discharge Pressure on Net Unit HR Results

- A cross heat exchanger was found to be quite beneficial in improving the performance of the ADA capture system. Heat exchanger effectiveness values between 0 and 1 were considered. When an idealized effectiveness of 1.0 was assumed, the addition of a XHTX was found to decrease net unit HR by 12.0, 14.4 and 14.0 percent for the Illinois #6, PRB, and ND Lignite coals, respectively (Figure 16.5).

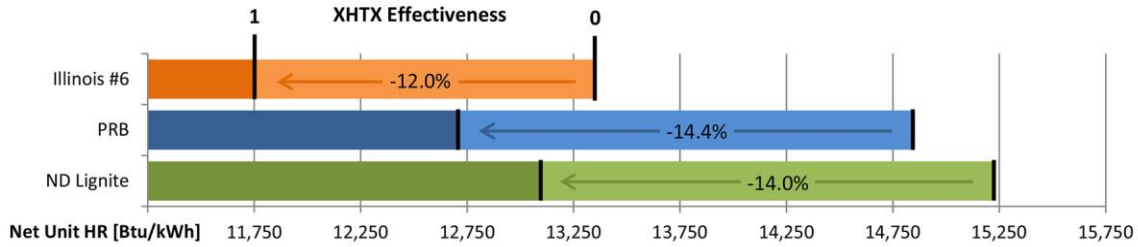

Figure 16.5: Effect of XHTX on Net Unit HR Results

- Waste heat from both the CO_2 compressors and the flue gas cooler was found to be capable of heating boiler combustion air, the CO_2 rich sorbent, and boiler feedwater. Individual heat integration cases were considered (heat from a single source being used in a single sink) along with cases where multiple heat integration cases were implemented simultaneously. The best performing case was HI ALL, where all four individual heat integration cases were modeled at the same time. For this case, net unit HR was found to decrease by 7.4, 9.0, and 8.6 percent for the Illinois #6, PRB, and ND Lignite coals, respectively (Figure 16.6).

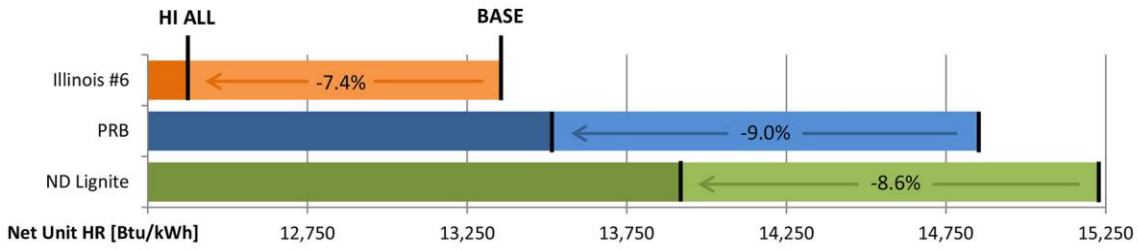

Figure 16.6: Effect of HI ALL on Net Unit HR

- Increasing the CO_2 concentration entering the adsorber was not found to be beneficial for the ADA capture system. For the cases and coals examined, an increase in CO_2 concentration (accomplished through CO_2 recycle) always resulted in a predicted increase in net unit HR.

- It was found that changes in the operating conditions of the ADA CO_2 capture system, the addition of a XHTX, and heat integration can all have a positive impact on net unit HR. To demonstrate the maximum possible benefit from implementing all of these improvements, cases with ideal adsorber and regenerator temperatures, zero water adsorption, a XHTX (with an effectiveness of 1), and HI ALL were modeled. Net unit HR was found to decrease by 16.6, 20.2, and 19.3 percent for the Illinois #6, PRB, and ND Lignite coals, respectively (Figure 16.7).

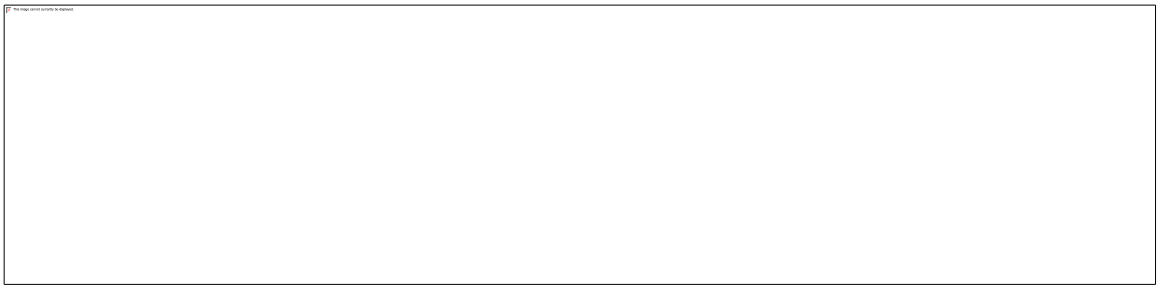

Figure 16.7: Effect of HI ALL, 0 Moist. Adsorption, a XTHX and Ideal ADS Temps. on Net Unit HR

- Net unit HR improvements approaching 20 percent are predicted for a PC plant equipped with the ADA CO_2 capture system. These improvements were due to changes in the operating conditions of the system, the addition of a XHTX, and waste heat integration.

Areas, which should be investigated for additional improvements in net unit HR include:

1. Develop sorbents with improved CO_2 and H_2O capture properties
2. Redesign CO_2 adsorber vessel and associated flue gas cleanup equipment to reduce flue gas pressure drop and booster fan power.

References

[1] Energy Research Center, “Investigation on Flue Gas & Condensing Heat Exchanger (CHX) Cooling Water Cooling Processes and CHX Design.” Prepared for ADA-ES, Inc. September 2014.

[2] Walsh, M. “Wet FGD Types and Fundamentals.” Marsulex Environmental Technologies. 2008.

[3] Sargent & Lundy LLC. “Wet Flue Gas Desulfurization Technology Evaluation.” Prepared for the National Lime Association. January 2003.

[4] Krutka, H., Starns, T., Richard, M., Thitakamal, B. “Evaluation of Solid Sorbents as a Retrofit Technology for CO_2 Capture: Preliminary Techno-Economic Assessment of Solid Sorbents for Post-Combustion CO_2 Capture.” ADA-ES, Inc. 2011.

[5] Charles, J. “An Examination of Heat Rate Improvements Due to Waste Heat Integration in an Oxycombustion Pulverized Coal Power Plant.” M.S. thesis, Lehigh University, Bethlehem, PA. 2011.

[6] Berger, A., Bhown, A. “Selection of Optimal Solid Sorbents for CO_2 Capture Based on Gas Phase CO_2 Composition.” International Conference on Greenhouse Gas Technologies (GHGT-12), October 5-9, 2014, Austin, TX. EPRI, Palo Alto, CA.

[7] NETL/DOE. “Pulverized Coal Oxycombustion Power Plants.” Vol. 1: Bituminous Coal to Electric. 2008.

Appendix

Table A.1: Mass & Energy Balance of Excel Adsorber Model (Initial Verification Case)

ADSORBER	Inlet Streams								Outlet Streams				
Stream	**2**	**13**	**14**	**16**	**18**	**20**	**21**	**22**	**4**	**12**	**15**	**17**	**19**
T [°F]	104	248	65	65	65	104	104	104	104	104	99	99	99
P [psia]	20.6	15.9	50.0	50.0	50.0	20.0	18.8	16.9	15.7	20.4	30.0	30.0	30.0
MIXED	[lbmol/hr]								[lbmol/hr]				
AR	1,433	0	0	0	0	0	0	0	1,421	12	0	0	0
CO_2	23,557	0	0	0	0	0	0	0	2,356	170	0	0	0
H_2O	8,071	0	1,131,827	435,048	120,780	0	0	0	8,005	66	1,131,827	435,048	120,780
N_2	119,004	0	0	0	0	0	0	0	118,024	980	0	0	0
O_2	4,247	0	0	0	0	0	0	0	4,212	35	0	0	0
SO_2	0	0	0	0	0	0	0	0	0	0	0	0	0
	[mol-frac]								[mol-frac]				
AR	0.0092	0.0000	0.0000	0.0000	0.0000	0.0000	0.0000	0.0000	0.0106	0.0093	0.0000	0.0000	0.0000
CO_2	0.1507	0.0000	0.0000	0.0000	0.0000	0.0000	0.0000	0.0000	0.0176	0.1346	0.0000	0.0000	0.0000
H_2O	0.0516	0.0000	1.0000	1.0000	1.0000	0.0000	0.0000	0.0000	0.0597	0.0526	1.0000	1.0000	1.0000
N_2	0.7613	0.0000	0.0000	0.0000	0.0000	0.0000	0.0000	0.0000	0.8807	0.7758	0.0000	0.0000	0.0000
O_2	0.0272	0.0000	0.0000	0.0000	0.0000	0.0000	0.0000	0.0000	0.0314	0.0277	0.0000	0.0000	0.0000
SO_2	0.0000	0.0000	0.0000	0.0000	0.0000	0.0000	0.0000	0.0000	0.0000	0.0000	0.0000	0.0000	0.0000
	[lb/hr]								[lb/hr]				
AR	57,245	0	0	0	0	0	0	0	56,774	471	0	0	0
CO_2	1,036,739	0	0	0	0	0	0	0	103,674	7,482	0	0	0
H_2O	145,401	0	20,390,162	7,837,500	2,175,883	0	0	0	144,204	1,197	20,390,162	7,837,500	2,175,883
N_2	3,333,716	0	0	0	0	0	0	0	3,306,263	27,453	0	0	0
O_2	135,899	0	0	0	0	0	0	0	134,780	1,119	0	0	0
SO_2	0	0	0	0	0	0	0	0	0	0	0	0	0
$\dot{m}_{MIXED}$	4,709,001	0	20,390,162	7,837,500	2,175,883				3,745,695	37,723	20,390,162	7,837,500	2,175,883
h (77°F) [Btu/lb]	167.03		45.10	45.10	45.10				151.07	165.22	45.10	45.10	45.10
h (T) [Btu/lb]	186.59		33.24	33.24	33.24				177.65	185.59	67.16	67.16	67.16
SOLIDS	[lb/hr]								[lb/hr]				
SORBENT	0	13,031,199	0	0	0	0	0	0	0	13,031,199	0	0	0
ADS CO2	0	479,965	0	0	0	125,779	453,053	346,732	0	1,405,528	0	0	0
ADS H2O	0	0	0	0	0	0	0	0	0	0	0	0	0
Mass Balance													
Total Mass Flow [lb/hr]*	4,709,001	13,511,164							3,745,695	14,474,450			
Sum in/out [lb/hr]	18,220,165								18,220,144				
Results [%]	0.0001												
Energy Balance													
Q [Btu/hr]*	92,071,886	577,564,609	-241,810,865	-92,946,424	-25,804,216	73,832,055	265,942,058	203,531,470	99,557,609	97,418,122	449,761,733	172,877,861	47,995,151
Sum in/out [Btu/hr]	852,380,571								867,610,476				
Results [%]	-1.7867												

*Calculated Using Mass or Energy Balance Equations

Table A.2: Mass & Energy Balance of Excel Stripper Model (Initial Verification Case)

STRIPPER	Inlet Streams			Outlet Streams			
Stream	**7**	**23**	**24**	**9**	**11**	**25**	**26**
T [°F]	279	104	400	248	248	274	248
P [psia]	18.0	18.0	45.0	15.9	15.9	45.0	15.9
MIXED	[lbmol/hr]			[lbmol/hr]			
AR	11	17	0	28	0	0	0
CO_2	14,139	170	0	35,341	0	0	0
H_2O	44	66	59,539	111	0	59,539	0
N_2	647	971	0	1,618	0	0	0
O_2	26	40	0	66	0	0	0
SO_2	0	0	0	0	0	0	0
	[mol-frac]			[mol-frac]			
AR	0.0007	0.0132	0.0000	0.0007	0.0000	0.0000	0.0000
CO_2	0.9510	0.1346	0.0000	0.9510	0.0000	0.0000	0.0000
H_2O	0.0030	0.0523	1.0000	0.0030	0.0000	1.0000	0.0000
N_2	0.0435	0.7686	0.0000	0.0435	0.0000	0.0000	0.0000
O_2	0.0018	0.0313	0.0000	0.0018	0.0000	0.0000	0.0000
SO_2	0.0000	0.0000	0.0000	0.0000	0.0000	0.0000	0.0000
	[lb/hr]			[lb/hr]			
AR	444	666	0	1,110	0	0	0
CO_2	622,255	7,482	0	1,555,335	0	0	0
H_2O	793	1,189	1,072,613	1,996	0	1,072,613	0
N_2	18,138	27,194	0	45,321	0	0	0
O_2	845	1,266	0	2,110	0	0	0
SO_2	0	0	0	0	0	0	0
$\dot{m}_{MIXED}$	642,474	37,797	1,072,613	1,605,872	0	1,072,613	
h (77°F) [Btu/lb]	216.08	164.78	45.10	216.09		45.10	
h (T) [Btu/lb]	259.81	184.98	1236.65	252.84		243.65	
SOLIDS	[lb/hr]			[lb/hr]			
SORBENT	0	13,031,199	0	0	13,031,199	0	0
ADS CO2	0	1,405,528	0	0	479,965	0	925,563
ADS H2O	0	0	0	0	0	0	0
Mass Balance							
Total Mass Flow [lb/hr]*	642,474	14,474,524	1,072,613	1,605,872	13,511,164	1,072,613	
Sum in/out [lb/hr]	16,189,612			16,189,649			
Results [%]	-0.0002						
Energy Balance							
Q [Btu/hr]*	28,097,745	98,757,896	1,278,073,584	59,028,638	577,333,258	212,967,137	543,305,481
Sum in/out [Btu/hr]	1,404,929,224			1,392,634,514			
Results [%]	0.8751						

*Calculated Using Mass or Energy Balance Equations

Table A.3: Mass & Energy Balance of Aspen Plus Adsorber Model (Initial Verification Case)

ADSORBER	Inlet Streams								Outlet Streams				
Stream	**2**	**13**	**14**	**16**	**18**	**20**	**21**	**22**	**4**	**12**	**15**	**17**	**19**
Aspen Stream Name	**FGAS9**	**LEAN4**	**ADS3-CW1**	**ADS2-CW1**	**ADS1-CW1**	**ADS1CO22**	**ADS2CO22**	**ADS3CO22**	**ADS3-1**	**RICH1**	**ADS3-CW3**	**ADS2-CW3**	**ADS1-CW3**
T [°F]	104	248	65	65	65	104	104	104	104	104	99	99	99
P [psia]	20.6	15.9	50.0	50.0	50.0	20.4	18.2	16.4	15.7	19.5	30.0	30.0	30.0
MIXED	[lbmol/hr]								[lbmol/hr]				
AR	0	0	0	0	0	0	0	0	0	0	0	0	0
CO_2	31,459	0	0	0	0	0	0	0	3,146	223	0	0	0
H_2O	13,832	0	1,433,910	586,607	171,101	0	0	0	13,718	114	1,433,910	586,607	171,101
N_2	196,136	0	0	0	0	0	0	0	194,521	1,615	0	0	0
O_2	14,756	0	0	0	0	0	0	0	14,635	122	0	0	0
SO_2	5	0	0	0	0	0	0	0	5	0	0	0	0
	[mol-frac]								[mol-frac]				
AR	0.0000	0.0000	0.0000	0.0000	0.0000	0.0000	0.0000	0.0000	0.0000	0.0000	0.0000	0.0000	0.0000
CO_2	0.1228	0.0000	0.0000	0.0000	0.0000	0.0000	0.0000	0.0000	0.0139	0.1075	0.0000	0.0000	0.0000
H_2O	0.0540	0.0000	1.0000	1.0000	1.0000	0.0000	0.0000	0.0000	0.0607	0.0549	1.0000	1.0000	1.0000
N_2	0.7654	0.0000	0.0000	0.0000	0.0000	0.0000	0.0000	0.0000	0.8604	0.7787	0.0000	0.0000	0.0000
O_2	0.0576	0.0000	0.0000	0.0000	0.0000	0.0000	0.0000	0.0000	0.0647	0.0586	0.0000	0.0000	0.0000
SO_2	0.0000	0.0000	0.0000	0.0000	0.0000	0.0000	0.0000	0.0000	0.0000	0.0000	0.0000	0.0000	0.0000
	[lb/hr]								[lb/hr]				
AR	0	0	0	0	0	0	0	0	0	0	0	0	0
CO_2	1,384,500	0	0	0	0	0	0	0	138,453	9,817	0	0	0
H_2O	249,184	0	25,832,300	10,567,900	3,082,430	0	0	0	247,132	2,052	25,832,300	10,567,900	3,082,430
N_2	5,494,440	0	0	0	0	0	0	0	5,449,200	45,247	0	0	0
O_2	472,189	0	0	0	0	0	0	0	468,300	3,888	0	0	0
SO_2	342	0	0	0	0	0	0	0	339	3	0	0	0
$\dot{m}_{MIXED}$	7,600,655	0	25,832,300	10,567,900	3,082,430				6,303,424	61,007	25,832,300	10,567,900	3,082,430
h (77°F) [Btu/lb]	179.00		45.10	45.10	45.10				171.41	177.99	45.10	45.10	45.10
h (T) [Btu/lb]	185.55		33.26	33.26	33.26				178.25	184.60	67.14	67.17	67.18
SOLIDS	[lb/hr]								[lb/hr]				
SORBENT	0	16,660,600	0	0	0	0	0	0	0	16660600	0	0	0
ADS CO2	0	580,174	0	0	0	192,365	610,444	433,418	0	1,816,400	0	0	0
ADS H2O	0	0	0	0	0	0	0	0	0	0	0	0	0
Mass Balance													
Total Mass Flow [lb/hr]*	7,600,655	17,240,774							6,303,424	18,538,007			
Sum in/out [lb/hr]	24,841,429								24,841,431				
Results [%]	0.0000												
Energy Balance													
Q [Btu/hr]*	49,777,545	737,155,129	-305,883,381	-125,135,779	-36,499,426	112,918,255	358,330,628	254,416,366	43,111,094	124,087,571	569,470,128	233,245,233	68,058,067
Sum in/out [Btu/hr]	1,045,079,338								1,037,972,093				
Results [%]	0.6801												

*Calculated Using Mass or Energy Balance Equations

Table A.4: Mass & Energy Balance of Aspen Plus Stripper Model (Initial Verification Case)

STRIPPER	Inlet Streams			Outlet Streams			
Stream	**7**	**23**	**24**	**9**	**11**	**25**	**26**
Aspen Stream Name	**RECYCLE3**	**RICH3**	**REG-EXT2**	**GAS-2**	**LEAN1**	**COND**	**CO2-1**
T [°F]	279	104	400	241	248	274	248
P [psia]	18.0	18.0	45.0	15.9	15.9	45.0	15.9
MIXED		[lbmol/hr]			[lbmol/hr]		
AR	0	0	0	0	0	0	0
CO_2	17,862	1,205	0	47,157	0	0	0
H_2O	72	118	77,144	190	0	77,144	0
N_2	1,019	1,671	0	2,690	0	0	0
O_2	77	126	0	202	0	0	0
SO_2	0	0	0	0	0	0	0
		[mol-frac]			[mol-frac]		
AR	0.0000	0.0000	0.0000	0.0000	0.0000	0.0000	0.0000
CO_2	0.9386	0.3862	0.0000	0.9386	0.0000	0.0000	0.0000
H_2O	0.0038	0.0378	1.0000	0.0038	0.0000	1.0000	0.0000
N_2	0.0535	0.5356	0.0000	0.0535	0.0000	0.0000	0.0000
O_2	0.0040	0.0403	0.0000	0.0040	0.0000	0.0000	0.0000
SO_2	0.0000	0.0000	0.0000	0.0000	0.0000	0.0000	0.0000
		[lb/hr]			[lb/hr]		
AR	0	0	0	0	0	0	0
CO_2	786,092	53,039	0	2,075,360	0	0	0
H_2O	1,295	2,123	1,389,780	3,418	0	1,389,780	0
N_2	28,546	46,816	0	75,362	0	0	0
O_2	2,453	4,023	0	6,477	0	0	0
SO_2	2	3	0	5	0	0	0
$\dot{m}_{MIXED}$	818,388	106,005	1,389,780	2,160,621	0	1,389,780	
h (77°F) [Btu/lb]	215.75	190.43	45.10	215.75		45.10	
h (T) [Btu/lb]	259.56	200.28	1236.46	250.92		243.65	
SOLIDS		[lb/hr]			[lb/hr]		
SORBENT	0	16,660,600	0	0	16,660,600	0	0
ADS CO2	0	1,816,400	0	0	580,174	0	1,236,230
ADS H2O	0	0	0	0	0	0	0
Mass Balance							
Total Mass Flow [lb/hr]*	818,388	18,583,005	1,389,780	2,160,621	17,240,774	1,389,780	
Sum in/out [lb/hr]	20,791,172			20,791,175			
Results [%]	0.0000						
Energy Balance							
Q [Btu/hr]*	35,854,146	126,449,446	1,655,735,810	75,977,533	736,859,852	275,940,593	725,667,010
Sum in/out [Btu/hr]	1,818,039,401			1,814,444,988			
Results [%]	0.1977						

*Calculated Using Mass or Energy Balance Equations

Investigation on Flue Gas & Condensing Heat Exchanger (CHX) Cooling Water Cooling Processes and CHX Design

LEHIGH UNIVERSITY

Investigation on Flue Gas & Condensing Heat Exchanger(CHX) Cooling Water Cooling Processes and CHX Design

Energy Research Center

Prepared for:

ADA-ES, Inc.

Prepared by:

Energy Research Center
Lehigh University
177 ATLSS Dr
Bethlehem, PA 18015

9/12/2014

Executive Summary

The ADA CO_2 capture system is designed to adsorb CO_2 at a flue gas inlet temperature of 104°F. In order to overcome the pressure drop of the flue gas passing through the CO_2 adsorber, the flue gas leaving the wet FGD must be compressed to higher pressure and temperature; which ADA estimated to be 21.7 psia and 219°F. ADA assumed the flue gas would then be cooled down from 219°F to 104°F.

The ERC conducted an investigation on the impacts of changes in flue gas flow rate, inlet and outlet flue gas temperatures of the flue gas cooling system, and the possible use of a refrigeration system to reduce the cooling water temperature entering the CHX on power and capital costs of the flue gas cooling system. The calculation results show the flue gas flow rate will significantly affect the power needed by the flue gas cooling system. When the flue gas mass flow rate increases from 7,343,850 lb/hr to 10,634,586 lb/hr with a fixed exit gas temperature, the total power needed by the flue gas cooling system with refrigeration increases by 2 to 3 times. In contrast, the installed capital cost of the CHX is relatively insensitive to flue gas flow rate for fixed exit gas temperature as shown in Table 1E and Table 2E.

Table E1. Total Power Needed of Flue Gas Cooling System with Refrigeration System

Total Power of Flue Gas Cooling System with Refrigeration System (MW)					
$T, P_{FGAS,in}$ / $T_{FGAS,out}$.°F / $\dot{m}_{FGAS}$	219°F, 21.7psia				
	100	104	110	120	130
10,634,586 ln/hr	31.41	28.16	23.16	17.91	12.04
9,561,430 lb/hr	23.53	21.42	19.29	12.82	8.95
8,452,640 lb/hr	16.32	16.47	13.54	9.58	7.07
7,343,850 lb/hr	11.02	10.14	8.44	6.38	7.56

Table E2. Installed Capital Costs of CHX

Installed Capital Costs of CHX (Million $)					
$T, P_{FGAS,in}$ / $T_{FGAS,out}$.°F / $\dot{m}_{FGAS}$	219°F, 21.7psia				
	100	104	110	120	130
10,634,586 ln/hr	16.68	14.82	12.98	9.27	7.42
9,561,430 lb/hr	14.82	12.98	11.12	9.27	7.42
8,452,640 lb/hr	14.84	12.98	11.12	9.27	7.43
7,343,850 lb/hr	14.84	12.99	11.12	9.29	5.56

These results indicate the design of flue gas cooling system is primarily determined by flue gas inlet and outlet temperatures and pressures. The same design of the flue gas cooling system can be used for different flue gas flow rates.

The flue gas flow rate is determined by power plant net power and coal type. A flue gas mass flow rate of 10,634,586 lb/hr, calculated for a unit burning PRB coal with a 550MW net power, was chosen to investigate the effect of different inlet and outlet flue gas temperatures and pressures.

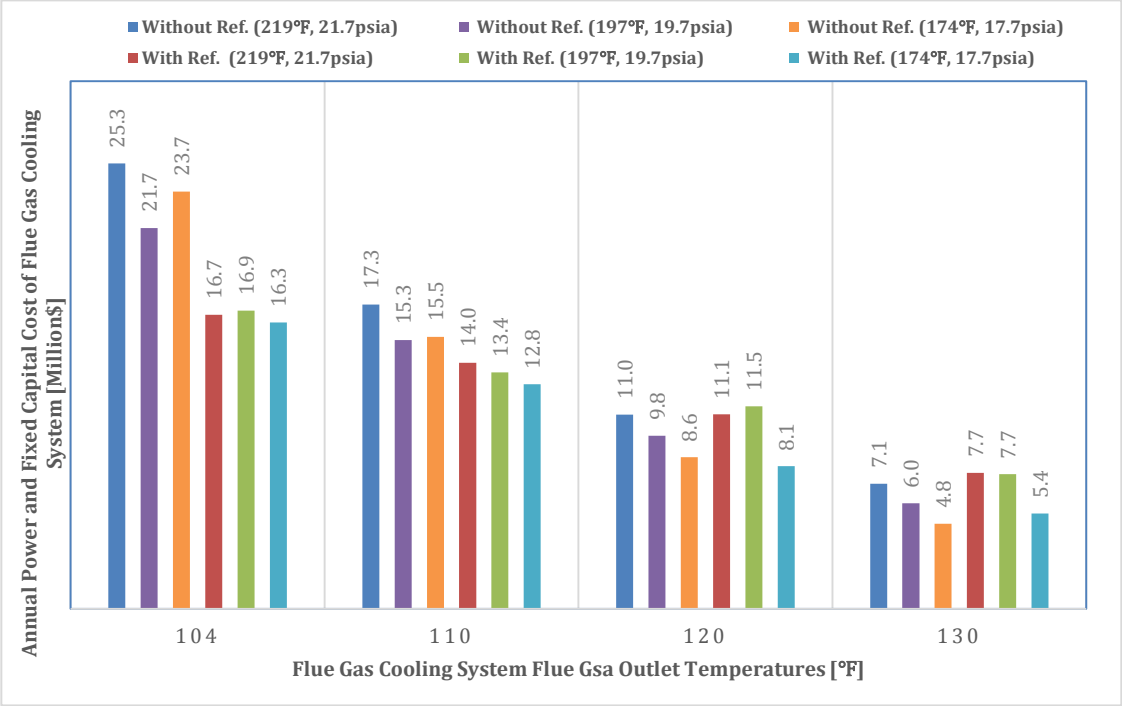

Figure E1. Annual Power and Fixed Costs of Flue Gas Cooling System

Figure E1 shows the annual power and fixed capital costs are relatively insensitive to the flue gas temperature and pressure at the inlet to the flue gas cooling system.

When a flue gas outlet temperature is lower than ~110°F, the flue gas cooling system with a refrigeration system has lower power and capital costs than the system without refrigeration. For a flue gas outlet temperature higher than ~115°F, the flue gas cooling system with refrigeration system costs slightly more in power and capital costs than a system without refrigeration.

1. Flue Gas and CHX Cooling Water Cooling Processes

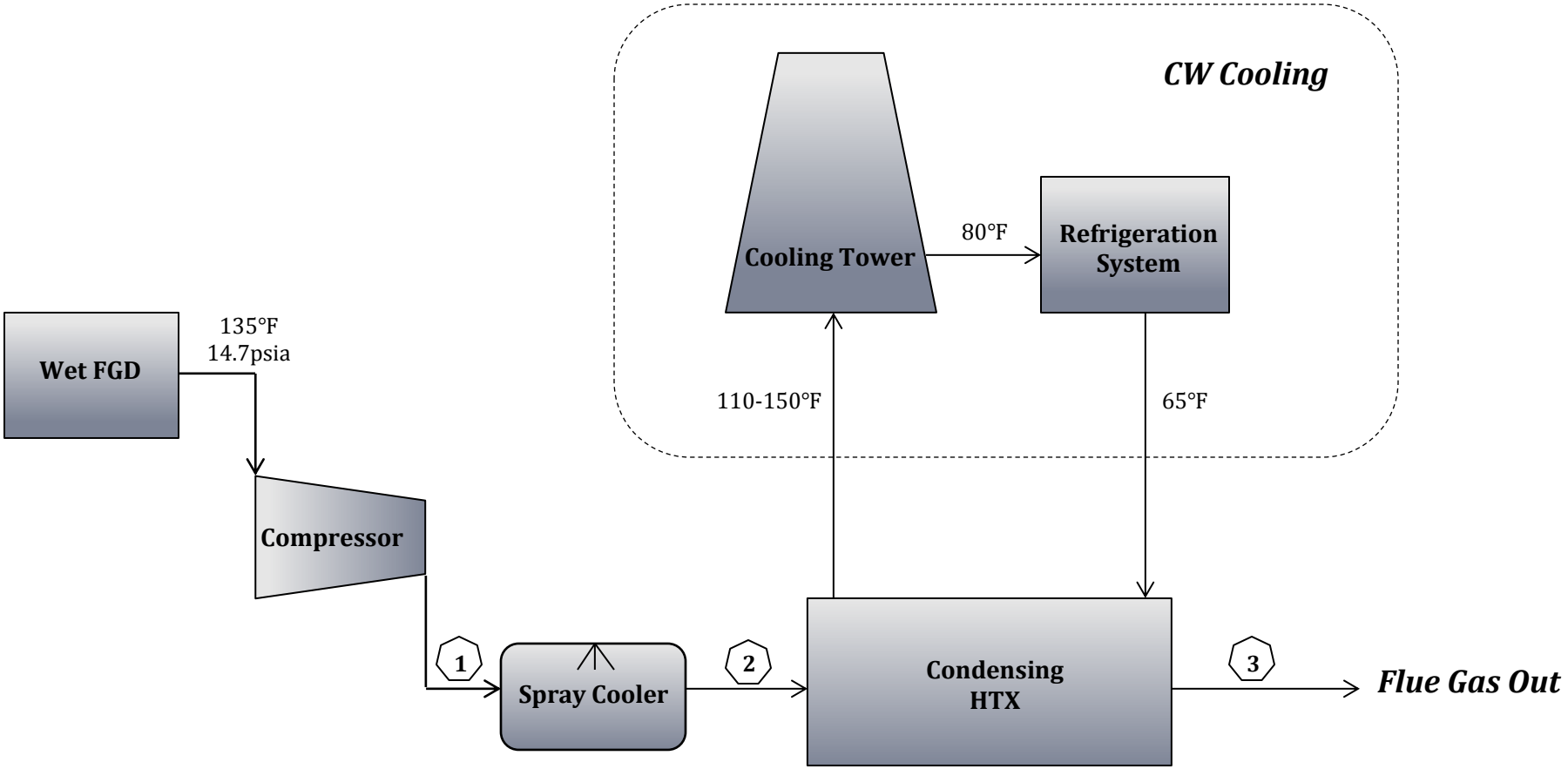

Figure 1. Flue Gas and Cooling Water Cooling Processes

1-1 Flue Gas Cooling Process

To cool down the high temperature and pressure flue gas from 219℉ to 104℉, the ERC has developed the flue gas cooling system model shown in Figure 1 which consists of a spray cooler, condensing heat exchanger (CHX) and CHX cooling water cooling system.

Previous study done by the ERC shows that the CHX tube surface area and power consumption will decrease with flue gas going through spray cooler before it enters the CHX. Introducing a spray cooler will not only decrease the CHX inlet flue gas temperature but also make it possible to avoid using corrosion resistant alloy tube which is relatively expensive compared to stainless steel tube. Therefore, the spray cooler was used to cool the flue gas down in this investigation.

Figure 1 shows the flue gas leaves the wet FGD at 135℉, 14.7 psia then leaves the flue gas compressor at 219℉, 21.7 psia. The high temperature and pressure flue gas is then cooled down to 104℉ by using the spray cooler and condensing heat eachanger in sequence.

Figure 2 shows moisture content vs. flue gas temperature in the flue gas cooling process for the case with spray cooler and without spray cooler called base case. The moisture content of flue gas in cooling process has to be lower than the moisture content in saturated vapor partial pressure of flue gas which is the black curve in Figure 2.

The three state points (1, 2 & 3) marked in Figure 1 and Figure 2 represent the flue gas leaving the compressor, spray cooler and CHX representatively. The conditions of flue gas in these positions will be changed to optimize the CHX design.

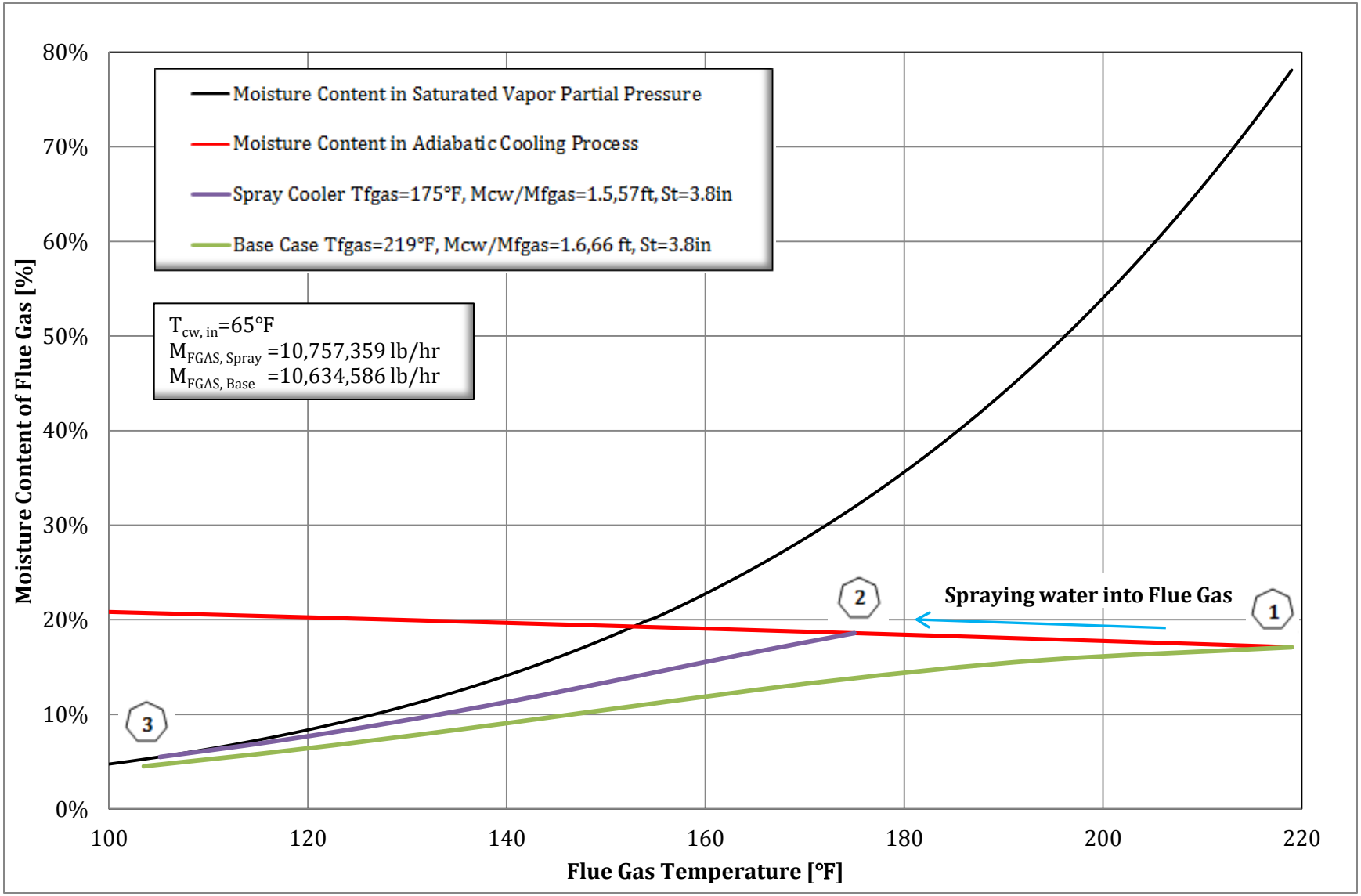

Figure 2. Moisture Content vs. Flue Gas Temperature in Flue Gas Cooling Process

1-2 Cooling Water Cooling Process

The cooling water loop consists of cooling tower and a vapor compression refrigeration system. The cooling tower cools the cooling water that is leaving the CHX from the temperature of 110-150°F down to 80°F and subsequently the cooling water leaves the refrigeration system at 65°F.

ASPEN Plus [1] was used to calculate compressor power of refrigeration cycle. The compressor efficiency was assumed to be 0.8. Assume ambient air temperature is 70°F.

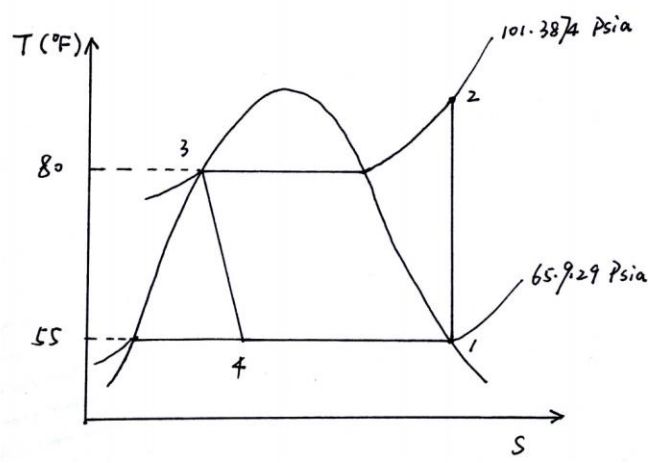

Figure 3. T-S diagram of R134a for the temperature of cooling water out of evaporator is 65°F

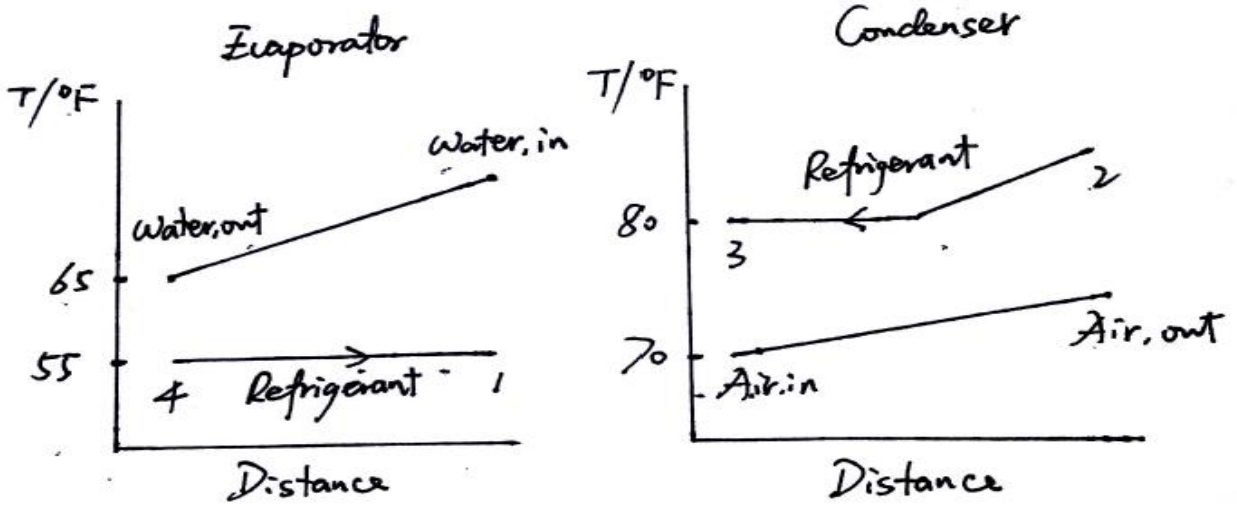

Figure 4. Temperature vs. Distance in Evaporator and Condenser of Refrigeration System

2. CHX Design and Results Analysis

To investigate the impact of different flue gas flow rates and different CHX inlet and outlet temperatures with corresponding pressures on CHX tube surface area and power needed, a series of CHX design cases were conducted. Four different flue gas mass flow rates, 10634586 lb/hr, 9561430 lb/hr, 8452640lb/hr and 7343850lb/hr and the CHX inlet flue gas temperatures of 219°F, 197°F and 174°F corresponding to flue gas compressor outlet pressures of 21.7psia, 19.7psia and 17.7 psia respectively were taken to conduct these design calculations.

Table 1 shows the flue gas temperatures and pressures in three different compressor outlet conditions at flue gas mass flow rate of 10,634,586 lb/hr for the particular unit burning PRB coal. The temperatures and pressures at three state points marked in Figure 1 are also presented in Table 1. States 1, 2 and 3 are the flue gas compressor outlet, the spray cooler and the CHX outlet respectively. In addition, for each flue gas flow rate and CHX inlet flue gas temperature with corresponding pressure, five different target CHX outlet temperatures were set to analyze the sensitivity of target CHX outlet temperature variation on CHX tube surface area and power needed which is also shown in Table 1.

Table 1. Flue Gas Temperatures for Three Different Flue Gas Compressor Outlet Conditions at Flue Gas Mass Flow Rate of 10,634,586 lb/hr

Flue Gas Temperatures Passing Through Spray Cooler and CHX (°F) $\dot{m}_{FGAS} = 10,634,586$ lb/hr															
Case / State Point	**A**					**B**					**C**				
1	219 (21.7psia)					197 (19.7 psia)					174 (17.7 psia)				
2	175 (21.6 psia)					165°F (19.6 psia)					155 (17.6 psia)				
3	100	104	110	120	130	100	104	110	120	130	100	104	110	120	130

Similarly, the CHX designs were also conducted at the flue gas mass flow rate of 7,343,850 lb/hr, 8,452,640 lb/hr and 9,561,430 lb/hr. For different flue gas mass flow rates, the flue gas temperatures at state 2 which is the spray cooler outlet, would be chosen specifically due to different flue gas pressure drops.

Table 2A. Flue Gas Conditions before Entering Flue Gas Cooling System

Flue Gas			
FGAS $Temp_{in}$ [°F]	FGAS Mass Flow $Rate_{in}$ [lb/hr]	FGAS $Pressure_{in}$ [psia]	FGAS TARGET $Temp_{out}$ [°F]
219/197/174	7,343,850/8,452,640/ 9,561,430/10,634,586	21.7/19.7/17.7	100/104/110/120/130
Flue Gas Composition			
FGAS CO_2 [%]	FGAS O_2 [%]	FGAS N_2 [%]	FGAS H_2O [%]
11.32	4.93	66.65	17.10
Cooling Water			
CW $Temp_{in}$ [°F]	$\frac{\dot{m}_{CW}}{\dot{m}_{FGAS}}$	CW Mass Flow $Rate_{in}$ [lb/hr]	
65.0/80.0	0.8-1.8	$0.8 \times 10^7 - 1.8 \times 10^7$	

Table 2B. CHX Design Geometry

Heat Exchanger		**HX1**	**HX2**	**HX3**	**HX4**	**HX5**	**HX6**
	Units	Duct Geometry					
Width of Flue Gas Duct	ft	40	40	40	40	40	40
Height of Flue Gas Duct	ft	40	40	40	40	40	40
Length of HX Section	ft	-	-	-	-	-	-
Longitudinal Direction # of Row	-	-	-	-	-	-	-
Transverse Direction # of Column	-	125	125	125	125	125	125
	Units	Tube Geometry					
Transverse Tube Spacing Pitch	in	3.8	3.8	3.8	3.8	3.8	3.8
Longitudinal Tube Spacing Pitch	in	6.5	6.5	6.5	6.5	6.5	6.5
Outside Diameter of Tube	in	2.875	2.875	2.875	2.875	2.875	2.875
Inside Diameter of Tube	in	2.469	2.469	2.469	2.469	2.469	2.469
Staggered or Inline Arrangement	-	Inline	Inline	Inline	Inline	Inline	Inline

2-1 CHX Design Results

Based on previous study [2] on CHX design, the size of cross section of CHX, tube size and arrangement were fixed. The CHX lengths and mass flow rate ratios between cooling water and flue gas were changed to achieve feasible CHX designs.

The CHX tube surface area and power needed are two important parameters considered to conduct an economic and practical design.

Table 3 shows the total power of ID fan, CW pump of the CHX and refrigeration cycle compressor. The refrigeration cycle compressor power shown in Table 4 does not change significantly compared to total power needed due to the temperature range of refrigeration is fixed and the compressor power is only related to cooling water mass flow rate. Table 6 shows the CHX outlet flue gas moisture content. Table 5 and Table 7 present the length and heat transfer surface area of CHX. Table 8 shows the capital cost of the CHX including manufacturing and installation cost. The detailed design results are shown in appendix.

Table 3. Total Power of ID Fan, Cooling Water Pump Power of CHX and Refrigeration Cycle Compressor

ID Fan, Cooling Water Pump Power of CHX and Refrigeration Cycle Compressor Power (MW)															
$T, P_{FGAS,in}$ / $T_{FGAS,out}$°F / $\dot{m}_{FGAS}$	219°F, 21.7psia					197°F, 19.7psia					174°F, 17.7psia				
	100	104	110	120	130	100	104	110	120	130	100	104	110	120	130
10,634,586 ln/hr	31.41	28.16	23.16	17.91	12.04	31.76	28.78	22.28	18.78	11.90	29.09	27.65	21.13	12.82	8.36
9,561,430 lb/hr	23.53	21.42	19.29	12.82	8.95	21.77	19.80	16.52	12.56	8.14	20.49	20.03	16.17	13.15	8.96
8,452,640 lb/hr	16.32	16.47	13.54	9.58	7.07	15.89	13.85	11.98	9.03	7.45	14.87	13.44	10.96	8.69	6.35
7,343,850 lb/hr	11.02	10.14	8.44	6.38	7.56	11.32	10.81	9.76	6.34	4.66	10.11	8.81	7.28	6.19	4.05

Table 4. Refrigeration Cycle Compressor Power

Refrigeration Cycle Compressor Power (MW)															
$T, P_{FGAS,in}$ / $T_{FGAS,out}$°F / $\dot{m}_{FGAS}$	219°F, 21.7psia					197°F, 19.7psia					174°F, 17.7psia				
	100	104	110	120	130	100	104	110	120	130	100	104	110	120	130
10,634,586 ln/hr	4.73	4.67	4.35	4.28	3.42	4.96	4.96	4.50	4.81	3.88	4.57	5.10	4.64	3.40	2.41
9,561,430 lb/hr	4.47	4.47	4.47	3.63	2.94	4.18	4.18	3.90	3.90	3.07	3.89	4.45	4.17	4.45	3.89
8,452,640 lb/hr	3.83	4.07	3.83	3.21	2.72	3.69	3.57	3.45	3.69	3.20	3.68	3.68	3.44	3.56	3.19
7,343,850 lb/hr	3.22	3.22	3.00	2.57	3.54	3.42	3.53	3.53	2.78	2.35	3.10	2.99	2.77	2.99	2.35

Table 5. Length of CHX

Length of CHX (ft)															
$T, P_{FGAS,in}$ / $T_{FGAS,out}$.°F / $\dot{m}_{FGAS}$	219°F, 21.7psia					197°F, 19.7psia					174°F, 17.7psia				
	100	104	110	120	130	100	104	110	120	130	100	104	110	120	130
10,634,586 ln/hr	66	57	51	36	30	57	51	42	30	24	57	42	36	30	24
9,561,430 lb/hr	57	51	42	36	30	57	51	42	30	24	57	42	36	24	18
8,452,640 lb/hr	57	51	42	36	30	57	51	42	30	24	51	42	36	24	18
7,343,850 lb/hr	57	51	42	36	24	51	42	36	30	24	51	42	36	24	18

Table 6. CHX Outlet Flue Gas Moisture Content

CHX Outlet Flue Gas Moisture Content [%]															
$T, P_{FGAS,in}$ / $T_{FGAS,out}$.°F / $\dot{m}_{FGAS}$	219°F, 21.7psia					197°F, 19.7psia					174°F, 17.7psia				
	100	104	110	120	130	100	104	110	120	130	100	104	110	120	130
10,634,586 ln/hr	4.74	5.29	6.24	7.97	9.85	5.17	5.82	6.94	8.89	10.81	5.64	6.58	7.77	9.71	11.80
9,561,430 lb/hr	4.83	5.50	6.28	7.99	9.83	5.21	5.85	6.86	8.88	10.87	5.84	6.45	7.55	10.14	12.24
8,452,640 lb/hr	4.70	5.11	6.12	7.70	9.39	5.10	5.78	6.66	8.46	10.30	5.80	6.50	7.55	10.06	12.17
7,343,850 lb/hr	4.66	5.20	6.23	7.84	9.60	5.08	5.66	6.63	8.48	10.32	5.72	6.48	7.58	9.79	12.04

Table 7. Surface Area of CHX Tubes

Stainless Steel Tube Surface Area (ft²)															
$T, P_{FGAS,in}$ / $T_{FGAS,out}$ / $\dot{m}_{FGAS}$	219°F, 21.7psia					197°F, 19.7psia					174°F, 17.7psia				
	100	104	110	120	130	100	104	110	120	130	100	104	110	120	130
10,634,586 ln/hr	404029	358965	314266	224501	179622	358965	314266	269385	179622	134740	358965	269385	224501	179622	134740
9,561,430 lb/hr	358965	314266	269385	224501	179622	358965	314266	269385	179622	134740	358965	269385	224501	134740	89859
8,452,640 lb/hr	100* +358865	314266	269385	224501	100* +179522	100* +358865	100* +314166	269385	179622	134740	314266	269385	224501	134740	89859
7,343,850 lb/hr	100* +358865	100* +314166	269385	100* +224401	134740	100* +314166	269385	224501	179622	134740	100* +314166	269385	224501	134740	89859

***Surface Area of Nickel Alloy 22**

Table 8. Installed Capital Cost of CHX

Capital Costs of CHX Including Manufacturing & Installation Costs (Million $)															
$T, P_{FGAS,in}$ / $T_{FGAS,out}$.°F / $\dot{m}_{FGAS}$	219°F, 21.7psia					197°F, 19.7psia					174°F, 17.7psia				
	100	104	110	120	130	100	104	110	120	130	100	104	110	120	130
10,634,586 ln/hr	16.68	14.82	12.98	9.27	7.42	14.82	12.98	11.12	7.42	5.56	14.82	11.12	9.27	7.42	5.56
9,561,430 lb/hr	14.82	12.98	11.12	9.27	7.42	14.82	12.98	11.12	7.42	5.56	14.82	11.12	9.27	5.56	3.71
8,452,640 lb/hr	14.84	12.98	11.12	9.27	7.43	14.82	12.99	11.12	7.42	5.56	12.98	11.12	9.27	5.56	3.71
7,343,850 lb/hr	14.84	12.99	11.12	9.29	5.56	12.99	11.12	9.27	7.42	5.56	12.99	11.12	9.27	5.56	3.71

2-2 Results Analysis

The results presented in section 2-2 indicate the total power needed and capital cost of the CHX will not change significantly with different CHX inlet flue gas temperatures and pressures. However, the total power needed of ID fan, CW pump of CHX and refrigeration cycle compressor is sensitive to flue gas mass flow rate and CHX flue gas outlet temperature.

Figure 5 and Figure 6 show the total power needed decreases when CHX flue gas outlet temperature increases or flue gas mass flow rate decreases. The effects of changes in CHX inlet flue gas temperature at constant CHX flue gas exit temperature shown in Figure 5 or constant CHX flue gas mass flow rate shown in Figure 6 on total power of ID fan, CW pump and refrigeration compressor are relatively small.

Figure 7 presents the flue gas moisture content vs. different flue gas temperatures at the outlet of the CHX. Basically, the flue gas at the CHX outlet is saturated and the moisture content will increase when the flue gas exit temperature increases.

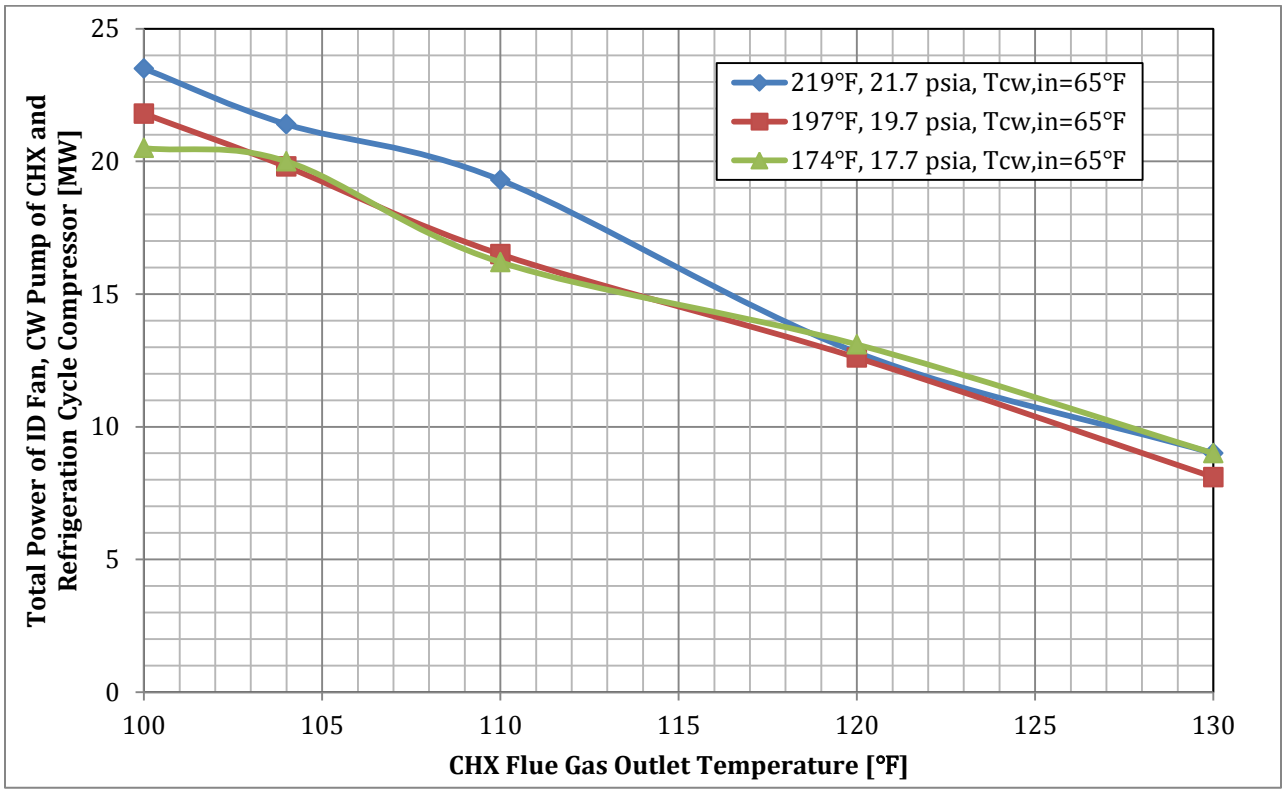

Figure 5. Total Power Needed vs. CHX Flue Gas Exit Temperature at Flue Gas Mass Flow Rate of 10,634,586 lb/hr

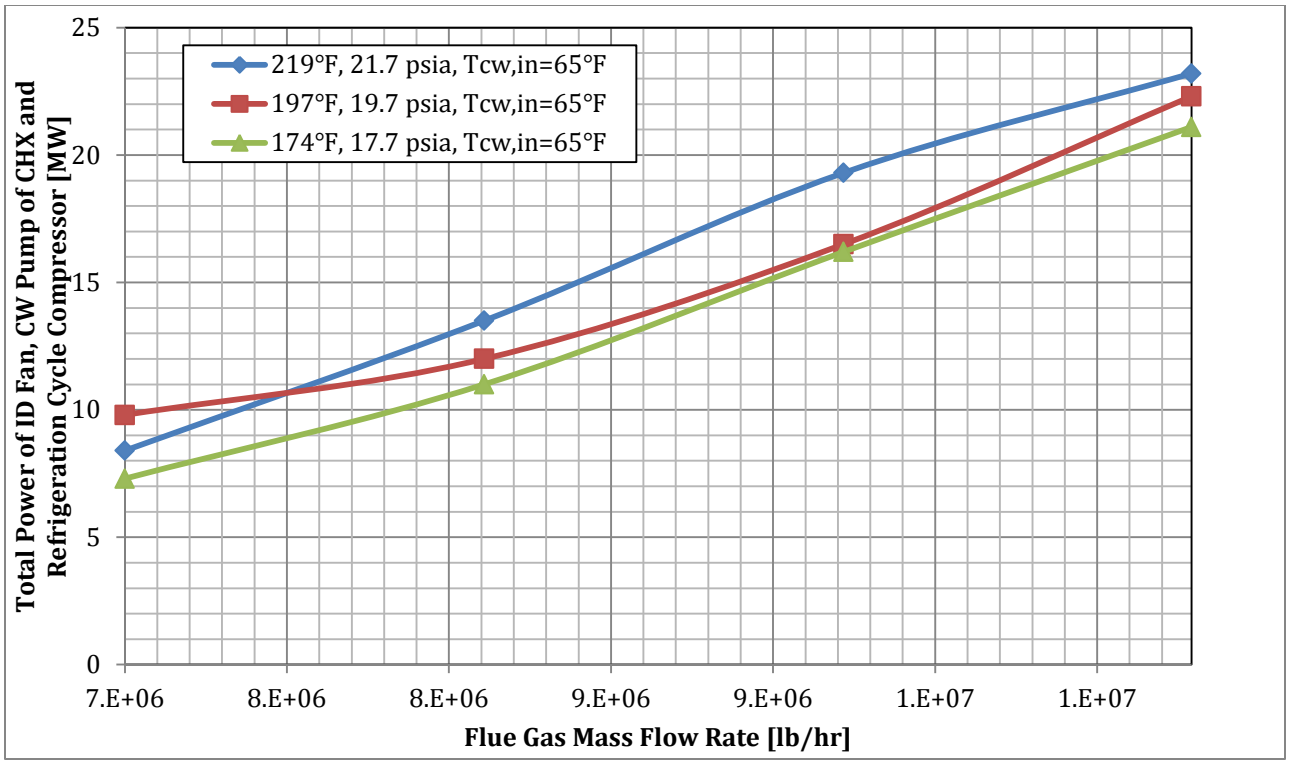

Figure 6. Total Power Needed vs. Flue Gas Mass Flow Rate at Flue Gas Outlet Temperature of 110°F

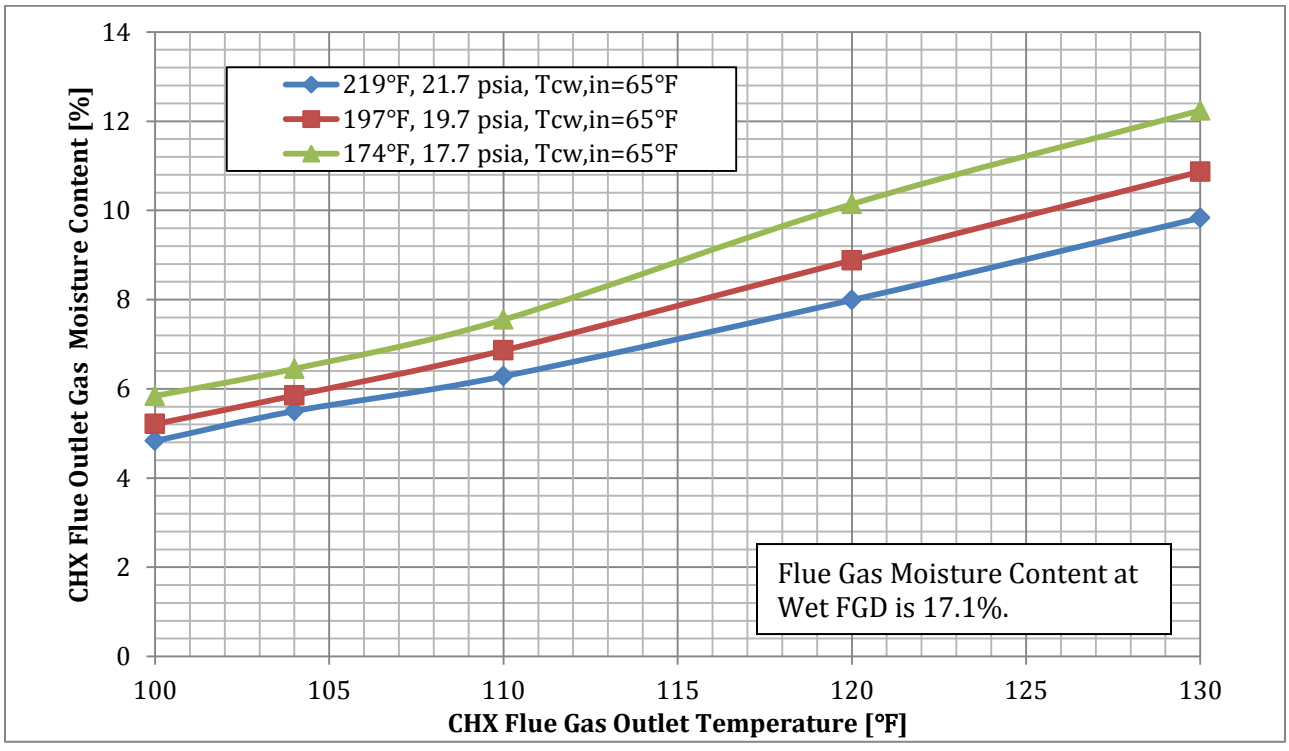

Figure 7. CHX Flue Gas Outlet Moisture Content vs. CHX Flue Gas Outlet Temprature at Flue Gas Mass Flow Rate of 10,634,586 lb/hr

2-3 Cost Analysis of Flue Gas Cooling System with & without Refrigeration System

The refrigeration system used to cool cooling water from 80°F down to 65°F is a large part of power and capital cost of the whole flue gas cooling system. The CHX cooling water inlet temperature of 80°F which is cooling tower outlet temperature can be taken to conduct new designs to avoid using refrigeration system. However, the power cost of ID fan, CW pump of CHX and refrigeration compressor and the capital cost of CHX will increase.

The flue gas mass flow rate of 10,634,586 lb/hr and the CHX cross sectional area of 40 ft by 40 ft were fixed in this investigation. The mass flow rate ratio between cooling water and flue gas was controlled within 1.8. The CHX flue gas exit temperatures of 104°F, 110°F, 120°F and 130°F were taken in this comparison.

The circulating cooling water temperatures returning to cooling tower will be different with or without refrigeration system. Therefore, the heat loads and the operating costs of the cooling tower will be different.

The analysis of power and capital cost of the flue gas cooling system with and without refrigeration system was done to discuss whether the refrigeration system is necessary or beneficial.

2-3-1 Power Cost Estimation

$$P_{Total} = P_{ID\ Fan} + P_{CW\ Pump} + P_{Ref.Comp.}$$

The total power in this investigation consists of ID fan power, cooling water pump power of CHX and refrigeration compressor power. There is an assumption that the cooling system would be used 7000 hours per year. A power cost of $0.07/kWh was assumed. The annual total power cost can be calculated by the equation below:

$$Annual\ Power\ Cost = P_{Total}(kW) * \frac{7000\ hrs}{year} * \$0.07/kWh$$

2-3-2 Installed Capital Cost Estimation of CHX [3]

The capital costs of CHX consist of the material cost and fabrication and installation costs. The type of tube material used will have a major influence on what percentage of the total cost is tube material cost alone. The heat exchange surfaces, the tubes themselves, will be the main contributor to the material cost due to the very large surface area (>100,000 ft^2). Information in the published literature on heat exchanger costs led to basing the fabrication

and installation costs off of a factor of the raw tube material cost. Fabrication and material costs from the literature were identified as percentages of total capital heat exchanger cost for shell and tube heat exchangers. It was found that as the heat exchanger size increases, the ratio of material cost to total cost rises and the ratio of fabrication cost to total cost decreases. For a standard carbon steel heat exchanger, the ratios eventually plateau to where labor cost is roughly three times the cost of the tubing material. This trend is seen in Figure 8. As more expensive materials such as stainless steel and nickel alloys are used, the cost of the heat exchanger is dominated by the tube material cost. For example, with the use of high Nickel Alloy C-276 tubing, the percentage of the total heat exchanger cost that consists of tube material cost is 88%. For estimation purposes, the labor cost involved in assembling a heat exchanger from a relatively expensive tube material was assumed to be the same as the labor cost for fabricating a carbon steel heat exchanger of the same size.

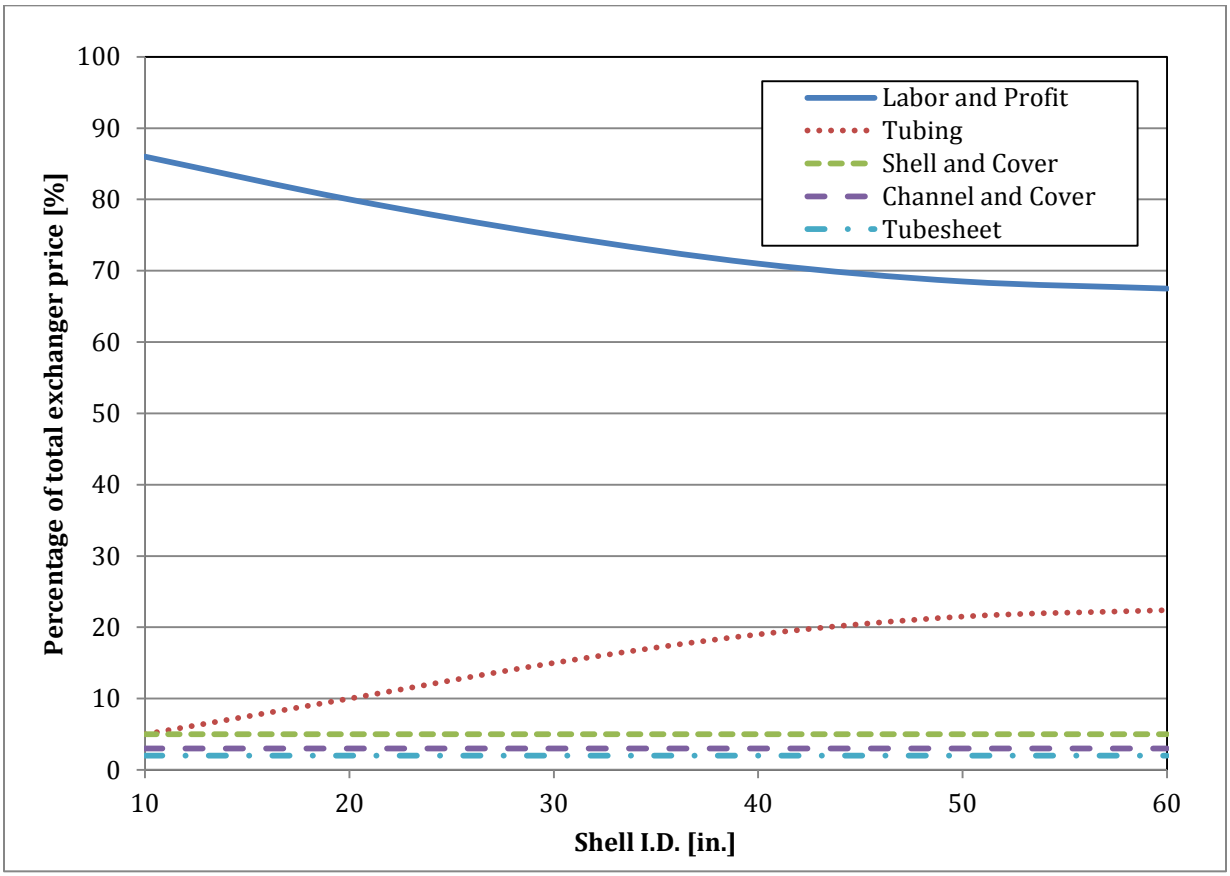

Figure 8. Heat Exchanger Ratio of Costs

The principal difference between shell and tube heat exchangers that were investigated for costing purposes and the tube bundle heat exchangers investigated in this study is that the shell and tube heat exchangers are manufactured and assembled at the factory and then shipped as a complete unit, whereas with the heat exchangers investigated here, the tubes would be assembled into bundles, shipped to the plant and then installed into a duct at the plant. For this reason, it was assumed that the cost factor used in the literature for manufacture and assembly for shell and tube heat exchangers was going to be much the same as the factor used for manufacture and plant installation of the tube bundle heat exchangers investigated here. Figure 8 shows that as heat exchanger surface area increases, the ratio of material cost to total cost rises and the ratio of fabrication cost to total cost decreases. To determine the appropriate factors between fabrication and assembly cost and tube material cost, four cases in the available literature with large heat exchanger surface areas were studied. The calculations showed that the average factor for manufacture and assembly for carbon steel tube heat exchangers is 3.00 times the cost of the material as seen in Table 9. An extra 30% was added to this factor for any unaccounted costs, making the total factor for manufacture and installation of a tube bundle heat exchanger to be 3.90 times the carbon steel tube material cost.

Table 9. Heat Exchanger Cost Factors

	(Tube Material) / Total	(Manufacture and Assembly)/Total	Ratio
Case 1	20.58	59.42	2.89
Case 2	20.42	59.58	2.92
Case 3	18.90	61.10	3.23
Case 4	20.10	59.90	2.98
Average	**20.00**	**60.00**	**3.00**

Cost of stainless steel tubing was found by getting quotes from manufacturers. Stainless Steel 304 tubing in the OD of 2.875” and 0.203” wall thickness was quoted at $12.98/ft [4]. A ratio that is generally used when comparing the cost of stainless steel 304 tubing to carbon steel tubing is 2.80. This would indicate that carbon steel tubing with the same dimensions of the stainless steel 304 tubing mentioned above would cost approximately $4.64/ft. Using the factor mentioned above of 3.90, the manufacture and installation cost would be $14.89/ft. This manufacture and installation cost applies for any tube material. For example, for stainless steel 304 tubing which costs $12.98/ft, the relative manufacture and

installation factor is 1.394 making the cost to be the same as carbon steel manufacture and installation at $18.10/ft.

An investigation into the cost of Nickel Alloy 22 tubing led to a cost of $22.00/lb [5]. For a 2.875" OD and 0.203" wall thickness, this translates to $141.26/ft. A manufacture and installation cost of $18.10/ft leads to a relative factor of 0.128. The material cost dominates the total capital cost of the heat exchanger for expensive materials. Table 10 shows the relative cost factors and total cost for each type of tube material that was considered.

Table 10. Cost Factors for Different Tubes

Carbon Steel		
Type	**Relative Cost Factor**	**Cost/ft ($/ft)**
Tube Material Cost	1.00	$4.64
Manufacture and Installation Cost	3.90	$18.10
Total	**4.90**	$28.74
SS 304		
Type	**Relative Cost Factor**	**Cost/ft ($/ft)**
Tube Material Cost	1.00	$12.98
Manufacture and Installation Cost	1.394	$18.10
Total	**2.394**	$31.08
Ni Alloy 22		
Type	**Relative Cost Factor**	**Cost/ft ($/ft)**
Tube Material Cost	1.00	$141.26
Manufacture and Installation Cost	0.128	$18.10
Total	**1.128**	$159.36

The total installed cost based on the factors above was converted into an annual fixed cost that takes into consideration capital amortization and tax and insurance costs. A monthly payment was derived using the following equation:

$$PF = \frac{i(1+i)^n}{(1+i)^n - 1}$$

where PF stands for the monthly payment factor, n is the period of the loan in months and i is the interest rate per month. The period of loan for this research was 20 years and the annual interest rate was taken to be 4%. This gives a monthly payment factor of 0.00606. This monthly payment factor was used to calculate the annual fixed cost using the following equation:

$$AFC = (12 * PF + 0.015) * (Total\ Installed\ Cost)$$

where AFC stands for annual fixed cost, PF is the monthly payment factor, 0.015 is a factor to take into account taxes and insurance and the total installed cost was explained before. This annual fixed cost does not take into account the power requirements for the full scale heat exchanger.

2-4-3 Installed Capital Cost Estimation of Refrigeration System

The installation cost data of refrigeration system can be found with different tons of refrigeration. [6] The assumption of installation cost equals to equipment cost was made to estimate total installed capital cost of refrigeration system. Figure 9 shows the installation cost per ton of refrigeration changes in total tons of refrigeration in year of 2003.

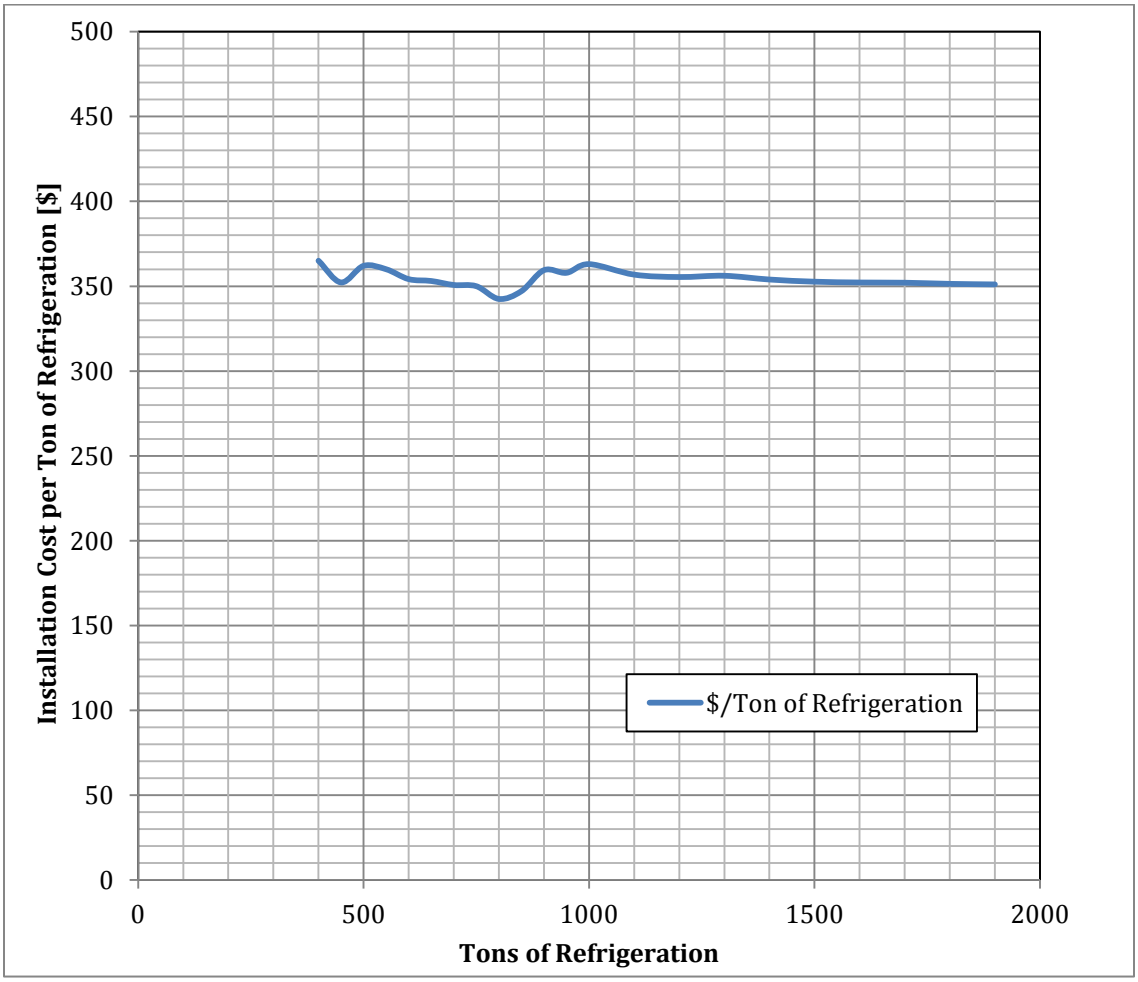

Figure 9. Installation Cost per Ton of Refrigeration vs. Total Tons of Refrigeration

Figure 9 shows the installation cost per ton of refrigeration approaches $350/ton when the total tons of refrigeration increases. Therefore, the estimated installed capital cost is $700/ton in year of 2003.

Considering inflation rate, the refrigeration system installed capital cost per ton of refrigeration in year of 2014 is $906.74/ton. The total installed capital cost of refrigeration system can be calculated by following equation:

$$Total\ Installed\ Cost = \$906.74/ton * (Total\ Tons\ of\ Refrigeration)$$

The annual fixed cost of refrigeration system can be calculated using same method of CHX annual fixed cost calculation.

2-4-4 Cost Estimation Calculation Example

The conditions of $\dot{m}_{FGAS} = 10634586$ lb/hr, $T_{FGAS,in} = 219$°F, $P_{FGAS,in} = 21.7$psia, $T_{FGAS,out} = 104$°F, $T_{CW,in} = 65$°F were taken to calculate this cost estimation example.

Total Power Cost

The calculated total power is shown below:

$$\begin{aligned} P_{Total} &= P_{ID\ Fan} + P_{CW\ Pump} + P_{Ref.Comp.} \\ &= 10108.61\text{kW} + 13386.65\text{kW} + 4667.34\text{kW} \\ &= 28162.6\text{kW} \end{aligned}$$

The annual operating hour was assumed 7000 hours and the dollar cost per kilowatt-hour was $0.07. The annual power cost was calculated using following equation:

$$Annual\ Power\ Cost = P_{Total}(\text{kW}) * \frac{7000\ \text{hrs}}{\text{year}} * \frac{\$0.07}{\text{kWh}}$$

$$=28162.6\text{kW} * \frac{7000\ \text{hrs}}{\text{year}} * \frac{\$0.07}{\text{kWh}}$$

=13.80 Million $

Installed Capital Cost of CHX

The CHX design result for this case shows the total heat transfer area needed is 0 ft^2 of nickel alloy 22 tube and 358965 ft^2 stainless steel tube. For a 2.875" OD and 0.203" wall thickness, these translate to 0 ft nickel alloy 22 tube and 476920.77 ft stainless steel tube. The tube material and installation costs can be found in section 2-4-2 which are $159.36/ft nickel alloy 22 and $31.08/ft for stainless steel tube. The total installed CHX cost is:

$$Total\ Installed\ CHX\ Cost = 0\text{ft} * \frac{\$159.36}{\text{ft}} + 476920.77\text{ft} * \frac{\$31.08}{\text{ft}}$$
$$= 14.82\ \text{Million}\ \$$$

The period of loan was assumed 20 years and the annual interest rate was taken to be 4%. The annual CHX fixed cost can be derived by following equations where PF stands for the monthly payment factor, n is the period of the loan in months and *i* is the interest rate per month:

$$PF = \frac{i(1+i)^n}{(1+i)^n - 1}$$
$$= \frac{\frac{4\%}{12}\left(1+\frac{4\%}{12}\right)^{240}}{\left(1+\frac{4\%}{12}\right)^{240} - 1}$$
$$= 0.00606$$

The annual CHX fixed cost is:

$$Annual\ Fixed\ Cost\ of\ CHX = (12 * PF + 0.015) * (Total\ Installed\ Cost)$$
$$= (12 * 0.00606 + 0.015) * 14.82\ \text{Million}\ \$$$
$$= 1.300\ \text{Million}\ \$/\text{year}$$

Installed Capital Cost of Refrigeration System

In this particular case, the refrigeration capacity is 20170 tons. The total installed capital cost is

$$20170\ tons\ \times \frac{\$906.74}{ton} = 18.29\ \text{Million}\ \$$$

The annual refrigeration system fixed cost is:

$$Annual\ Fixed\ Cost\ of\ Ref.\ Sys. = (12 * PF + 0.015) * (Total\ Installed\ Cost)$$
$$= (12 * 0.00606 + 0.015) * 18.29 \text{ Million \$}$$
$$= 1.604 \text{ Million \$}$$

2-4-5 Results Comparison

Table 11 compares the CHX design results of the cooling system with and without refrigeration system. Table 12 then shows the annual power and CHX capital costs of the cooling system with refrigeration system are much lower. Furthermore, the cooling tower heat dissipations of the cases without refrigeration system are large than the cases with refrigeration system. However, compared to the total cooling water mass flow rate of 550MW power plant which is >100,000,000 lb/hr typically, the cooling water flow rate of this flue gas cooling system is so small that the cooling tower heat dissipations can be ignored in cost analysis and no new cooling tower needs to be constructed.

Table 11. Estimated ID Fan, CW Pump of CHX and Refrigeration Compressor Power for Various CHX Designs

CHX Design Results with/without Refrigeration System $\dot{m}_{FGAS} = 10,634,586$ lb/hr													
$T, P_{FGAS,in}$ / $T_{FGAS,out}$ °F		219°F, 21.7psia				197°F, 19.7psia				174°F, 17.7psia			
		104	110	120	130	104	110	120	130	104	110	120	130
$T_{CW,in}$ [°F]	with Ref.	65	65	65	65	65	65	65	65	65	65	65	65
	w/o Ref.	80	80	80	80	80	80	80	80	80	80	80	80
$T_{CW,out}$ [°F]	with Ref.	139.34	139.41	131.00	134.44	129.58	130.32	116.57	116.61	121.03	120.64	120.04	130.58
	w/o Ref.	152.91	147.38	143.70	140.28	142.02	141.02	136.47	131.20	142.61	138.59	129.04	121.09
$P_{ID\ Fan}$ [MW]	with Ref.	10.11	9.10	6.72	5.64	9.54	8.45	5.83	4.57	8.99	7.72	6.49	5.10
	w/o Ref.	19.55	13.00	9.46	7.02	15.05	12.66	8.79	6.10	22.00	14.04	8.04	5.03
$P_{CW\ Pump}$ [MW]	with Ref.	13.39	9.71	6.91	2.98	14.28	9.34	8.14	3.45	13.56	8.77	2.93	0.85
	w/o Ref.	26.55	18.98	10.72	5.83	25.48	17.75	9.30	4.82	21.74	14.52	7.90	3.82
$P_{Ref.\ Comp}$ [MW]	with Ref.	4.67	4.35	4.28	3.42	4.96	4.50	4.81	3.88	5.10	4.64	3.40	2.41
	w/o Ref.	0	0	0	0	0	0	0	0	0	0	0	0
P_{Total} [MW]	with Ref.	28.2	23.2	17.9	12.0	28.8	22.3	18.8	11.9	27.6	21.1	12.8	8.4
	w/o Ref.	46.1	31.98	20.18	12.85	40.53	30.41	18.09	10.92	43.74	28.56	15.94	8.85
Length of CHX [ft]	with Ref.	57	51	36	30	51	42	30	24	42	36	30	24
	w/o Ref.	102	72	51	36	78	66	48	30	96	66	36	24
Heat Transfer Area[ft²]	with Ref.	358965	314266	224501	179622	314266	269385	179622	134740	269385	224501	179622	134740
	w/o Ref.	19253.34* +654063.4	100.02* +448809.8	99.95* +314165.7	224503.2	100* +493691	99.98* +103928.5	269384.6	179621.8	99.99* +628335.4	99.98* +403928.5	224503.2	134740.3

***Surface Area of Nickel Alloy 22**

Note: $T_{CW,in} = 65$°F (with Ref.); $T_{CW,in} = 80$°F (w/o Ref.)

Table 12. Cost and Cooling Tower Heat Load Comparison between Flue Gas Cooling System with & without Refrigeration System

Cost and Cooling Tower Heat Load Comparison between Flue Gas Cooling System with & without Refrigeration System													
$T, P_{FGAS,in}$ / $T_{FGAS,out}$ °F		219°F, 21.7psia				197°F, 19.7psia				174°F, 17.7psia			
		104	110	120	130	104	110	120	130	104	110	120	130
Annual Refrigeration Sys. Capital Cost [Milli $]	with Ref.	1.604	1.497	1.471	1.176	1.706	1.546	1.652	1.333	1.753	1.594	1.169	0.829
	w/o Ref.	0	0	0	0	0	0	0	0	0	0	0	0
Annual CHX Capital Cost [Milli $]	with Ref.	1.300	1.139	0.813	0.651	1.139	0.975	0.651	0.488	0.975	0.813	0.651	0.488
	w/o Ref.	2.726	1.627	1.139	0.813	1.790	0.378	0.975	0.651	2.278	1.465	0.813	0.488
Cooling Tower Heat Dissipation [BTUs/hr]	with Ref.	1.200E+09	1.121E+09	9.762E+08	8.217E+08	1.108E+09	1.016E+09	8.572E+08	6.918E+08	9.880E+08	8.919E+08	7.247E+08	5.467E+08
	w/o Ref.	1.224E+09	1.145E+09	9.936E+08	8.430E+08	1.131E+09	1.047E+09	8.780E+08	7.137E+08	1.004E+09	9.392E+08	7.599E+08	5.709E+08
Total Annual Power Cost [Milli $]	**with Ref.**	**13.80**	**11.35**	**8.77**	**5.90**	**14.10**	**10.92**	**9.20**	**5.83**	**13.55**	**10.35**	**6.28**	**4.10**
	w/o Ref.	**22.59**	**15.67**	**9.89**	**6.30**	**19.86**	**14.90**	**8.86**	**5.35**	**21.43**	**14.00**	**7.81**	**4.34**
Total Annual Capital Cost [Milli $]	**with Ref.**	**2.904**	**2.636**	**2.284**	**1.827**	**2.845**	**2.521**	**2.303**	**1.821**	**2.728**	**2.407**	**1.82**	**1.317**
	w/o Ref.	**2.726**	**1.627**	**1.139**	**0.813**	**1.79**	**0.378**	**0.975**	**0.651**	**2.278**	**1.465**	**0.813**	**0.488**

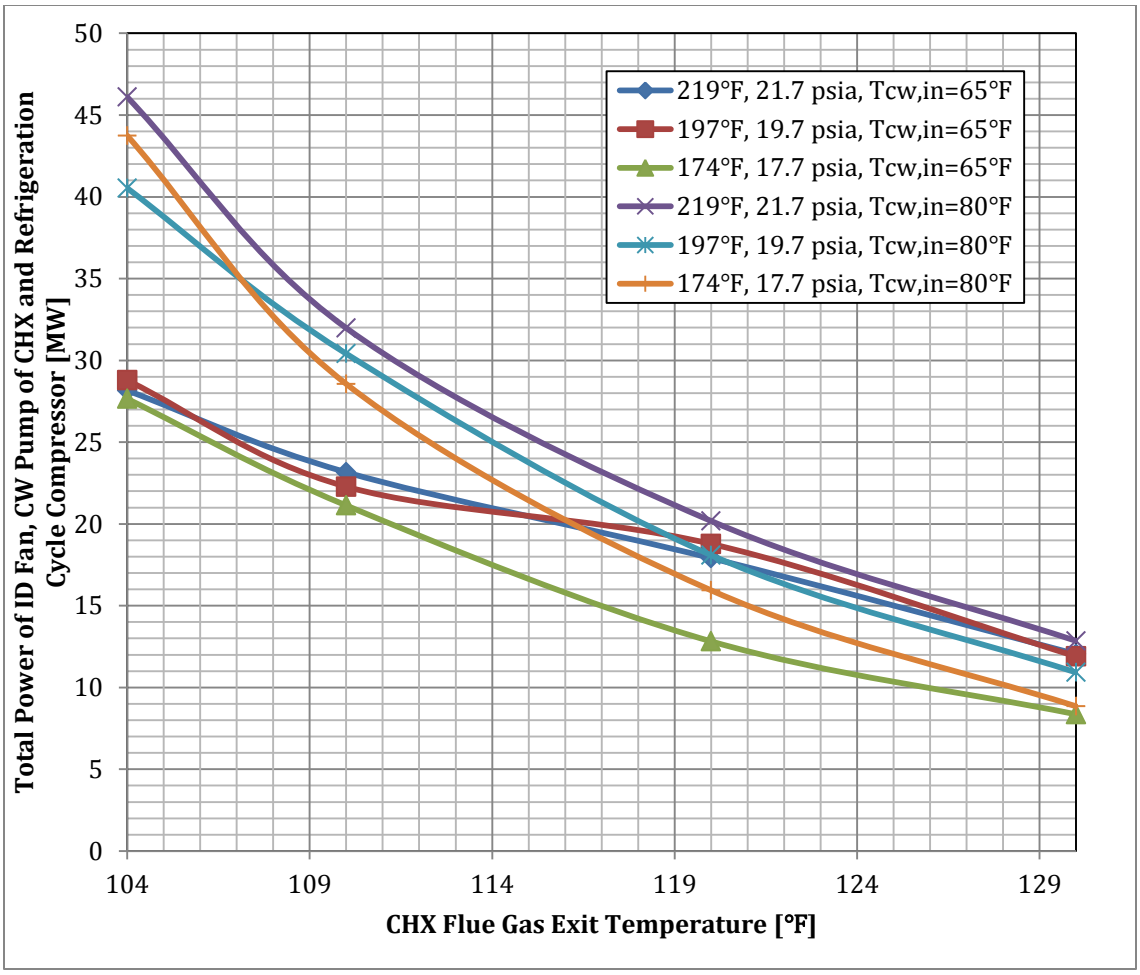

Figure 10. Total Power Needed vs. CHX Flue Gas Exit Temperature for T_{CW}=65°F and T_{CW}=80°F at the Flue Gas Mass Flow Rate of 10,634,586 lb/hr

Figure 10 shows the total power of ID fan, CW pump of CHX and refrigeration compressor of the cooling system with and without refrigeration system for three different CHX inlet temperatures and pressures. At the lower (<110°F) CHX flue gas exit temperature, the total power needed for the cooling system without refrigeration system is significantly larger than that with refrigeration system. The effect of changes in CHX inlet temperatures and pressures on total power cost is relatively small.

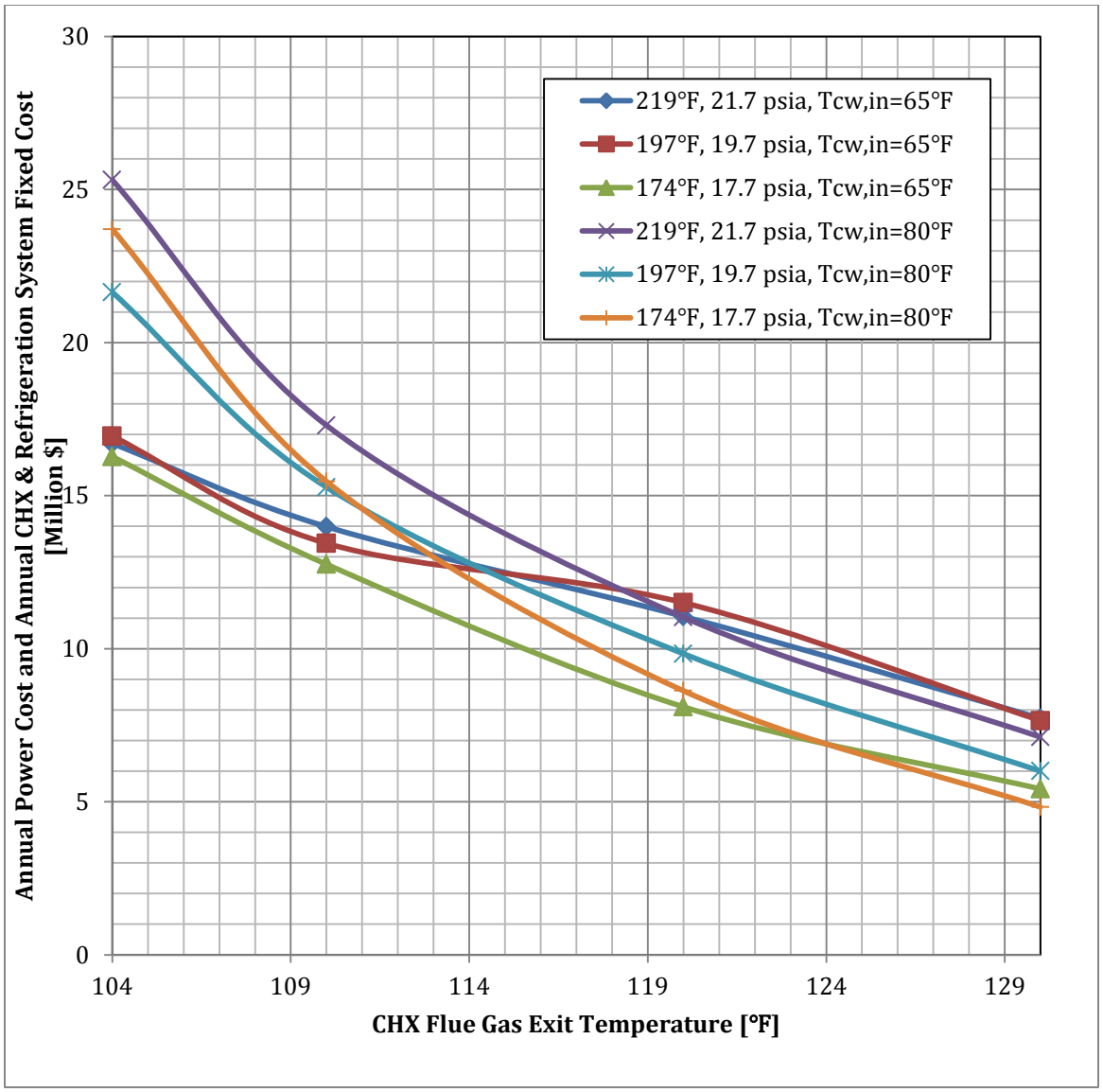

Figure 11. Annual Power Cost and Annual CHX & Refrigeration System Fixed Cost vs. CHX Flue Gas Exit Temperature at the Flue Gas Mass Flow Rate of 10,634,586 lb/hr

Figure 11 presents the annual power and fixed costs are not too different at CHX flue gas exit temperatures higher than 115°F. However, at the CHX outlet flue gas temperature lower than 110°F, the annual power and fixed costs of the system without refrigeration system are much larger than the system with refrigeration system.

3. Conclusion

In this investigation, the ERC has developed a flue gas cooling system model to cool compressed high temperature flue gas from 219°F to 104°F in the base case which the conditions were assumed by ADA. To optimize the CO_2 capture system performance, the impact of CHX inlet flue gas temperature and pressure, CHX outlet flue gas temperature, flue gas mass flow rate and CHX cooling water inlet temperature on the power consumption and capital cost of the flue gas cooling system was investigated.

The CHX design results show that the flue gas mass flow rate will significantly affect the power needed and capital cost of the flue gas cooling system. To cool down larger mass flow rate of flue gas, more heat transfer areas are needed that means a larger size CHX and lager capital cost. The total power of ID fan and cooling water pump of CHX will increase due to the flue gas side and cooling water side pressure drops increase.

At fixed flue gas mass flow rate, the different CHX inlet flue gas temperatures and pressures will not affect the total power needed and capital costs a lot. However, the CHX outlet flue gas temperatures changes from 104°F to 130°F, the power needed and capital costs of the cooling system with or without refrigeration system both decrease. The flue gas cooling system designs without refrigeration system which the CHX inlet cooling water temperature of 80°F were conducted. The results show that at the CHX outlet flue gas temperatures equal to and lower than 110°F, the cooling system with refrigeration system is more economical; at the CHX outlet flue gas temperature higher than 115°F, the cooling system with refrigeration system costs a little bit more than the cooling system without refrigeration system.

To determine the final design of the flue gas cooling system, the effect of changes in parameters like CHX outlet temperatures, flue gas mass flow rates and etc. on the whole CO_2 capture system power consumption and capital cost should be taken into account.

4. Appendix

4.1 CHX Design Results with Cooling Water Inlet Temperature of 65°F

$T_{FGAS,\ in}$=219°F, $T_{FGAS,\ out}$=100°F, P_{FGAS}=21.7psia, $\dot{m}_{FGAS}$=10634586 lb/hr		
Case		**With Spray Cooler**
	Units	Temperatures and Condensation Rate
Flue Gas Mass Flow Rate	lb/hr	10757359.10
CW Mass Flow Rate	lb/hr	16351185.83 (1.52)
Flue Gas Inlet Temp	°F	175
Flue Gas Outlet Temp	°F	100.24
CW Inlet Temp	°F	65.03
CW Outlet Temp	°F	141.49
Inlet y_{H2O}	%	18.59
Outlet y_{H2O}	%	4.74
Condensation Rate	lb/hr	1001948
	Units	Pressure Drop in CHX
Flue Gas Side ΔP	psi	2.252
Total CW Side ΔP	psi	870.795
	Units	Power
ID Fan Power	kW	11217.93
CW Pump Power	kW	15461.62
Refrigeration Compressor Power (T_{CW} From 80°F to 65 °F)	kW	4729.23
Annual Power Cost (7000hr/yr, $70/Million kWh)	Milli$	15.39
	Units	Geometry
Total Duct Length	ft	66
Total # of Row	-	108
Nickel Alloy 22 Tube Surface Area	ft^2	0
Stainless Steel Tube Surface Area	ft^2	404029
Total Capital Cost (Including Manufacture & Installation Cost)	Milli$	16.68

$T_{FGAS, in}$=219°F, $T_{FGAS, out}$=104°F, P_{FGAS}=21.7psia, $\dot{m}_{FGAS}$=10634586 lb/hr		
Case		**With Spray Cooler**
	Units	Temperatures and Condensation Rate
Flue Gas Mass Flow Rate	lb/hr	10757359.10
CW Mass Flow Rate	lb/hr	16136038.65 (1.5)
Flue Gas Inlet Temp	°F	175
Flue Gas Outlet Temp	°F	103.9
CW Inlet Temp	°F	64.66
CW Outlet Temp	°F	139.34
Inlet y_{H2O}	%	18.59
Outlet y_{H2O}	%	5.29
Condensation Rate	lb/hr	967181
	Units	Pressure Drop in CHX
Flue Gas Side ΔP	psi	2.019
Total CW Side ΔP	psi	763.985
	Units	Power
ID Fan Power	kW	10108.61
CW Pump Power	kW	13386.65
Refrigeration Compressor Power (T_{CW} From 80°F to 65 °F)	kW	4667.34
Annual Power Cost (7000hr/yr, $70/Million kWh)	Milli$	13.80
	Units	Geometry
Total Duct Length	ft	57
Total # of Row	-	96
Nickel Alloy 22 Tube Surface Area	ft^2	0
Stainless Steel Tube Surface Area	ft^2	358965
Total Capital Cost (Including Manufacture & Installation Cost)	Milli$	14.82

$T_{FGAS,\ in}$=219°F, $T_{FGAS,\ out}$=110°F, P_{FGAS}=21.7psia, $\dot{m}_{FGAS}$=10634586 lb/hr		
Case		**With Spray Cooler**
	Units	Temperatures and Condensation Rate
Flue Gas Mass Flow Rate	lb/hr	10757359.10
CW Mass Flow Rate	lb/hr	15060302.74 (1.4)
Flue Gas Inlet Temp	°F	175
Flue Gas Outlet Temp	°F	109.88
CW Inlet Temp	°F	64.60
CW Outlet Temp	°F	139.41
Inlet y_{H2O}	%	18.59
Outlet y_{H2O}	%	6.24
Condensation Rate	lb/hr	907241
	Units	Pressure Drop in CHX
Flue Gas Side ΔP	psi	1.798
Total CW Side ΔP	psi	593.485
	Units	Power
ID Fan Power	kW	9096.63
CW Pump Power	kW	9705.84
Refrigeration Compressor Power (T_{CW} From 80°F to 65 °F)	kW	4354.89
Annual Power Cost (7000hr/yr, $70/Million kWh)	Milli$	11.35
	Units	Geometry
Total Duct Length	ft	51
Total # of Row	-	84
Nickel Alloy 22 Tube Surface Area	ft^2	0
Stainless Steel Tube Surface Area	ft^2	314265.8
Total Capital Cost (Including Manufacture & Installation Cost)	Milli$	12.98

$T_{FGAS,\ in}$=219°F, $T_{FGAS,\ out}$=120°F, P_{FGAS}=21.7psia, $\dot{m}_{FGAS}$=10634586 lb/hr		
Case		**With Spray Cooler**
	Units	Temperatures and Condensation Rate
Flue Gas Mass Flow Rate	lb/hr	10757359.10
CW Mass Flow Rate	lb/hr	14791368.76 (1.375)
Flue Gas Inlet Temp	°F	175
Flue Gas Outlet Temp	°F	119.82
CW Inlet Temp	°F	64.41
CW Outlet Temp	°F	131.00
Inlet y_{H2O}	%	18.59
Outlet y_{H2O}	%	7.97
Condensation Rate	lb/hr	795137
	Units	Pressure Drop in CHX
Flue Gas Side ΔP	psi	1.31
Total CW Side ΔP	psi	430.312
	Units	Power
ID Fan Power	kW	6718.1
CW Pump Power	kW	6911.65
Refrigeration Compressor Power (T_{CW} From 80°F to 65 °F)	kW	4277.33
Annual Power Cost (7000hr/yr, $70/Million kWh)	Milli$	8.77
	Units	Geometry
Total Duct Length	ft	36
Total # of Row	-	60
Nickel Alloy 22 Tube Surface Area	ft^2	0
Stainless Steel Tube Surface Area	ft^2	224501.4
Total Capital Cost (Including Manufacture & Installation Cost)	Milli$	9.27

$T_{FGAS,\ in}$=219°F, $T_{FGAS,\ out}$=130°F, P_{FGAS}=21.7psia, $\dot{m}_{FGAS}$=10634586 lb/hr		
Case		**With Spray Cooler**
	Units	Temperatures and Condensation Rate
Flue Gas Mass Flow Rate	lb/hr	10757359.10
CW Mass Flow Rate	lb/hr	11833095.01 (1.1)
Flue Gas Inlet Temp	°F	175
Flue Gas Outlet Temp	°F	130.34
CW Inlet Temp	°F	64.94
CW Outlet Temp	°F	134.44
Inlet y_{H2O}	%	18.59
Outlet y_{H2O}	%	9.85
Condensation Rate	lb/hr	667577
	Units	Pressure Drop in CHX
Flue Gas Side ΔP	psi	1.081
Total CW Side ΔP	psi	231.957
	Units	Power
ID Fan Power	kW	5638.62
CW Pump Power	kW	2980.55
Refrigeration Compressor Power (T_{CW} From 80°F to 65 °F)	kW	3422.02
Annual Power Cost (7000hr/yr, $70/Million kWh)	Milli$	5.90
	Units	Geometry
Total Duct Length	ft	30
Total # of Row	-	48
Nickel Alloy 22 Tube Surface Area	ft^2	0
Stainless Steel Tube Surface Area	ft^2	179621.5
Total Capital Cost (Including Manufacture & Installation Cost)	Milli$	7.42

$T_{FGAS,\ in}$=197°F, $T_{FGAS,\ out}$=100°F, P_{FGAS}=19.7psia, $\dot{m}_{FGAS}$=10634586 lb/hr		
Case		**With Spray Cooler**
	Units	Temperatures and Condensation Rate
Flue Gas Mass Flow Rate	lb/hr	10723341.37
CW Mass Flow Rate	lb/hr	17157346.19 (1.6)
Flue Gas Inlet Temp	°F	165
Flue Gas Outlet Temp	°F	99.95
CW Inlet Temp	°F	64.91
CW Outlet Temp	°F	132.57
Inlet y_{H2O}	%	18.18
Outlet y_{H2O}	%	5.17
Condensation Rate	lb/hr	941020
	Units	Pressure Drop in CHX
Flue Gas Side ΔP	psi	2.180
Total CW Side ΔP	psi	861.871
	Units	Power
ID Fan Power	kW	10742.95
CW Pump Power	kW	16057.66
Refrigeration Compressor Power (T_{CW} From 80°F to 65 °F)	kW	4962.63
Annual Power Cost (7000hr/yr, $70/Million kWh)	Milli$	15.56
	Units	Geometry
Total Duct Length	ft	57
Total # of Row	-	96
Nickel Alloy 22 Tube Surface Area	ft^2	0
Stainless Steel Tube Surface Area	ft^2	358965.1
Total Capital Cost (Including Manufacture & Installation Cost)	Milli$	14.82

$T_{FGAS,\ in}$=197°F, $T_{FGAS,\ out}$=104°F, P_{FGAS}=19.7psia, $\dot{m}_{FGAS}$=10634586 lb/hr		
Case		**With Spray Cooler**
	Units	Temperatures and Condensation Rate
Flue Gas Mass Flow Rate	lb/hr	10723341.37
CW Mass Flow Rate	lb/hr	17157346.19 (1.6)
Flue Gas Inlet Temp	°F	165
Flue Gas Outlet Temp	°F	103.86
CW Inlet Temp	°F	64.97
CW Outlet Temp	°F	129.58
Inlet y_{H2O}	%	18.18
Outlet y_{H2O}	%	5.82
Condensation Rate	lb/hr	900076
	Units	Pressure Drop in CHX
Flue Gas Side ΔP	psi	1.924
Total CW Side ΔP	psi	766.402
	Units	Power
ID Fan Power	kW	9541.71
CW Pump Power	kW	14278.96
Refrigeration Compressor Power (T_{CW} From 80°F to 65 °F)	kW	4962.63
Annual Power Cost (7000hr/yr, $70/Million kWh)	Milli$	14.10
	Units	Geometry
Total Duct Length	ft	51
Total # of Row	-	84
Nickel Alloy 22 Tube Surface Area	ft^2	0
Stainless Steel Tube Surface Area	ft^2	314266.1
Total Capital Cost (Including Manufacture & Installation Cost)	Milli$	12.98

$T_{FGAS,\ in}$=197°F, $T_{FGAS,\ out}$=110°F, P_{FGAS}=19.7psia, $\dot{m}_{FGAS}$=10634586 lb/hr		
Case		**With Spray Cooler**
	Units	Temperatures and Condensation Rate
Flue Gas Mass Flow Rate	lb/hr	10723341.37
CW Mass Flow Rate	lb/hr	15548844.99 (1.45)
Flue Gas Inlet Temp	°F	165
Flue Gas Outlet Temp	°F	110.35
CW Inlet Temp	°F	64.96
CW Outlet Temp	°F	130.32
Inlet y_{H2O}	%	18.18
Outlet y_{H2O}	%	6.94
Condensation Rate	lb/hr	828405
	Units	Pressure Drop in CHX
Flue Gas Side ΔP	psi	1.684
Total CW Side ΔP	psi	553.282
	Units	Power
ID Fan Power	kW	8445.83
CW Pump Power	kW	9341.91
Refrigeration Compressor Power (T_{CW} From 80°F to 65 °F)	kW	4496.57
Annual Power Cost (7000hr/yr, $70/Million kWh)	Milli$	10.92
	Units	Geometry
Total Duct Length	ft	42
Total # of Row	-	72
Nickel Alloy 22 Tube Surface Area	ft^2	0
Stainless Steel Tube Surface Area	ft^2	269384.6
Total Capital Cost (Including Manufacture & Installation Cost)	Milli$	11.12

$T_{FGAS,\ in}$=197°F, $T_{FGAS,\ out}$=120°F, P_{FGAS}=19.7psia, $\dot{m}_{FGAS}$=10634586 lb/hr		
Case		**With Spray Cooler**
	Units	Temperatures and Condensation Rate
Flue Gas Mass Flow Rate	lb/hr	10723341.37
CW Mass Flow Rate	lb/hr	16621179.12 (1.55)
Flue Gas Inlet Temp	°F	165
Flue Gas Outlet Temp	°F	120.08
CW Inlet Temp	°F	64.95
CW Outlet Temp	°F	116.57
Inlet y_{H2O}	%	18.18
Outlet y_{H2O}	%	8.89
Condensation Rate	lb/hr	699262
	Units	Pressure Drop in CHX
Flue Gas Side ΔP	psi	1.147
Total CW Side ΔP	psi	451.128
	Units	Power
ID Fan Power	kW	5827.73
CW Pump Power	kW	8142.38
Refrigeration Compressor Power (T_{CW} From 80°F to 65 °F)	kW	4807.53
Annual Power Cost (7000hr/yr, $70/Million kWh)	Milli$	9.20
	Units	Geometry
Total Duct Length	ft	30
Total # of Row	-	48
Nickel Alloy 22 Tube Surface Area	ft^2	0
Stainless Steel Tube Surface Area	ft^2	179621.8
Total Capital Cost (Including Manufacture & Installation Cost)	Milli$	7.42

$T_{FGAS,\ in}$=197°F, $T_{FGAS,\ out}$=130°F, P_{FGAS}=19.7psia, $\dot{m}_{FGAS}$=10634586 lb/hr		
Case		**With Spray Cooler**
	Units	Temperatures and Condensation Rate
Flue Gas Mass Flow Rate	lb/hr	10723341.37
CW Mass Flow Rate	lb/hr	13404176.71 (1.25)
Flue Gas Inlet Temp	°F	165
Flue Gas Outlet Temp	°F	129.82
CW Inlet Temp	°F	64.95
CW Outlet Temp	°F	116.61
Inlet y_{H2O}	%	18.18
Outlet y_{H2O}	%	10.81
Condensation Rate	lb/hr	566563
	Units	Pressure Drop in CHX
Flue Gas Side ΔP	psi	0.885
Total CW Side ΔP	psi	237.19
	Units	Power
ID Fan Power	kW	4569.12
CW Pump Power	kW	3452.44
Refrigeration Compressor Power (T_{CW} From 80°F to 65 °F)	kW	3876.15
Annual Power Cost (7000hr/yr, $70/Million kWh)	Milli$	5.83
	Units	Geometry
Total Duct Length	ft	24
Total # of Row	-	36
Nickel Alloy 22 Tube Surface Area	ft^2	0
Stainless Steel Tube Surface Area	ft^2	134740.3
Total Capital Cost (Including Manufacture & Installation Cost)	Milli$	5.56

$T_{FGAS,\,in}$=174°F, $T_{FGAS,\,out}$=100°F, P_{FGAS}=17.7psia, $\dot{m}_{FGAS}$=10634586lb/hr		
Case		**With Spray Cooler**
	Units	Temperatures and Condensation Rate
Flue Gas Mass Flow Rate	lb/hr	10686971.12
CW Mass Flow Rate	lb/hr	15816717.26 (1.48)
Flue Gas Inlet Temp	°F	155
Flue Gas Outlet Temp	°F	99.47
CW Inlet Temp	°F	64.56
CW Outlet Temp	°F	131.91
Inlet y_{H2O}	%	17.75
Outlet y_{H2O}	%	5.64
Condensation Rate	lb/hr	875305
	Units	Pressure Drop in CHX
Flue Gas Side ΔP	psi	2.425
Total CW Side ΔP	psi	735.17
	Units	Power
ID Fan Power	kW	11886.36
CW Pump Power	kW	12626.81
Refrigeration Compressor Power (T_{CW} From 80°F to 65 °F)	kW	4574.87
Annual Power Cost (7000hr/yr, $70/Million kWh)	Milli$	14.25
	Units	Geometry
Total Duct Length	ft	57
Total # of Row	-	96
Nickel Alloy 22 Tube Surface Area	ft^2	0
Stainless Steel Tube Surface Area	ft^2	358965.1
Total Capital Cost (Including Manufacture & Installation Cost)	Milli$	14.82

$T_{FGAS,\,in}$=174°F, $T_{FGAS,\,out}$=104°F, P_{FGAS}=17.7psia, $\dot{m}_{FGAS}$=10634586lb/hr		
Case		**With Spray Cooler**
	Units	Temperatures and Condensation Rate
Flue Gas Mass Flow Rate	lb/hr	10686971.12
CW Mass Flow Rate	lb/hr	17633502.35 (1.65)
Flue Gas Inlet Temp	°F	155
Flue Gas Outlet Temp	°F	104.26
CW Inlet Temp	°F	64.77
CW Outlet Temp	°F	121.03
Inlet y_{H2O}	%	17.75
Outlet y_{H2O}	%	6.58
Condensation Rate	lb/hr	814962.2
	Units	Pressure Drop in CHX
Flue Gas Side ΔP	psi	1.826
Total CW Side ΔP	psi	708.248
	Units	Power
ID Fan Power	kW	8987.75
CW Pump Power	kW	13561.66
Refrigeration Compressor Power (T_{CW} From 80°F to 65 °F)	kW	5099.84
Annual Power Cost (7000hr/yr, $70/Million kWh)	Milli$	13.55
	Units	Geometry
Total Duct Length	ft	42
Total # of Row	-	72
Nickel Alloy 22 Tube Surface Area	ft^2	0
Stainless Steel Tube Surface Area	ft^2	269384.6
Total Capital Cost (Including Manufacture & Installation Cost)	Milli$	11.12

$T_{FGAS,\,in}$=174°F, $T_{FGAS,\,out}$=110°F, P_{FGAS}=17.7psia, $\dot{m}_{FGAS}$=10634586lb/hr		
Case		**With Spray Cooler**
	Units	Temperatures and Condensation Rate
Flue Gas Mass Flow Rate	lb/hr	10686971.12
CW Mass Flow Rate	lb/hr	16030456.68 (1.5)
Flue Gas Inlet Temp	°F	155
Flue Gas Outlet Temp	°F	110.41
CW Inlet Temp	°F	64.81
CW Outlet Temp	°F	120.64
Inlet y_{H2O}	%	17.75
Outlet y_{H2O}	%	7.77
Condensation Rate	lb/hr	737746
	Units	Pressure Drop in CHX
Flue Gas Side ΔP	psi	1.552
Total CW Side ΔP	psi	504.054
	Units	Power
ID Fan Power	kW	7718.2
CW Pump Power	kW	8774.31
Refrigeration Compressor Power (T_{CW} From 80°F to 65 °F)	kW	4636.76
Annual Power Cost (7000hr/yr, $70/Million kWh)	Milli$	10.35
	Units	Geometry
Total Duct Length	ft	36
Total # of Row	-	60
Nickel Alloy 22 Tube Surface Area	ft^2	0
Stainless Steel Tube Surface Area	ft^2	224501.4
Total Capital Cost (Including Manufacture & Installation Cost)	Milli$	9.27

$T_{FGAS,\,in}$=174°F, $T_{FGAS,\,out}$=120°F, P_{FGAS}=17.7psia, $\dot{m}_{FGAS}$=10634586lb/hr		
Case		**With Spray Cooler**
	Units	Temperatures and Condensation Rate
Flue Gas Mass Flow Rate	lb/hr	10686971.12
CW Mass Flow Rate	lb/hr	11755668.23 (1.1)
Flue Gas Inlet Temp	°F	155
Flue Gas Outlet Temp	°F	120.04
CW Inlet Temp	°F	64.43
CW Outlet Temp	°F	126.65
Inlet y_{H2O}	%	17.75
Outlet y_{H2O}	%	9.71
Condensation Rate	lb/hr	607253.7
	Units	Pressure Drop in CHX
Flue Gas Side ΔP	psi	1.281
Total CW Side ΔP	psi	229.316
	Units	Power
ID Fan Power	kW	6494.88
CW Pump Power	kW	2927.32
Refrigeration Compressor Power (T_{CW} From 80°F to 65 °F)	kW	3399.65
Annual Power Cost (7000hr/yr, $70/Million kWh)	Milli$	6.28
	Units	Geometry
Total Duct Length	ft	30
Total # of Row	-	48
Nickel Alloy 22 Tube Surface Area	ft^2	0
Stainless Steel Tube Surface Area	ft^2	179621.8
Total Capital Cost (Including Manufacture & Installation Cost)	Milli$	7.42

$T_{FGAS,\,in}$=174°F, $T_{FGAS,\,out}$=130°F, P_{FGAS}=17.7psia, $\dot{m}_{FGAS}$=10634586lb/hr		
Case		**With Spray Cooler**
	Units	Temperatures and Condensation Rate
Flue Gas Mass Flow Rate	lb/hr	10686971.12
CW Mass Flow Rate	lb/hr	8335837.47 (0.78)
Flue Gas Inlet Temp	°F	155
Flue Gas Outlet Temp	°F	129.64
CW Inlet Temp	°F	64.54
CW Outlet Temp	°F	130.58
Inlet y_{H2O}	%	17.75
Outlet y_{H2O}	%	11.80
Condensation Rate	lb/hr	459631
	Units	Pressure Drop in CHX
Flue Gas Side ΔP	psi	0.990
Total CW Side ΔP	psi	93.964
	Units	Power
ID Fan Power	kW	5099.40
CW Pump Power	kW	850.55
Refrigeration Compressor Power (T_{CW} From 80°F to 65 °F)	kW	2410.10
Annual Power Cost (7000hr/yr, $70/Million kWh)	Milli$	4.10
	Units	Geometry
Total Duct Length	ft	24
Total # of Row	-	36
Nickel Alloy 22 Tube Surface Area	ft^2	0
Stainless Steel Tube Surface Area	ft^2	134740.3
Total Capital Cost (Including Manufacture & Installation Cost)	Milli$	5.56

$T_{FGAS,\ in}$=219°F, $T_{FGAS,\ out}$=100°F, P_{FGAS}=21.7psia, $\dot{m}_{FGAS}$=9561430lb/hr		
Case		**With Spray Cooler**
	Units	Temperatures and Condensation Rate
Flue Gas Mass Flow Rate	lb/hr	9671813.00
CW Mass Flow Rate	lb/hr	15474900.80 (1.6)
Flue Gas Inlet Temp	°F	175
Flue Gas Outlet Temp	°F	100.75
CW Inlet Temp	°F	64.87
CW Outlet Temp	°F	137.15
Inlet y_{H2O}	%	18.59
Outlet y_{H2O}	%	4.83
Condensation Rate	lb/hr	895,682
	Units	Pressure Drop in CHX
Flue Gas Side ΔP	psi	1.611
Total CW Side ΔP	psi	704.694
	Units	Power
ID Fan Power	kW	7213.25
CW Pump Power	kW	11841.83
Refrigeration Compressor Power (T_{CW} From 80°F to 65 °F)	kW	4474.94
Annual Power Cost (7000hr/yr, $70/Million kWh)	Milli$	11.53
	Units	Geometry
Total Duct Length	ft	57
Total # of Row	-	96
Nickel Alloy 22 Tube Surface Area	ft^2	0
Stainless Steel Tube Surface Area	ft^2	358965.1
Total Capital Cost (Including Manufacture & Installation Cost)	Milli$	14.82

$T_{FGAS,\ in}$=219°F, $T_{FGAS,\ out}$=104°F, P_{FGAS}=21.7psia, $\dot{m}_{FGAS}$=9561430lb/hr		
Case		**With Spray Cooler**
	Units	Temperatures and Condensation Rate
Flue Gas Mass Flow Rate	lb/hr	9,659,565
CW Mass Flow Rate	lb/hr	15,474,901 (1.6)
Flue Gas Inlet Temp	°F	175
Flue Gas Outlet Temp	°F	105.13
CW Inlet Temp	°F	64.95
CW Outlet Temp	°F	134.07
Inlet y_{H2O}	%	18.59
Outlet y_{H2O}	%	5.50
Condensation Rate	lb/hr	858,106
	Units	Pressure Drop in CHX
Flue Gas Side ΔP	psi	1.424
Total CW Side ΔP	psi	626.573
	Units	Power
ID Fan Power	kW	6415.86
CW Pump Power	kW	10529.04
Refrigeration Compressor Power (T_{CW} From 80°F to 65 °F)	kW	4474.94
Annual Power Cost (7000hr/yr, $70/Million kWh)	Milli$	10.50
	Units	Geometry
Total Duct Length	ft	51
Total # of Row	-	84
Nickel Alloy 22 Tube Surface Area	ft^2	0
Stainless Steel Tube Surface Area	ft^2	314265.8
Total Capital Cost (Including Manufacture & Installation Cost)	Milli$	12.98

$T_{FGAS,\ in}$=219°F, $T_{FGAS,\ out}$=110°F, P_{FGAS}=21.7psia, $\dot{m}_{FGAS}$=9561430lb/hr		
Case		**With Spray Cooler**
	Units	Temperatures and Condensation Rate
Flue Gas Mass Flow Rate	lb/hr	9671813.00
CW Mass Flow Rate	lb/hr	15474900.80 (1.6)
Flue Gas Inlet Temp	°F	175
Flue Gas Outlet Temp	°F	109.8
CW Inlet Temp	°F	64.53
CW Outlet Temp	°F	130
Inlet y_{H2O}	%	18.59
Outlet y_{H2O}	%	6.28
Condensation Rate	lb/hr	813,773
	Units	Pressure Drop in CHX
Flue Gas Side ΔP	psi	1.233
Total CW Side ΔP	psi	548.592
	Units	Power
ID Fan Power	kW	5597.45
CW Pump Power	kW	9218.62
Refrigeration Compressor Power (T_{CW} From 80°F to 65 °F)	kW	4474.94
Annual Power Cost (7000hr/yr, $70/Million kWh)	Milli$	9.45
	Units	Geometry
Total Duct Length	ft	42
Total # of Row	-	72
Nickel Alloy 22 Tube Surface Area	ft^2	0
Stainless Steel Tube Surface Area	ft^2	269385.3
Total Capital Cost (Including Manufacture & Installation Cost)	Milli$	11.12

$T_{FGAS, in}$=219°F, $T_{FGAS, out}$=120°F, P_{FGAS}=21.7psia, $\dot{m}_{FGAS}$=9561430lb/hr		
Case		**With Spray Cooler**
	Units	Temperatures and Condensation Rate
Flue Gas Mass Flow Rate	lb/hr	9671813.00
CW Mass Flow Rate	lb/hr	12573356.90 (1.3)
Flue Gas Inlet Temp	°F	175
Flue Gas Outlet Temp	°F	120.09
CW Inlet Temp	°F	64.92
CW Outlet Temp	°F	135.12
Inlet y_{H2O}	%	18.59
Outlet y_{H2O}	%	7.99
Condensation Rate	lb/hr	713,623
	Units	Pressure Drop in CHX
Flue Gas Side ΔP	psi	1.063
Total CW Side ΔP	psi	313.405
	Units	Power
ID Fan Power	kW	4912.64
CW Pump Power	kW	4279.03
Refrigeration Compressor Power (T_{CW} From 80°F to 65 °F)	kW	3633.03
Annual Power Cost (7000hr/yr, $70/Million kWh)	Milli$	6.28
	Units	Geometry
Total Duct Length	ft	36
Total # of Row	-	60
Nickel Alloy 22 Tube Surface Area	ft^2	0
Stainless Steel Tube Surface Area	ft^2	224501.4
Total Capital Cost (Including Manufacture & Installation Cost)	Milli$	9.27

$T_{FGAS,\ in}$=219°F, $T_{FGAS,\ out}$=130°F, P_{FGAS}=21.7psia, $\dot{m}_{FGAS}$=9561430lb/hr		
Case		**With Spray Cooler**
	Units	Temperatures and Condensation Rate
Flue Gas Mass Flow Rate	lb/hr	9671813.00
CW Mass Flow Rate	lb/hr	10155403.65 (1.05)
Flue Gas Inlet Temp	°F	175
Flue Gas Outlet Temp	°F	130.17
CW Inlet Temp	°F	64.80
CW Outlet Temp	°F	137.74
Inlet y_{H2O}	%	18.59
Outlet y_{H2O}	%	9.83
Condensation Rate	lb/hr	601568
	Units	Pressure Drop in CHX
Flue Gas Side ΔP	psi	0.875
Total CW Side ΔP	psi	172.277
	Units	Power
ID Fan Power	kW	4113.37
CW Pump Power	kW	1899.83
Refrigeration Compressor Power (T_{CW} From 80°F to 65 °F)	kW	2937.31
Annual Power Cost (7000hr/yr, $70/Million kWh)	Milli$	4.39
	Units	Geometry
Total Duct Length	ft	30
Total # of Row	-	48
Nickel Alloy 22 Tube Surface Area	ft^2	0
Stainless Steel Tube Surface Area	ft^2	179621.8
Total Capital Cost (Including Manufacture & Installation Cost)	Milli$	7.42

$T_{FGAS, in}$=197°F, $T_{FGAS, out}$=100°F, P_{FGAS}=19.7psia, $\dot{m}_{FGAS}$=9561430lb/hr		
Case		**With Spray Cooler**
	Units	Temperatures and Condensation Rate
Flue Gas Mass Flow Rate	lb/hr	9641229.00
CW Mass Flow Rate	lb/hr	14461843.50 (1.5)
Flue Gas Inlet Temp	°F	165
Flue Gas Outlet Temp	°F	100.21
CW Inlet Temp	°F	64.48
CW Outlet Temp	°F	136.39
Inlet y_{H2O}	%	18.18
Outlet y_{H2O}	%	5.21
Condensation Rate	lb/hr	843,589
	Units	Pressure Drop in CHX
Flue Gas Side ΔP	psi	1.772
Total CW Side ΔP	psi	617.477
	Units	Power
ID Fan Power	kW	7892.27
CW Pump Power	kW	9696.92
Refrigeration Compressor Power (T_{CW} From 80°F to 65 °F)	kW	4181.88
Annual Power Cost (7000hr/yr, $70/Million kWh)	Milli$	10.67
	Units	Geometry
Total Duct Length	ft	57
Total # of Row	-	96
Nickel Alloy 22 Tube Surface Area	ft^2	0
Stainless Steel Tube Surface Area	ft^2	358965.1
Total Capital Cost (Including Manufacture & Installation Cost)	Milli$	14.82

$T_{FGAS, in}$=197°F, $T_{FGAS, out}$=104°F, P_{FGAS}=19.7psia, $\dot{m}_{FGAS}$=9561430lb/hr		
Case		**With Spray Cooler**
	Units	Temperatures and Condensation Rate
Flue Gas Mass Flow Rate	lb/hr	9,641,229
CW Mass Flow Rate	lb/hr	14,461,844 (1.5)
Flue Gas Inlet Temp	°F	165
Flue Gas Outlet Temp	°F	104.12
CW Inlet Temp	°F	64.85
CW Outlet Temp	°F	133.54
Inlet y_{H2O}	%	18.18
Outlet y_{H2O}	%	5.85
Condensation Rate	lb/hr	807,504
	Units	Pressure Drop in CHX
Flue Gas Side ΔP	psi	1.562
Total CW Side ΔP	psi	549.008
	Units	Power
ID Fan Power	kW	6995.73
CW Pump Power	kW	8621.7
Refrigeration Compressor Power (T_{CW} From 80°F to 65 °F)	kW	4181.88
Annual Power Cost (7000hr/yr, $70/Million kWh)	Milli$	9.70
	Units	Geometry
Total Duct Length	ft	51
Total # of Row	-	84
Nickel Alloy 22 Tube Surface Area	ft^2	0
Stainless Steel Tube Surface Area	ft^2	314265.8
Total Capital Cost (Including Manufacture & Installation Cost)	Milli$	12.98

$T_{FGAS,\ in}$=197°F, $T_{FGAS,\ out}$=110°F, P_{FGAS}=19.7psia, $\dot{m}_{FGAS}$=9561430lb/hr		
Case		**With Spray Cooler**
	Units	Temperatures and Condensation Rate
Flue Gas Mass Flow Rate	lb/hr	9641229.00
CW Mass Flow Rate	lb/hr	13497720.60 (1.4)
Flue Gas Inlet Temp	°F	165
Flue Gas Outlet Temp	°F	109.95
CW Inlet Temp	°F	64.88
CW Outlet Temp	°F	132.95
Inlet y_{H2O}	%	18.18
Outlet y_{H2O}	%	6.86
Condensation Rate	lb/hr	749,253
	Units	Pressure Drop in CHX
Flue Gas Side ΔP	psi	1.363
Total CW Side ΔP	psi	419.943
	Units	Power
ID Fan Power	kW	6157.07
CW Pump Power	kW	6155.19
Refrigeration Compressor Power (T_{CW} From 80°F to 65 °F)	kW	3902.99
Annual Power Cost (7000hr/yr, $70/Million kWh)	Milli$	7.95
	Units	Geometry
Total Duct Length	ft	42
Total # of Row	-	72
Nickel Alloy 22 Tube Surface Area	ft^2	0
Stainless Steel Tube Surface Area	ft^2	269385.3
Total Capital Cost (Including Manufacture & Installation Cost)	Milli$	11.12

$T_{FGAS,\ in}$=197°F, $T_{FGAS,\ out}$=120°F, P_{FGAS}=19.7psia, $\dot{m}_{FGAS}$=9561430lb/hr		
Case		**With Spray Cooler**
	Units	Temperatures and Condensation Rate
Flue Gas Mass Flow Rate	lb/hr	9641229.00
CW Mass Flow Rate	lb/hr	13497720.60 (1.4)
Flue Gas Inlet Temp	°F	165
Flue Gas Outlet Temp	°F	120.30
CW Inlet Temp	°F	64.85
CW Outlet Temp	°F	121.94
Inlet y_{H2O}	%	18.18
Outlet y_{H2O}	%	8.88
Condensation Rate	lb/hr	629,346
	Units	Pressure Drop in CHX
Flue Gas Side ΔP	psi	0.930
Total CW Side ΔP	psi	300.438
	Units	Power
ID Fan Power	kW	4256.35
CW Pump Power	kW	4403.58
Refrigeration Compressor Power (T_{CW} From 80°F to 65 °F)	kW	3902.99
Annual Power Cost (7000hr/yr, $70/Million kWh)	Milli$	6.16
	Units	Geometry
Total Duct Length	ft	30
Total # of Row	-	48
Nickel Alloy 22 Tube Surface Area	ft^2	0
Stainless Steel Tube Surface Area	ft^2	179621.8
Total Capital Cost (Including Manufacture & Installation Cost)	Milli$	7.42

$T_{FGAS,\ in}$=197°F, $T_{FGAS,\ out}$=130°F, P_{FGAS}=19.7psia, $\dot{m}_{FGAS}$=9561430lb/hr		
Case		**With Spray Cooler**
	Units	Temperatures and Condensation Rate
Flue Gas Mass Flow Rate	lb/hr	9641229.00
CW Mass Flow Rate	lb/hr	10605351.90 (1.1)
Flue Gas Inlet Temp	°F	165
Flue Gas Outlet Temp	°F	130.36
CW Inlet Temp	°F	64.83
CW Outlet Temp	°F	123.00
Inlet y_{H2O}	%	18.18
Outlet y_{H2O}	%	10.87
Condensation Rate	lb/hr	506113
	Units	Pressure Drop in CHX
Flue Gas Side ΔP	psi	0.719
Total CW Side ΔP	psi	150.241
	Units	Power
ID Fan Power	kW	3340.49
CW Pump Power	kW	1730.24
Refrigeration Compressor Power (T_{CW} From 80°F to 65 °F)	kW	3067.81
Annual Power Cost (7000hr/yr, $70/Million kWh)	Milli$	3.99
	Units	Geometry
Total Duct Length	ft	24
Total # of Row	-	36
Nickel Alloy 22 Tube Surface Area	ft^2	0
Stainless Steel Tube Surface Area	ft^2	134740.3
Total Capital Cost (Including Manufacture & Installation Cost)	Milli$	5.56

$T_{FGAS, in}$=174°F, $T_{FGAS, out}$=100°F, P_{FGAS}=17.7psia, $\dot{m}_{FGAS}$=9561430lb/hr		
Case		**With Spray Cooler**
	Units	Temperatures and Condensation Rate
Flue Gas Mass Flow Rate	lb/hr	9608528.00
CW Mass Flow Rate	lb/hr	13451939.20 (1.4)
Flue Gas Inlet Temp	°F	155
Flue Gas Outlet Temp	°F	100.83
CW Inlet Temp	°F	65.3
CW Outlet Temp	°F	135.3
Inlet y_{H2O}	%	17.75
Outlet y_{H2O}	%	5.84
Condensation Rate	lb/hr	775,315
	Units	Pressure Drop in CHX
Flue Gas Side ΔP	psi	1.979
Total CW Side ΔP	psi	535.891
	Units	Power
ID Fan Power	kW	8774.95
CW Pump Power	kW	7828.01
Refrigeration Compressor Power (T_{CW} From 80°F to 65 °F)	kW	3890.32
Annual Power Cost (7000hr/yr, $70/Million kWh)	Milli$	10.04
	Units	Geometry
Total Duct Length	ft	57
Total # of Row	-	96
Nickel Alloy 22 Tube Surface Area	ft^2	0
Stainless Steel Tube Surface Area	ft^2	358965.1
Total Capital Cost (Including Manufacture & Installation Cost)	Milli$	14.82

$T_{FGAS, in}$=174°F, $T_{FGAS, out}$=104°F, P_{FGAS}=17.7psia, $\dot{m}_{FGAS}$=9561430lb/hr		
Case		**With Spray Cooler**
	Units	Temperatures and Condensation Rate
Flue Gas Mass Flow Rate	lb/hr	9,608,528
CW Mass Flow Rate	lb/hr	15,373,645 (1.6)
Flue Gas Inlet Temp	°F	155
Flue Gas Outlet Temp	°F	103.59
CW Inlet Temp	°F	64.63
CW Outlet Temp	°F	123.26
Inlet y_{H2O}	%	17.75
Outlet y_{H2O}	%	6.45
Condensation Rate	lb/hr	740,626
	Units	Pressure Drop in CHX
Flue Gas Side ΔP	psi	1.476
Total CW Side ΔP	psi	542.001
	Units	Power
ID Fan Power	kW	6534.72
CW Pump Power	kW	9048.28
Refrigeration Compressor Power (T_{CW} From 80°F to 65 °F)	kW	4445.86
Annual Power Cost (7000hr/yr, $70/Million kWh)	Milli$	9.81
	Units	Geometry
Total Duct Length	ft	42
Total # of Row	-	72
Nickel Alloy 22 Tube Surface Area	ft^2	0
Stainless Steel Tube Surface Area	ft^2	269384.3
Total Capital Cost (Including Manufacture & Installation Cost)	Milli$	11.12

$T_{FGAS,\ in}$=174°F, $T_{FGAS,\ out}$=110°F, P_{FGAS}=17.7psia, $\dot{m}_{FGAS}$=9561430lb/hr		
Case		**With Spray Cooler**
	Units	Temperatures and Condensation Rate
Flue Gas Mass Flow Rate	lb/hr	9608528.00
CW Mass Flow Rate	lb/hr	14412792.00 (1.5)
Flue Gas Inlet Temp	°F	155
Flue Gas Outlet Temp	°F	109.31
CW Inlet Temp	°F	64.75
CW Outlet Temp	°F	121.7
Inlet y_{H2O}	%	17.75
Outlet y_{H2O}	%	7.55
Condensation Rate	lb/hr	676,316
	Units	Pressure Drop in CHX
Flue Gas Side ΔP	psi	1.252
Total CW Side ΔP	psi	409.717
	Units	Power
ID Fan Power	kW	5591.28
CW Pump Power	kW	6412.43
Refrigeration Compressor Power (T_{CW} From 80°F to 65 °F)	kW	4167.72
Annual Power Cost (7000hr/yr, $70/Million kWh)	Milli$	7.92
	Units	Geometry
Total Duct Length	ft	36
Total # of Row	-	60
Nickel Alloy 22 Tube Surface Area	ft^2	0
Stainless Steel Tube Surface Area	ft^2	224501.4
Total Capital Cost (Including Manufacture & Installation Cost)	Milli$	9.27

$T_{FGAS,\ in}$=174°F, $T_{FGAS,\ out}$=120°F, P_{FGAS}=17.7psia, $\dot{m}_{FGAS}$=9561430lb/hr		
Case		**With Spray Cooler**
	Units	Temperatures and Condensation Rate
Flue Gas Mass Flow Rate	lb/hr	9608528.00
CW Mass Flow Rate	lb/hr	15373644.80 (1.6)
Flue Gas Inlet Temp	°F	155
Flue Gas Outlet Temp	°F	120.95
CW Inlet Temp	°F	65.54
CW Outlet Temp	°F	106.54
Inlet y_{H2O}	%	17.74
Outlet y_{H2O}	%	10.14
Condensation Rate	lb/hr	518,981
	Units	Pressure Drop in CHX
Flue Gas Side ΔP	psi	0.772
Total CW Side ΔP	psi	310.396
	Units	Power
ID Fan Power	kW	2851.63
CW Pump Power	kW	4086.12
Refrigeration Compressor Power (T_{CW} From 80°F to 65 °F)	kW	4445.86
Annual Power Cost (7000hr/yr, $70/Million kWh)	Milli$	5.58
	Units	Geometry
Total Duct Length	ft	24
Total # of Row	-	36
Nickel Alloy 22 Tube Surface Area	ft^2	0
Stainless Steel Tube Surface Area	ft^2	134739.8
Total Capital Cost (Including Manufacture & Installation Cost)	Milli$	5.56

$T_{FGAS,\ in}$=174°F, $T_{FGAS,\ out}$=130°F, P_{FGAS}=17.7psia, $\dot{m}_{FGAS}$=9561430lb/hr		
Case		**With Spray Cooler**
	Units	Temperatures and Condensation Rate
Flue Gas Mass Flow Rate	lb/hr	9608528.00
CW Mass Flow Rate	lb/hr	13451939.20 (1.4)
Flue Gas Inlet Temp	°F	155
Flue Gas Outlet Temp	°F	130.18
CW Inlet Temp	°F	65.22
CW Outlet Temp	°F	99.95
Inlet y_{H2O}	%	17.74
Outlet y_{H2O}	%	12.24
Condensation Rate	lb/hr	384553
	Units	Pressure Drop in CHX
Flue Gas Side ΔP	psi	0.530
Total CW Side ΔP	psi	179.518
	Units	Power
ID Fan Power	kW	2448.72
CW Pump Power	kW	2622.31
Refrigeration Compressor Power (T_{CW} From 80°F to 65 °F)	kW	3890.32
Annual Power Cost (7000hr/yr, $70/Million kWh)	Milli$	4.39
	Units	Geometry
Total Duct Length	ft	18
Total # of Row	-	24
Nickel Alloy 22 Tube Surface Area	ft^2	0
Stainless Steel Tube Surface Area	ft^2	89858.9
Total Capital Cost (Including Manufacture & Installation Cost)	Milli$	3.71

$T_{FGAS,\ in}$=219°F, $T_{FGAS,\ out}$=100°F, P_{FGAS}=21.7psia, $\dot{m}_{FGAS}$=8452640lb/hr		
Case		**With Spray Cooler**
	Units	Temperatures and Condensation Rate
Flue Gas Mass Flow Rate	lb/hr	8539395.00
CW Mass Flow Rate	lb/hr	13236062.25 (1.55)
Flue Gas Inlet Temp	°F	180
Flue Gas Outlet Temp	°F	100.5
CW Inlet Temp	°F	64.67
CW Outlet Temp	°F	139.88
Inlet y_{H2O}	%	18.43
Outlet y_{H2O}	%	4.7
Condensation Rate	lb/hr	787,196
	Units	Pressure Drop in CHX
Flue Gas Side ΔP	psi	1.263
Total CW Side ΔP	psi	519.884
	Units	Power
ID Fan Power	kW	5022.25
CW Pump Power	kW	7472.33
Refrigeration Compressor Power (T_{CW} From 80°F to 65 °F)	kW	3827.68
Annual Power Cost (7000hr/yr, $70/Million kWh)	Milli$	8.00
	Units	Geometry
Total Duct Length	ft	57
Total # of Row	-	96
Nickel Alloy 22 Tube Surface Area	ft^2	100
Stainless Steel Tube Surface Area	ft^2	358865
Total Capital Cost (Including Manufacture & Installation Cost)	Milli$	14.84

$T_{FGAS,\ in}$=219°F, $T_{FGAS,\ out}$=104°F, P_{FGAS}=21.7psia, $\dot{m}_{FGAS}$=8452640lb/hr		
Case		**With Spray Cooler**
	Units	Temperatures and Condensation Rate
Flue Gas Mass Flow Rate	lb/hr	8,539,395
CW Mass Flow Rate	lb/hr	14,090,002 (1.65)
Flue Gas Inlet Temp	°F	180
Flue Gas Outlet Temp	°F	103.43
CW Inlet Temp	°F	64.96
CW Outlet Temp	°F	133.76
Inlet y_{H2O}	%	18.42
Outlet y_{H2O}	%	5.11
Condensation Rate	lb/hr	766,905
	Units	Pressure Drop in CHX
Flue Gas Side ΔP	psi	1.107
Total CW Side ΔP	psi	522.302
	Units	Power
ID Fan Power	kW	4406.15
CW Pump Power	kW	7991.4
Refrigeration Compressor Power (T_{CW} From 80°F to 65 °F)	kW	4074.50
Annual Power Cost (7000hr/yr, $70/Million kWh)	Milli$	8.07
	Units	Geometry
Total Duct Length	ft	51
Total # of Row	-	84
Nickel Alloy 22 Tube Surface Area	ft^2	0
Stainless Steel Tube Surface Area	ft^2	314265.8
Total Capital Cost (Including Manufacture & Installation Cost)	Milli$	12.98

$T_{FGAS,\ in}$=219°F, $T_{FGAS,\ out}$=110°F, P_{FGAS}=21.7psia, $\dot{m}_{FGAS}$=8452640lb/hr		
Case		**With Spray Cooler**
	Units	Temperatures and Condensation Rate
Flue Gas Mass Flow Rate	lb/hr	8539395.00
CW Mass Flow Rate	lb/hr	13236062.25 (1.55)
Flue Gas Inlet Temp	°F	180
Flue Gas Outlet Temp	°F	110.18
CW Inlet Temp	°F	64.96
CW Outlet Temp	°F	133.14
Inlet y_{H2O}	%	18.42
Outlet y_{H2O}	%	6.12
Condensation Rate	lb/hr	716,342
	Units	Pressure Drop in CHX
Flue Gas Side ΔP	psi	0.967
Total CW Side ΔP	psi	404.562
	Units	Power
ID Fan Power	kW	3894.68
CW Pump Power	kW	5814.78
Refrigeration Compressor Power (T_{CW} From 80°F to 65 °F)	kW	3827.68
Annual Power Cost (7000hr/yr, $70/Million kWh)	Milli$	6.63
	Units	Geometry
Total Duct Length	ft	42
Total # of Row	-	72
Nickel Alloy 22 Tube Surface Area	ft^2	0
Stainless Steel Tube Surface Area	ft^2	269385.3
Total Capital Cost (Including Manufacture & Installation Cost)	Milli$	11.12

$T_{FGAS,\ in}$=219°F, $T_{FGAS,\ out}$=120°F, P_{FGAS}=21.7psia, $\dot{m}_{FGAS}$=8452640lb/hr		
Case		**With Spray Cooler**
	Units	Temperatures and Condensation Rate
Flue Gas Mass Flow Rate	lb/hr	8539395.00
CW Mass Flow Rate	lb/hr	11101213.50 (1.3)
Flue Gas Inlet Temp	°F	180
Flue Gas Outlet Temp	°F	119.98
CW Inlet Temp	°F	64.88
CW Outlet Temp	°F	136.58
Inlet y_{H2O}	%	18.43
Outlet y_{H2O}	%	7.7
Condensation Rate	lb/hr	634,970
	Units	Pressure Drop in CHX
Flue Gas Side ΔP	psi	0.831
Total CW Side ΔP	psi	246.083
	Units	Power
ID Fan Power	kW	3404.49
CW Pump Power	kW	2966.48
Refrigeration Compressor Power (T_{CW} From 80°F to 65 °F)	kW	3210.24
Annual Power Cost (7000hr/yr, $70/Million kWh)	Milli$	4.69
	Units	Geometry
Total Duct Length	ft	36
Total # of Row	-	60
Nickel Alloy 22 Tube Surface Area	ft^2	100.1
Stainless Steel Tube Surface Area	ft^2	224501.4
Total Capital Cost (Including Manufacture & Installation Cost)	Milli$	9.27

$T_{FGAS,\ in}$=219°F, $T_{FGAS,\ out}$=130°F, P_{FGAS}=21.7psia, $\dot{m}_{FGAS}$=8452640lb/hr		
Case		**With Spray Cooler**
	Units	Temperatures and Condensation Rate
Flue Gas Mass Flow Rate	lb/hr	8539395.00
CW Mass Flow Rate	lb/hr	9393334.50 (1.1)
Flue Gas Inlet Temp	°F	180
Flue Gas Outlet Temp	°F	129.81
CW Inlet Temp	°F	180
CW Outlet Temp	°F	129.81
Inlet y_{H2O}	%	18.43
Outlet y_{H2O}	%	9.39
Condensation Rate	lb/hr	545111
	Units	Pressure Drop in CHX
Flue Gas Side ΔP	psi	0.681
Total CW Side ΔP	psi	148.172
	Units	Power
ID Fan Power	kW	2838.22
CW Pump Power	kW	1511.38
Refrigeration Compressor Power (T_{CW} From 80°F to 65 °F)	kW	2716.59
Annual Power Cost (7000hr/yr, $70/Million kWh)	Milli$	3.46
	Units	Geometry
Total Duct Length	ft	30
Total # of Row	-	48
Nickel Alloy 22 Tube Surface Area	ft^2	99.95
Stainless Steel Tube Surface Area	ft^2	179621.8
Total Capital Cost (Including Manufacture & Installation Cost)	Milli$	7.43

$T_{FGAS,\ in}$=197°F, $T_{FGAS,\ out}$=100°F, P_{FGAS}=19.7psia, $\dot{m}_{FGAS}$=8452640lb/hr		
Case		**With Spray Cooler**
	Units	Temperatures and Condensation Rate
Flue Gas Mass Flow Rate	lb/hr	8512340.00
CW Mass Flow Rate	lb/hr	12768510.00 (1.5)
Flue Gas Inlet Temp	°F	170
Flue Gas Outlet Temp	°F	100.16
CW Inlet Temp	°F	65.04
CW Outlet Temp	°F	138.17
Inlet y_{H2O}	%	18.16
Outlet y_{H2O}	%	5.1
Condensation Rate	lb/hr	748,948
	Units	Pressure Drop in CHX
Flue Gas Side ΔP	psi	1.388
Total CW Side ΔP	psi	484.602
	Units	Power
ID Fan Power	kW	5480.28
CW Pump Power	kW	6719.18
Refrigeration Compressor Power (T_{CW} From 80°F to 65 °F)	kW	3692.71
Annual Power Cost (7000hr/yr, $70/Million kWh)	Milli$	7.79
	Units	Geometry
Total Duct Length	ft	57
Total # of Row	-	96
Nickel Alloy 22 Tube Surface Area	ft^2	100
Stainless Steel Tube Surface Area	ft^2	358865
Total Capital Cost (Including Manufacture & Installation Cost)	Milli$	14.82

$T_{FGAS,\ in}$=197°F, $T_{FGAS,\ out}$=104°F, P_{FGAS}=19.7psia, $\dot{m}_{FGAS}$=8452640lb/hr		
Case		**With Spray Cooler**
	Units	Temperatures and Condensation Rate
Flue Gas Mass Flow Rate	lb/hr	8512340.00
CW Mass Flow Rate	lb/hr	12342893.00 (1.4)
Flue Gas Inlet Temp	°F	170
Flue Gas Outlet Temp	°F	104.43
CW Inlet Temp	°F	64.49
CW Outlet Temp	°F	136.57
Inlet y_{H2O}	%	18.16
Outlet y_{H2O}	%	5.78
Condensation Rate	lb/hr	714890
	Units	Pressure Drop in CHX
Flue Gas Side ΔP	psi	1.227
Total CW Side ΔP	psi	403.389
	Units	Power
ID Fan Power	kW	4878.27
CW Pump Power	kW	5406.71
Refrigeration Compressor Power (T_{CW} From 80°F to 65 °F)	kW	3569.67
Annual Power Cost (7000hr/yr, $70/Million kWh)	Milli$	6.79
	Units	Geometry
Total Duct Length	ft	51
Total # of Row	-	84
Nickel Alloy 22 Tube Surface Area	ft^2	99.95
Stainless Steel Tube Surface Area	ft^2	314165.7
Total Capital Cost (Including Manufacture & Installation Cost)	Milli$	12.99

$T_{FGAS,\ in}$=197°F, $T_{FGAS,\ out}$=110°F, P_{FGAS}=19.7psia, $\dot{m}_{FGAS}$=8452640lb/hr		
Case		**With Spray Cooler**
	Units	Temperatures and Condensation Rate
Flue Gas Mass Flow Rate	lb/hr	8512340.00
CW Mass Flow Rate	lb/hr	11917276.00 (1.4)
Flue Gas Inlet Temp	°F	170
Flue Gas Outlet Temp	°F	109.8
CW Inlet Temp	°F	64.79
CW Outlet Temp	°F	134.61
Inlet y_{H2O}	%	18.16
Outlet y_{H2O}	%	6.66
Condensation Rate	lb/hr	670,461
	Units	Pressure Drop in CHX
Flue Gas Side ΔP	psi	1.065
Total CW Side ΔP	psi	329.697
	Units	Power
ID Fan Power	kW	4267.58
CW Pump Power	kW	4266.58
Refrigeration Compressor Power (T_{CW} From 80°F to 65 °F)	kW	3445.88
Annual Power Cost (7000hr/yr, $70/Million kWh)	Milli$	5.87
	Units	Geometry
Total Duct Length	ft	42
Total # of Row	-	72
Nickel Alloy 22 Tube Surface Area	ft^2	0
Stainless Steel Tube Surface Area	ft^2	269385.3
Total Capital Cost (Including Manufacture & Installation Cost)	Milli$	11.12

$T_{FGAS,\ in}$=197°F, $T_{FGAS,\ out}$=120°F, P_{FGAS}=19.7psia, $\dot{m}_{FGAS}$=8452640lb/hr		
Case		**With Spray Cooler**
	Units	Temperatures and Condensation Rate
Flue Gas Mass Flow Rate	lb/hr	8512340.00
CW Mass Flow Rate	lb/hr	12768510.00 (1.5)
Flue Gas Inlet Temp	°F	170
Flue Gas Outlet Temp	°F	119.82
CW Inlet Temp	°F	64.88
CW Outlet Temp	°F	120.85
Inlet y_{H2O}	%	64.88
Outlet y_{H2O}	%	8.46
Condensation Rate	lb/hr	576,254
	Units	Pressure Drop in CHX
Flue Gas Side ΔP	psi	0.724
Total CW Side ΔP	psi	269.806
	Units	Power
ID Fan Power	kW	2929.9
CW Pump Power	kW	3740.92
Refrigeration Compressor Power (T_{CW} From 80°F to 65 °F)	kW	3692.71
Annual Power Cost (7000hr/yr, $70/Million kWh)	Milli$	5.08
	Units	Geometry
Total Duct Length	ft	30
Total # of Row	-	48
Nickel Alloy 22 Tube Surface Area	ft^2	0
Stainless Steel Tube Surface Area	ft^2	179621.8
Total Capital Cost (Including Manufacture & Installation Cost)	Milli$	7.42

$T_{FGAS,\ in}$=197°F, $T_{FGAS,\ out}$=130°F, P_{FGAS}=19.7psia, $\dot{m}_{FGAS}$=8452640lb/hr		
Case		**With Spray Cooler**
	Units	Temperatures and Condensation Rate
Flue Gas Mass Flow Rate	lb/hr	8512340.00
CW Mass Flow Rate	lb/hr	11066042.00 (1.3)
Flue Gas Inlet Temp	°F	170
Flue Gas Outlet Temp	°F	129.64
CW Inlet Temp	°F	64.93
CW Outlet Temp	°F	118.23
Inlet y_{H2O}	%	18.15
Outlet y_{H2O}	%	10.3
Condensation Rate	lb/hr	476883
	Units	Pressure Drop in CHX
Flue Gas Side ΔP	psi	0.557
Total CW Side ΔP	psi	163.383
	Units	Power
ID Fan Power	kW	2290.55
CW Pump Power	kW	1963.3
Refrigeration Compressor Power (T_{CW} From 80°F to 65 °F)	kW	3199.80
Annual Power Cost (7000hr/yr, $70/Million kWh)	Milli$	3.65
	Units	Geometry
Total Duct Length	ft	24
Total # of Row	-	36
Nickel Alloy 22 Tube Surface Area	ft^2	0
Stainless Steel Tube Surface Area	ft^2	134740.3
Total Capital Cost (Including Manufacture & Installation Cost)	Milli$	5.56

$T_{FGAS,\ in}$=174°F, $T_{FGAS,\ out}$=100°F, P_{FGAS}=17.7psia, $\dot{m}_{FGAS}$=8452640lb/hr		
Case		**With Spray Cooler**
	Units	Temperatures and Condensation Rate
Flue Gas Mass Flow Rate	lb/hr	8494277.00
CW Mass Flow Rate	lb/hr	12741415.50 (1.5)
Flue Gas Inlet Temp	°F	155
Flue Gas Outlet Temp	°F	100.27
CW Inlet Temp	°F	64.74
CW Outlet Temp	°F	130.89
Inlet y_{H2O}	%	17.84
Outlet y_{H2O}	%	5.8
Condensation Rate	lb/hr	693,331
	Units	Pressure Drop in CHX
Flue Gas Side ΔP	psi	1.339
Total CW Side ΔP	psi	429.427
	Units	Power
ID Fan Power	kW	5241.48
CW Pump Power	kW	5941.52
Refrigeration Compressor Power (T_{CW} From 80°F to 65 °F)	kW	3684.50
Annual Power Cost (7000hr/yr, $70/Million kWh)	Milli$	7.29
	Units	Geometry
Total Duct Length	ft	51
Total # of Row	-	84
Nickel Alloy 22 Tube Surface Area	ft^2	0
Stainless Steel Tube Surface Area	ft^2	314266
Total Capital Cost (Including Manufacture & Installation Cost)	Milli$	12.98

$T_{FGAS, in}$=174°F, $T_{FGAS, out}$=104°F, P_{FGAS}=17.7psia, $\dot{m}_{FGAS}$=8452640lb/hr		
Case		**With Spray Cooler**
	Units	Temperatures and Condensation Rate
Flue Gas Mass Flow Rate	lb/hr	8,494,277
CW Mass Flow Rate	lb/hr	12,741,416 (1.5)
Flue Gas Inlet Temp	°F	155
Flue Gas Outlet Temp	°F	104.05
CW Inlet Temp	°F	64.94
CW Outlet Temp	°F	127.59
Inlet y_{H2O}	%	17.84
Outlet y_{H2O}	%	6.50
Condensation Rate	lb/hr	657,720
	Units	Pressure Drop in CHX
Flue Gas Side ΔP	psi	1.158
Total CW Side ΔP	psi	375.889
	Units	Power
ID Fan Power	kW	4549.92
CW Pump Power	kW	5200.78
Refrigeration Compressor Power (T_{CW} From 80°F to 65 °F)	kW	3684.50
Annual Power Cost (7000hr/yr, $70/Million kWh)	Milli$	6.58
	Units	Geometry
Total Duct Length	ft	42
Total # of Row	-	72
Nickel Alloy 22 Tube Surface Area	ft^2	0
Stainless Steel Tube Surface Area	ft^2	269384.3
Total Capital Cost (Including Manufacture & Installation Cost)	Milli$	11.12

$T_{FGAS,\ in}$=174°F, $T_{FGAS,\ out}$=110°F, P_{FGAS}=17.7psia, $\dot{m}_{FGAS}$=8452640lb/hr		
Case		**With Spray Cooler**
	Units	Temperatures and Condensation Rate
Flue Gas Mass Flow Rate	lb/hr	8494277.00
CW Mass Flow Rate	lb/hr	11891987.80 (1.4)
Flue Gas Inlet Temp	°F	155
Flue Gas Outlet Temp	°F	109.3
CW Inlet Temp	°F	64.37
CW Outlet Temp	°F	125.87
Inlet y_{H2O}	%	17.84
Outlet y_{H2O}	%	7.55
Condensation Rate	lb/hr	604,018
	Units	Pressure Drop in CHX
Flue Gas Side ΔP	psi	0.980
Total CW Side ΔP	psi	281.831
	Units	Power
ID Fan Power	kW	3882.01
CW Pump Power	kW	3639.43
Refrigeration Compressor Power (T_{CW} From 80°F to 65 °F)	kW	3439.17
Annual Power Cost (7000hr/yr, $70/Million kWh)	Milli$	5.37
	Units	Geometry
Total Duct Length	ft	36
Total # of Row	-	60
Nickel Alloy 22 Tube Surface Area	ft^2	0
Stainless Steel Tube Surface Area	ft^2	224501.4
Total Capital Cost (Including Manufacture & Installation Cost)	Milli$	9.27

$T_{FGAS, in}$=174°F, $T_{FGAS, out}$=120°F, P_{FGAS}=17.7psia, $\dot{m}_{FGAS}$=8452640lb/hr		
Case		**With Spray Cooler**
	Units	Temperatures and Condensation Rate
Flue Gas Mass Flow Rate	lb/hr	8494277.00
CW Mass Flow Rate	lb/hr	12316701.65 (1.45)
Flue Gas Inlet Temp	°F	155
Flue Gas Outlet Temp	°F	120.61
CW Inlet Temp	°F	64.98
CW Outlet Temp	°F	111.11
Inlet y_{H2O}	%	17.84
Outlet y_{H2O}	%	10.06
Condensation Rate	lb/hr	469,138
	Units	Pressure Drop in CHX
Flue Gas Side ΔP	psi	0.604
Total CW Side ΔP	psi	201.451
	Units	Power
ID Fan Power	kW	2431.88
CW Pump Power	kW	2694.35
Refrigeration Compressor Power (T_{CW} From 80°F to 65 °F)	kW	3561.46
Annual Power Cost (7000hr/yr, $70/Million kWh)	Milli$	4.26
	Units	Geometry
Total Duct Length	ft	24
Total # of Row	-	36
Nickel Alloy 22 Tube Surface Area	ft^2	0
Stainless Steel Tube Surface Area	ft^2	134739.8
Total Capital Cost (Including Manufacture & Installation Cost)	Milli$	5.56

$T_{FGAS,\ in}$=174°F, $T_{FGAS,\ out}$=130°F, P_{FGAS}=17.7psia, $\dot{m}_{FGAS}$=8452640lb/hr		
Case		**With Spray Cooler**
	Units	Temperatures and Condensation Rate
Flue Gas Mass Flow Rate	lb/hr	8494277.00
CW Mass Flow Rate	lb/hr	11042560.10 (1.3)
Flue Gas Inlet Temp	°F	155
Flue Gas Outlet Temp	°F	129.83
CW Inlet Temp	°F	65.36
CW Outlet Temp	°F	103.77
Inlet y_{H2O}	%	17.84
Outlet y_{H2O}	%	12.17
Condensation Rate	lb/hr	350160
	Units	Pressure Drop in CHX
Flue Gas Side ΔP	psi	0.414
Total CW Side ΔP	psi	122.136
	Units	Power
ID Fan Power	kW	1690.13
CW Pump Power	kW	1464.55
Refrigeration Compressor Power (T_{CW} From 80°F to 65 °F)	kW	3193.09
Annual Power Cost (7000hr/yr, $70/Million kWh)	Milli$	3.11
	Units	Geometry
Total Duct Length	ft	18
Total # of Row	-	24
Nickel Alloy 22 Tube Surface Area	ft^2	0
Stainless Steel Tube Surface Area	ft^2	89858.9
Total Capital Cost (Including Manufacture & Installation Cost)	Milli$	3.71

$T_{FGAS,\ in}$=219°F, $T_{FGAS,\ out}$=100°F, P_{FGAS}=21.7psia, $\dot{m}_{FGAS}$=7343850lb/hr		
Case		**With Spray Cooler**
	Units	Temperatures and Condensation Rate
Flue Gas Mass Flow Rate	lb/hr	7418893.24
CW Mass Flow Rate	lb/hr	11128339.86 (1.5)
Flue Gas Inlet Temp	°F	180
Flue Gas Outlet Temp	°F	100.19
CW Inlet Temp	°F	65.07
CW Outlet Temp	°F	142.93
Inlet y_{H2O}	%	18.42
Outlet y_{H2O}	%	4.66
Condensation Rate	lb/hr	685,283
	Units	Pressure Drop in CHX
Flue Gas Side ΔP	psi	0.958
Total CW Side ΔP	psi	371.157
	Units	Power
ID Fan Power	kW	3314.92
CW Pump Power	kW	4485.15
Refrigeration Compressor Power (T_{CW} From 80°F to 65 °F)	kW	3217.69
Annual Power Cost (7000hr/yr, $70/Million kWh)	Milli$	5.40
	Units	Geometry
Total Duct Length	ft	57
Total # of Row	-	96
Nickel Alloy 22 Tube Surface Area	ft^2	100
Stainless Steel Tube Surface Area	ft^2	358865
Total Capital Cost (Including Manufacture & Installation Cost)	Milli$	14.84

$T_{FGAS,\ in}$=219°F, $T_{FGAS,\ out}$=104°F, P_{FGAS}=21.7psia, $\dot{m}_{FGAS}$=7343850lb/hr		
Case		**With Spray Cooler**
	Units	Temperatures and Condensation Rate
Flue Gas Mass Flow Rate	lb/hr	7418893.24
CW Mass Flow Rate	lb/hr	11128339.86 (1.5)
Flue Gas Inlet Temp	°F	180
Flue Gas Outlet Temp	°F	103.94
CW Inlet Temp	°F	64.64
CW Outlet Temp	°F	139.75
Inlet y_{H2O}	%	18.42
Outlet y_{H2O}	%	5.20
Condensation Rate	lb/hr	662064
	Units	Pressure Drop in CHX
Flue Gas Side ΔP	psi	0.842
Total CW Side ΔP	psi	330.082
	Units	Power
ID Fan Power	kW	2931.72
CW Pump Power	kW	3988.8
Refrigeration Compressor Power (T_{CW} From 80°F to 65 °F)	kW	3217.70
Annual Power Cost (7000hr/yr, $70/Million kWh)	Milli$	4.97
	Units	Geometry
Total Duct Length	ft	51
Total # of Row	-	84
Nickel Alloy 22 Tube Surface Area	ft^2	99.95
Stainless Steel Tube Surface Area	ft^2	314165.7
Total Capital Cost (Including Manufacture & Installation Cost)	Milli$	12.99

$T_{FGAS,\ in}$=219°F, $T_{FGAS,\ out}$=110°F, P_{FGAS}=21.7psia, $\dot{m}_{FGAS}$=7343850lb/hr		
Case		**With Spray Cooler**
	Units	Temperatures and Condensation Rate
Flue Gas Mass Flow Rate	lb/hr	7418893.24
CW Mass Flow Rate	lb/hr	10386450.54 (1.4)
Flue Gas Inlet Temp	°F	180
Flue Gas Outlet Temp	°F	110.79
CW Inlet Temp	°F	64.64
CW Outlet Temp	°F	139.38
Inlet y_{H2O}	%	18.42
Outlet y_{H2O}	%	6.23
Condensation Rate	lb/hr	616,849
	Units	Pressure Drop in CHX
Flue Gas Side ΔP	psi	0.737
Total CW Side ΔP	psi	252.514
	Units	Power
ID Fan Power	kW	2590.03
CW Pump Power	kW	2848.02
Refrigeration Compressor Power (T_{CW} From 80°F to 65 °F)	kW	3003.68
Annual Power Cost (7000hr/yr, $70/Million kWh)	Milli$	4.14
	Units	Geometry
Total Duct Length	ft	42
Total # of Row	-	72
Nickel Alloy 22 Tube Surface Area	ft^2	0
Stainless Steel Tube Surface Area	ft^2	269385.3
Total Capital Cost (Including Manufacture & Installation Cost)	Milli$	11.12

$T_{FGAS, in}$=219°F, $T_{FGAS, out}$=120°F, P_{FGAS}=21.7psia, $\dot{m}_{FGAS}$=7343850lb/hr		
Case		**With Spray Cooler**
	Units	Temperatures and Condensation Rate
Flue Gas Mass Flow Rate	lb/hr	7418893.24
CW Mass Flow Rate	lb/hr	8902671.89 (1.2)
Flue Gas Inlet Temp	°F	180
Flue Gas Outlet Temp	°F	120.59
CW Inlet Temp	°F	65.04
CW Outlet Temp	°F	141.75
Inlet y_{H2O}	%	18.42
Outlet y_{H2O}	%	7.84
Condensation Rate	lb/hr	545026
	Units	Pressure Drop in CHX
Flue Gas Side ΔP	psi	0.632
Total CW Side ΔP	psi	160.31
	Units	Power
ID Fan Power	kW	2259.13
CW Pump Power	kW	1549.76
Refrigeration Compressor Power (T_{CW} From 80°F to 65 °F)	kW	2574.90
Annual Power Cost (7000hr/yr, $70/Million kWh)	Milli$	3.13
	Units	Geometry
Total Duct Length	ft	36
Total # of Row	-	60
Nickel Alloy 22 Tube Surface Area	ft^2	100.05
Stainless Steel Tube Surface Area	ft^2	224400.8
Total Capital Cost (Including Manufacture & Installation Cost)	Milli$	9.29

$T_{FGAS,\ in}$=219°F, $T_{FGAS,\ out}$=130°F, P_{FGAS}=21.7psia, $\dot{m}_{FGAS}$=7343850lb/hr		
Case		**With Spray Cooler**
	Units	Temperatures and Condensation Rate
Flue Gas Mass Flow Rate	lb/hr	7418893.24
CW Mass Flow Rate	lb/hr	12241173.85 (1.65)
Flue Gas Inlet Temp	°F	180
Flue Gas Outlet Temp	°F	130.44
CW Inlet Temp	°F	64.98
CW Outlet Temp	°F	112.57
Inlet y_{H2O}	%	18.41
Outlet y_{H2O}	%	9.60
Condensation Rate	lb/hr	462910
	Units	Pressure Drop in CHX
Flue Gas Side ΔP	psi	0.383
Total CW Side ΔP	psi	199.070
	Units	Power
ID Fan Power	kW	1376.07
CW Pump Power	kW	2646.17
Refrigeration Compressor Power (T_{CW} From 80°F to 65 °F)	kW	3539.84
Annual Power Cost (7000hr/yr, $70/Million kWh)	Milli$	3.71
	Units	Geometry
Total Duct Length	ft	24
Total # of Row	-	36
Nickel Alloy 22 Tube Surface Area	ft^2	0
Stainless Steel Tube Surface Area	ft^2	134740.3
Total Capital Cost (Including Manufacture & Installation Cost)	Milli$	5.56

$T_{FGAS,\ in}$=197°F, $T_{FGAS,\ out}$=100°F, P_{FGAS}=19.7psia, $\dot{m}_{FGAS}$=7343850lb/hr		
Case		**With Spray Cooler**
	Units	Temperatures and Condensation Rate
Flue Gas Mass Flow Rate	lb/hr	7395719.00
CW Mass Flow Rate	lb/hr	11833150.40 (1.6)
Flue Gas Inlet Temp	°F	170
Flue Gas Outlet Temp	°F	100.05
CW Inlet Temp	°F	64.9
CW Outlet Temp	°F	132.98
Inlet y_{H2O}	%	18.02
Outlet y_{H2O}	%	5.08
Condensation Rate	lb/hr	644,410
	Units	Pressure Drop in CHX
Flue Gas Side ΔP	psi	0.910
Total CW Side ΔP	psi	372.267
	Units	Power
ID Fan Power	kW	3116.84
CW Pump Power	kW	4783.51
Refrigeration Compressor Power (T_{CW} From 80°F to 65 °F)	kW	3422.02
Annual Power Cost (7000hr/yr, $70/Million kWh)	Milli$	5.55
	Units	Geometry
Total Duct Length	ft	54
Total # of Row	-	84
Nickel Alloy 22 Tube Surface Area	ft^2	100
Stainless Steel Tube Surface Area	ft^2	314166
Total Capital Cost (Including Manufacture & Installation Cost)	Milli$	12.99

$T_{FGAS, in}$=197°F, $T_{FGAS, out}$=104°F, P_{FGAS}=19.7psia, $\dot{m}_{FGAS}$=7343850lb/hr		
Case		**With Spray Cooler**
	Units	Temperatures and Condensation Rate
Flue Gas Mass Flow Rate	lb/hr	7,395,719
CW Mass Flow Rate	lb/hr	12,202,936 (1.65)
Flue Gas Inlet Temp	°F	170
Flue Gas Outlet Temp	°F	103.67
CW Inlet Temp	°F	64.47
CW Outlet Temp	°F	127.86
Inlet y_{H2O}	%	18.02
Outlet y_{H2O}	%	5.66
Condensation Rate	lb/hr	619,031
	Units	Pressure Drop in CHX
Flue Gas Side ΔP	psi	0.785
Total CW Side ΔP	psi	346.054
	Units	Power
ID Fan Power	kW	2699.07
CW Pump Power	kW	4585.64
Refrigeration Compressor Power (T_{CW} From 80°F to 65 °F)	kW	3528.65
Annual Power Cost (7000hr/yr, $70/Million kWh)	Milli$	5.30
	Units	Geometry
Total Duct Length	ft	42
Total # of Row	-	72
Nickel Alloy 22 Tube Surface Area	ft^2	0
Stainless Steel Tube Surface Area	ft^2	269384.3
Total Capital Cost (Including Manufacture & Installation Cost)	Milli$	11.12

$T_{FGAS,\ in}$=197°F, $T_{FGAS,\ out}$=110°F, P_{FGAS}=19.7psia, $\dot{m}_{FGAS}$=7343850lb/hr		
Case		**With Spray Cooler**
	Units	Temperatures and Condensation Rate
Flue Gas Mass Flow Rate	lb/hr	7395719.00
CW Mass Flow Rate	lb/hr	12202936.35 (1.65)
Flue Gas Inlet Temp	°F	170
Flue Gas Outlet Temp	°F	109.53
CW Inlet Temp	°F	64.78
CW Outlet Temp	°F	123.71
Inlet y_{H2O}	%	18.02
Outlet y_{H2O}	%	6.63
Condensation Rate	lb/hr	576,590
	Units	Pressure Drop in CHX
Flue Gas Side ΔP	psi	0.664
Total CW Side ΔP	psi	296.655
	Units	Power
ID Fan Power	kW	2301.11
CW Pump Power	kW	3931.04
Refrigeration Compressor Power (T_{CW} From 80°F to 65 °F)	kW	3528.65
Annual Power Cost (7000hr/yr, $70/Million kWh)	Milli$	4.78
	Units	Geometry
Total Duct Length	ft	36
Total # of Row	-	60
Nickel Alloy 22 Tube Surface Area	ft^2	0
Stainless Steel Tube Surface Area	ft^2	224501.4
Total Capital Cost (Including Manufacture & Installation Cost)	Milli$	9.27

$T_{FGAS, in}$=197°F, $T_{FGAS, out}$=120°F, P_{FGAS}=19.7psia, $\dot{m}_{FGAS}$=7343850lb/hr		
Case		**With Spray Cooler**
	Units	Temperatures and Condensation Rate
Flue Gas Mass Flow Rate	lb/hr	7395719.00
CW Mass Flow Rate	lb/hr	9614434.70 (1.3)
Flue Gas Inlet Temp	°F	170
Flue Gas Outlet Temp	°F	120.27
CW Inlet Temp	°F	64.47
CW Outlet Temp	°F	128.01
Inlet y_{H2O}	%	18.02
Outlet y_{H2O}	%	8.48
Condensation Rate	lb/hr	492,692
	Units	Pressure Drop in CHX
Flue Gas Side ΔP	psi	0.550
Total CW Side ΔP	psi	155.441
	Units	Power
ID Fan Power	kW	1940.29
CW Pump Power	kW	1622.87
Refrigeration Compressor Power (T_{CW} From 80°F to 65 °F)	kW	2779.97
Annual Power Cost (7000hr/yr, $70/Million kWh)	Milli$	3.11
	Units	Geometry
Total Duct Length	ft	30
Total # of Row	-	48
Nickel Alloy 22 Tube Surface Area	ft^2	0
Stainless Steel Tube Surface Area	ft^2	179620.6
Total Capital Cost (Including Manufacture & Installation Cost)	Milli$	7.42

$T_{FGAS,\ in}$=197°F, $T_{FGAS,\ out}$=130°F, P_{FGAS}=19.7psia, $\dot{m}_{FGAS}$=7343850lb/hr		
Case		**With Spray Cooler**
	Units	Temperatures and Condensation Rate
Flue Gas Mass Flow Rate	lb/hr	7395719.00
CW Mass Flow Rate	lb/hr	8135290.90 (1.1)
Flue Gas Inlet Temp	°F	170
Flue Gas Outlet Temp	°F	130.27
CW Inlet Temp	°F	64.65
CW Outlet Temp	°F	126.29
Inlet y_{H2O}	%	18.02
Outlet y_{H2O}	%	10.32
Condensation Rate	lb/hr	405811
	Units	Pressure Drop in CHX
Flue Gas Side ΔP	psi	0.423
Total CW Side ΔP	psi	89.888
	Units	Power
ID Fan Power	kW	1515.37
CW Pump Power	kW	794.08
Refrigeration Compressor Power (T_{CW} From 80°F to 65 °F)	kW	2352.68
Annual Power Cost (7000hr/yr, $70/Million kWh)	Milli$	2.28
	Units	Geometry
Total Duct Length	ft	24
Total # of Row	-	36
Nickel Alloy 22 Tube Surface Area	ft^2	0
Stainless Steel Tube Surface Area	ft^2	134740.3
Total Capital Cost (Including Manufacture & Installation Cost)	Milli$	5.56

$T_{FGAS, in}$=174°F, $T_{FGAS, out}$=100°F, P_{FGAS}=17.7psia, $\dot{m}_{FGAS}$=7343850lb/hr		
Case		**With Spray Cooler**
	Units	Temperatures and Condensation Rate
Flue Gas Mass Flow Rate	lb/hr	7380025.00
CW Mass Flow Rate	lb/hr	10701036.25 (1.45)
Flue Gas Inlet Temp	°F	155
Flue Gas Outlet Temp	°F	100.01
CW Inlet Temp	°F	65.03
CW Outlet Temp	°F	133.29
Inlet y_{H2O}	%	17.75
Outlet y_{H2O}	%	5.72
Condensation Rate	lb/hr	600,629
	Units	Pressure Drop in CHX
Flue Gas Side ΔP	psi	1.016
Total CW Side ΔP	psi	306.056
	Units	Power
ID Fan Power	kW	3457.86
CW Pump Power	kW	3556.43
Refrigeration Compressor Power (T_{CW} From 80°F to 65 °F)	kW	3095.40
Annual Power Cost (7000hr/yr, $70/Million kWh)	Milli$	4.95
	Units	Geometry
Total Duct Length	ft	54
Total # of Row	-	84
Nickel Alloy 22 Tube Surface Area	ft^2	100
Stainless Steel Tube Surface Area	ft^2	314166
Total Capital Cost (Including Manufacture & Installation Cost)	Milli$	12.99

$T_{FGAS, in}$=174°F, $T_{FGAS, out}$=104°F, P_{FGAS}=17.7psia, $\dot{m}_{FGAS}$=7343850lb/hr		
Case		**With Spray Cooler**
	Units	Temperatures and Condensation Rate
Flue Gas Mass Flow Rate	lb/hr	7,380,025
CW Mass Flow Rate	lb/hr	10,332,035 (1.4)
Flue Gas Inlet Temp	°F	155
Flue Gas Outlet Temp	°F	104.07
CW Inlet Temp	°F	64.66
CW Outlet Temp	°F	131.33
Inlet y_{H2O}	%	17.75
Outlet y_{H2O}	%	6.48
Condensation Rate	lb/hr	567,422
	Units	Pressure Drop in CHX
Flue Gas Side ΔP	psi	0.878
Total CW Side ΔP	psi	250.249
	Units	Power
ID Fan Power	kW	3010.01
CW Pump Power	kW	2807.67
Refrigeration Compressor Power (T_{CW} From 80°F to 65 °F)	kW	2988.02
Annual Power Cost (7000hr/yr, $70/Million kWh)	Milli$	4.31
	Units	Geometry
Total Duct Length	ft	42
Total # of Row	-	72
Nickel Alloy 22 Tube Surface Area	ft^2	0
Stainless Steel Tube Surface Area	ft^2	269384.3
Total Capital Cost (Including Manufacture & Installation Cost)	Milli$	11.12

$T_{FGAS, in}$=174°F, $T_{FGAS, out}$=110°F, P_{FGAS}=17.7psia, $\dot{m}_{FGAS}$=7343850lb/hr		
Case		**With Spray Cooler**
	Units	Temperatures and Condensation Rate
Flue Gas Mass Flow Rate	lb/hr	7380025.00
CW Mass Flow Rate	lb/hr	9594032.50 (1.3)
Flue Gas Inlet Temp	°F	155
Flue Gas Outlet Temp	°F	109.81
CW Inlet Temp	°F	64.83
CW Outlet Temp	°F	130.17
Inlet y_{H2O}	%	17.75
Outlet y_{H2O}	%	7.58
Condensation Rate	lb/hr	518,055
	Units	Pressure Drop in CHX
Flue Gas Side ΔP	psi	0.744
Total CW Side ΔP	psi	185.745
	Units	Power
ID Fan Power	kW	2570.2
CW Pump Power	kW	1935.13
Refrigeration Compressor Power (T_{CW} From 80°F to 65 °F)	kW	2774.75
Annual Power Cost (7000hr/yr, $70/Million kWh)	Milli$	3.57
	Units	Geometry
Total Duct Length	ft	36
Total # of Row	-	60
Nickel Alloy 22 Tube Surface Area	ft^2	0
Stainless Steel Tube Surface Area	ft^2	224501.4
Total Capital Cost (Including Manufacture & Installation Cost)	Milli$	9.27

$T_{FGAS,\ in}$=174°F, $T_{FGAS,\ out}$=120°F, P_{FGAS}=17.7psia, $\dot{m}_{FGAS}$=7343850lb/hr		
Case		**With Spray Cooler**
	Units	Temperatures and Condensation Rate
Flue Gas Mass Flow Rate	lb/hr	7380025.00
CW Mass Flow Rate	lb/hr	10332035.00 (1.4)
Flue Gas Inlet Temp	°F	155
Flue Gas Outlet Temp	°F	119.66
CW Inlet Temp	°F	64.96
CW Outlet Temp	°F	113.69
Inlet y_{H2O}	%	17.74
Outlet y_{H2O}	%	9.79
Condensation Rate	lb/hr	415,533
	Units	Pressure Drop in CHX
Flue Gas Side ΔP	psi	0.455
Total CW Side ΔP	psi	143.191
	Units	Power
ID Fan Power	kW	1590.89
CW Pump Power	kW	1606.53
Refrigeration Compressor Power (T_{CW} From 80°F to 65 °F)	kW	2988.02
Annual Power Cost (7000hr/yr, $70/Million kWh)	Milli$	3.03
	Units	Geometry
Total Duct Length	ft	24
Total # of Row	-	36
Nickel Alloy 22 Tube Surface Area	ft^2	0
Stainless Steel Tube Surface Area	ft^2	134739.8
Total Capital Cost (Including Manufacture & Installation Cost)	Milli$	5.56

$T_{FGAS,\ in}$=174°F, $T_{FGAS,\ out}$=130°F, P_{FGAS}=17.7psia, $\dot{m}_{FGAS}$=7343850lb/hr		
Case		**With Spray Cooler**
	Units	Temperatures and Condensation Rate
Flue Gas Mass Flow Rate	lb/hr	7380025.00
CW Mass Flow Rate	lb/hr	8118027.50 (1.1)
Flue Gas Inlet Temp	°F	155
Flue Gas Outlet Temp	°F	129.88
CW Inlet Temp	°F	64.98
CW Outlet Temp	°F	110.44
Inlet y_{H2O}	%	17.74
Outlet y_{H2O}	%	12.04
Condensation Rate	lb/hr	305384
	Units	Pressure Drop in CHX
Flue Gas Side ΔP	psi	0.312
Total CW Side ΔP	psi	67.152
	Units	Power
ID Fan Power	kW	1110.82
CW Pump Power	kW	591.97
Refrigeration Compressor Power (T_{CW} From 80°F to 65 °F)	kW	2347.46
Annual Power Cost (7000hr/yr, $70/Million kWh)	Milli$	1.98
	Units	Geometry
Total Duct Length	ft	18
Total # of Row	-	24
Nickel Alloy 22 Tube Surface Area	ft^2	0
Stainless Steel Tube Surface Area	ft^2	89858.9
Total Capital Cost (Including Manufacture & Installation Cost)	Milli$	3.71

4.2 CHX Design Results with Cooling Water Inlet Temperature of 80°F

$T_{FGAS,\,in}$=219°F, $T_{FGAS,\,out}$=104°F, P_{FGAS}=21.7psia, $\dot{m}_{FGAS}$=10634586lb/hr		
Case		**With Spray Cooler**
	Units	Temperatures and Condensation Rate
Flue Gas Mass Flow Rate	lb/hr	10757359.10
CW Mass Flow Rate	lb/hr	16781480.20 (1.56)
Flue Gas Inlet Temp	°F	175
Flue Gas Outlet Temp	°F	103.57
CW Inlet Temp	°F	79.90
CW Outlet Temp	°F	152.91
Inlet y_{H2O}	%	18.59
Outlet y_{H2O}	%	4.90
Condensation Rate	lb/hr	991966
	Units	Pressure Drop in CHX
Flue Gas Side ΔP	psi	3.882
Total CW Side ΔP	psi	1456.925
	Units	Power
ID Fan Power	kW	19554.81
CW Pump Power	kW	26549.55
Refrigeration Compressor Power (T_{CW} From 80°F to 65 °F)	kW	0
Annual Power Cost (7000hr/yr, $70/Million kWh)	Milli$	22.59
	Units	Geometry
Total Duct Length	ft	102
Total # of Row	-	180
Nickel Alloy 22 Tube Surface Area	ft^2	19253.34
Stainless Steel Tube Surface Area	ft^2	654063.4
Total Capital Cost (Including Manufacture & Installation Cost)	Milli$	31.08

$T_{FGAS,\ in}$=219°F, $T_{FGAS,\ out}$=110°F, P_{FGAS}=21.7psia, $\dot{m}_{FGAS}$=10634586lb/hr		
Case		**With Spray Cooler**
	Units	Temperatures and Condensation Rate
Flue Gas Mass Flow Rate	lb/hr	10757359.10
CW Mass Flow Rate	lb/hr	16996627.38 (1.58)
Flue Gas Inlet Temp	°F	175
Flue Gas Outlet Temp	°F	109.84
CW Inlet Temp	°F	79.89
CW Outlet Temp	°F	147.38
Inlet y_{H2O}	%	18.59
Outlet y_{H2O}	%	5.86
Condensation Rate	lb/hr	931799
	Units	Pressure Drop in CHX
Flue Gas Side ΔP	psi	2.572
Total CW Side ΔP	psi	1028.34
	Units	Power
ID Fan Power	kW	12995.47
CW Pump Power	kW	18979.64
Refrigeration Compressor Power (T_{CW} From 80°F to 65 °F)	kW	0
Annual Power Cost (7000hr/yr, $70/Million kWh)	Milli$	15.67
	Units	Geometry
Total Duct Length	ft	72
Total # of Row	-	120
Nickel Alloy 22 Tube Surface Area	ft^2	100.02
Stainless Steel Tube Surface Area	ft^2	448809.8
Total Capital Cost (Including Manufacture & Installation Cost)	Milli$	18.55

$T_{FGAS,\,in}$=219°F, $T_{FGAS,\,out}$=120°F, P_{FGAS}=21.7psia, $\dot{m}_{FGAS}$=10634586lb/hr		
Case		**With Spray Cooler**
	Units	Temperatures and Condensation Rate
Flue Gas Mass Flow Rate	lb/hr	10757359.10
CW Mass Flow Rate	lb/hr	15598170.69 (1.45)
Flue Gas Inlet Temp	°F	175
Flue Gas Outlet Temp	°F	120.01
CW Inlet Temp	°F	79.54
CW Outlet Temp	°F	143.70
Inlet y_{H2O}	%	18.59
Outlet y_{H2O}	%	7.64
Condensation Rate	lb/hr	816450
	Units	Pressure Drop in CHX
Flue Gas Side ΔP	psi	1.845
Total CW Side ΔP	psi	632.819
	Units	Power
ID Fan Power	kW	9459.81
CW Pump Power	kW	10718.71
Refrigeration Compressor Power (T_{CW} From 80°F to 65 °F)	kW	0
Annual Power Cost (7000hr/yr, $70/Million kWh)	Milli$	9.89
	Units	Geometry
Total Duct Length	ft	51
Total # of Row	-	84
Nickel Alloy 22 Tube Surface Area	ft^2	99.95
Stainless Steel Tube Surface Area	ft^2	314165.7
Total Capital Cost (Including Manufacture & Installation Cost)	Milli$	12.99

$T_{FGAS,\,in}$=219°F, $T_{FGAS,\,out}$=130°F, P_{FGAS}=21.7psia, $\dot{m}_{FGAS}$=10634586lb/hr		
Case		**With Spray Cooler**
	Units	Temperatures and Condensation Rate
Flue Gas Mass Flow Rate	lb/hr	10757359.10
CW Mass Flow Rate	lb/hr	13984566.83 (1.3)
Flue Gas Inlet Temp	°F	175
Flue Gas Outlet Temp	°F	130.00
CW Inlet Temp	°F	79.94
CW Outlet Temp	°F	140.28
Inlet y_{H2O}	%	18.59
Outlet y_{H2O}	%	9.52
Condensation Rate	lb/hr	690762
	Units	Pressure Drop in CHX
Flue Gas Side ΔP	psi	1.348
Total CW Side ΔP	psi	383.709
	Units	Power
ID Fan Power	kW	7021.32
CW Pump Power	kW	5826.95
Refrigeration Compressor Power (T_{CW} From 80°F to 65 °F)	kW	0
Annual Power Cost (7000hr/yr, $70/Million kWh)	Milli$	6.30
	Units	Geometry
Total Duct Length	ft	36
Total # of Row	-	60
Nickel Alloy 22 Tube Surface Area	ft^2	0
Stainless Steel Tube Surface Area	ft^2	224503.2
Total Capital Cost (Including Manufacture & Installation Cost)	Milli$	9.27

$T_{FGAS,\,in}$=197°F, $T_{FGAS,\,out}$=104°F, P_{FGAS}=19.7psia, $\dot{m}_{FGAS}$=10634586lb/hr		
Case		**With Spray Cooler**
	Units	Temperatures and Condensation Rate
Flue Gas Mass Flow Rate	lb/hr	10723341.37
CW Mass Flow Rate	lb/hr	18229680.33 (1.7)
Flue Gas Inlet Temp	°F	165
Flue Gas Outlet Temp	°F	104.14
CW Inlet Temp	°F	80.15
CW Outlet Temp	°F	142.02
Inlet y_{H2O}	%	18.18
Outlet y_{H2O}	%	5.41
Condensation Rate	lb/hr	925664
	Units	Pressure Drop in CHX
Flue Gas Side ΔP	psi	3.038
Total CW Side ΔP	psi	1286.947
	Units	Power
ID Fan Power	kW	15052.15
CW Pump Power	kW	25475.89
Refrigeration Compressor Power (T_{CW} From 80°F to 65 °F)	kW	0
Annual Power Cost (7000hr/yr, $70/Million kWh)	Milli$	19.86
	Units	Geometry
Total Duct Length	ft	78
Total # of Row	-	132
Nickel Alloy 22 Tube Surface Area	ft^2	100
Stainless Steel Tube Surface Area	ft^2	493691.2
Total Capital Cost (Including Manufacture & Installation Cost)	Milli$	20.41

$T_{FGAS,\,in}$=197°F, $T_{FGAS,\,out}$=110°F, P_{FGAS}=19.7psia, $\dot{m}_{FGAS}$=10634586lb/hr		
Case		**With Spray Cooler**
	Units	Temperatures and Condensation Rate
Flue Gas Mass Flow Rate	lb/hr	10723341.37
CW Mass Flow Rate	lb/hr	17157346.19 (1.6)
Flue Gas Inlet Temp	°F	165
Flue Gas Outlet Temp	°F	109.88
CW Inlet Temp	°F	80.04
CW Outlet Temp	°F	141.02
Inlet y_{H2O}	%	18.18
Outlet y_{H2O}	%	6.43
Condensation Rate	lb/hr	861379
	Units	Pressure Drop in CHX
Flue Gas Side ΔP	psi	2.529
Total CW Side ΔP	psi	952.74
	Units	Power
ID Fan Power	kW	12663.59
CW Pump Power	kW	17750.66
Refrigeration Compressor Power (T_{CW} From 80°F to 65 °F)	kW	0
Annual Power Cost (7000hr/yr, $70/Million kWh)	Milli$	14.90
	Units	Geometry
Total Duct Length	ft	66
Total # of Row	-	108
Nickel Alloy 22 Tube Surface Area	ft^2	99.98
Stainless Steel Tube Surface Area	ft^2	103928.5
Total Capital Cost (Including Manufacture & Installation Cost)	Milli$	4.31

$T_{FGAS,\,in}$=197°F, $T_{FGAS,\,out}$=120°F, P_{FGAS}=19.7psia, $\dot{m}_{FGAS}$=10634586lb/hr		
Case		**With Spray Cooler**
	Units	Temperatures and Condensation Rate
Flue Gas Mass Flow Rate	lb/hr	10723341.37
CW Mass Flow Rate	lb/hr	15548844.99 (1.45)
Flue Gas Inlet Temp	°F	165
Flue Gas Outlet Temp	°F	119.86
CW Inlet Temp	°F	79.28
CW Outlet Temp	°F	136.47
Inlet y_{H2O}	%	18.18
Outlet y_{H2O}	%	8.36
Condensation Rate	lb/hr	734955
	Units	Pressure Drop in CHX
Flue Gas Side ΔP	psi	1.727
Total CW Side ΔP	psi	550.815
	Units	Power
ID Fan Power	kW	8786.96
CW Pump Power	kW	9300.22
Refrigeration Compressor Power (T_{CW} From 80°F to 65 °F)	kW	0
Annual Power Cost (7000hr/yr, $70/Million kWh)	Milli$	8.86
	Units	Geometry
Total Duct Length	ft	48
Total # of Row	-	72
Nickel Alloy 22 Tube Surface Area	ft^2	0
Stainless Steel Tube Surface Area	ft^2	269384.6
Total Capital Cost (Including Manufacture & Installation Cost)	Milli$	11.12

$T_{FGAS,\,in}$=197°F, $T_{FGAS,\,out}$=130°F, P_{FGAS}=19.7psia, $\dot{m}_{FGAS}$=10634586lb/hr		
Case		**With Spray Cooler**
	Units	Temperatures and Condensation Rate
Flue Gas Mass Flow Rate	lb/hr	10723341.37
CW Mass Flow Rate	lb/hr	13940343.78 (1.3)
Flue Gas Inlet Temp	°F	165
Flue Gas Outlet Temp	°F	129.93
CW Inlet Temp	°F	79.90
CW Outlet Temp	°F	131.20
Inlet y_{H2O}	%	18.18
Outlet y_{H2O}	%	10.44
Condensation Rate	lb/hr	593151
	Units	Pressure Drop in CHX
Flue Gas Side ΔP	psi	1.179
Total CW Side ΔP	psi	318.193
	Units	Power
ID Fan Power	kW	6095.96
CW Pump Power	kW	4816.76
Refrigeration Compressor Power (T_{CW} From 80°F to 65 °F)	kW	0
Annual Power Cost (7000hr/yr, $70/Million kWh)	Milli$	5.35
	Units	Geometry
Total Duct Length	ft	30
Total # of Row	-	48
Nickel Alloy 22 Tube Surface Area	ft^2	0
Stainless Steel Tube Surface Area	ft^2	179621.8
Total Capital Cost (Including Manufacture & Installation Cost)	Milli$	7.42

$T_{FGAS,\,in}$=174°F, $T_{FGAS,\,out}$=104°F, P_{FGAS}=17.7psia, $\dot{m}_{FGAS}$=10634586lb/hr		
Case		**With Spray Cooler**
	Units	Temperatures and Condensation Rate
Flue Gas Mass Flow Rate	lb/hr	10686971.12
CW Mass Flow Rate	lb/hr	16030456.68 (1.5)
Flue Gas Inlet Temp	°F	155
Flue Gas Outlet Temp	°F	104.26
CW Inlet Temp	°F	79.28
CW Outlet Temp	°F	142.61
Inlet y_{H2O}	%	17.75
Outlet y_{H2O}	%	6.13
Condensation Rate	lb/hr	844269
	Units	Pressure Drop in CHX
Flue Gas Side ΔP	psi	4.423
Total CW Side ΔP	psi	1249.013
	Units	Power
ID Fan Power	kW	22000.10
CW Pump Power	kW	21742.17
Refrigeration Compressor Power (T_{CW} From 80°F to 65 °F)	kW	0
Annual Power Cost (7000hr/yr, $70/Million kWh)	Milli$	21.43
	Units	Geometry
Total Duct Length	ft	96
Total # of Row	-	168
Nickel Alloy 22 Tube Surface Area	ft^2	99.99
Stainless Steel Tube Surface Area	ft^2	628335.4
Total Capital Cost (Including Manufacture & Installation Cost)	Milli$	25.97

$T_{FGAS,\,in}$=174°F, $T_{FGAS,\,out}$=110°F, P_{FGAS}=17.7psia, $\dot{m}_{FGAS}$=10634586lb/hr		
Case		**With Spray Cooler**
	Units	Temperatures and Condensation Rate
Flue Gas Mass Flow Rate	lb/hr	10686971.12
CW Mass Flow Rate	lb/hr	16030456.68 (1.5)
Flue Gas Inlet Temp	°F	155
Flue Gas Outlet Temp	°F	109.84
CW Inlet Temp	°F	80.42
CW Outlet Temp	°F	138.59
Inlet y_{H2O}	%	17.75
Outlet y_{H2O}	%	7.14
Condensation Rate	lb/hr	778732
	Units	Pressure Drop in CHX
Flue Gas Side ΔP	psi	2.820
Total CW Side ΔP	psi	834.020
	Units	Power
ID Fan Power	kW	14044.61
CW Pump Power	kW	14518.18
Refrigeration Compressor Power (T_{CW} From 80°F to 65 °F)	kW	0
Annual Power Cost (7000hr/yr, $70/Million kWh)	Milli$	14.00
	Units	Geometry
Total Duct Length	ft	66
Total # of Row	-	108
Nickel Alloy 22 Tube Surface Area	ft^2	99.98
Stainless Steel Tube Surface Area	ft^2	403928.5
Total Capital Cost (Including Manufacture & Installation Cost)	Milli$	16.70

$T_{FGAS,\,in}$=174°F, $T_{FGAS,\,out}$=120°F, P_{FGAS}=17.7psia, $\dot{m}_{FGAS}$=10634586lb/hr		
Case		**With Spray Cooler**
	Units	Temperatures and Condensation Rate
Flue Gas Mass Flow Rate	lb/hr	10686971.12
CW Mass Flow Rate	lb/hr	15496108.12 (1.45)
Flue Gas Inlet Temp	°F	155
Flue Gas Outlet Temp	°F	119.74
CW Inlet Temp	°F	79.93
CW Outlet Temp	°F	129.04
Inlet y_{H2O}	%	17.75
Outlet y_{H2O}	%	9.26
Condensation Rate	lb/hr	637616
	Units	Pressure Drop in CHX
Flue Gas Side ΔP	psi	1.592
Total CW Side ΔP	psi	469.436
	Units	Power
ID Fan Power	kW	8036.37
CW Pump Power	kW	7899.3
Refrigeration Compressor Power (T_{CW} From 80°F to 65 °F)	kW	0
Annual Power Cost (7000hr/yr, $70/Million kWh)	Milli$	7.81
	Units	Geometry
Total Duct Length	ft	36
Total # of Row	-	60
Nickel Alloy 22 Tube Surface Area	ft^2	0
Stainless Steel Tube Surface Area	ft^2	224503.2
Total Capital Cost (Including Manufacture & Installation Cost)	Milli$	9.27

$T_{FGAS,\,in}$=174°F, $T_{FGAS,\,out}$=130°F, P_{FGAS}=17.7psia, $\dot{m}_{FGAS}$=10634586lb/hr		
Case		**With Spray Cooler**
	Units	Temperatures and Condensation Rate
Flue Gas Mass Flow Rate	lb/hr	10686971.12
CW Mass Flow Rate	lb/hr	13893062.46 (1.3)
Flue Gas Inlet Temp	°F	155
Flue Gas Outlet Temp	°F	129.69
CW Inlet Temp	°F	80.37
CW Outlet Temp	°F	121.09
Inlet y_{H2O}	%	17.75
Outlet y_{H2O}	%	11.59
Condensation Rate	lb/hr	475007
	Units	Pressure Drop in CHX
Flue Gas Side ΔP	psi	0.980
Total CW Side ΔP	psi	253.228
	Units	Power
ID Fan Power	kW	5028.96
CW Pump Power	kW	3820.3
Refrigeration Compressor Power (T_{CW} From 80°F to 65 °F)	kW	0
Annual Power Cost (7000hr/yr, $70/Million kWh)	Milli$	4.34
	Units	Geometry
Total Duct Length	ft	24
Total # of Row	-	36
Nickel Alloy 22 Tube Surface Area	ft^2	0
Stainless Steel Tube Surface Area	ft^2	134740.3
Total Capital Cost (Including Manufacture & Installation Cost)	Milli$	5.56

4.3 CHX Design Results Summary with Cooling Water Inlet Temperature of 65°F

Flue Gas Side Pressure Drop of CHX (psi)															
$T, P_{FGAS,in}$ / $T_{FGAS,out}$ / $\dot{m}_{FGAS}$	219°F, 21.7psia					197°F, 19.7psia					174°F, 17.7psia				
	100	104	110	120	130	100	104	110	120	130	100	104	110	120	130
10,634,586 lb/hr	2.252	2.019	1.798	1.310	1.081	2.180	1.924	1.684	1.147	0.885	2.425	1.826	1.552	1.281	0.990
9,561,430 lb/hr	1.611	1.424	1.233	1.063	0.875	1.772	1.562	1.363	0.930	0.719	1.979	1.476	1.252	0.772	0.530
8,452,640 lb/hr	1.263	1.107	0.967	0.831	0.681	1.388	1.227	1.065	0.724	0.557	1.339	1.158	0.980	0.604	0.414
7,343,850 lb/hr	0.958	0.842	0.737	0.632	0.383	0.910	0.785	0.664	0.550	0.423	1.016	0.878	0.744	0.455	0.312

Cooling Water Side Pressure Drop of CHX (psi)															
$T, P_{FGAS,in}$ / $T_{FGAS,out}$ / $\dot{m}_{FGAS}$	219°F, 21.7psia					197°F, 19.7psia					174°F, 17.7psia				
	100	104	110	120	130	100	104	110	120	130	100	104	110	120	130
10,634,586 lb/hr	870.795	763.985	593.485	430.312	231.957	861.871	766.402	553.282	451.128	237.19	735.17	708.248	504.054	229.316	93.964
9,561,430 lb/hr	704.694	626.573	548.592	313.405	172.277	617.477	549.008	419.943	300.438	150.241	535.891	542.001	409.717	310.396	179.518
8,452,640 lb/hr	519.884	522.302	404.562	246.083	148.172	484.602	403.389	329.697	269.806	163.383	429.427	375.889	281.831	201.451	122.136
7,343,850 lb/hr	371.157	330.082	252.514	160.31	199.070	372.267	346.054	296.655	155.441	89.888	306.056	250.249	185.745	143.191	67.152

ID Fan Power of CHX (kW)															
$T, P_{FGAS,in}$ / $T_{FGAS,out}$ / $\dot{m}_{FGAS}$	219°F, 21.7psia					197°F, 19.7psia					174°F, 17.7psia				
	100	104	110	120	130	100	104	110	120	130	100	104	110	120	130
10,634,586 lb/hr	11217.93	10108.61	9096.63	6718.10	5638.62	10742.95	9541.71	8445.83	5827.73	4569.12	11886.36	8987.75	7718.2	6494.88	5099.40
9,561,430 lb/hr	7213.25	6415.86	5597.45	4912.64	4113.37	7892.27	6995.73	6457.07	4256.35	3340.49	8774.95	6534.72	5591.28	3518.53	2448.72
8,452,640 lb/hr	5022.25	4406.15	3894.68	3404.49	2838.22	5480.28	4878.27	4267.58	2351.00	2290.55	5241.48	4549.92	3882.01	2431.88	1690.13
7,343,850 lb/hr	3314.92	2931.72	2590.03	2259.13	1376.07	3116.84	2699.07	2301.11	1940.29	1515.37	3457.86	3010.01	2570.20	1590.89	1110.82

Cooling Water Pump Power of CHX (kW)															
$T, P_{FGAS,in}$ / $T_{FGAS,out}$ / $\dot{m}_{FGAS}$	219°F, 21.7psia					197°F, 19.7psia					174°F, 17.7psia				
	100	104	110	120	130	100	104	110	120	130	100	104	110	120	130
10,634,586 lb/hr	15461.62	13386.65	9705.84	6911.65	2980.55	16057.66	14278.96	9341.91	8142.38	3452.44	12626.81	13561.66	8774.31	2927.32	850.55
9,561,430 lb/hr	11841.83	10529.04	9218.62	4279.03	1899.83	9696.92	8621.70	6155.19	4403.58	1730.24	7828.01	9048.28	6412.43	5181.84	2622.31
8,452,640 lb/hr	7472.33	7991.4	5814.78	2966.48	1511.38	6719.18	5406.71	4266.58	2986.89	1963.30	5941.52	5200.78	3639.43	2694.35	1464.55
7,343,850 lb/hr	4485.15	3988.80	2848.02	1549.76	2646.17	4783.51	4585.64	3931.04	1622.87	794.08	3556.43	2807.67	1935.13	1606.53	591.97

Refrigeration Cycle Compressor Power (kW)															
$T, P_{FGAS,in}$ / $T_{FGAS,out}$ / $\dot{m}_{FGAS}$	219°F, 21.7psia					197°F, 19.7psia					174°F, 17.7psia				
	100	104	110	120	130	100	104	110	120	130	100	104	110	120	130
10,634,586 lb/hr	4729.23	4667.34	4354.89	4277.33	3422.02	4962.63	4962.63	4496.57	4807.53	3876.15	4574.87	5099.84	4636.76	3399.65	2410.10
9,561,430 lb/hr	4474.94	4474.94	4474.94	3633.03	2937.31	4181.88	4181.88	3902.99	3902.99	3067.81	3890.32	4445.86	4167.72	4445.86	3890.32
8,452,640 lb/hr	3827.68	4074.50	3827.68	3210.24	2716.59	3692.71	3569.67	3445.88	3692.71	3199.80	3684.50	3684.50	3439.17	3561.46	3193.09
7,343,850 lb/hr	3217.69	3217.70	3003.68	2574.90	3539.84	3422.02	3528.65	3528.65	2779.97	2352.68	3095.40	2988.02	2774.75	2988.02	2347.46

Moisture Content at the Outlet of CHX (%)															
$T, P_{FGAS,in}$ / $T_{FGAS,out}$ / $\dot{m}_{FGAS}$	219°F, 21.7psia					197°F, 19.7psia					174°F, 17.7psia				
	100	104	110	120	130	100	104	110	120	130	100	104	110	120	130
10,634,586 lb/hr	4.74	5.29	6.24	7.97	9.85	5.17	5.82	6.94	8.89	10.81	5.64	6.58	7.77	9.71	11.80
9,561,430 lb/hr	4.83	5.50	6.28	7.99	9.83	5.21	5.85	6.86	8.88	10.87	5.84	6.45	7.55	10.14	12.24
8,452,640 lb/hr	4.70	5.11	6.12	7.70	9.39	5.10	5.78	6.66	8.46	10.30	5.80	6.50	7.55	10.06	12.17
7,343,850 lb/hr	4.66	5.20	6.23	7.84	9.60	5.08	5.66	6.63	8.48	10.32	5.72	6.48	7.58	9.79	12.04

Length of CHX (ft)															
$T, P_{FGAS,in}$ / $T_{FGAS,out}$ / $\dot{m}_{FGAS}$	219°F, 21.7psia					197°F, 19.7psia					174°F, 17.7psia				
	100	104	110	120	130	100	104	110	120	130	100	104	110	120	130
10,634,586 lb/hr	66	57	51	36	30	57	51	42	30	24	57	42	36	30	24
9,561,430 lb/hr	57	51	42	36	30	57	51	42	30	24	57	42	36	24	18
8,452,640 lb/hr	57	51	42	36	30	57	51	42	30	24	51	42	36	24	18
7,343,850 lb/hr	57	51	42	36	24	51	42	36	30	24	51	42	36	24	18

Stainless Steel Tube Surface Area, No Nickel Alloy Needed (ft^2) [or Nickel Alloy + Stainless Steel]															
$T, P_{FGAS,in}$ / $T_{FGAS,out}$ / $\dot{m}_{FGAS}$	219°F, 21.7psia					197°F, 19.7psia					174°F, 17.7psia				
	100	104	110	120	130	100	104	110	120	130	100	104	110	120	130
10,634,586 lb/hr	404029	358965	314266	224501	179622	358965	314266	269385	179622	134740	358965	269385	224501	179622	134740
9,561,430 lb/hr	358965	314266	269385	224501	179622	358965	314266	269385	179622	134740	358965	269385	224501	134740	89859
8,452,640 lb/hr	100* +358865	314266	269385	224501	100* +179522	100* +358865	100* +314166	269385	179622	134740	314266	269385	224501	134740	89859
7,343,850 lb/hr	100* +358865	100* +314166	269385	100* +224401	134740	100* +314166	269385	224501	179622	134740	100* +314166	269385	224501	134740	89859

***Surface Area of Nickel Alloy**

Refrigeration Capacity [BTUs/hr]															
$T, P_{FGAS,in}$ / $T_{FGAS,out}$ / $\dot{m}_{FGAS}$	219°F, 21.7psia					197°F, 19.7psia					174°F, 17.7psia				
	100	104	110	120	130	100	104	110	120	130	100	104	110	120	130
10,634,586 lb/hr	2.453E+08	2.420E+08	2.259E+08	2.219E+08	1.775E+08	2.574E+08	2.574E+08	2.332E+08	2.493E+08	2.011E+08	2.373E+08	2.645E+08	2.405E+08	1.763E+08	1.250E+08
9,561,430 lb/hr	2.321E+08	2.321E+08	2.321E+08	1.886E+08	1.523E+08	2.169E+08	2.169E+08	2.025E+08	2.025E+08	1.591E+08	2.018E+08	2.306E+08	2.162E+08	2.306E+08	2.018E+08
8,452,640 lb/hr	1.985E+08	2.114E+08	1.985E+08	1.665E+08	1.409E+08	1.915E+08	1.851E+08	1.788E+08	1.915E+08	1.660E+08	1.911E+08	1.911E+08	1.784E+08	1.848E+08	1.656E+08
7,343,850 lb/hr	1.669E+08	1.669E+08	1.558E+08	1.335E+08	1.836E+08	1.775E+08	1.830E+08	1.830E+08	1.442E+08	1.220E+08	1.605E+08	1.550E+08	1.439E+08	1.550E+08	1.218E+08

Cooling Tower Heat Dissipation [BTUs/hr]															
$T, P_{FGAS,in}$ / $T_{FGAS,out}$ / $\dot{m}_{FGAS}$	219°F, 21.7psia					197°F, 19.7psia					174°F, 17.7psia				
	100	104	110	120	130	100	104	110	120	130	100	104	110	120	130
10,634,586 lb/hr	1.251E+09	1.200E+09	1.121E+09	9.762E+08	8.217E+08	1.159E+09	1.108E+09	1.016E+09	8.572E+08	6.918E+08	1.058E+09	9.880E+08	8.919E+08	7.247E+08	5.467E+08
9,561,430 lb/hr	1.117E+09	1.069E+09	1.006E+09	8.816E+08	7.387E+08	1.032E+09	9.912E+08	9.172E+08	7.686E+08	6.151E+08	9.457E+08	8.957E+08	8.172E+08	6.386E+08	4.701E+08
8,452,640 lb/hr	9.911E+08	9.688E+08	9.019E+08	7.946E+08	6.088E+08	9.343E+08	8.834E+08	8.296E+08	7.131E+08	5.890E+08	8.395E+08	7.975E+08	7.239E+08	5.679E+08	4.281E+08
7,343,850 lb/hr	8.672E+08	8.318E+08	7.725E+08	6.833E+08	5.823E+08	8.044E+08	7.671E+08	7.164E+08	6.058E+08	4.986E+08	7.308E+08	6.853E+08	6.252E+08	5.031E+08	3.689E+08

4.4 CHX Design Results Summary with Cooling Water Inlet Temperature of 80°F and Flue Gas Mass Flow Rate of 10,634,586 lb/hr

Design Results of CHX without Refrigeration System and Flue Gas Mass Flue Rate of 10634586 lb/hr												
$T, P_{FGAS,in}$ / $T_{FGAS,out}$	219°F, 21.7psia				197°F, 19.7psia				174°F, 17.7psia			
	104	110	120	130	104	110	120	130	104	110	120	130
Flue Gas Side Pressure Drop [psi]	3.882	2.572	1.845	1.348	3.038	2.529	1.727	1.179	4.423	2.820	1.592	0.980
CW Side Pressure Drop [psi]	1456.925	1028.34	632.819	383.709	1286.947	952.74	550.815	318.193	1249.013	834.020	469.436	253.228
$T_{CW,out}$ [°F]	152.91	147.38	143.70	140.28	142.02	141.02	136.47	131.20	142.61	138.59	129.04	121.09
$P_{ID\ Fan}$ [MW]	19.55	13.00	9.46	7.02	15.05	12.66	8.79	6.10	22.00	14.04	8.04	5.03
$P_{CW\ Pump}$ [MW]	26.55	18.98	10.72	5.83	25.48	17.75	9.30	4.82	21.74	14.52	7.90	3.82
CHX Outlet Moisture Content [%]	4.90	5.86	7.64	9.52	5.41	6.43	8.36	10.44	6.13	7.14	9.28	11.59
Length of CHX [ft]	102	72	51	36	78	66	48	30	96	66	36	24
Heat Transfer Area[ft²]	19253* +654063	100* +448810	100* +314166	224503	100* +493691	100* +103929	269385	179622	100* +628335	100* +403929	224503	134740
Annual Power Cost [Milli $]	22.59	15.67	9.89	6.30	19.86	14.90	8.86	5.35	21.43	14.00	7.81	4.34
CHX Capital Cost [Milli $]	25.42	15.26	10.69	7.62	16.81	13.75	9.18	6.12	21.37	13.75	7.62	4.56

***Surface Area of Nickel Alloy**

Reference

[1]. Aspen Plus for Chemicals & Polymers. Retrieved from http://www.aspentech.com/products/aspen-plus.aspx.

[2]. Geol, Nipun. *Design and Performance Analyses of Condensing Heat Exchangers for Recovering Water and Waste Heat from Flue Gas*. Lehigh University, 2012.

[3]. Hazell, Daniel. *Modeling and Optimization of Condensing Heat Exchangers for Cooling Boiler Flue Gas*. Lehigh University, 2011.

[4]. Stainless Steel Tube Price. Retrieved from http://brismet.com/wp-content/uploads/2014/04/Base-Price-Sheet-1013.pdf.

[5]. Nickle Alloy C22 Tube Price. Retrieved from http://zbzhenlan.en.alibaba.com/product/1484997323-220039655/Nickel_Alloy_Hastelloy_C22_UNS_N06022_Strip.html.

[6]. Means, R. S. (2003). RSMeans Mechanical Cost Data. *RS Means Company,26*.